ORIGINS AND ZONING OF THE BUCKHORN GOLD SKARN, NE WASHINGTON

A

THESIS

Presented to the Faculty

of the University of Alaska Fairbanks

in Partial Fulfillment of the Requirements

for the Degree of

MASTER OF SCIENCE

By

Michelle L. Deal, B.S.

Fairbanks, Alaska

December 2012

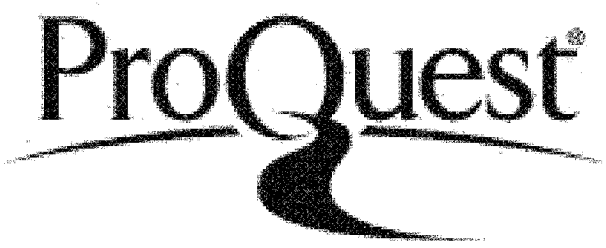

ProQuest LLC
789 East Eisenhower Parkway
P.O. Box 1346
Ann Arbor, MI 48106-1346

ORIGINS AND ZONING OF THE BUCKHORN GOLD SKARN, NE WASHINGTON

By

Michelle L. Deal

RECOMMENDED:

Advisory Committee Chair

Chair, Department of Geology and Geophysics

APPROVED:

Dean, College of Natural Science and Mathematics

Dean of the Graduate School

11/29/2012

Date

Abstract

The Buckhorn Deposit was discovered in the mid 1980's and is composed of two separate Au-Bi deposits: the Gold Bowl and the Southwest Zone. The Southwest Zone is the larger of the two and is blind and stratabound. The Gold Bowl is exposed on the surface. Jurassic and Eocene plutonic rocks are present in the immediate area, indicating a complex geologic history and two potential mineralization ages. To determine the source- and thus the age- of gold mineralization I use chemical analyses of (>300) igneous rocks, X-ray Fluorescence (XRF) determination of (>200) Bi/Au, Cu/Au, and Cu/Pb ratios throughout the ore zones, Fe:Mg ratios of skarn clinopyroxenes determined by EMP analyses, calc-silicate mineral zoning, surface and underground mapping, and Ar^{40}/Ar^{39} dating of Au-intergrown skarn hornblende. Chemical classification of igneous rocks distinguishes seven potential source intrusions in the immediate Buckhorn area. Metal zoning (Bi/Au, Cu/Au, and Cu/Pb) throughout the entire deposit showcases the lack of relationship between the Gold Bowl and the Southwest Zone, allowing for multiple source and remobilization interpretations. However, the techniques employed all indicate an east to west ore fluid migration across the Southwest Zone and reveal a newly-unrecognized zoned Jurassic pluton SE and below the deposit as the source.

Table of Contents

Page

List of Figures

Page

List of Tables

Page

List of Appendices

Page

Acknowledgements

I began working on the Buckhorn deposit in the summer of 2008 as a geology technician: hauling core boxes, taking pictures, collecting soil samples, and curiously staring at the pretty green and red rocks. In the summers of 2009 and 2010, I returned in the capacity of a geologist and spent both summers logging core and studying the garnet-pyroxene-sulfide rich rocks with the exploration team. I finished a Bachelor's degree in geology in 2009, and a Bachelor's degree in environmental science in 2010. During the 2010 school year, I began the search for a graduate school. Thank you, Dr. John Buchanan, for the best advice possible concerning finding a graduate school. He told me "find an advisor you like, not a school. It doesn't matter where you go, as long as you have a good advisor to lead you." He was right.

In the summer of 2010, I moved to Fairbanks, Alaska to attend the University of Alaska and work on a MSc. degree on the Buckhorn deposit. None of this would have been possible without the financial and logistical support that I received from Kinross-Kettle River Operations. I formally thank Peter Cooper and the exploration department at Kettle River, for painstakingly ensuring that I received the funding necessary for undertaking this degree. On an informal note, I thank both Rod Willard and Josh Ellis for... everything: for setting up this funding, for being so supportive, and for always being around to have a beer and bat ideas back and forth.

In wading through the guts of the project: collecting, preparing, and analyzing an absolutely obscene number of samples, I have several people I would like to thank. A huge 'thanks' to Dr. Ken Severin and the AIL (Advanced Instrumentation Laboratory) for an exceptional amount of help in developing microprobe and XRF routines tailored to what I needed most. In collecting samples from historic drill core, underground exposures, and surface outcrop, I thank the exploration 'techs.' Thanks to Chad Flom, Colton Halback, Justin Wilson, and Chip Sykes for keeping sample collection fun with dirty jokes, water balloon fights, and a running commentary of ridiculous-ness. I miss you guys already. A ton of thanks to Sam Murphy for being suckered into making innumerable pressed pellets and cutting thin section billets, for always being supportive, and for understanding the mercurial moods from too many consecutive all-nighters.

I also thank my committee: Dr. Ken Severin, Dr. Mary Keskinen, Dr. Robert Hickey, and Dr. Rainer Newberry, for help developing my project proposal and providing valuable insight and ideas, and keeping things interesting. Thanks to Robert Hickey for the loan of his Gold Bowl thin sections and for making the time to undertake a couple of day- long underground mapping expeditions.

On a personal note, thanks to the creator and many distributors of Redbull for many well-timed caffeinated rescues. Thanks to my family for being supportive, entertainingly unusual, often inappropriate, and awesome. Thanks to my little brother, George, for not killing me for leaving you with it all. I love you! Thanks to my colleagues, friends, and partners-in-crime: Jill Kooistra and Bonnie Broman, this roller-

coaster ride would not have been the same without you to struggle through with and enjoy with. Thank you for all the nights spent in the collaborative homework (and wine drinking) effort and for all the fun we have had reminding ourselves that life goes on outside of our office walls. I am grateful that our chosen careers guarantee we will always have the opportunity to share a drink and a story. Thank you for always being around to commiserate with and for all ideas, advice, help, and adventures we have shared and will share in the future - you two are unsurpassable.

Finally, and most importantly- all my thanks to my advisor, professor, and friend, Dr. Rainer Newberry. You have made this an unparallelable experience, and I am so grateful to have worked with you. Thank you, for making not one, not two, but three trips to Buckhorn (at the risk of life and limb); for never letting any of us feel lost or abandoned; and for always being right alongside for the long nights spent on the microprobe and microscope searching for tiny, itty-bitty gold grains. The shrine is under construction, and you can rest assured that whether it is due to the number of believers or the devotion of one believer- you'll always be able to a produce a good lightning strike. You made this project fun, and I really appreciate you and everything you have done. You are truly the best!

Thanks!

1. Introduction

1.1 Introductory statement

This thesis concerns the Buckhorn Gold Skarn deposit in NE Washington State (Fig. 1.1). Skarn deposits are one of the most intriguing types of deposits due to their highly variable ore elements, high grades, and poorly understood nature. Even the meaning of the word 'skarn' is ambiguous. It is derived from the Medieval Swedish word meaning '(bodily) waste' and referred to the calc-silicate gangue present in some Swedish magnetite deposits. It is generally considered (e.g., AGI Glossary of Geology, Klaus et al., 2011) "calcium-bearing silicates derived from nearly pure limestone and dolomite with the introduction of large amounts of Si, Al, Fe and Mg..."

Skarns derived from limestone are calcic; those from dolomite are magnesian. The two have different but relatively well-defined patterns of silicate and ore distribution (Meinert et al., 2005). Skarn deposits host a multitude of different ore elements, and skarns are generally classified by the predominant ore element. Major skarn types include Cu, Mo, W, Sn, Fe, and, Au. Each skarn type has somewhat different calc-silicate minerals and (or) mineral compositions and ore zoning patterns (e.g., Einaudi et al., 1981). However, there can be wide variations within a single 'type,' and this is particularly true of calcic gold skarns, such as Buckhorn. It is difficult to explore for and to exploit an ore deposit unless one knows something about its formation: the fluid deposition patterns, grade patterns, and ore controls.

Gold skarns make up a small percentage of all skarn deposits, but are of interest because they host some of the world's highest average gold grades. Fortitude, Nixon

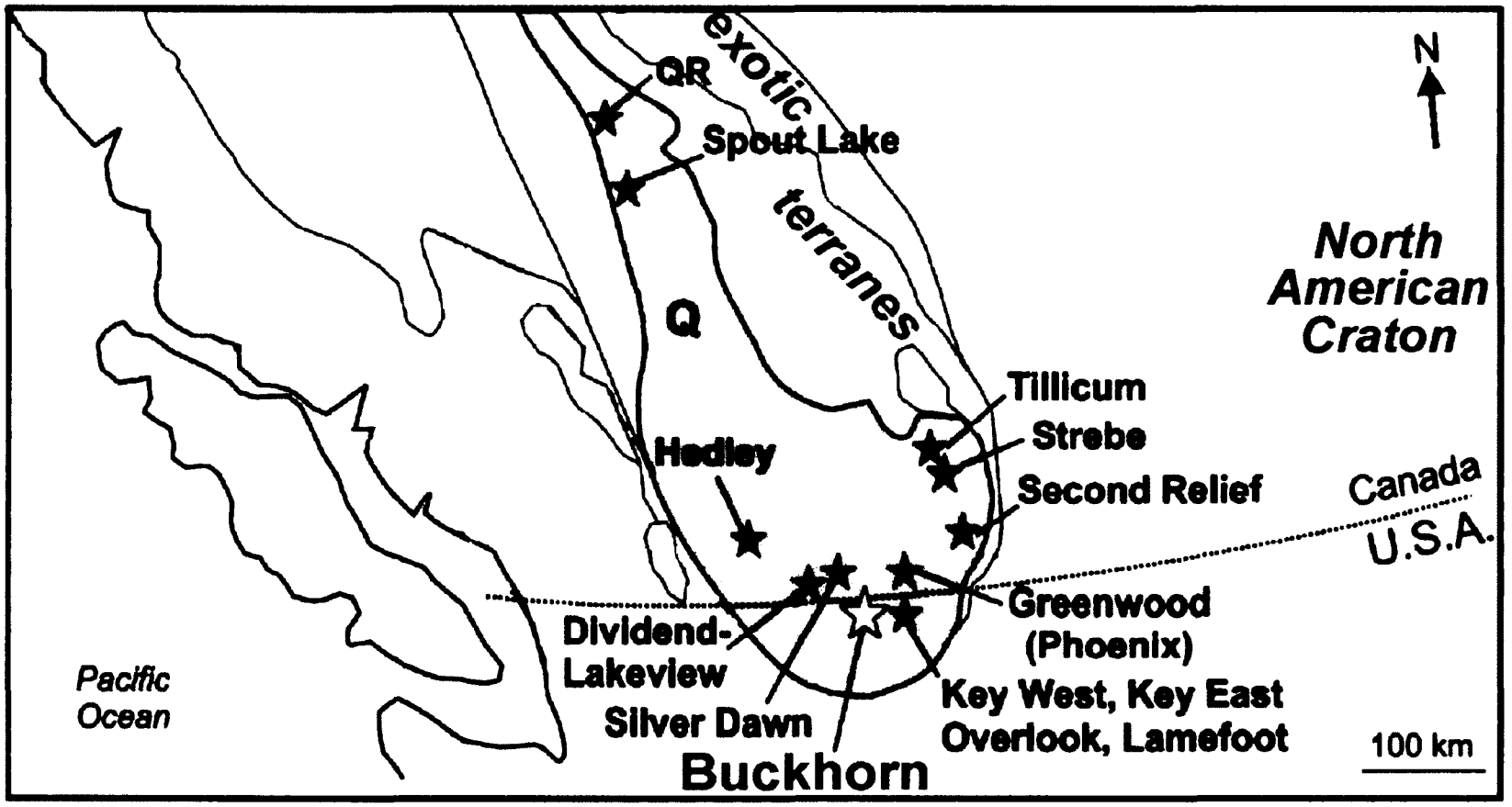

Figure 1.1. Location map of the Buckhorn deposit. Other Au-bearing skarns (such as the Hedley deposit) in the southern portion of the Quesnel terrane (Q, shaded area) are shown as well. Modified from Gaspar (2005).

Fork, Hedley, and Buckhorn are gold skarns found in Nevada, Alaska, British Columbia, and Washington, respectively. Besides the presence of gold there are limited similarities and none has been thoroughly studied. Some generalizations are possible: most gold skarns are calcic and are Fe-clinopyroxene-rich; gold grades are generally higher with distance from the intrusion; Bi- and Te- minerals are ubiquitously associated; and the spatially associated pluton displays a low oxidation state (Meinert et al., 2005).

The gold skarn at Fortitude (Nevada) is located near a granodiorite-hosted porphyry copper deposit (Myers and Meinert, 1991); for uncertain reasons the skarns which accompany most Cu porphyry deposits are instead Cu-rich and relatively Au-poor (Figs. 1.2 and 1.3). The skarn at Nixon Fork (Alaska) is present as vertical 'pipes,' instead of surrounding the nearby (quartz monzonite) pluton, and copper is an abundant by-product (Newberry et al., 2010). However, extensive weathering, which extends far below the surface, obscures the geology. Hedley (British Columbia, Canada) and Buckhorn (Washington) are both located within the Quesnel terrain, approximately 100 km (60 miles) apart (Fig. 1.1), and are associated with Jurassic plutons but display many differences. The host rock at Hedley is a Triassic calcareous siltstone, the spatially associated pluton is a gabbro, and the ore is arsenopyrite-rich and Cu-poor (Ettlinger et al., 1992). Hedley is one of the largest known gold skarns, but because it was mostly mined in the 1920's and 30's, the skarn was studied after most ore was gone. Gold ore at Hedley is hosted by scapolite-sulfide replaced clinopyroxene-rich skarn, distal to the pluton (Fig. 1.4), but adjacent to an intermediate composition dike. Ray and Dawson

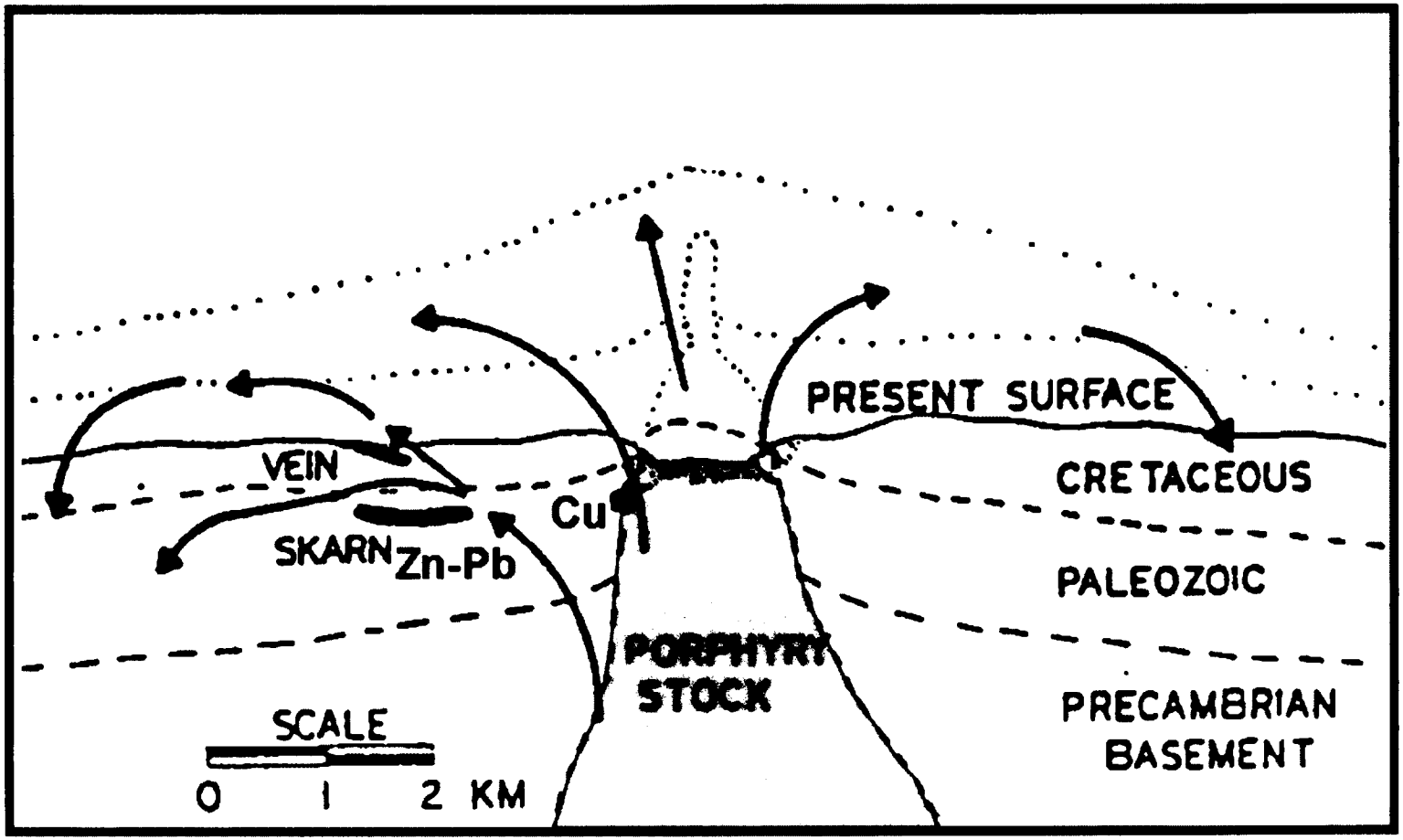

Figure 1.2. Cartoon portrayal of skarn in porphyry systems. Note the relationship between skarn and the intrusion present. Modified from Meinert 1997.

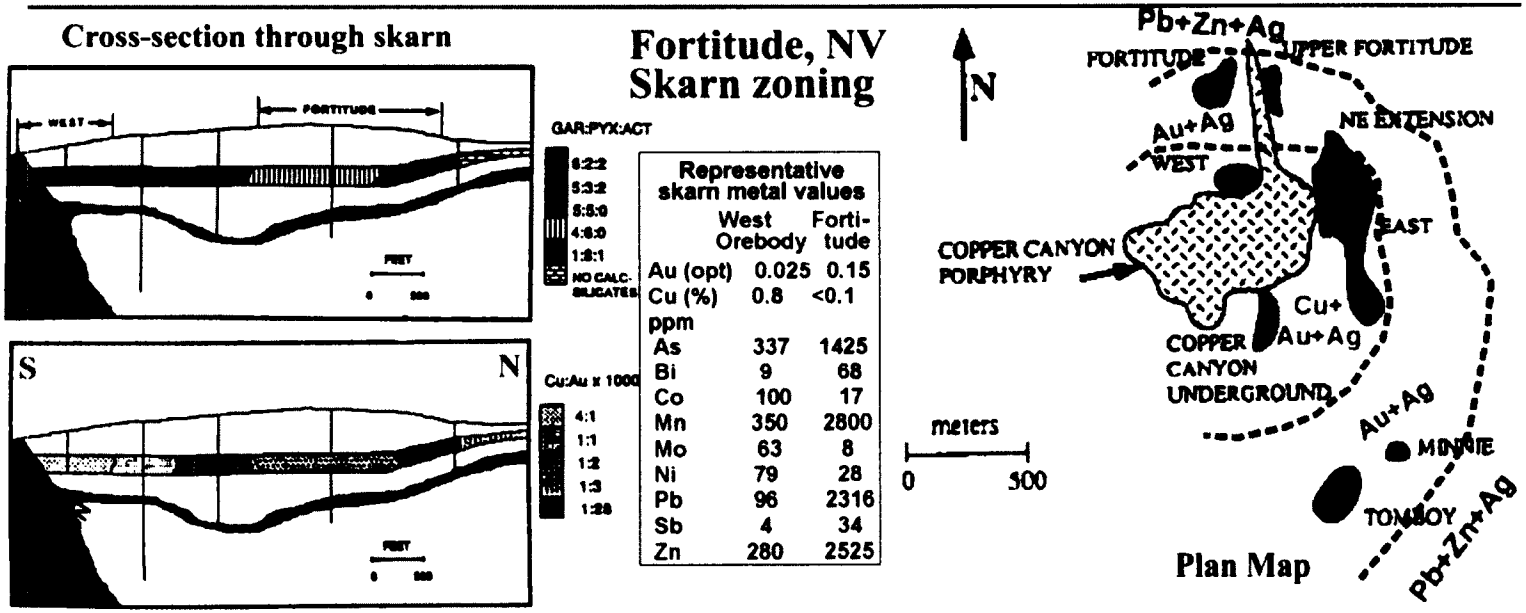

Figure 1.3. Silicate and metal zoning in the Fortitude deposit , NV. Fortitude is a Cu-Au skarn in Lander County, Nevada (40°55'N, -117°13'E). Map on far right shows the overall metal zoning; the cartoon cross-sections on the left show mineral and Cu/Au zoning. Box in the center contrasts metals present in skarn adjacent to the Copper Canyon pluton (West Orebody) to those present in the Fortitude skarn, 3,000 feet (.9 km) from the porphyry stock. Modified from Myers and Meinert (1991).

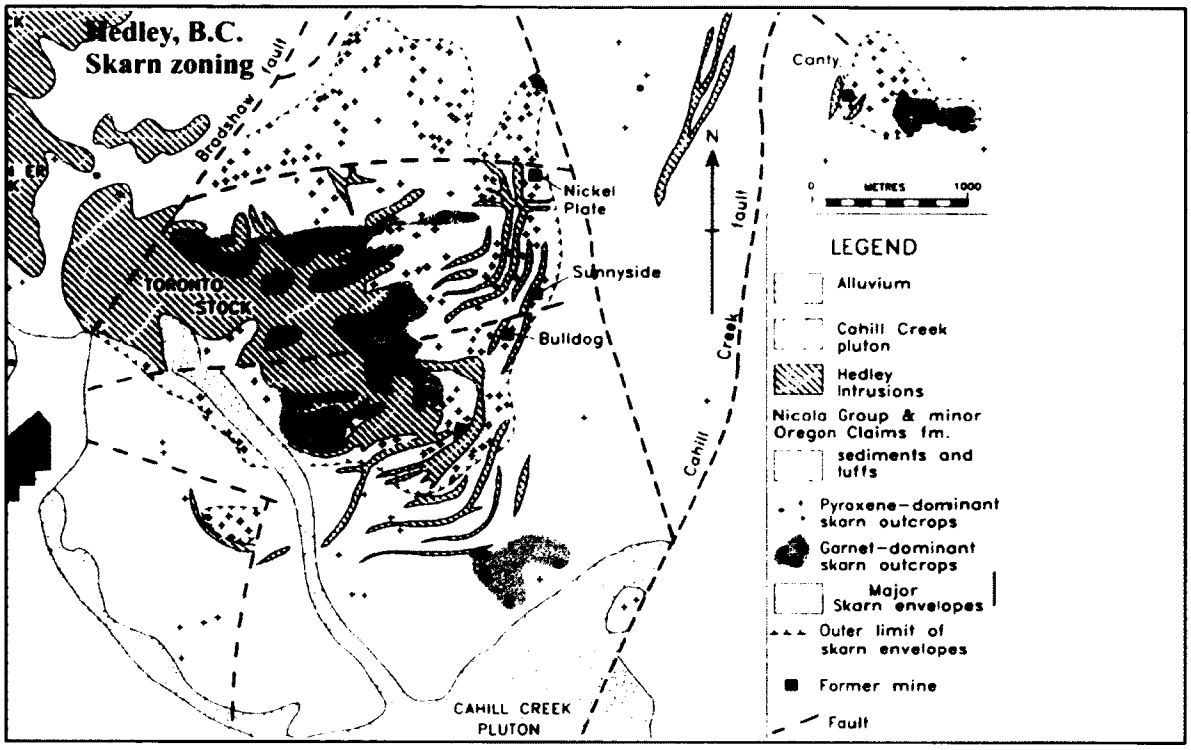

Figure 1.4. Silicate zoning in the Hedley skarn deposit. Pyroxene-rich skarn (green) occurs distal to plutonic bodies and contains the ore deposits. Garnet-rich skarn (brown) is barren. The Nickel Plate deposit is located at 49°22'N and 120°3'W. Modified from Ray et al. (1992).

(1994) ascribe the gold deposition at Hedley to introduction of non-igneous water some time after garnet-pyroxene skarn formation.

In sum, given the considerable variations between gold-rich skarns, the best way to explore for more Buckhorn-like gold skarns in northeast Washington is to better understand the Buckhorn skarn. The Hedley deposit is simply not a good model for exploration in the Buckhorn area.

1.2 Formation and evolution of skarn deposits

This section is synthesized from several different overviews of skarn deposits, and describes commonly observed features and patterns generally accepted to be characteristic of skarn deposits. The works referenced in this synopsis include: Atkinson and Einaudi (1978), Einaudi and Burt (1982), Einaudi et al. (1981), Meinert et al. (1980), Meinert (1983), Meinert (1992), Meinert (1997), Meinert et al. (2005), Newberry (1982), Newberry (1998), and Ray et al. (1990).

Most skarn deposits are considered the products of reactions between igneous-derived fluids that move outward and upward into carbonate-rich host rocks. However, skarn formation is more complicated, as calc-silicate minerals are also formed during contact metamorphism of mixed calcareous rocks, and these minerals are partly destroyed during later circulation of lower-temperature fluids. The suite of rocks and minerals--including massive sulfide or oxide replacement of marble--created in this fashion comprises a deposit type described as a 'skarn deposit.'

Skarn deposits are generally modeled as forming in three overlapping stages: metamorphism, prograde skarn, and retrograde skarn. Metamorphism occurs as the pluton heats the host rock and perhaps drives off water due to dehydration reactions in the non-carbonate rocks. No components (besides water) are added at this time, but recrystallization of components already present is common. This recrystallization creates "hornfels," which is generally recognizable by its fine-grained nature, pale colors, and partly preserved sedimentary layering or banding. Types of homfels are generally

classified by color, reflecting their mineralogy. Pelitic hornfels from metamorphism of pelitic rocks, for example, is common as a dark biotite and (or) quartz-rich hornfels. In contrast, calc-silicate hornfels forms from metamorphism of impure carbonate rock. The minerals made in this fashion (through isochemical metamorphism) are commonly the same minerals which are created metasomatically during prograde skarn formation. A major distinction between metamorphically formed minerals and minerals formed during prograde skarn formation is composition; sedimentary rocks contain abundant aluminum and magnesium but lesser iron, and metamorphically formed minerals will retain that distinctive chemistry. Thus 'metamorphic' calc-silicates are generally iron-poor. Formation of hornfels (and the recrystallization of limestone to marble) may be of regional extent, with the metamorphic aureole potentially extending kilometers from the responsible plutons.

1.2.1 Prograde skarn formation

As igneous-derived fluids—rich in Si, Al, Fe, Mg, and other elements—percolate into carbonate rocks, they react with the rock, dissolving calcite and precipitating calc-silicate minerals. In carbonate rocks near the fluid source, the stable mineral assemblage is dominated by garnet. Garnet is an abundant mineral because it can have a variety of different compositions, reflecting differences in local conditions (e.g. oxidation state) and it is typically an Fe-rich phase. The "garnet zone" changes outward into a pyroxene-rich zone (Fig. 1.3 and 1.4). Beyond the pyroxene zone, there may or may not be an 'outer zone' containing Ca-rich minerals (e.g. idocrase or wollastonite) adjacent to marble. The outer zone (if present) is in contact with marble: recrystallized (and potentially bleached)

but with no added components. This change in the prograde mineral assemblage (garnet-rich to pyroxene-rich to marble) can be used to infer the fluid source.

Metasomatic changes also take place in igneous rocks from the diffusion of calcium ions from the carbonate rocks. Rocks formed from such chemical changes are called 'endoskarn.' The amount and type of endoskarn alteration varies between skarns, but generally includes the conversion of potassium feldspar to plagioclase and the conversion of amphibole to pyroxene. Endoskarn can also include the complete conversion of igneous rock into an ambiguous garnet-rich assemblage. Endoskarn can occur in both the source pluton and other igneous rocks, especially those interlayered with carbonate rock, such as dikes, sills, and volcanic flows.

At temperatures greater than about 350°-400°C (depending on pressure and concentration of CO_2 in the fluid phase), the predominant minerals formed in carbonate rocks are calcic garnet and calcic clinopyroxene. The solubility of many ore metals in hydrothermal solution is pH-dependent, with higher pH causing a decrease in solubility. As increasing pH results from dissolving carbonate, a variety of metals also precipitate, typically as sulfide or oxide minerals, but also as native metals (e.g. gold). Such reactions are especially prolific at or near the most carbonate-rich zone, frequently referred to as the 'marble front.'

During skarn growth, garnet invariably replaces pyroxene, which either replaces even more Ca-rich minerals (such as wollastonite or idocrase) or directly replaces calcite. Hence, garnet-rich skarn is closer to the fluid source and is generally metal-poor relative to pyroxene-rich skarn. Both the garnet-and pyroxene-rich zones grow with time,

producing an increasingly larger zoned skarn. Such zoning is present at scales ranging from district (Hedley, Fig. 1.4) to hand-specimen. At the Fortitude gold skarn, for example (Fig. 1.3), the mineralogy progressively changes from garnet-rich to pyroxene-rich and the Cu: Au ratio changes from high to low with increasing distance from the source porphyry copper pluton. Other metals that increase with distance include Bi, As, Pb, and Zn; Mo, Ni, and Co decrease with increasing distance (Fig. 1.3).

Clinopyroxene preferentially incorporates Mg^{2+} (due to its smaller size) relative to the larger Fe^{2+} and Mn^{2+} ions. As Mg^{2+} becomes depleted from the solution, Fe^{2+} and Mn^{2+} become enriched. Fluids that have traveled farther and have precipitated more pyroxene become increasingly depleted in Mg^{2+}. Thus, skarn clinopyroxenes generally become increasingly iron-rich with distance from the fluid source (Meinert, 1992). Consequently, compositions of clinopyroxene from samples in a skarn also provide information about the directions of fluid flow.

1.2.2 Retrograde skarn formation and destruction

At temperatures below approximately 350-400°C (depending on pressure, oxidation state, and concentration CO_2 in the fluid) anhydrous calc-silicate minerals become unstable with respect to hydrous calc-silicate minerals and hydrous assemblages + calcite. If lower-temperature water passes through the previously-formed skarn, it will cause such hydration and carbonation reactions—but such will <u>not</u> happen unless lower-temperature fluids ARE circulated. This final stage is called 'retrograde,' because many of the reactions involve adding H_2O and (or) CO_2 back into minerals. The water circulating at these temperatures is unlikely to be of magmatic origin, but the heat from

the pluton is sufficient to cause circulation (and heating) of groundwater. The retrograde phase does not necessarily introduce new components but clearly causes a re-arrangement of the components already present: breaking down the anhydrous minerals to create hydrous calc-silicates. Two typical reactions are the conversion of Ca pyroxene to Ca amphibole + quartz + calcite ± an Fe-phase (e.g., pyrite, pyrrhotite, magnetite or hematite) and conversion of garnet to epidote + quartz + calcite ± an Fe-phase. At lower temperatures, iron-rich garnet and pyroxene simply break down into quartz + calcite + Fe mineral without any calc-silicate.

A variation on this pattern apparently happens when lower-temperature fluids encounter marble. In such cases, a hydrosilicate assemblage can directly form, without any preliminary 'prograde' minerals, as seen at some tungsten skarns (Newberry, 1998). Biotite is likely to form in this manner, but amphibole and epidote do so as well. Magnetite and sulfide precipitation can accompany this direct replacement of carbonate minerals by hydrous silicates. Despite the lower temperature of formation, calling this 'retrograde' is inappropriate, as no prograde minerals are being altered. Other terms, such as 'hydrosilicate' or 'low temperature' more accurately reflect the reaction and have been employed.

1.3 Previous work

1.3.1 General setting and characteristics

The Buckhorn Mountain area was unsuccessfully explored in the 1960s to late 1980s, primarily because attention was focused on the 'skarn' located adjacent to the Buckhorn

pluton (Fig. 1.5). Working to the south of the historic magnetite-rich ores, Crown Resources discovered gold skarn in 1988 in the Gold Bowl (GB, Fig. 1.5) area and eventually the blind Southwest Zone (SWZ, Fig. 1.5). Mining operations began in 2008 and are anticipated to finish in 2015 unless new resources are discovered. Regional mineral exploration around Buckhorn Mountain has unearthed a series of epithermal deposits associated with Early Tertiary extension and volcanism (Curlew and Republic Districts), other small skarn deposits (Key West, Key East, and Overlook, Fig. 1.1), and a possible metamorphosed volcanogenic massive sulfide deposit (Lamefoot, Fig. 1.1).

The stratigraphy of the immediate Buckhorn area varies widely over short distances (Cheney et al., 1994) and is complicated by regional thrusting, contact metamorphism, generally poor exposures, and limited age control. An example: the basaltic rocks overlying the skarn-hosting sedimentary package are considered Jurassic and correlated with one volcanic unit in Canada by some workers; they are considered Triassic and correlated with a different volcanic unit by others. To add to the confusion, most refer to the volcanic rocks as 'andesite' (e.g., Ray, 2009) despite their basaltic chemical compositions (Gaspar, 2005). Most workers consider the sedimentary rocks late Paleozoic.

Historically, the Buckhorn deposit has been broken into two predominant ore bodies, the "Gold Bowl" and the "Southwest Zone" (Fig. 1.5). Additionally, a small skarn prospect ("Mike's Skarn") was discovered west of the Gold Bowl in 2009 (Fig. 1.5). The Gold Bowl is locally exposed on the surface, and is near a large granodioritic pluton (Buckhorn Pluton, Fig. 1.6). It is reported to consist of mostly epidote-garnet

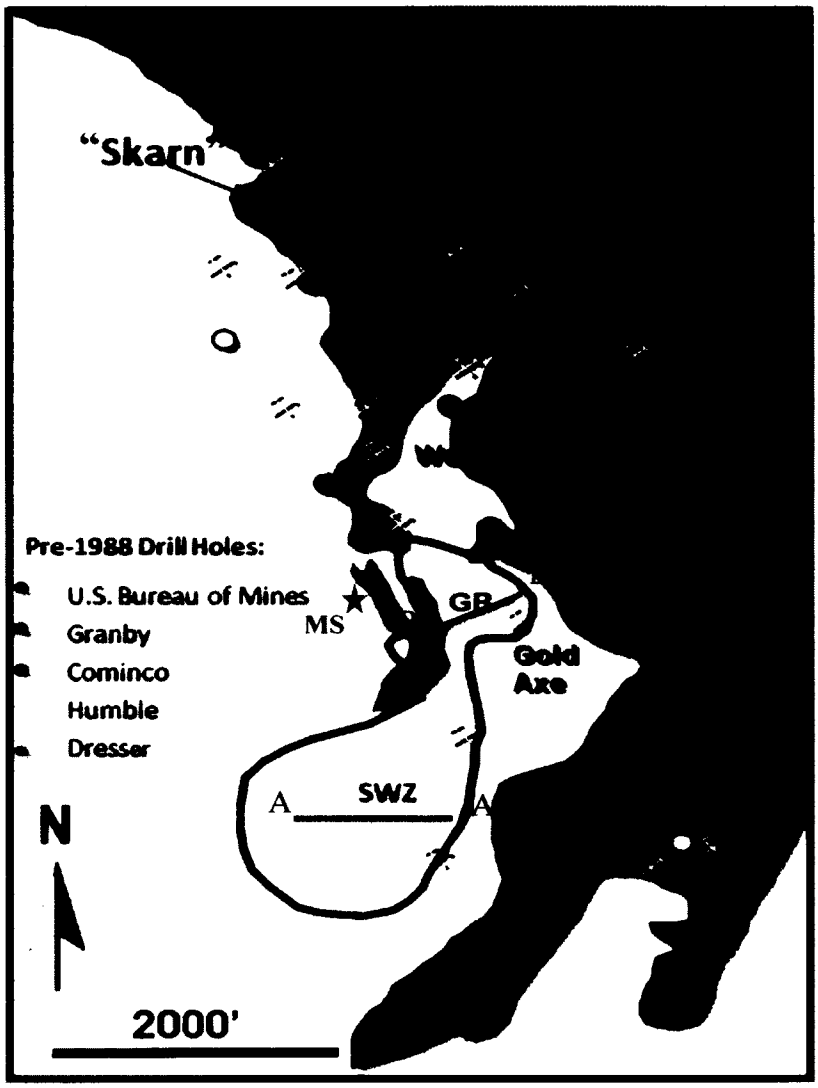

Figure 1.5. Map showing locations of historic workings near Buckhorn. The Roosevelt Mine (shown above) is located at 118°58'33"N and 48°56'37"W. Drilling shown is pre-1988. 'Skarn' as identified on the map is actually a mixture of endoskarn, calc-silicate hornfels, and minor exoskarn. GB = Gold Bowl. SWZ = Southwest Zone. MS (red star) = Mike's Skarn. Picks = historic prospect locations. Black lines represent cross section locations for Figures 1.8 and 1.9. Modified from Cooper (writ. comm., 2010).

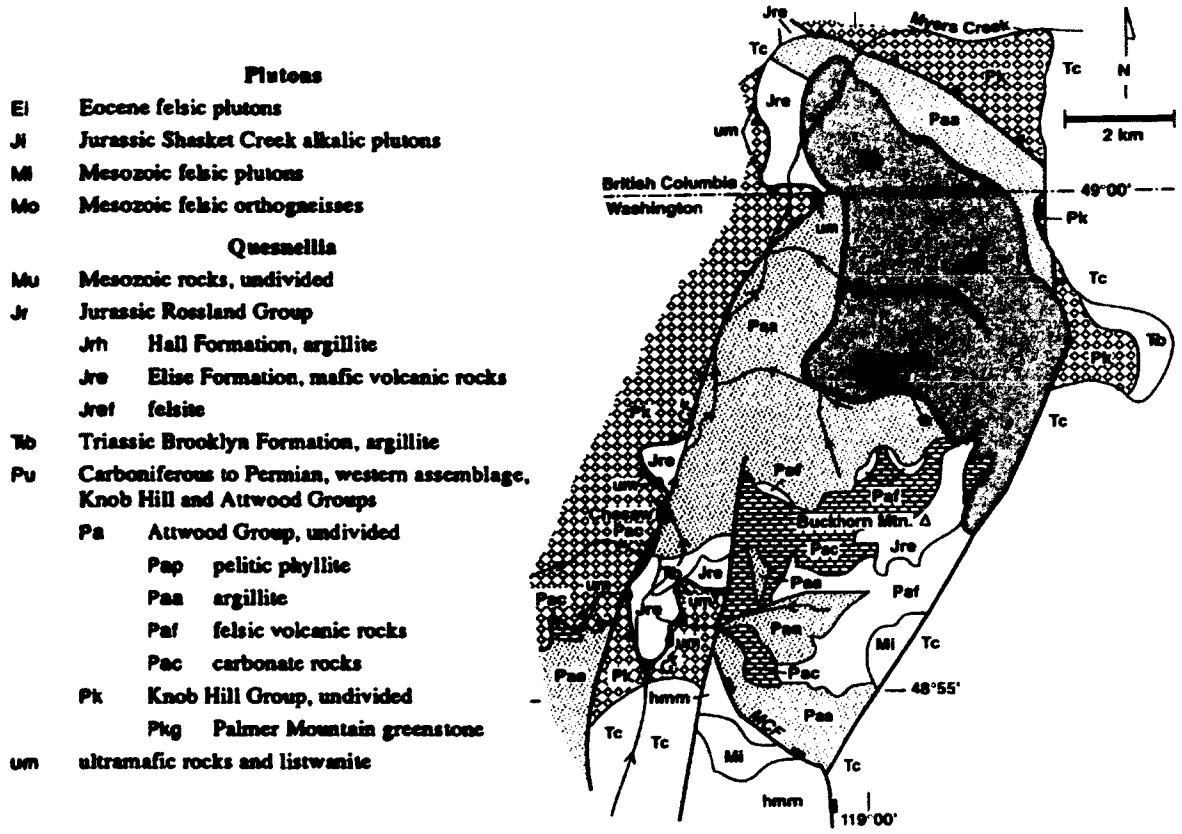

Figure 1.6. Geologic map of the Buckhorn area. The extent of the Buckhorn Pluton is shown above in pink and marked "Mi" in the legend. Tc = Toroda Creek Graben. Modified from Cheney et al. (1994).

dominated endoskarn and less altered igneous rocks with erratic grade distributions (Hickey, 1992). The Southwest Zone is a 'blind' deposit which was discovered in 1991. It is said to consist primarily of pyroxene-rich skarn (Gaspar, 2005) hosted by marble. The host rock stratigraphy in the Southwest Zone is dominated by a thick, relatively pure carbonate sequence underlain by meta-pelitic sediments and overlain by meta-basalt (Fig. 1.7). The carbonate package in the Southwest Zone is notably thicker than is reported anywhere else in the area. The contacts between major units may be structural (McMillen, 1979) and are certainly deformed. Barren calc-silicate rocks are intermittently present throughout the upper part of the section; ore-bearing skarn is reported to be restricted to the Buckhorn Marble (Gaspar, 2005).

A typical cross-section through the Southwest Zone (Fig. 1.8) shows a large body of marble that becomes thinner and increasingly replaced by 'skarn' to the east sandwiched between volcanic rocks above and metaclastic rocks below. The ore body remains of approximately constant thickness even as the skarn thickness drastically increases. That is, the volume of barren 'skarn' increases towards the east. The ore body is commonly in the lower part of the skarn adjacent to the marble ('marble front') but not invariably so (Fig. 1.8). Grade within the Southwest Zone increases from east to west (Cooper, writ. comm., 2010) and is variable within the skarn package. Notably, quartz porphyry dikes cut across all rock types and do not appear to be the locus of skarn formation (Fig. 1.8; Ray, 2009). The thinning of the marble to the east is variably interpreted as either a stratigraphic pinch-out or a large, recumbent isoclinal fold that was overthrust by the volcanic rocks. The latter is compatible with regional contractional

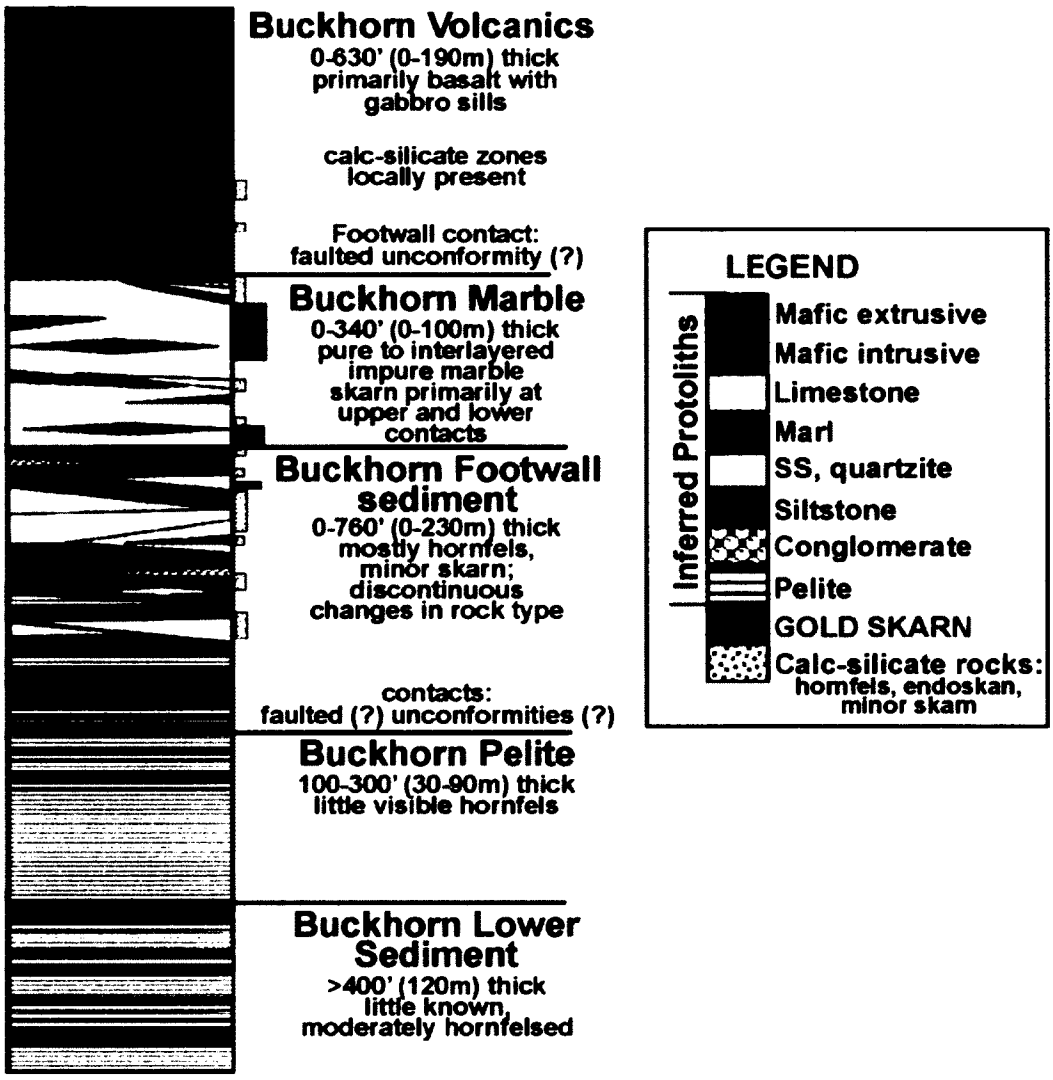

Figure 1.7. Simplified schematic stratigraphy at the Southwest Zone. Modified from Doler (writ. comm, 2009).

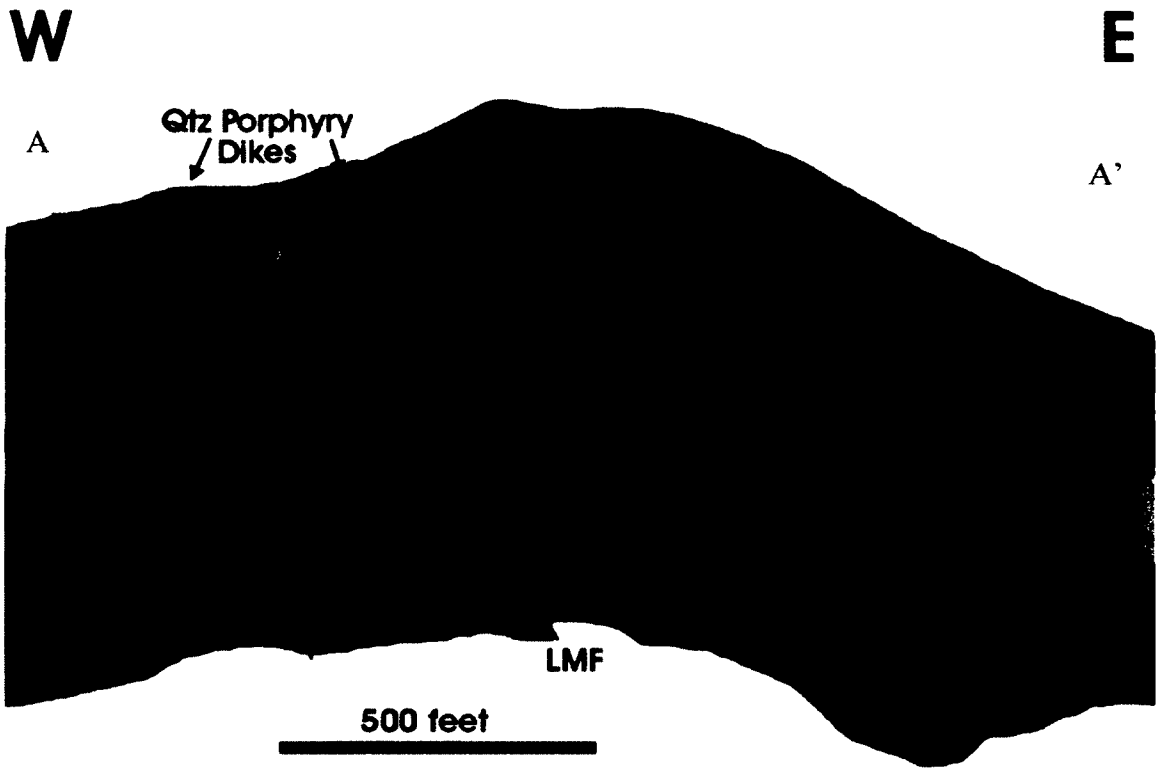

Figure 1.8. Cartoon cross section of the Southwest Zone. Location of the section is shown on Figure 1.5. Modified from K. McCaughney (writ. comm., 2011).

tectonics and with locally seen foliation and deformation, especially in the overlying volcanic rocks (McMillen, 1979).

The Gold Bowl area is considerably more complex as there is little (if any) marble present, no stratigraphic markers, and a series of ore bodies defined by drilling that are irregular in size and shape (Fig. 1.9). Based on limited data available early in the exploration history, Hickey (1992) described the Gold Bowl as a zoned deposit, with "proximal garnet-magnetite-sulfide, intermediate garnet-pyroxene-epidote-sulfide, and distal pyroxene and hornfels assemblages."

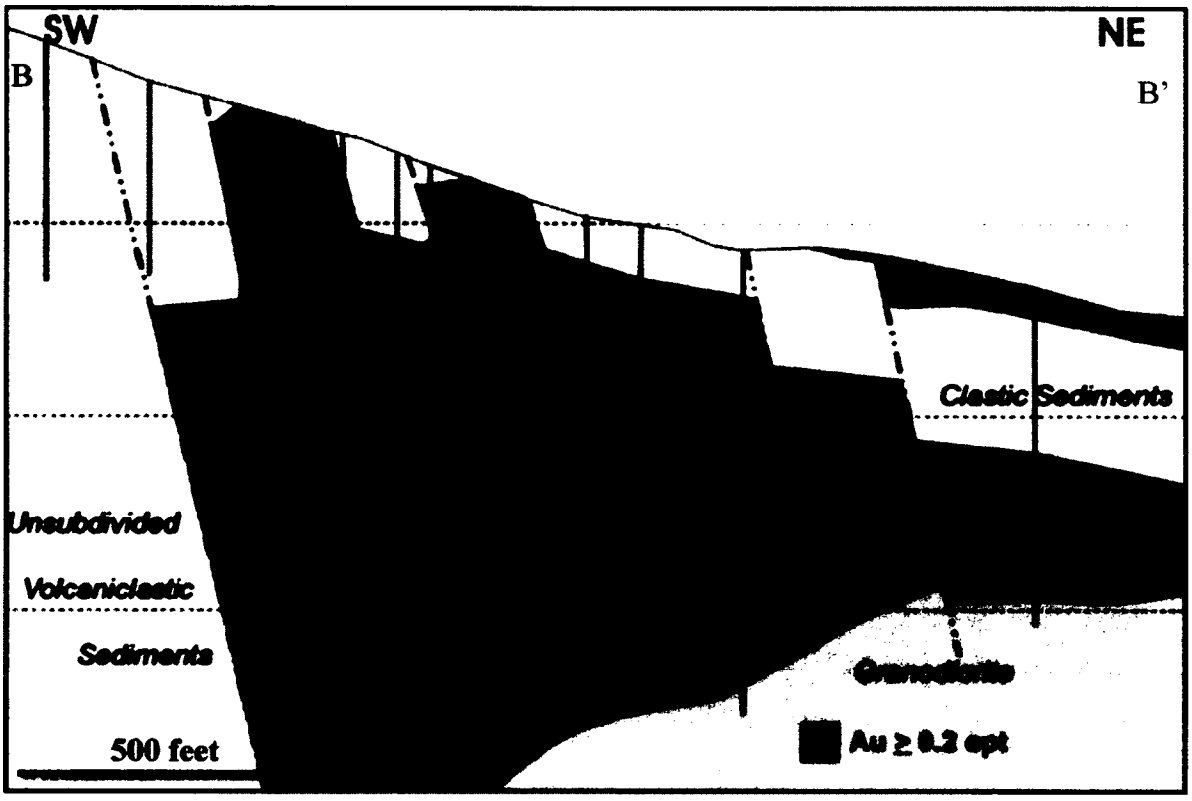

Figure 1.9. Cartoon cross section of the Gold Bowl. The section highlights the seemingly erratic pockets of minable grade skarn. Modified from Cooper (writ. comm., 2010). Location shown on Figure 1.5.

Finally, north of the Gold Bowl enormous magnetite bodies occur; they are collectively grouped and referred to as the 'the magnetic mine' (Fig. 1.5). The Magnetic Mine was mined in the 1940s for iron ore and is now exposed as a cliff face of variably weathered massive magnetite surrounded by scattered smaller workings. The magnetite locally contains remnant garnet skarn fragments but otherwise appears to be only magnetite with minor chalcopyrite.

1.3.2 Mineralization

Similar to other gold skarns (Ray, 2006), the gold at Buckhorn is tiny (microns in size) and associated with bismuth and tellurium minerals (Gaspar, 2005). Unlike Hedley, scapolite has not been reported. Assay data from two drill holes provided by Hickey (1990) indicates that the Gold Bowl mineralization is anomalous in Bi, Cu, Pb, Zn, As, and Sb; the latter three rarely concentrate above a few hundred ppm. Hickey (1992) also reports a strong Au-Bi correlation at Gold Bowl. His data indicate a Bi:Au ratio of approximately 60:1, which is higher than those typically seen with plutonic-related gold deposits (5-20:1, Flanigan et al., 2000), but not excessively so.

Gaspar (2005) presents the most complete dataset on the Southwest Zone available, but he made no attempt to relate his petrographic observations or microprobe analyses to a geologic context. Gaspar (2005) provides several hundred microprobe analyses of garnet (grossular to andradite), pyroxene (diopside to hedenbergite), amphibole (actinolite to hornblende), and epidote-clinozoisite with no spatial distribution of the minerals or the compositions. Data from Gaspar (2005) shows that Southwest Zone gold (3 grains) is silver-poor and that sulfide minerals present in the deposit include

arsenopyrite, chalcopyrite, sphalerite, pyrrhotite, and galena. Gaspar (2005) notes that Au is variably present with Bi^{o}. However, exactly where the gold is located in the skarn and its distribution and timing relative to host minerals and to a potential causative pluton have not been described.

1.3.3 Igneous rocks

The Buckhorn pluton is, by far, the most extensively exposed body in the Buckhorn area. It covers an area approximately 8 km by 5 km and stretches into Canada (Fig. 1.6). The pluton has a general NW-SE trend and is abruptly cut off by the NNE-trending Toroda Creek Graben (Fig. 1.6) Pearson (1967) and Hickey (1992) noted a more mafic marginal phase present on its southwestern side.

Gaspar (2005) showed that the simple concept of a single Buckhorn pluton (e.g. Fig. 1.6) did not describe the variations in plutonic rocks of the area. Based on LA-ICP-MS U-Pb dating of zircons, Gaspar (2005) identified 3 different Jurassic igneous bodies (Buckhorn pluton, granodiorite dikes, and quartz porphyry dikes) and two different Eocene stocks (Roosevelt Granodiorite and Pink Granite) in the immediate Buckhorn area (Fig. 1.10). In addition, undated 'andesitic' dikes cut across much of the area and are of presumed Tertiary age (Fig. 1.11). Further, the Mesozoic basaltic rocks above the sedimentary package are almost certainly fed by gabbroic bodies—these have been identified in regional mapping. The Buckhorn pluton is itself zoned, with a mafic and finer-grained outer portion (Pearson, 1967; Hickey, 1992). Finally, based on mapping in the Gold Bowl area, Ray (2009) suggested an 'early' diorite, distinct from and earlier than the marginal diorite of the Buckhorn pluton.

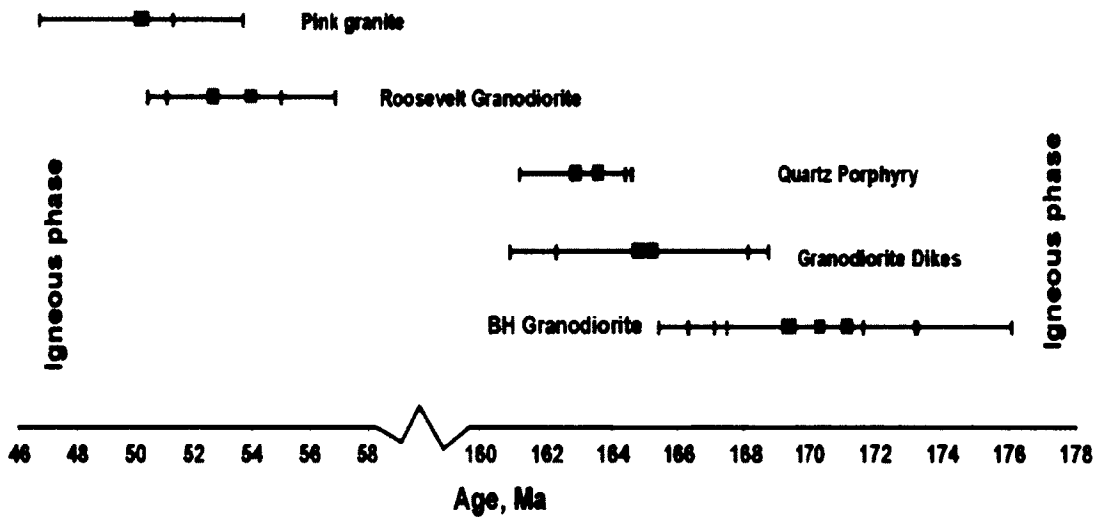

Figure 1.10. U-Pb ages reported for Buckhorn area igneous rocks. Error bars are 1 sigma age uncertainties. Boxes represent ages derived from individual samples. Graph is based on data reported in Gaspar (2005).

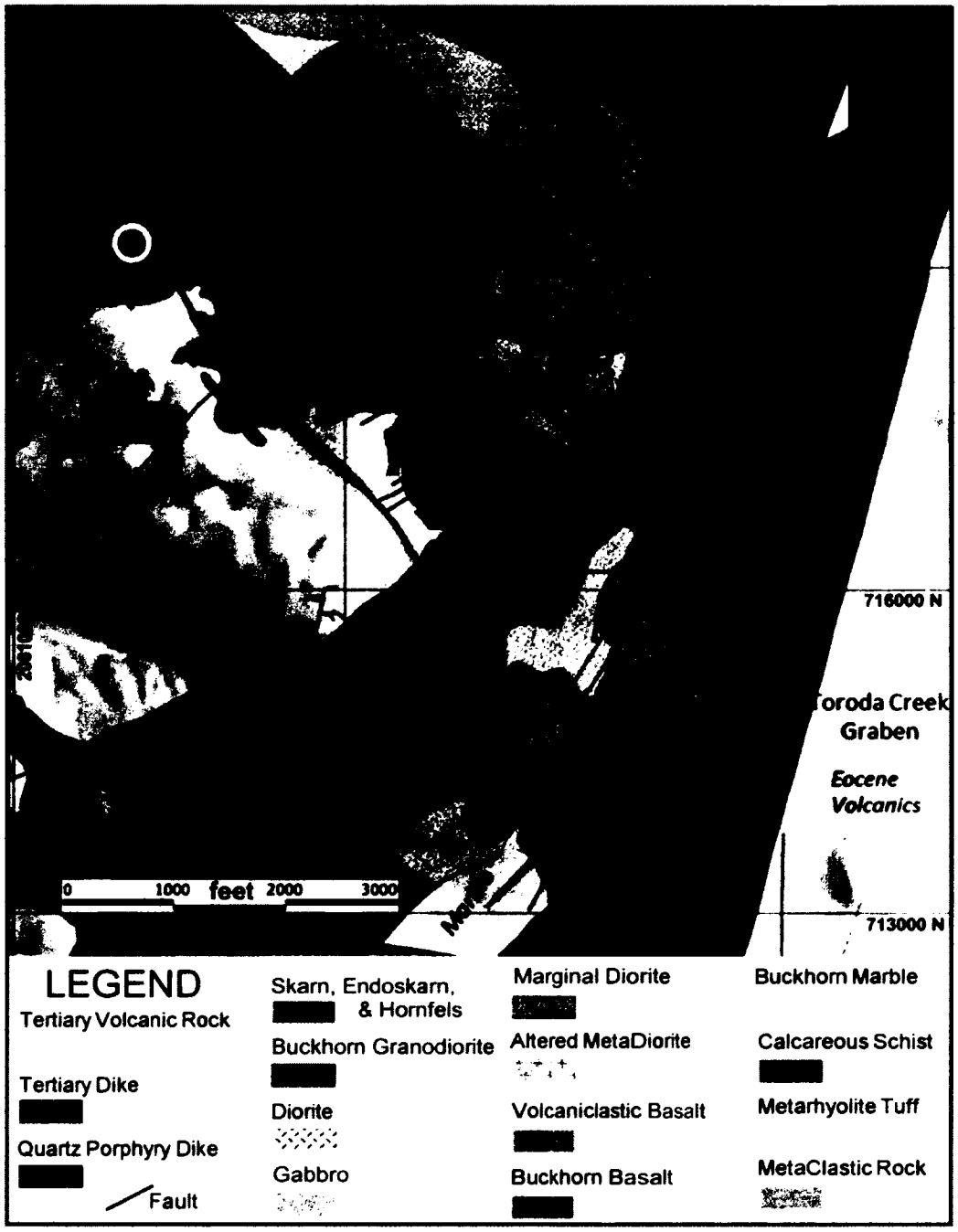

Figure 1.11. General geology map of the Buckhorn area. Locations of the three main skarn deposits are marked as follows: GB= Gold Bowl, SWZ= Southwest Zone, MS= Mike's Skarn. Modified from Ellis (writ. comm., 2011).

Thus, previous workers have identified at least seven different intrusive phases, any or all of which could be confused with each other and associated with skarn and (or) Au deposition. Core logging at the Buckhorn deposit, however, has codes for fourteen different plutonic igneous options (Table 1.1), and eight more for volcanic rocks, allowing for abundant categorical overlaps and suggesting far more intrusions are present than those broken out by Gaspar (2005).

Table 1.1.- Intrusive Lithology Codes at Buckhorn Mine.

40	Intrusive Lithology Codes	
	41	Granodiorite
	411	Granodiorite Dike
	42	Diorite
	421	Marginal (Border) Diorite
	422	"Early " Diorite
	43	Monzonite
	44	Feldspar Porphyry
	45	Biotite Porphyry
	46	Hornblende Porphyry
	47	Siliceous ("rhyolite") Quartz Porphyry (QP)
	471	Aphanitic no mafic QP dike
	472	Phaneritic, Bio-Hbled QP equivalent
	48	Qtz Monzonite/Qtz Diorite
	49	Andesite Prophyry

The presence of both Jurassic and Eocene intrusions combined with the numerous early Eocene epithermal systems nearby have generated debate on the age and origins of the gold mineralization at Buckhorn. Gaspar (2005), for example, proposed that the Southwest Zone was caused by the Eocene Roosevelt granodiorite, a unit he identified near the Roosevelt workings (Fig. 1.5). Various workers have proposed that both skarn

and mineralization are Jurassic, that the skarn and the mineralization are Eocene, and that the skarn is Jurassic and barren while the mineralization is Eocene and overprints the skarn.

1.4 Thesis objectives

Although considerable information is available on the Buckhorn area, most of the details necessary for a full understanding of the skarns are still missing. My goals were to:

1) Use feldspar staining and obtain hand-held X-Ray Fluorescence (XRF) data and quantitative XRF analyses on the least altered igneous rocks from the region to sort out the various igneous bodies in the Buckhorn area.

2) Use petrographic, X-Ray Diffraction (XRD) and XRF techniques to better categorize the skarn and host rocks at Buckhorn.

3) Determine the age, origin, relative timing, and metal associations relative to gold deposition.

4) Use mineral, mineral composition, and elemental zoning to determine the likely source of ore fluids and the direction towards the causative pluton(s), and

5) Summarize recognizable patterns beneficial to further exploration.

Because the Southwest Zone is described as the most simple of the skarns in the area (uniform marble host) and because I have logged many more drill holes from the Southwest Zone (2009-2011) than from other parts of Buckhorn, I focused this study on the Southwest Zone. However, to give the study more general value and to tie into the

Gold Bowl work of Hickey (1992), I also provide some data for the Gold Bowl area and further north.

1.5 Methods

Aside from standard petrographic, core logging, mapping, and XRD techniques, my principal research tools are the Electron Microprobe (EMP) and X-Ray Fluorescence (XRF) Analyzer at the Advanced Instrumentation Laboratory of UAF. Quantitative EMP analyses were performed on a Cameca SX-50 using wavelength-dispersive techniques (WDS). Semi-quantitative EMP analyses were performed by energy dispersive techniques (EDS). Both types of EMP analyses were performed on carbon coated polished thin sections using specialized routines, detailed in Appendix A1, Tables A1 – A2. I also employed a Panalytical Axios WDS-XRF Analyzer on a 37mm analysis area of both polished rock slabs and pressed pellets; any specialized routines developed are described in Appendix A1, Tables A3 – A4.

I acquired quantitative microprobe analyses of pyroxenes using a specialized routine customized for skarn clinopyroxene. I analyzed for Fe, Mg, Mn, Si and Ca with 10 second peak and background counting times. I used beam conditions of 15 kV and 20nA with a 5 micron diameter beam. I employed natural, well-characterized minerals as both primary and secondary standards.

I used a different specialized routine to analyze gold grains; the routine quantitatively measured Au, Ag, and Hg in metals. Beam conditions were 15kV and 20nA with a 1 micron diameter beam to best analyze tiny gold grains. The pyroxene and

the gold routines were both evaluated for accuracy and precision using natural mineral secondary standards.

I developed an XRF analytical routine for metals in the Buckhorn skarn. I devised it to accurately analyze Cu, Ni, Zn, W, Pb, As, Sb, Mo, Ag, Bi, Te, and Au, with the assumptions that Fe, Bi, As, Pb and Cu were likely in large concentrations and the other elements at moderate to low concentrations. Inter-element interferences were important considerations. The routine was designed to measure trace elements in pulp samples which had been pressed into 37 mm pellets. Matrix corrections used the rhodium Compton peak method, as described in Potts (1987). Operating conditions were 60 kV and 66 mA, with individual element peak and background counting times of 10 to 260 seconds, depending on the element. Well-characterized artificial and natural standards pressed into 37 mm pellets were employed as primary and secondary standards.

I analyzed for major elements using the IQ+ routine common to PanAnlytical Axios XRF and employed well-characterized, internationally certified standard reference materials, pressed to 37 mm pellets, as secondary standards. Data gathered from this routine was utilized to calculate Cross, Iddings, Pirsson and Washington (CIPW) norms. I used a specialized routine developed specifically for measuring Rb, Sr, Y, Zr, and Nb on 37 mm pellets. This routine (described in Lough et al., 2012) used a 60 kV, 66 mA beam with peak and background counting times of 10-60 seconds, depending on the element

1.6 Notes on terminology:

Skarn has been defined as a "...metamorphic zone developed in the contact area around igneous intrusions when carbonate rocks are invaded and replaced with chemical elements that originate from the nearby igneous body. The typical rock of a skarn is hornfels..." (Evans, 1987). That is, most workers restrict the word to mean replaced carbonate rocks, and there is considerable confusion between skarn and hornfels-- the latter being simply metamorphic in origin, with no added constituents. Any definition of a rock which is based on its inferred origin is problematic, as no one *actually watched* the rock form. In fact, calc silicate rocks formed by regional metamorphism, by contact metamorphism, and by metasomatism (addition of components; the classic criterion for 'skarn' *per se*) are idealized distinctions that are commonly difficult to distinguish. Recognizing this problem, Meinert et al., (2005) defines skarn simply as a calc-silicate (typically calcic garnet and pyroxene) rock of any origins.

Why all this is more than mere semantics is: the variable metal grades present in skarn (broad sense of the word) deposits can often be ascribed to the barren character of the metamorphic calc-silicates as opposed to the ore-bearing metasomatic calc-silicates. This is further confused by the zoning of ores typically present in metasomatic skarn and by the fact that igneous rocks (especially calcic igneous rocks) can also be metasomatically converted to (usually) barren calc-silicates.

In this thesis I will refer to metamorphic 'skarn' as 'calc-silicate hornfels.' Other definitions necessary for this thesis include 'exoskarn' and 'endoskarn.' Endoskarn is

skarn which is formed in/from a non-carbonate host rock while exoskarn (or 'skarn') is skarn formed in/from a purely carbonate host rock, keeping in mind that distinction between these two skarn types is not always easy or possible.

2. Igneous Rocks

2.1 Introduction

One purpose of this thesis is to better understand the igneous rocks of the Buckhorn area, and determine which, if any, are associated with the skarn deposits. The difficulty of modeling the igneous rock distribution in the Buckhorn area stems from historic logging procedures for igneous rocks in the mine area. The current logging codes allow for fourteen different lithologic options (Table 1.1) for the intrusive rocks alone. Adding 8 more for the volcanic package allows for abundant categorical overlaps and suggests an enormous number of intrusions present. In contrast, U-Pb dating (Gaspar, 2005) indicates three Jurassic and two Eocene intrusions. Making sense of all the various igneous rocks logged is a key challenge.

2.2 Overview of classification techniques

My objective, in regards to the intrusions, is to provide quantitative criteria for recognizing and distinguishing the igneous bodies present. Visual identification of the igneous rocks is haphazard (at best) due to varying textures and mineralogy within a given body, with the added complication of superimposed alteration. The quantitative criteria I employed are, in contrast, based on major and minor element chemical analysis of samples from both the surface and the subsurface. Based on my compositional and textural data, I distinguished nine igneous rock types, two of which were not previously recognized.

The only internationally accepted classification of plutonic rocks is the International Union of the Geological Sciences (IUGS) scheme (Le Bas and Streckeisen, 1991) based on the modal mineralogy (i.e., minerals actually present in unaltered rocks). Accurate identification of modal mineralogy (especially feldspars) in both altered and unaltered samples is facilitated by staining with concentrated (52%) HF followed by immersion in a saturated Na-Cobaltinitrite solution. Quartz remains grey, plagioclase stays chalky white or adopts a faint green tint, and K-feldspar turns yellow (Lyons, 1971). The relative amounts of quartz, plagioclase, and alkali feldspar can then be estimated. Unfortunately, the health hazards involved in using concentrated HF make such a procedure impossible on Kinross property.

Unofficially, plutonic rocks can be classified based on their chemical compositions, using a variety of different schemes. I utilized the classification diagram of Streckheisen and Le Maitre (1979), which employs ratios of calculated mineral abundances ("CIPW norm"---see chapter 1) based on the major oxide analysis. Using this technique and based on several hundred XRF major element analyses, I condensed the original 14 lithologic options (Table 1.1) into seven.

I tested the accuracy of major and minor element analyses by comparing XRF compositions, determined with the Panalytical IQ+ software (chapter 1), of pressed pellets from six international standards to their published and certified compositions (Table 2.1). For most samples and most major elements the relative deviation between measured and published values was small: <1 to 6%. The light elements Na, Mg, and Al,

however, gave measured oxide values that commonly deviated from published values by more than 6 relative percent (Table 2.1). For all but the samples with very high and very low MgO, for example, IQ+ gave wt % MgO values that were low by 15-24 relative percent. Oppositely, IQ+ yielded wt % Na_2O values that were 7-21 relative percent too high. Because the CIPW normative classification scheme depends on the calculated values of albite (Na feldspar), anorthite (Ca feldspar), orthoclase (K-feldspar) and quartz, the net result is that the calculated albite values are slightly higher than they should be. However, the effect on the normative ratios used in classifying igneous rocks (%anorthite/(anorthite + orthoclase) and % quartz/(quartz + total feldspar)) is insignificant (Table 2.2). That is, despite the small systematic errors in major element composition calculated using IQ+, the effect on igneous rock classification is likely to be minor.

For minor elements the deviations between measured and published values are much smaller, usually 0-10 relative percent (Table 2.1). In the few cases where the trace elements are in unusually low concentration, e.g., 6 ppm Rb in NIM-N (Table 2.1), a small absolute error causes a large relative difference. However, for typical rock concentrations of these elements (e.g., 20-250 ppm Rb) the relative differences between measured and published are generally less than 5 percent of the concentration. For the purposes of this study, the differences are negligible.

Table 2.1. Summary of UAF XRF analyses* of certified standards.

	JG-2			JF-1			JB-2			W-2			NIM-N			MRG-1		
wt %	Meas	Publ	%Δ	Meas	Publ	%Δ	Meas	Publ	%Δ	Meas	Publ	%Δ	Meas	Publ	%Δ	Meas	Publ	%Δ
SiO_2	75.5	76.8	**2**	66.8	67.0	**0.4**	52.0	52.2	**0.4**	51.2	52.4	**2**	50.8	52.4	**3**	39.8	39.1	**-2**
TiO_2	0.05	0.05	**-6**	0.01	0.01	**1**	1.18	1.19	**1**	1.08	1.06	**-2**	0.18	0.19	**5**	3.97	3.77	**-5**
Al_2O_3	13.4	12.6	**-6**	18.7	18.1	**-3**	15.4	14.7	**-5**	17.7	15.4	**-15**	18.5	16.7	**-1**	9.27	8.64	**-7**
Fe_2O_3	1.06	0.99	**-7**	0.11	0.08		14.1	14.3	**2**	10.4	10.7	**3**	9.28	8.91	**-4**	17.7	17.9	**1**
MgO	0.06	0.05		0.04	0.01		3.91	4.62	**15**	4.98	6.07	**18**	5.64	7.3	**23**	13.2	13.5	**2**
CaO	0.82	0.77	**-6**	1.03	0.93	**-11**	9.89	9.82	**-1**	10.6	10.9	**2**	11.7	11.5	**-2**	14.6	14.7	**1**
MnO	0.02	0.02	**-11**	0	0		0.23	0.22	**-5**	0.17	0.16	**-6**	0.19	0.18	**-6**	0.18	0.17	**-6**
Na_2O	4.31	3.84	**-12**	3.67	3.56	**-3**	2.71	2.24	**-21**	2.83	2.34	**-21**	3.02	2.66	**-14**	0.81	0.76	**-7**
K_2O	4.67	4.71	**1**	9.38	10.1	**7**	0.4	0.42	**5**	0.62	0.63	**2**	0.25	0.25	**0**	0.17	0.18	**6**
P2O5	0.01	0		0.01	0.01	**1**	0.11	0.11	**0**	0.17	0.13	**-31**	0.02	0.03		0.09	0.08	
ppm																		
Rb	272	297	**8**	256	264	**3**	7	6	**-15**	21	20	**-6**	4	6	**38**	8	9	**13**
Sr	17	16	**-6**	159	163	**2**	186	178	**-5**	203	194	**-5**	266	260	**-2**	270	266	**-1**
Y	95	89	**-6**	6	5	**-5**	25	26	**3**	23	24	**6**	7	7	**7**	13	14	**5**
Zr	99	97	**-2**	38	41	**7**	52	52	**0**	99	94	**-5**	18	21	**12**	111	109	**-2**
Nb	13	14	**7**	1	1	**7**	1	1	**-1**	8	9	**10**	1	2	**10**	21	20	**-5**

* Major oxides determined using the Panalytical program 'IQ+'; minor elements using wavelength dispersive technique (WDS routine) described in text.

Table 2.2 Comparisons between normative mineralogy calculated for certified standards from UAF measured (Meas) and published (Publ) chemical analyses.

Normative Mineral	JB-2		JF-1		JG-2		MRG-1		NIM-N		W-2	
	Meas	Publ	Meas	Publ	Meas	Publ	Meas	Publ	Meas	Publ	Meas	Publ
Quartz	4.50	5.70	7.30	5.80	31.3	34.3				0.0	2.57	3.40
Albite	23.3	19.2	31.1	30.2	35.6	32.6	0.50	0.50	26.0	23.0	23.0	20.0
Orthoclase	2.40	2.50	55.6	59.9	27.7	27.9	0.10	0.10	1.00	1.00	4.00	4.00
Anorthite	29.0	29.2	5.00	3.50	3.40	3.20	21.6	20.2	37.0	33.0	33.0	30.0
Nepheline							3.80	3.60				
Leucite							0.80	0.90				
Diopside	16.9	16.5		0.25	0.50	0.51	34.9	33.0	18.2	19.7	14.9	19.7
Hypersthene	19.8	22.3	0.24		1.30	1.20			9.30	21.3	18.5	19.4
Olivine							25.80	27.90	6.80			
Larnite							2.70	4.30				
Ilmenite	2.30	2.30	0.0	0.0	0.09	0.09	7.70	7.40	0.30	0.40	2.10	2.00
Magnetite	2.10	2.10	0.0	0.0	0.16	0.14	2.60	2.70	1.40	1.30	1.50	1.60
An/(An+Or)	92.0	92.0	8.0	5.0	11.0	10.0	100.0	100.0	96.0	96.0	90.0	89.0
Q/(Q+F)*	8.0	10.0	7.00	6.00	32.0	35.0	-17.0	-18.0	0.0	0.0	4.00	6.00

*Negative values indicate ratio is feldspathoid / (total feldspathoid + feldspar). Q= quartz. F= feldspar.

To save time and expense, the igneous rocks--all of which are fine- to medium-grained were analyzed by XRF on a polished 4 cm slab of rock. I tested the precision and accuracy of this method by analyzing multiple polished slabs of the same typical sample (BS076) and by comparing the analyses of pulverized pressed pellets to slabs of the same rocks for both major oxide (Table 2.3) and trace element (Table 2.4) compositions. BS076, with a typical grain size of 1-3 mm, is on the upper end of grain sizes for the igneous rocks included in this study, and most likely to show variability in polished slab analysis. Comparison of major element concentrations (Table 2.3, Fig. 2.1) shows negligible differences among the different slabs and between slabs and pellets except for FeO and MgO. These two elements are under-reported by about 15-20 relative percent in the slab analyses. MnO is also lower for the slab, but the values are so small that the differences for this study are not significant. Notably, those oxides used in calculating the CIPW norms for quartz, feldspars, and feldspathoids (Tables 2.2, 2.3) show tiny relative differences between polished slab and pressed pellet.

Minor elements determined by IQ+ (Fig. 2.2) show clearly different values for pressed pellets versus polished slabs for sample BS076. For most elements (except S) pressed pellet concentrations are 15-30 relative percent higher than those measured for the polished slabs. However, for quantitative trace element comparisons of the igneous rocks I employed a specially designed XRF routine (see section 1.5). Using this routine on the polished slabs and pressed pellets of sample BS076, I found much smaller variations between individual samples (Table 2.4, Fig. 2.3) than I found for the values determined using IQ+ (Fig. 2.2).

Table 2.3. Major element composition comparisons for BS076 polished slabs and pressed pellets using IQ+

Sample	Weight % Oxide										
	SiO_2	Al_2O_3	Na_2O	CaO	FeO	K_2O	MgO	TiO_2	P_2O_5	BaO	MnO
PELLETS											
PP1	64.1	16.6	4.71	4.65	3.79	2.60	2.29	0.63	0.38	0.13	0.06
PP2	63.9	16.7	4.56	4.63	4.00	2.56	2.52	0.62	0.40	0.14	0.05
PP3	63.9	16.6	4.67	4.61	3.98	2.59	2.37	0.64	0.39	0.13	0.06
PP4	64.4	16.5	4.66	4.63	3.82	2.65	2.11	0.62	0.39	0.13	0.06
PP5	64.4	16.2	4.73	4.67	3.72	2.67	2.36	0.64	0.38	0.14	0.06
Avgerage	64.15	16.53	4.67	4.64	3.86	2.61	2.33	0.63	0.39	0.13	0.06
2 Sigma	0.51	0.40	0.14	0.05	0.24	0.09	0.30	0.02	0.01	0.01	0.01
SLABS											
SL1	65.2	16.3	4.83	4.77	3.27	2.63	1.80	0.64	0.36	0.14	0.04
SL2	65.5	16.2	4.76	4.69	2.99	2.73	1.97	0.62	0.35	0.15	0.05
SL3	65.2	16.4	4.89	4.86	3.01	2.63	1.81	0.59	0.38	0.14	0.05
SL4	64.8	16.6	4.86	4.90	3.12	2.63	1.95	0.62	0.40	0.14	0.05
SL4#2	64.7	16.7	4.89	4.79	3.14	2.58	2.00	0.64	0.38	0.15	0.05
SL5	65.3	16.6	4.84	4.72	2.99	2.58	1.80	0.61	0.37	0.14	0.04
SL5#2	65.5	16.4	4.72	4.59	3.14	2.55	1.90	0.58	0.38	0.15	0.04
SL6	65.1	16.5	4.71	4.82	3.14	2.67	1.93	0.58	0.38	0.15	0.05
SL7	65.5	16.2	4.79	4.82	3.01	2.64	1.93	0.57	0.34	0.15	0.05
SL7#2	65.4	16.3	4.75	4.69	2.92	2.80	1.97	0.59	0.34	0.15	0.05
Average	65.23	16.41	4.80	4.77	3.07	2.65	1.91	0.61	0.37	0.15	0.05
2 Sigma	0.58	0.31	0.13	0.18	0.21	0.15	0.15	0.05	0.04	0.01	0.01
%Δ	**-2**	**1**	**-3**	**-3**	**20**	**-1**	**18**	**4**	**6**	**-8**	**22**

Table 2.4 Minor element composition comparisons for BS076 polished slabs and pressed pellets using the XRF routine specially designed for these elements

Sample	# Analyses	Average concentration (ppm) Rb	Sr	Y	Zr	Nb
SLABS						
BS-76 #1	3	62	928	13	131	8
BS-76 #2	3	63	908	12	135	9
BS-76 #3	3	60	954	12	132	8
BS-76 #4	3	62	966	13	135	9
BS-76 #5	3	62	933	12	135	9
BS-76 #6	3	62	937	12	133	8
BS-76 #7	3	63	902	12	131	9
Average		62	933	12	133	9
2 x SD		2	44	1.3	3.6	0.6
PELLETS						
BS-76PP-1	7	68	851	15	159	10
BS-76PP-2	5	68	848	15	160	10
BS-76PP-3	5	68	856	15	158	10
BS-76PP-4	4	68	851	15	160	10
Average		68	851	15	159	10
2 x SD		0.8	19	0.4	3.0	0.4
PP vs. Slab	**% Δ**	**9**	**-10**	**18**	**16**	**16**

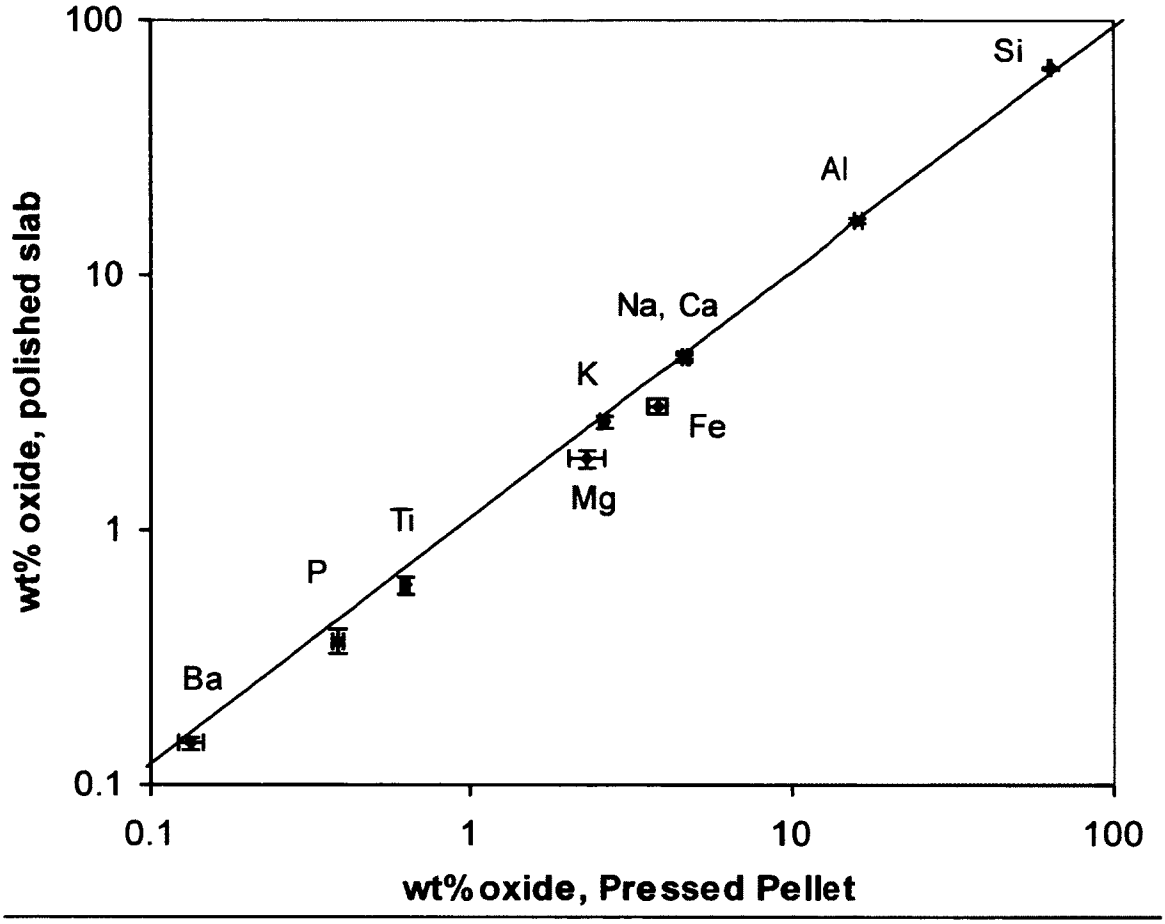

Figure 2.1. Major element composition comparisons for sample BS076- average polished slab vs. pressed pellet. Error bars represent 2 sigma calculated from least five different sub-samples of BS076. Major element concentrations for all elements except Mg and Fe show very close correlation between slab and pressed pellet values. Data from Table 2.3.

Further, for most of the elements the differences in concentrations between the two types are insignificant (less than 2 sigma) except for Zr (Table 2.4). Zr concentrations of pressed pellets are about 15% higher than those from polished slabs. However, since I consistently used polished slabs for igneous rock compositions this error should not be of importance.

In sum, the analytical procedures used for chemical analyses of Buckhorn igneous rocks are adequate to show differences between different rocks, as the within-sample variability is small, as shown by repeated tests on BS076. Absolute concentrations are expected to be close to real values given that there is good agreement between concentrations for polished slabs and pressed pellets for BS076. Further there is good agreement between measured and published values for six randomly-chosen certified standards (Table 2.1). Problematic elements include Mg, Na, and Fe, but none show sufficiently serious deviations to cause

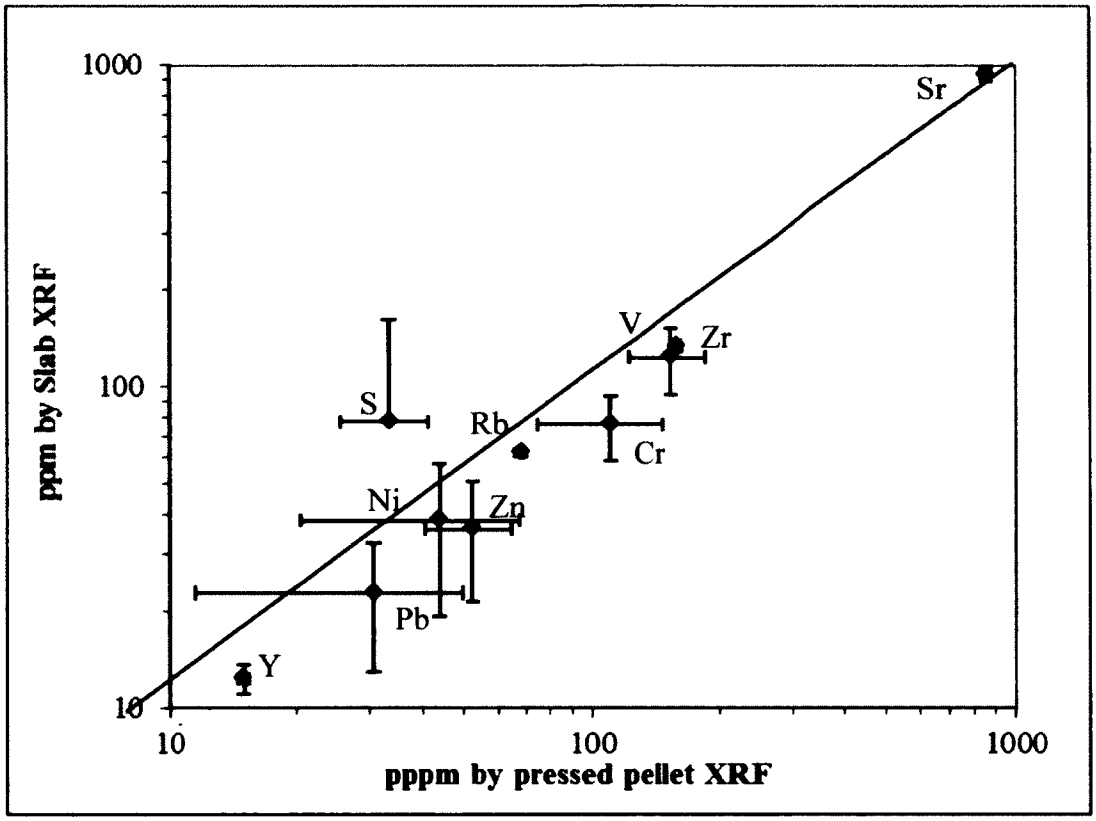

Figure 2.2. Minor element concentrations (using IQ+) for sample BS076. Comparison between polished slabs versus pressed pellets. Error bars represent 2 sigma calculated from at least five different sub-samples of BS076. Pressed pellets typically yield concentrations 15-30% higher than the polished slabs for all the elements shown. None of these elements, however, are employed in classification of the rocks.

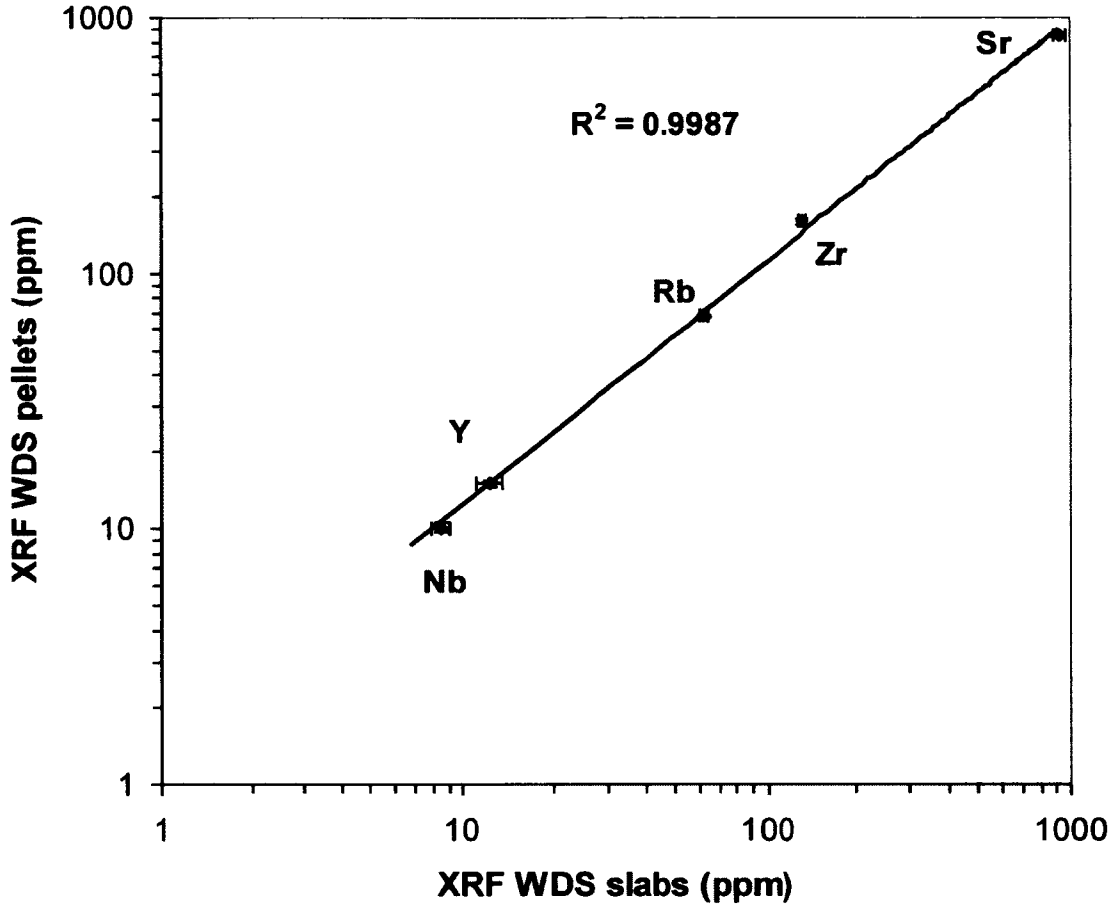

Figure 2.3. Minor element concentrations (using specially designed XRF routine) comparison for sample BS076: polished slabs versus pressed pellets. Error bars represent 2 sigma calculated from at least five different sub-samples of BS076. For all elements except Zr, the concentrations from pressed pellet and polished slabs are indistinguishable (within 2 sigma); however the absolute values for Zr, Nb, and Y by pressed pellets are 16-18 relative percent higher than the polished slab concentrations.

problems in normative classification (Table 2.2) or classification using other elements (e.g., Si, Ti). Because all of my igneous rock analyses are for polished slabs (not a combination of slabs and pellets), the values are adequate for my needs.

2.3 Buckhorn pluton

The Buckhorn pluton is a large mid-Jurassic body with an original surface area of at least 40 km^2 (Fig. 1.6). The southeastern contact is in part a graben-bounding normal fault; the overall NNW-SSE elongation suggests it continued well past the current fault contact. The pluton is compositionally variable; based on modal and normative analyses it consists of quartz monzonite, quartz monzodiorite, tonalite, and granodiorite (Figs. 2.4, 2.5) and possesses a mafic margin at least along the southern contact. The pluton is cut by granodiorite dikes which are not distinguishable from the main pluton either in composition or in hand sample. They are identified by their finer-grained (chilled) margins and changes in physical relief. The dikes vary in strike from NNW to NNE (Fig. 2.6).

Alteration present in the Buckhorn pluton is basically restricted to weak propylitization(chlorite + epidote ± calcite, sphene) and rare endoskarn. The pluton is fine-to medium-grained (usually 1-3 mm) and is generally subequigranular with potassium feldspar interstitial to plagioclase. In cases where a sample was noted as weakly porphyritic (feldspar phenocrystic), an accompanying variation in the modal mineralogy suggested the sample was a dike. Rock compositions are 71-63 wt. % SiO_2, 0.2 to 0.6 wt. % TiO_2 (Fig. 2.7) and 86 to 194 ppm Zr (Fig.2.8). The margin of the

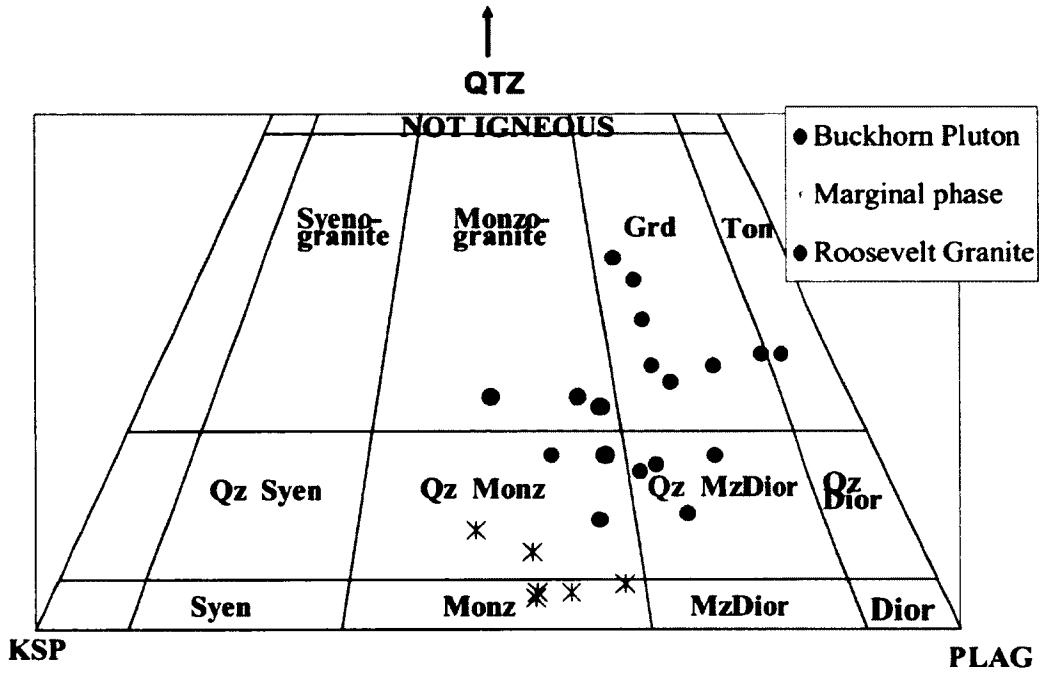

Figure 2.4. Modal classification of selected igneous rock samples. Modal mineralogy comparison of the Buckhorn Pluton, the Marginal phase, and the Roosevelt Granite. Diagram from Le Maitre (2002). Monz = Monzonite, Syen = Syenite, Dior = Diorite, Qz and QTZ = Quartz, Grd = Granodiorite, Ton = Tonalite, KSP = Alkali feldspars, and PLAG = plagioclase feldspar.

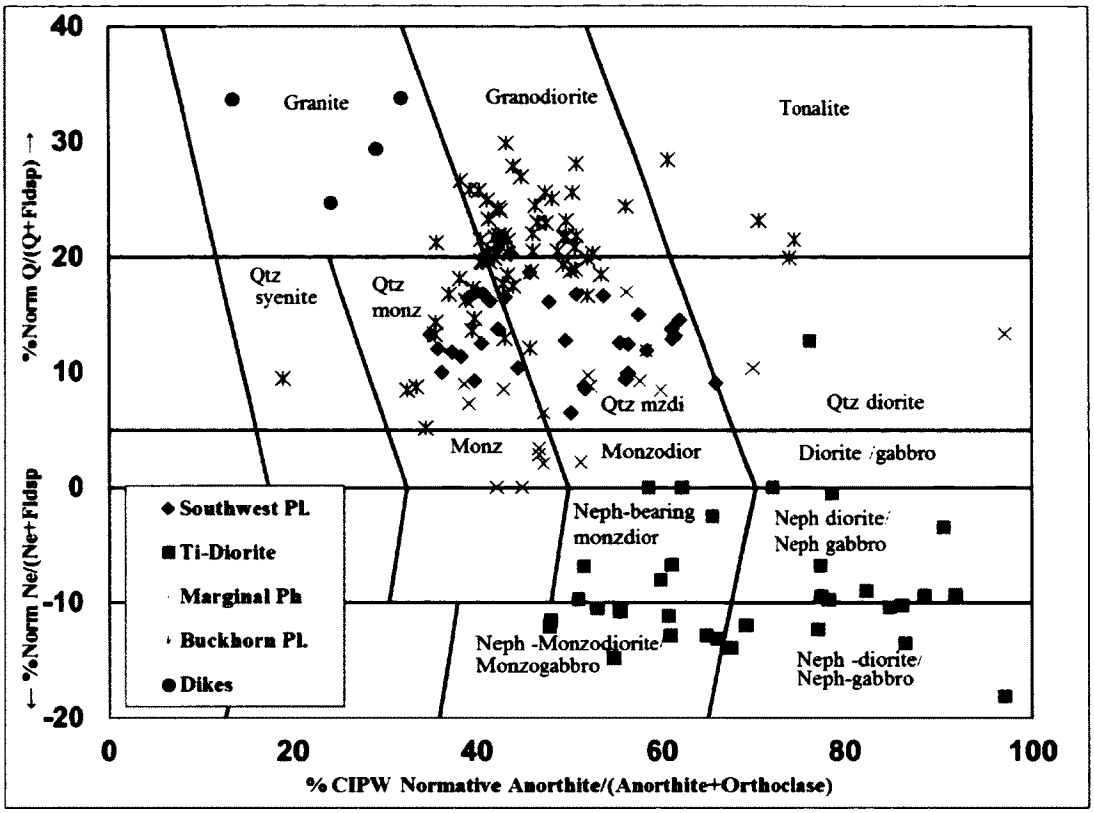

Figure 2.5. Classification of igneous rocks from the Buckhorn area using the CIPW normative scheme of Streckheisen and Le Maitre (1979). Data from this study. The wide scatter of data points are a result of the utilization of mobile elements (modified by hydrothermal alteration) in the classification scheme. Mobile elements are subject to remobilization and reconcentration during alteration. Pl. = pluton, Ph = phase, Neph = nepheline, Qtz = quartz, Monz = monzonite, and Dior = diorite.

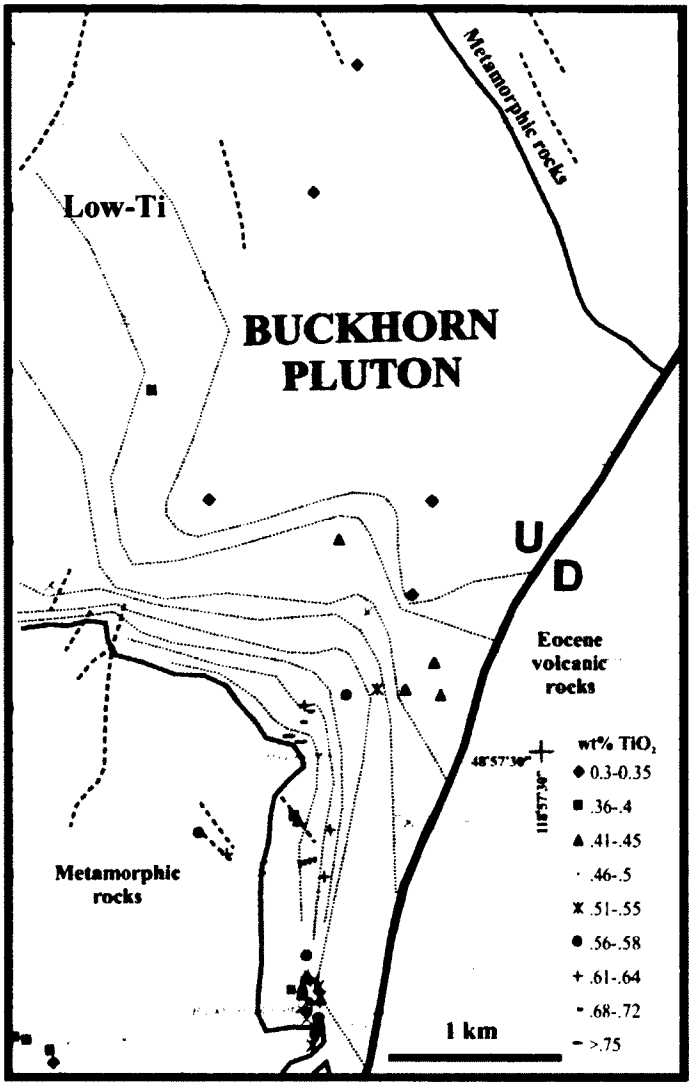

Figure 2.6. Map of the Buckhorn pluton showing TiO_2 compositional variation. Dikes are depicted as red dashed lines. Zoning in wt % TiO_2 shown by dashed, black, hand-drawn contour lines. TiO_2 content increases toward the SW margins of the mapped pluton, highlighting transition from the main body (Buckhorn pluton) to the Marginal Phase (Fig. 1.11). Pluton outline (dark black line) and some dikes from Pearson (1967). Compositional data from Hickey (1992) and this study.

pluton has a distinguishably different composition, although the gradational change between the two confirms that they are the same intrusion.

This gradational change is clearly demonstrated by gradational variation in TiO_2 concentrations (Fig. 2.6) which systematically decrease from the center of the pluton to the western margin. The available samples indicate the pluton is at least asymmetrically zoned. If there is an eastern mafic margin comparable to the western one it must be much narrower or cut off by the Toroda Creek graben's bounding fault (Fig. 2.6).

2.4. Marginal phase of the Buckhorn pluton

The marginal phase is present along the western rim of the Buckhorn pluton and as dikes throughout the Buckhorn area (Fig. 2.6) including underground in the Gold Bowl (see Chapter 3, Section 4). It gradationally merges with the main Buckhorn pluton, although sharp contacts are present in a few hand specimens. Hand sample mineralogy determined from selected NaCobaltinitrate stained samples suggests the marginal phase ranges between monzonite and quartz monzonite (Fig.2.4). Normative analyses of many samples indicate the unit also includes monzodiorite and quartz monzodiorite (Fig. 2.5). The marginal phase is generally subequigranular with grains less than 2mm(mafic minerals occasionally to 3 mm), and potassium feldspar is always interstitial to plagioclase. Alteration within the marginal phase is also limited to weak propylitization and very rare endoskarn. Variably intense shear zones cut this phase and can thoroughly obscure original fabrics, but are only locally present. Rock compositions are 54-63 wt % SiO_2, 0.4-0.8wt % TiO_2 (Fig. 2.7) and 86-94 ppm Zr (Fig.2.8). The more mafic composition, finer grain size, and the overall gradational compositional changes with

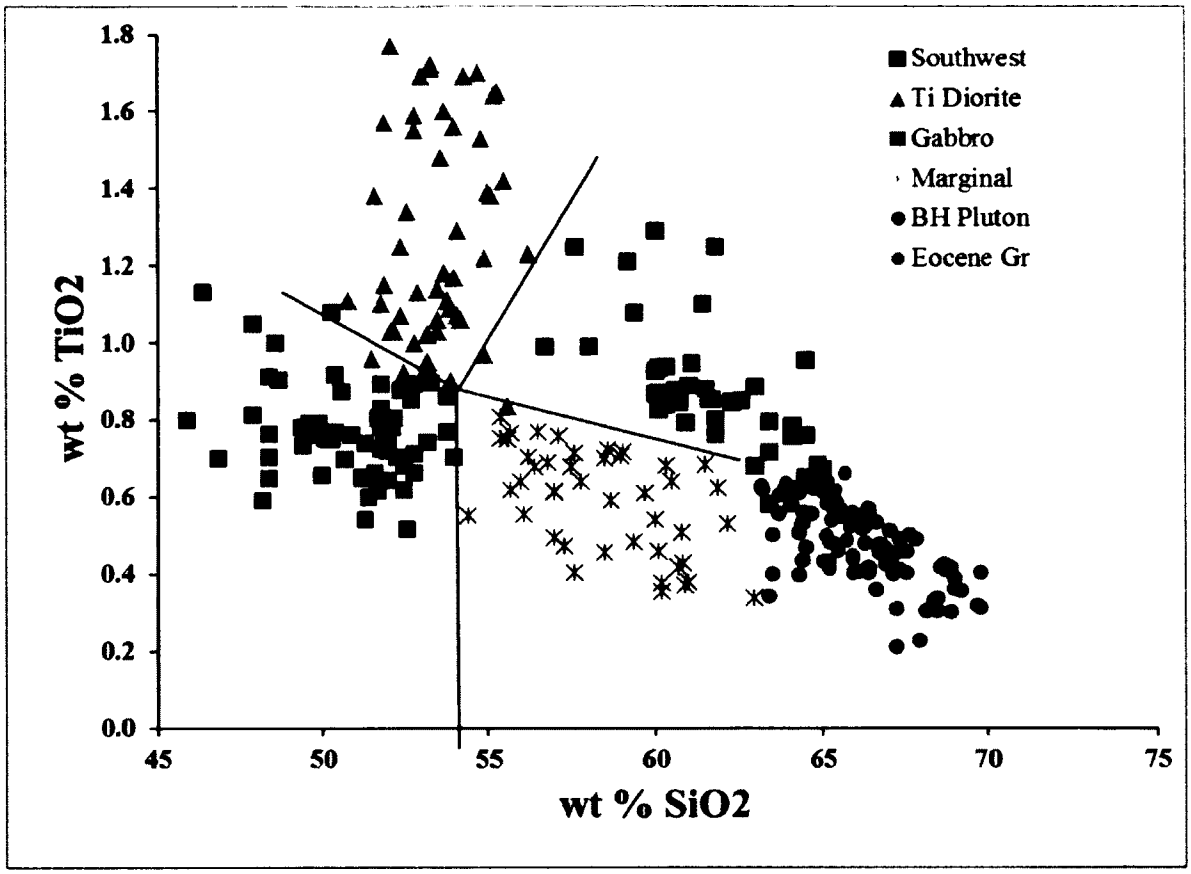

Figure 2.7. Igneous rock comparison based on wt % SiO_2 and wt % TiO_2. Data collected from XRF analysis of polished slabs. With the exception of the Eocene Roosevelt granite, which plots in the border area between the Southwest and the Buckhorn plutons, the igneous rocks are well-distinguished on this diagram.

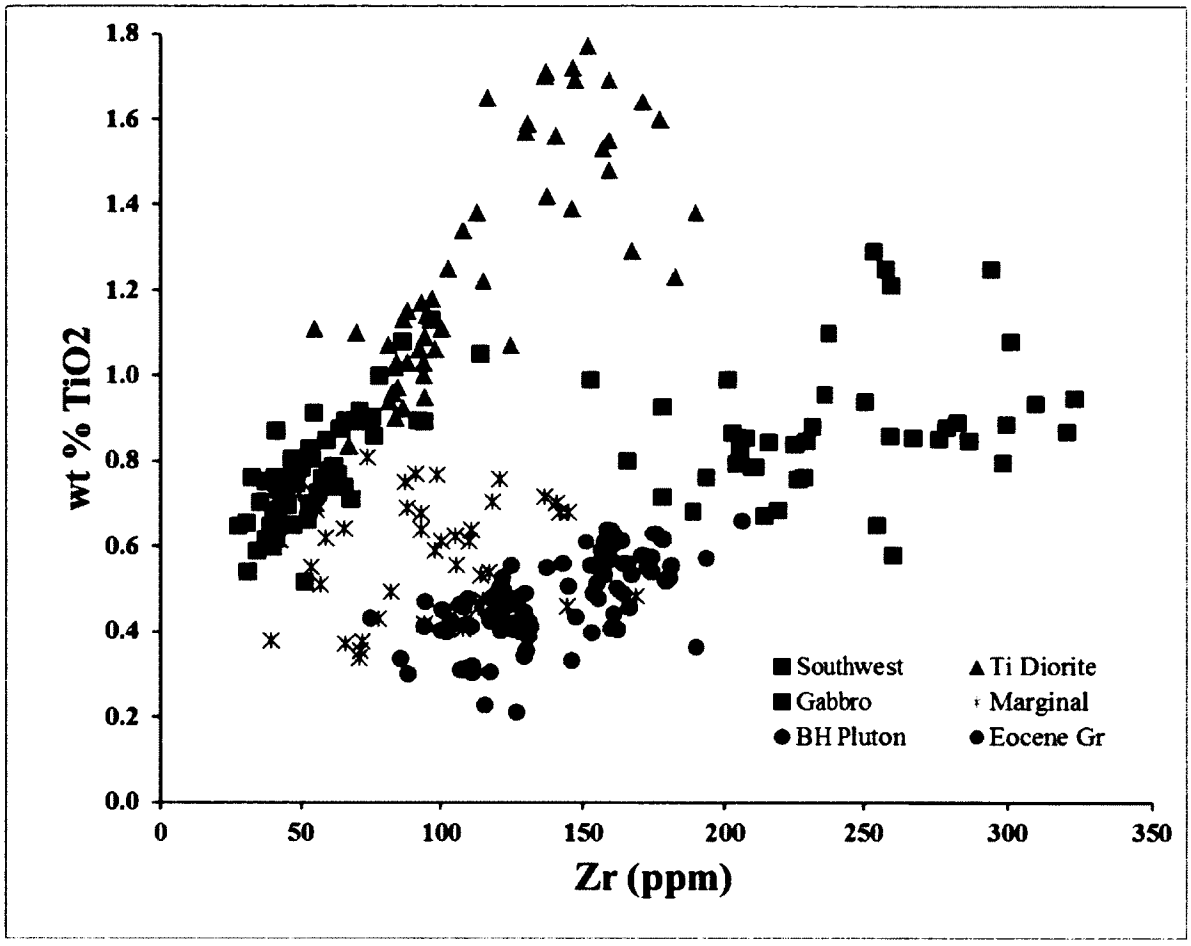

Figure 2.8. Igneous rock comparisons based on ppm Zr and wt % TiO_2. Compositions determined by XRF analysis of polished slabs. Note the minor overlap between the marginal and main phases of the Buckhorn pluton; otherwise the units are generally well-distinguished on this plot.

respect to the Buckhorn pluton (Fig. 2.6), support the conjecture (Hickey, 1990) that it is a chilled margin to the main pluton.

2.5. Ti diorite

The Ti diorite was one of two new intrusions identified as a result of my research, and it is the marginal phase of the Southwest Pluton (see section 2.6). In hand sample, this intrusion is recognizable by its dominantly mafic mineralogy and complete lack of easily-identified quartz. Detailed examination following HF leach and NaCobaltinitrate staining indicates the composition ranges between diorite and monzodiorite (Fig. 2.9). It is typically dark, often black, and subequigranular, with a grain size typically less than 1-2 mm. Potassium feldspar is rare but where present is interstitial to plagioclase, and I was able to identify quartz in only two samples. Local porphyritic zones contain feldspar phenocrysts 1-5 mm wide. Normative compositional classification (Fig. 2.5) indicates that the Ti diorite is, in fact, a diorite, although the high Na_2O concentrations yield significant normative nepheline in most analyzed samples and causes them to plot as Ne-diorites. (It is possible that the slightly high Na_2O concentrations given by IQ+ (Table 2.1) add to this problem.) Exactly what minerals are present that give rise to the nepheline-normative composition is not known; XRD analyses of selected samples indicate abundant albite and less mica. Additional compositional characteristics (Fig. 2.7) include low SiO_2 (46-56 wt %) and high titanium (0.9 – 1.8 wt % TiO_2). This unit also has modest Zr (70 - 190 ppm; Fig. 2.8).

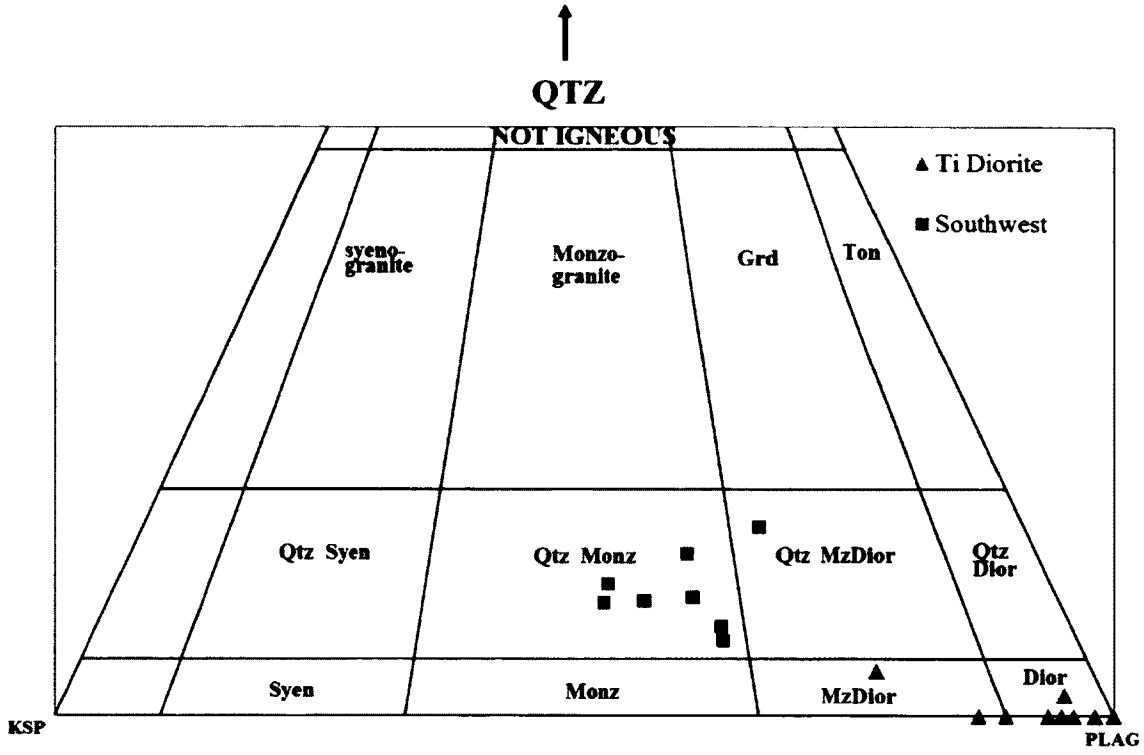

Figure 2.9. Modal classification of samples from the Southwest pluton and Ti Diorite. Classification scheme and rock types as in Fig. 2.4. Diagram from Le Maitre (2002). Dior = diorite, KSP = alkali feldspar, PLAG = plagioclase feldspar, Monz = monzonite, Grd = granodiorite, Ton = tonalite, Syen = syenite, and Qtz = quartz.

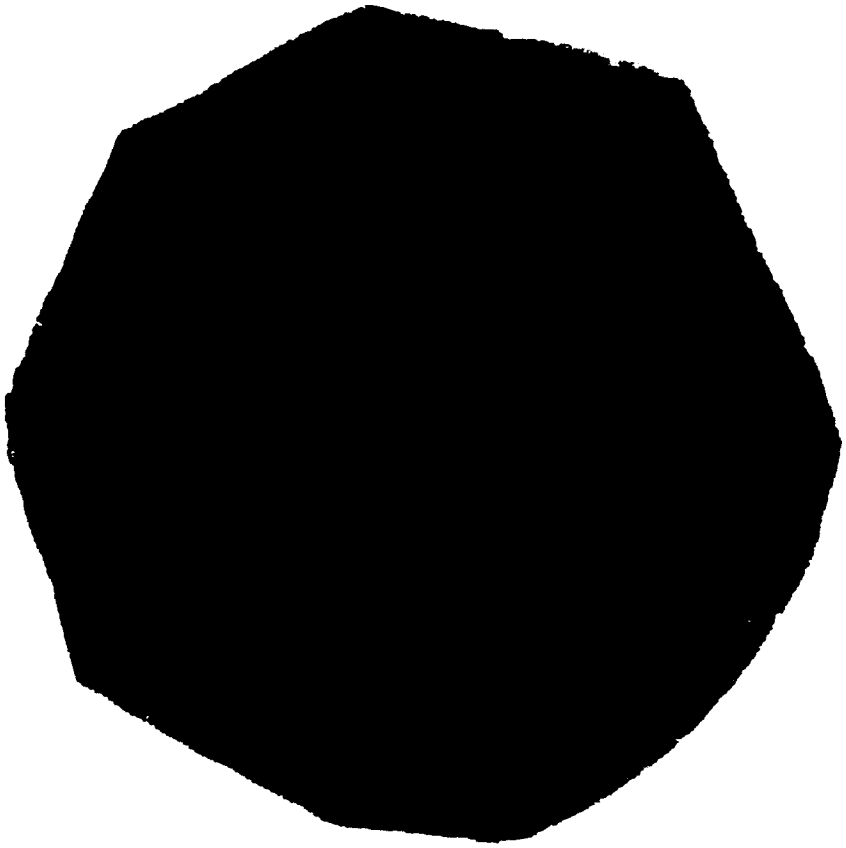

Figure 2.10. K-feldspar veinlet (stained yellow) in Ti diorite sample. Sample was taken from D09-512-150'. Many such veinlets were identified after HF etch and staining of Ti-diorite samples. Sample diameter is 4 cm.

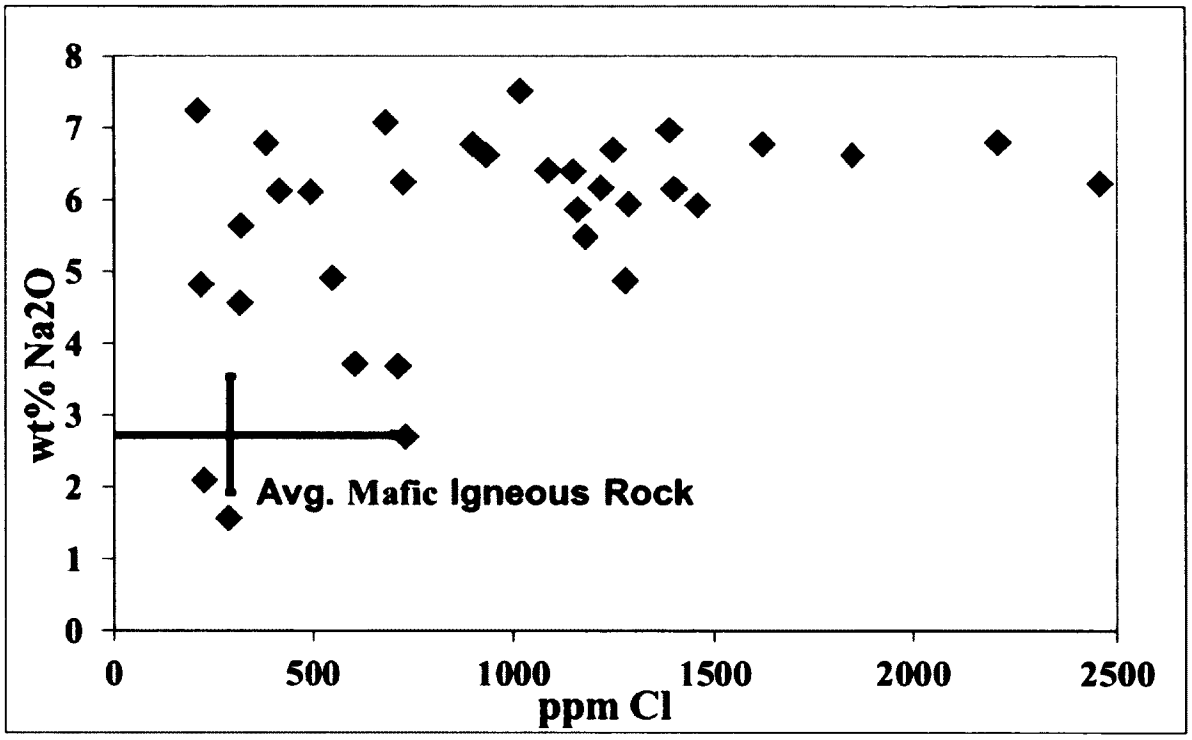

Figure 2.11. ppm Cl vs. wt % Na_2O for less-altered samples of Ti diorite. Average Cl and Na_2O from 'mafic igneous rocks' are from 7450 analyses of mafic rocks (Mutschler et al., 1981) with 1 sigma error bars.

The Ti-diorite is the most altered of the intrusions in the region; it has weak potassic alteration in the form of small, millimeter-scale, veinlets (Fig. 2.10)and moderate to intense sodic alteration accompanied by anomalous Cl (Fig. 2.11). The elevated Cl requires a small amount of Cl-rich mineral, perhaps scapolite (?). However, given the enormous Na content of these rocks, the principal mineral present must be albite. Such is indicated by XRD of representative samples.

2.6 Southwest pluton

The body now termed 'Southwest pluton' was not previously recognized in the Buckhorn area. It displays a visually gradational contact with Ti-diorite (Fig. 2.12), which is adjacent to metamorphic rocks as an outer margin, suggesting that the Ti Diorite is an early crystallizing phase of the Southwest Pluton. Samples of this pluton were selected away from these gradational contacts, obscuring some of the compositionally transitional evidence. In hand sample, SW pluton samples are light to medium grey in color (Fig. 2.12), and decidedly porphyritic; plagioclase and mafic minerals are usually 1-4 mm while the interstitial potassium feldspar and quartz are notably smaller (<2 mm). The hand sample mineralogy after HF etching and Na Cobaltinitrite staining includes lesser quartz and elevated K-feldspar: the samples are invariably quartz monzonite (Fig. 2.9). Normative mineral classification (Fig. 2.5) indicates quartz monzonite and quartz monzodiorite, the latter possibly representing more-altered samples that were not etched and stained. The Southwest pluton has moderateSiO_2 (57-65 wt %), moderate TiO_2 (0.6 - 1.3 wt. %; Fig. 2.7) and elevated Zr (153 – 323 ppm; Fig. 2.8). The high Zr is especially

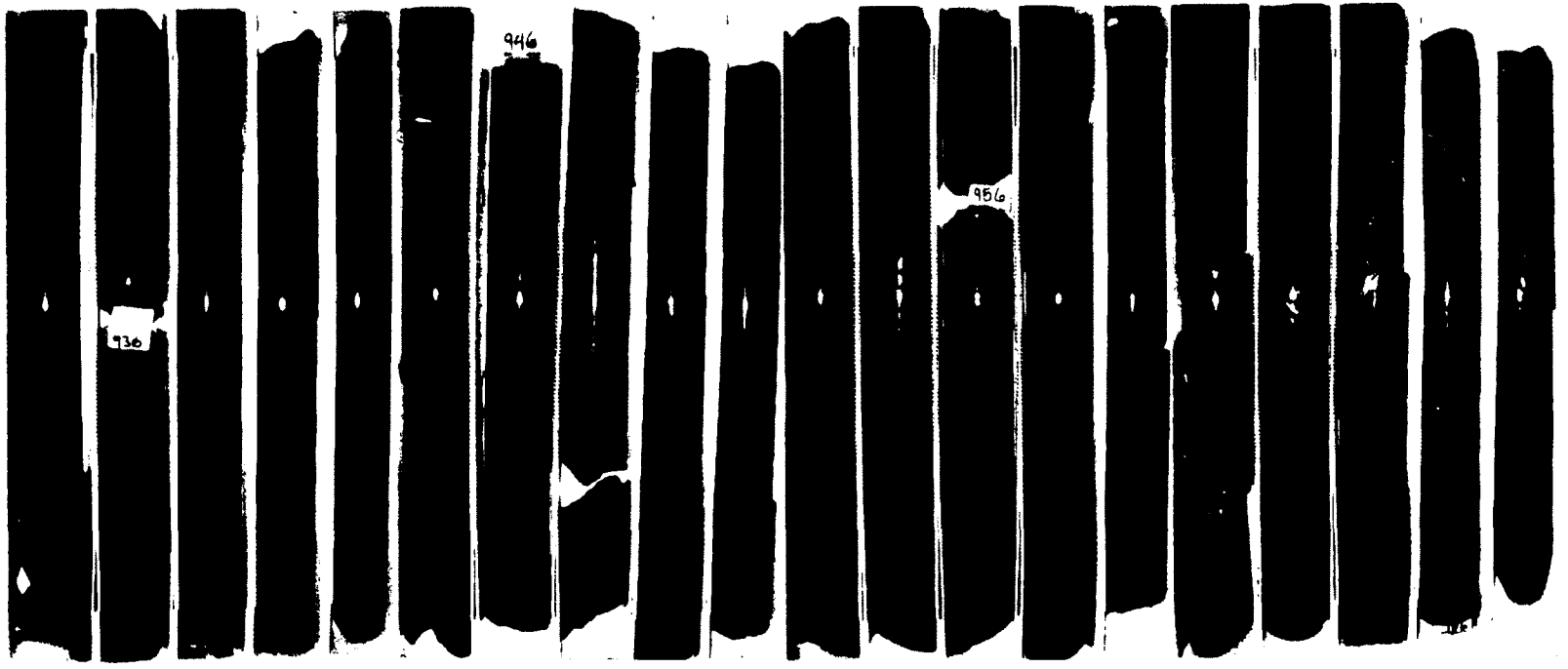

Figure 2.12. Transition from Ti Diorite (left) to Southwest pluton (right) in drill core from D09-590. Vertical scale is 2 feet (0.6 meters). Total length of the interval shown is 40 feet (12 meters). Note the absence of a clearly defined break.

diagnostic: no other igneous rock in the Buckhorn area analyzed in this study or by any previous worker (e.g., Hickey, 1992; Gaspar, 2005) has a Zr concentration above 200 ppm. This is a unique magmatic body in the Buckhorn area.

Also unique to the Southwest pluton is its variable magnetic susceptibility (MS). My measurements on the dated Jurassic plutons yield values of .02-.05 $x10^{-3}$SI, whereas the Eocene intrusions have magnetic susceptibilities of 15 -20 $x10^{-3}$SI (Appendix 2A). In contrast, samples from the Southwest pluton yield values of 0.05 to 18x 10^{-3}SI. Because the samples with MS greater than 3 uniformly contain 0.1-1% disseminated (secondary) pyrrhotite, it is most likely that the higher MS samples also contain secondary magnetite.

Based on where I encountered the Southwest pluton on the surface and in drill core intercepts, this body extends from the Roosevelt Mine area to the SW, mostly SE of the Southwest Zone (Fig. 2.13). The extent of the pluton is still poorly constrained. Outside of the Roosevelt mine area I have not encountered this rock type on the surface, nor have I found evidence for it in drill core outside of the area noted on Fig. 2.13. Given its high Zr content, this rock is easily identified using a hand-held XRF.

2.7 Roosevelt granite

The Roosevelt Granite (identified by Gaspar (2005) as a granodiorite) is only known to occur on the east side of the southern half of the deposit, near the Roosevelt Mine (Figs. 1.3, 2.14). Based on several drill hole intercepts, Gaspar (2005) recognized it as a separate pluton. It is compositionally difficult to distinguish from the Jurassic plutonic rocks (Fig. 2.5) but visually distinguishable by its unaltered appearance and common mafic clots. It also displays a distinctly higher magnetic susceptibility

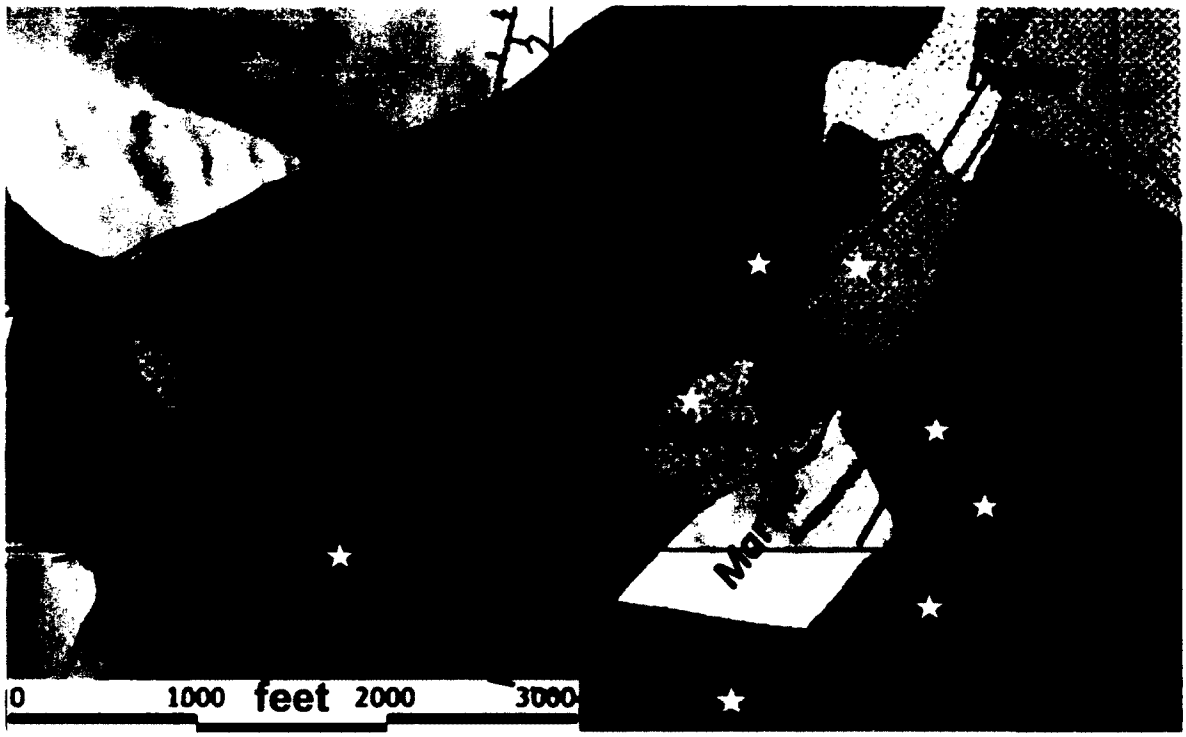

Figure. 2.13. Geologic map of the SW Buckhorn area showing known locations (yellow stars) of the SW pluton (outlined in red dashed line) in vertical drill holes. Black dashed line encloses approximate area of the volcanic package that I examined in detail. Southwest Zone (SWZ) workings are located at approximately 48°75'N, 119°00'E.

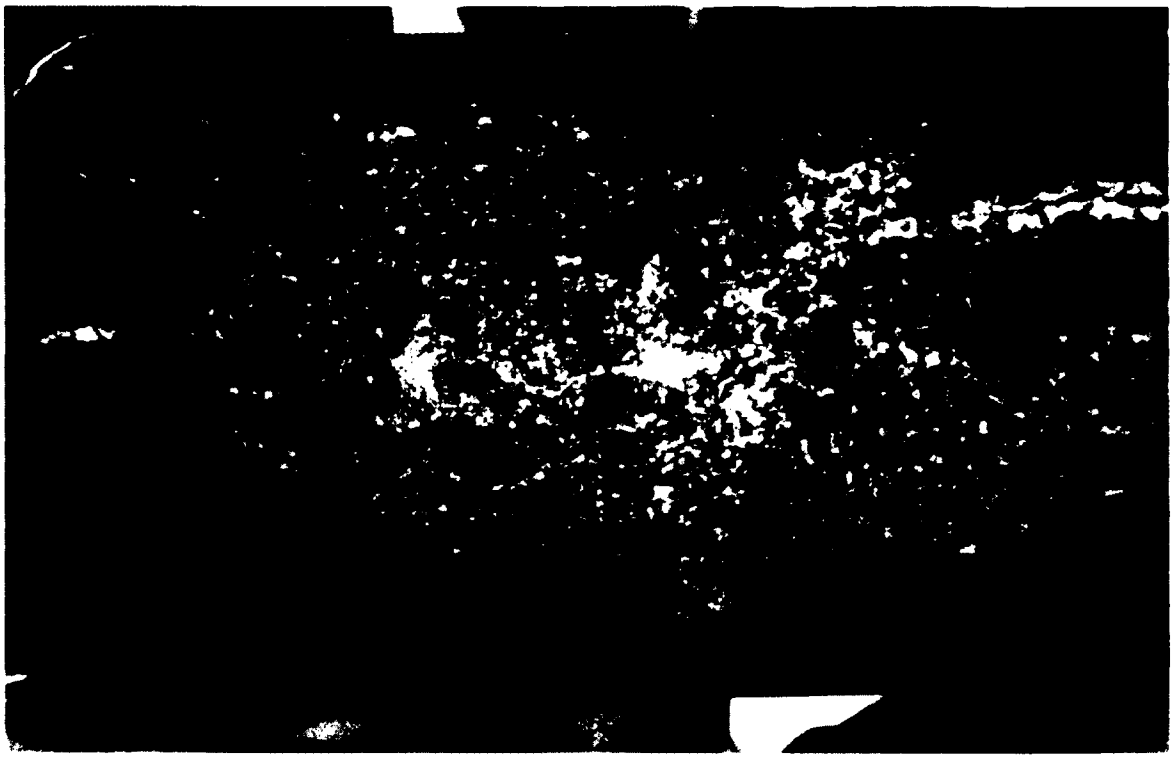

Figure 2.14. Equigranular basaltic rock (gabbro). The interval was originally logged as an andesite flow.

(15-20 $x10^{-3}$ SI) than the Jurassic plutonic rocks. Its color ranges from light to medium gray; it is typically medium-grained, and slightly porphyritic with multiply intergrown hornblende phenocrysts (glomeroporphyritic texture). The modal mineralogy of 4samples indicates it is mostly granite with minor quartz monzonite (Fig. 2.4). Aside from its unaltered appearance, the evidence for Eocene age is from a U-Pb zircon age of 55 Ma (Gaspar, 2005). At its only known surface occurrence (Fig. 2.15) the Roosevelt granite outcrops as a NNW-striking dike. Based on drill core intercepts described by Gaspar (2005) and the airborne magnetic map, it widens at depth and can be considered a pluton. This pluton, based on lack of hydrothermal alteration and limited spatial distribution, is unlikely to be associated with significant mineralization at Buckhorn.

2.8 Assorted Buckhorn area dikes

2.8.1 Granodiorite dikes

A series of granodiorite dikes intrude the Buckhorn pluton (Fig. 2.6). These dikes are not visually or compositionally distinguishable from the main portion of the pluton. They were initially identified by field observations (e.g., Pearson, 1967) and confirmed by U-Pb dating (Gaspar, 2005). The granodiorite dike samples yield a weighted average U-Pb age of 165 Ma, whereas those of the Buckhorn pluton are 169 Ma (Fig.1.10) (Gaspar, 2005). As the weighted averages of these two groups do not overlap, they likely represent different intrusive events. The few dikes that have been analyzed (e.g., Gaspar, 2005) do, in fact, have a granodioritic composition. Also lumped in this group are dikes

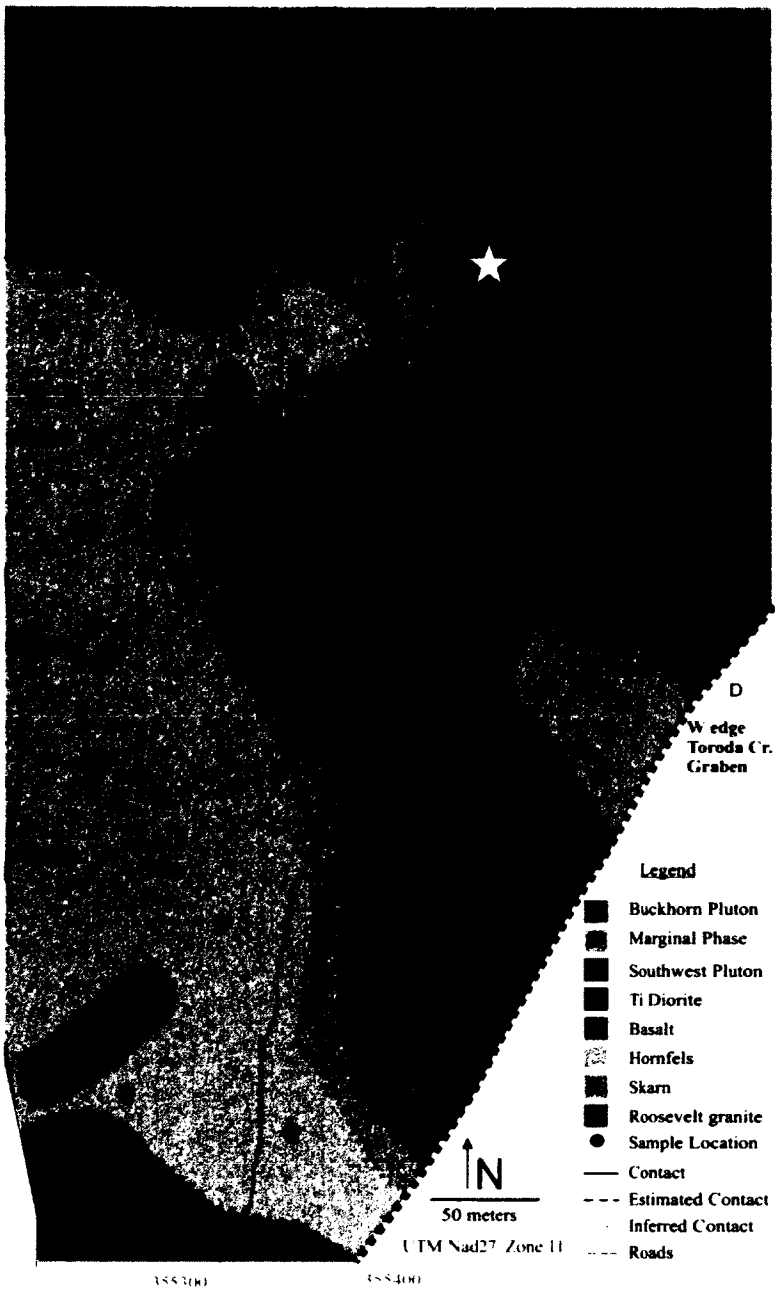

Figure 2.15. Detailed geologic map of the Roosevelt Mine area (1 km ESE of the Southwest Zone). Yellow star marks the location of the Roosevelt Mine adit. Southwest Pluton and Ti Diorite marked in the same color and lumped into one category for this map.

of broadly Buckhorn pluton composition that intrude rocks other than the Buckhorn pluton (Fig. 2.6). These include rocks with compositions ranging from quartz monzonite and quartz monzodiorite to granodiorite. They might represent offshoots of the Buckhorn pluton or an older or younger pluton of broadly similar age and composition.

2.8.2 Quartz porphyry dikes

The quartz porphyry dikes are identifiable without recourse to compositional data. The groundmass is very fine-grained, white to light grey in color, with 1-4 mm quartz phenocrysts ("eyes") present throughout. Compositionally, these dikes are recognizable because they contain >75wt % SiO_2 and < 0.1% TiO_2. Their low Zr concentrations (60-70 ppm) make them unlikely candidates for fractionates of the other Jurassic plutons, as such values are out of line with the drop in TiO_2 and rise in Zr seen in the Buckhorn and SW plutons (Fig. 2.8). The few mafic minerals originally present have been completely chloritized. The dikes cut both the Southwest Zone and Gold Bowl and generally strike NW (Fig. 1.11). The dikes cut across skarn and marble (Figs. 2.16, 2.17) and are not altered outside of weak propylitic alteration. U-Pb radiometric dating on zircons indicates a Jurassic age, approximately 163 Ma (Gaspar, 2005), compatible with their apparently cross-cutting relations to the deposit and to other plutonic rocks.

2.8.3 Eocene dikes

These dikes characteristically trend NE-SW (Fig. 1.11) and are easily identified on aeromagnetic maps by their high magnetic signature (magnetic susceptibility of 15-

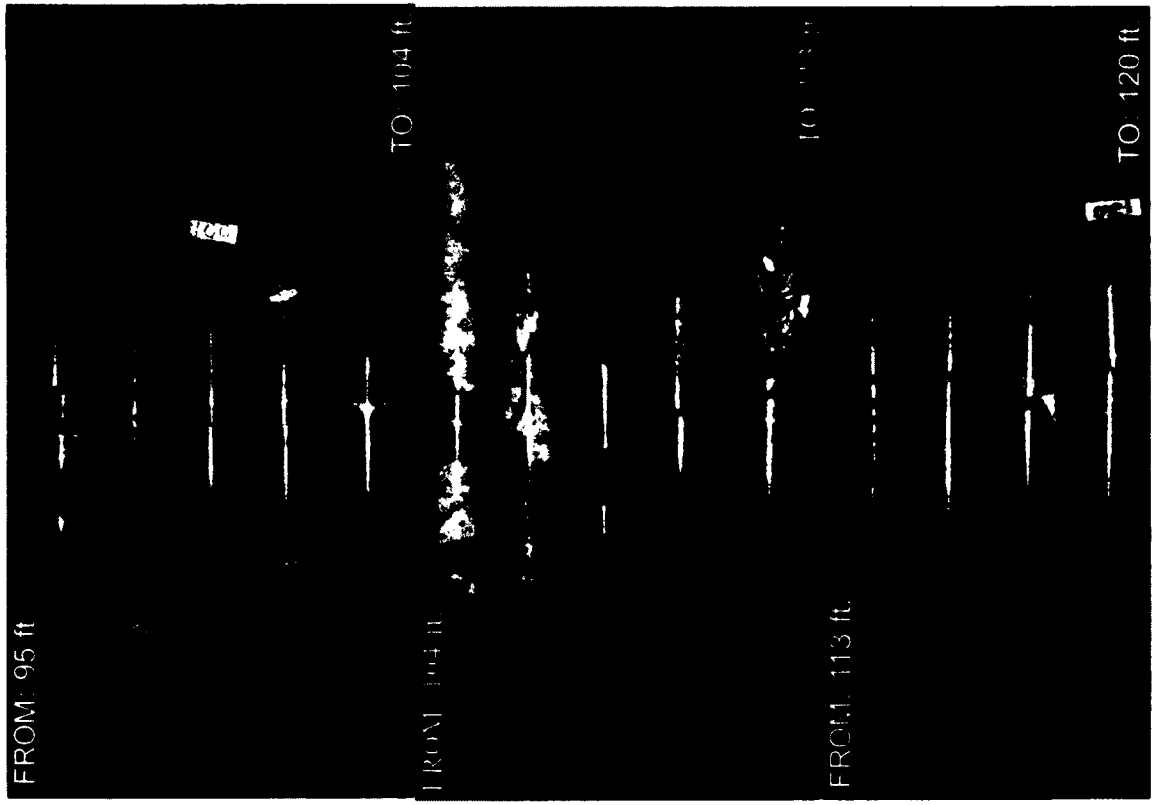

Figure 2.16. Relationship between quartz porphyry dike and skarn in D06-226. QP= Quartz porphyry dike. Green lines = approximate contacts between marble and quartz porphyry dike at 108 ft.). Blue line = contact between skarn and marble (at 104.5 ft.). Each drill core box is 2 feet (.6 m) in length.

Figure 2.17. Relationship between quartz porphyry dike, skarn, and marble in D06-264. QP = quartz porphyry dikes. Green lines represents contacts between units. Note that QP dike has pyroxene skarn on one side and unaltered marble on the other. Lack of skarn on both sides and lack of garnet between QP and clinopyroxene skarn indicate the skarn is not zoned around the dike. Rather, the dike apparently intruded along the skarn-marble contact.

$20x10^{-3}$ SI). In the field, they can be identified by their medium to dark brown color, fine- to medium-grained nature, and low-weathering relief. I have not noted hydrothermal alteration in these dikes. Based on two analyses, they are andesite.

2.9 Volcanic package

The southern half of the Buckhorn deposit is overlain by a complex volcanic package (Fig. 1.11). The package includes flows, sills, and volcaniclastic sedimentary rocks, all variably hornfelsed and endoskarn-altered. The flows are compositionally basaltic with $SiO_2$of 46 – 54 wt %, TiO_2 of 0.5 - 0.9 wt % (Fig. 2.7) and low Zr (28 - 94 ppm; Fig. 2.8). In hand sample, two varieties are commonly noted: an equigranular, medium gray, medium-grained rock that likely represents sills or dikes (Fig.2.14) and a porphyritic variety with 1-5 mm hornblende phenocrysts. The porphyritic flows have historically been called "augite porphyry"; however, the phenocrysts are, in fact, hornblende. The shapes range from 'typical' amphibole to 'possible pyroxene,' but XRF and XRD analysis conclusively identify them as hornblende. Most likely, these were originally augite but were replaced either while still in a magmatic matrix or shortly after emplacement. Such flows exhibit autobrecciation textures with the porphyritic portions of flow as large clasts in a fine-grained matrix (Fig.2.18). Associated with these are volcaniclastic rocks that display clear bedding (Fig. 2.19) but possess basaltic compositions. I mapped for two days in the volcanic package, 2,000 ft. (0.6 km) west-southwest of the Southwest Zone (Fig. 2.13), and noted approximately 30% flow-textured rocks, 20% gabbroic rocks, 10% volcaniclastic rocks, and 40% rocks with basaltic compositions and ambiguous textures.

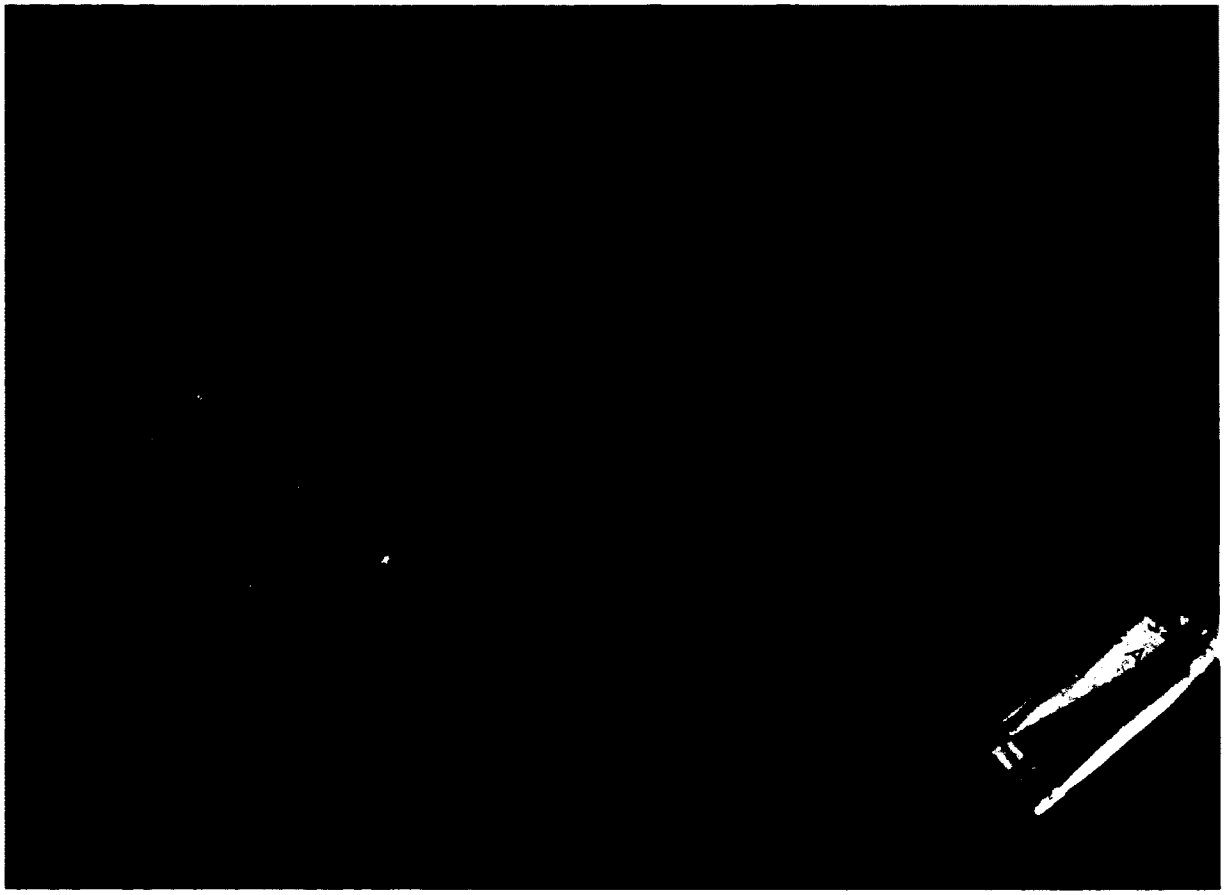

Figure 2.18. Surface exposure of autobrecciated (?) hornblende-porphyritic basalt flow with a finer-grained basalt matrix. Red Bull can is 2" (5 cm) across. Contacts between texturally different blocks are drawn with marker on the outcrop to highlight individual breccia 'clasts'.

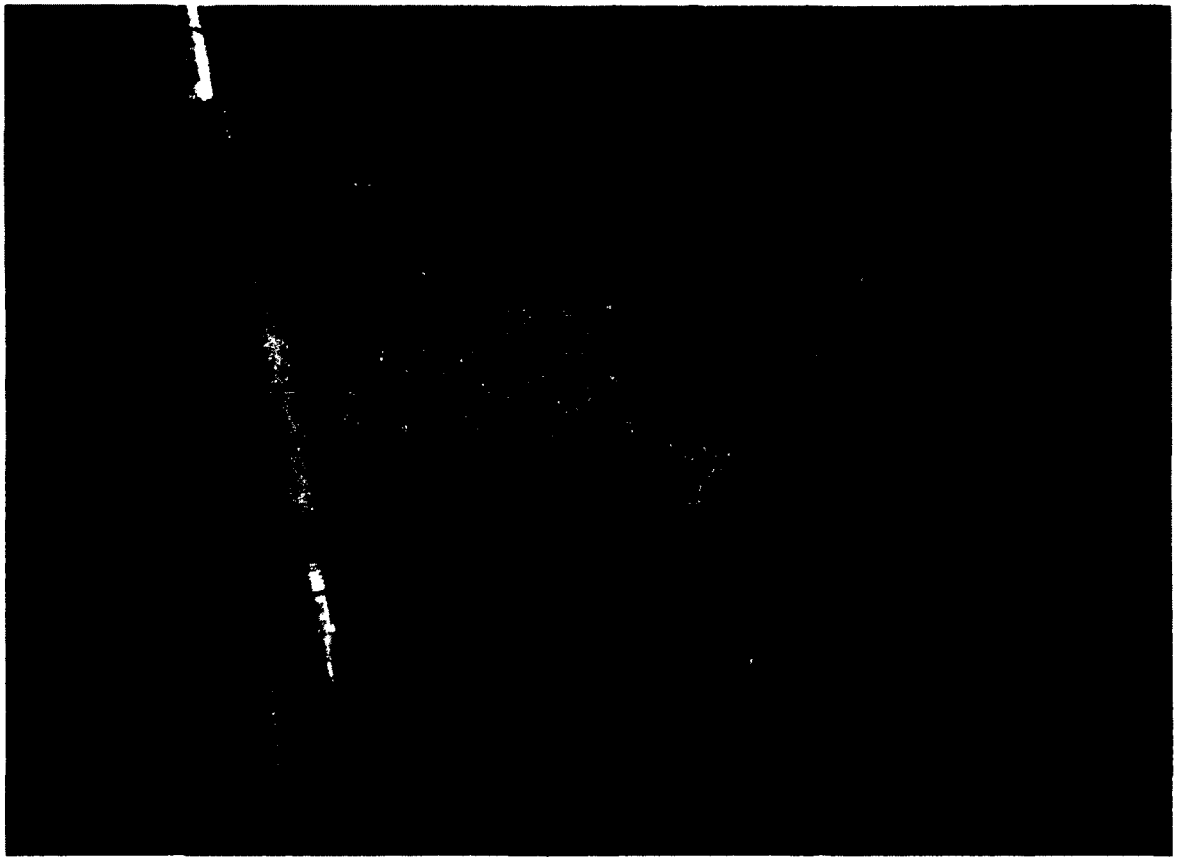

Figure 2.19. Surface exposure of basaltic composition volcaniclastic rock. Sample taken from 2 km west of the Southwest Zone. Similar-appearing rocks were noted underground in the Gold Bowl workings. Exposed pencil length is 4" (10 cm).

The sills are medium-grained (1-3 mm) and contain about 50% mafic minerals. Compositionally, they are indistinguishable from the flows. Underground they are difficult to identify and are locally pervasively altered. Both the flows and the sills contain endoskarn alteration (Section 1.3), suggesting they were present before the skarn event. Much of the pale green hornfels noted in the Southwest Zone may be derived from such rock.

The volcaniclastic portions of this package are also difficult to recognize except in sawed slabs where the texture is less ambiguous. They consist of sand-sized clasts with an overall grossly igneous appearance (indistinguishable from igneous rocks underground). The clasts vary in size and composition but large samples possess SiO_2 and TiO_2contents that fall within the range of the intrusive and extrusive volcanic rocks. Such rocks are also present underground in the Gold Bowl workings.

2.10 Roosevelt area mapping

The most complex intrusive rock relationships I have found are concentrated near the historic Roosevelt Mine area on the east side of the Southwest Zone (Fig. 2.15). Numerous unpublished Kinross maps of the area display serious discrepancies not easily reconciled, largely due to difficulties in distinguishing the various rock types. This is a complicated area for several reasons: the outcrop exposures are poor and limited and there are 6 different igneous rocks with variably superimposed alteration present (Fig. 2.15).

The Buckhorn pluton and its marginal phase seem to simply wrap around that east side of this area, although in the northwestern part Buckhorn pluton is directly adjacent to metavolcanic and metasedimentary rocks without any intervening marginal phase. The Roosevelt granite occurs as a narrow, NNW-striking dike that might continue to the SE edge of the map area. Underground investigation of the partly collapsed workings of the Roosevelt Mine with a magnetic susceptibility meter showed a dike approximately 20 feet (7 meters) wide in the workings, in line with the 4 surface samples. A detailed aeromagnetic map of the region suggests that the dike is underlain by an oval shaped body approximately 50 meters in diameter.

Also intermittently exposed are basaltic rocks of the volcanic package and small, irregularly shaped dikes (?) of the Southwest pluton. (I also found one sample of Ti diorite but to simplify the map included it with SW pluton). The sporadic outcrops of SW pluton suggest that the pluton itself is likely in the shallow subsurface.

2.11Conclusion

The best way to distinguish between the different igneous bodies at Buckhorn is compositionally, specifically by using immobile elements. Normative classification schemes were originally employed to reduce the twenty-two igneous rock codes used by the mine into fewer categories. However, normative classification diagrams are ultimately based on abundances of very mobile elements, namely Na, K, and Ca. These mobile elements are easily removed, added, or redistributed during even weak alteration, making the categories used to classify the different igneous rocks variable and broad.

The seemingly optimal immobile elements used here were zirconium (Zr) and titanium (Ti). These elements are present in tiny minerals (e.g., zircon, ilmenite, Ti-magnetite) and likely distributed homogeneously throughout a sample.

Also variable between the different intrusions is the intensity and type of alteration. The Buckhorn pluton, marginal phase, and quartz porphyry dikes all show weak to moderate propylitic alteration which manifests itself by the partial conversion of plagioclase to epidote and chloritization of mafic minerals. The Southwest pluton's hydrothermal alteration is evidenced by secondary pyrrhotite and secondary magnetite, making the pluton variably magnetic. The Ti diorite, marginal phase of the Southwest pluton, is the most altered intrusion and hosts both potassic and intense albitic alteration.

Endoskarn alteration is present within the overlying basalt package and portions of the marginal phase (to the Buckhorn Pluton). However, the most intensely altered intrusive is the margin of the Southwest pluton (Ti diorite) suggesting that heated fluids migrated out from the outer margins of that pluton. This makes it the suspected source of the mineralizing fluid for the Buckhorn gold skarn.

I now recognize nine distinguishable igneous rocks in the Buckhorn region. Of these nine, two are likely marginal phases to larger plutons, as documented in drill core (Fig. 2.12), map relations (Fig., 2.15), and progressive changes in chemical composition (e.g., Fig. 2.6). The quartz porphyry and Eocene andesite dikes are easily distinguished; both are compositionally identifiable and the latter identified by high magnetic susceptibility. The granodiorite dikes are compositionally and visually indistinguishable from the main phase of the Buckhorn pluton, and distinction of these is only noted by the

extent of a granodiorite body in drill core or surface exposure. The Roosevelt granite is best recognized by its complete lack of alteration and high magnetic susceptibility, although at first glance, it appears similar to the Southwest pluton. The older, overlying basaltic package is generally either compositionally OR visually identifiable depending on the part of the package.

The newly identified SW pluton is of particular interest because its location makes it a logical source for the Southwest Zone mineralization (Fig. 2.13). I pursue this possibility (Chapter 3) through examination of zoning in the skarn and mineralization of the Southwest Zone.

3. The Buckhorn skarn: mineralogy, zoning, mineral compositional zoning

3.1 Introduction

Mineral and rock identification for the skarn at Buckhorn has almost entirely been based on hand specimen identification; this is adequate for garnet most of the time, as this mineral is inevitably red-brown at Buckhorn. The other common minerals—pyroxene, epidote, amphibole, chlorite, phlogopite—are various shades of green. My comparison of rock descriptions made for a Kinross reference rock exhibit and the actual mineralogy (based on XRD analysis and thin section petrography) showed that the two were in poor agreement. Based on such evidence, the actual minerals present at Buckhorn and their distributions are poorly constrained. The purpose of this chapter is to elucidate the mineralogy and its spatial distribution by combining hand specimen observations with major and minor element analyses of approximately 300 skarn-related rocks from the deposit. These show distinct differences between the various parts of the Buckhorn system. In particular, I recognize that the western portion of the Southwest Zone is mineralogically quite distinct from the rest. Finally, by combining with clinopyroxene compositional distribution, I infer that the Southwest Zone is systematically unrelated to the Gold Bowl with respect to the source of mineralization, and that the former is sourced by a pluton to the SE of the Southwest Zone.

3.2 Mineralogy and mineral distribution

The major non-ore minerals and their relative abundances in the various parts of the Buckhorn system are listed in Table 3.1. Perhaps most notably, I have recognized

(via hand-held XRF, XRD, and petrography) phlogopite as a relatively common constituent of the Southwest Zone skarn, especially near the marble front. Conversely, I have not seen it at Gold Bowl. Similarly, I have seen stilpnomelane in several thin sections from the Southwest Zone but not from Gold Bowl. Other differences in mineralogy can be ascribed to the hornfels-rich nature of the host at Gold Bowl.

Table 3.1 Non-ore minerals and their relative abundances in underground exposures of the Buckhorn area.

Mineral	**Gold Bowl**	**Southwest Zone**
Garnet	A	C
Pyroxene	A	A
Amphibole	A	C
Epidote	A	C
Quartz	C	o
Phlogopite	r	C
Stilpnomelane	n	r
Magnetite	r*	o
Pyrrhotite	o*	C

A = abundant (>20%), C = common (5-20%), o = occurs (1-5%), r = rare (<1%), n = not reported. * = variably abundant in drill core at depth (Fig. 1.9).

3.2.1 Southwest Zone

The key difficulty in sorting out the mineralogy and mineral distribution in the Southwest Zone is that it appears to vary both vertically, in a single exposure, and also laterally across the ore body. To clarify these relations I begin by describing three representative drill holes, taken from the eastern (D09-534), central (D09-545) and western (D07-404) parts of the Southwest Zone (Fig. 3.1).

3.2.1. a Eastern most SW Zone

I chose drill hole D09-534 to represent the eastern portion of the Southwest Zone. A simplified graphic representation of the geology and assay values is shown in Figure 3.2. The overlying volcanic package is roughly 380 feet (116 meters) thick. Beneath the volcanic package are approximately 150 feet (46 meters) of skarn that is either locally pyroxene dominant or sulfide/oxide dominant (pyrrhotite/magnetite). Below that skarn interval, finely intercalated layers of hornfels and skarn occur; the skarn becomes more garnet-rich with depth (Fig. 3.3 a-f).

3.2.1.b Central SW Zone

Drill hole D09-545 (Fig. 3.4) represents the central part of the Southwest Zone. The volcanic package is approximately 350 feet (107 meters) thick and makes a transition into marble through a complex structural zone (the nature of which is still subject to debate).

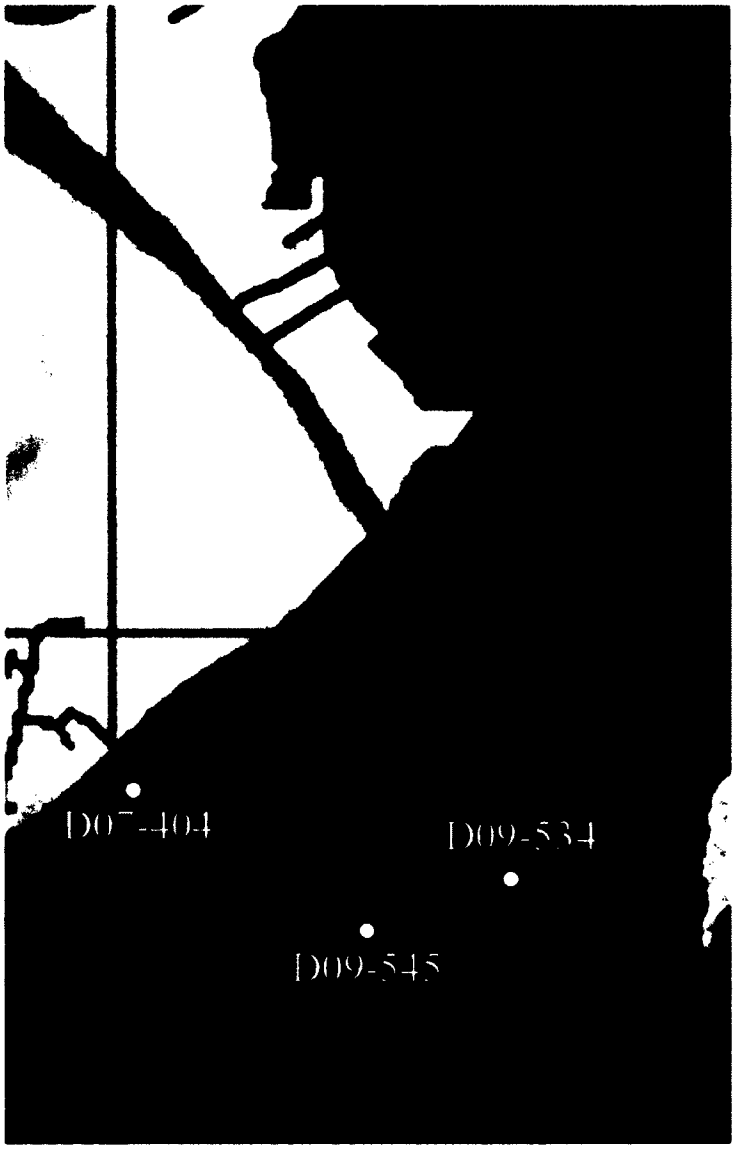

Figure 3.1. Location map for cross section drill holes described in sections 3.2 a-c. The black lines are underground workings; blue lines are faults at the surface; dark brown 'blobs' are ore shells for the respective portions of the deposit projected to the surface. GB = Gold Bowl. SWZ = Southwest Zone. Rock at the surface throughout this area is meta-basalt. Red dashed line separates 'western' from 'main' Southwest Zone. SWZ is located at 48°75'N, 119°00'E.

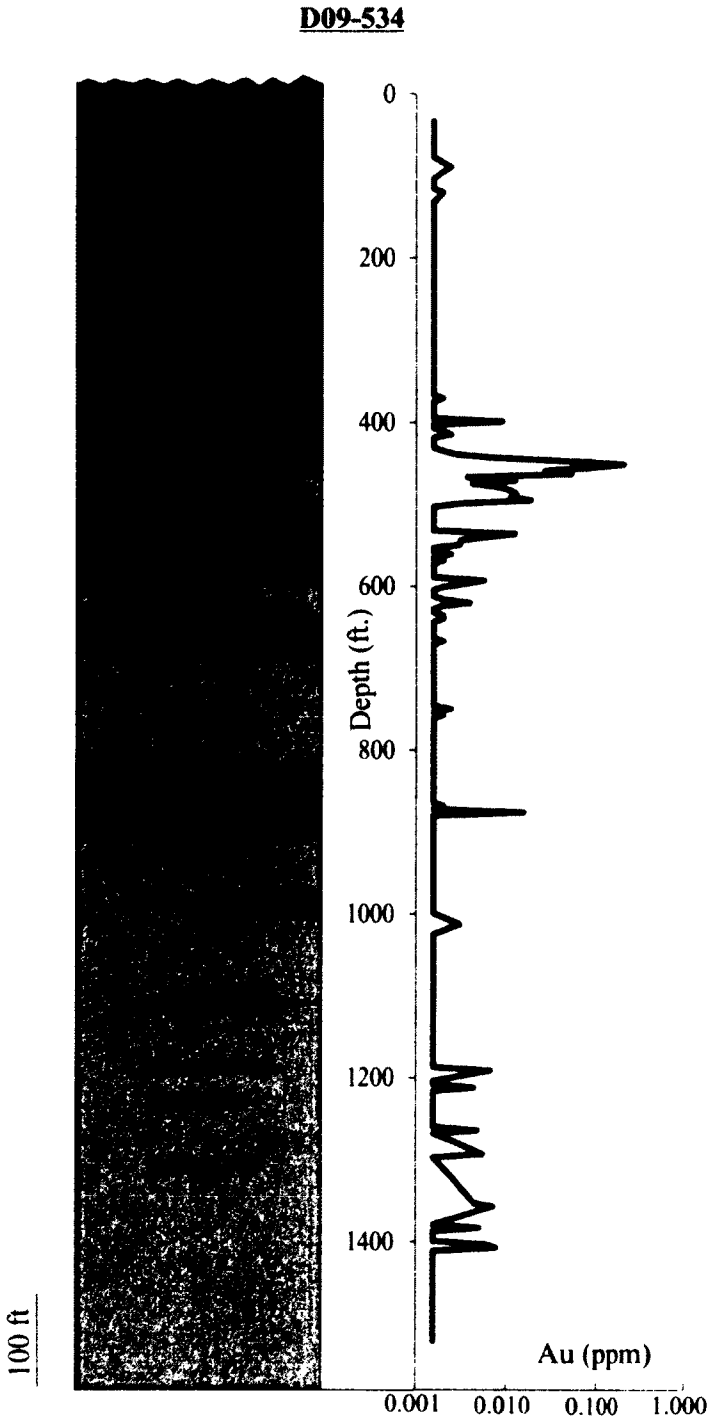

Figure 3.2. Graphical representation of drill hole D09-534. Log Au assay values on right. The bulk of the grade is at the bottom of the uppermost skarn layer.

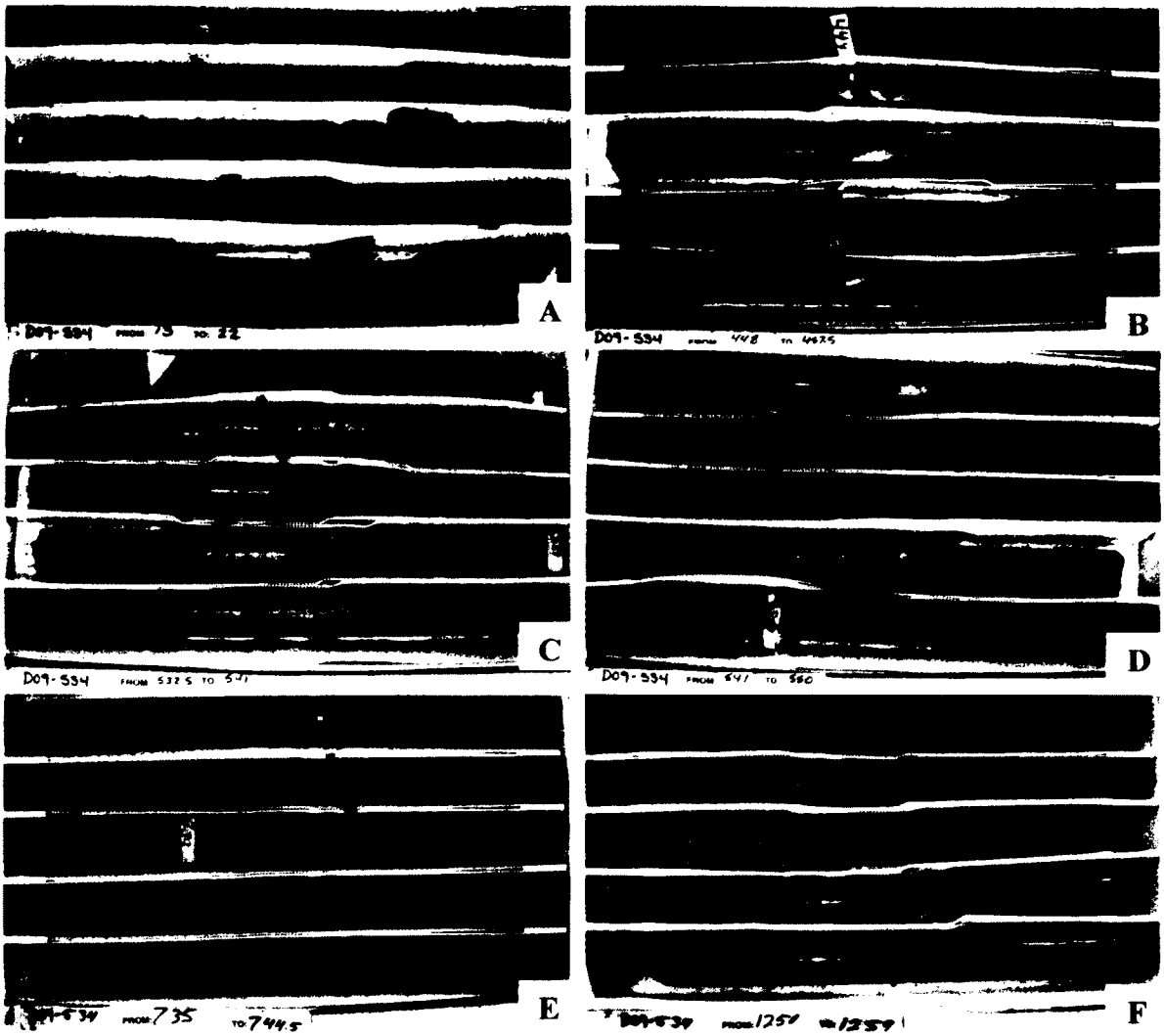

Figure 3.3 (a-f). Core photos of representative intervals for drill hole D09-534. A- Typical basaltic rock. B- Interleaved pyroxene and garnet skarn. C- Calc-silicate hornfels (banded) with transition into pyrrhotite dominant skarn. D- Transition with depth from pyrrhotite rich skarn to magnetite + clinopyroxene dominant skarn. E- Classic example of skarn vs. hornfels with darker interval of likely metasomatic (skarn) garnet in the center. F- Calc-silicate hornfels. Each core box is 2 feet (0.6 m) long. Po = pyrrhotite. Gar = garnet. Green line marks transitions between units when they occur in the interval displayed.

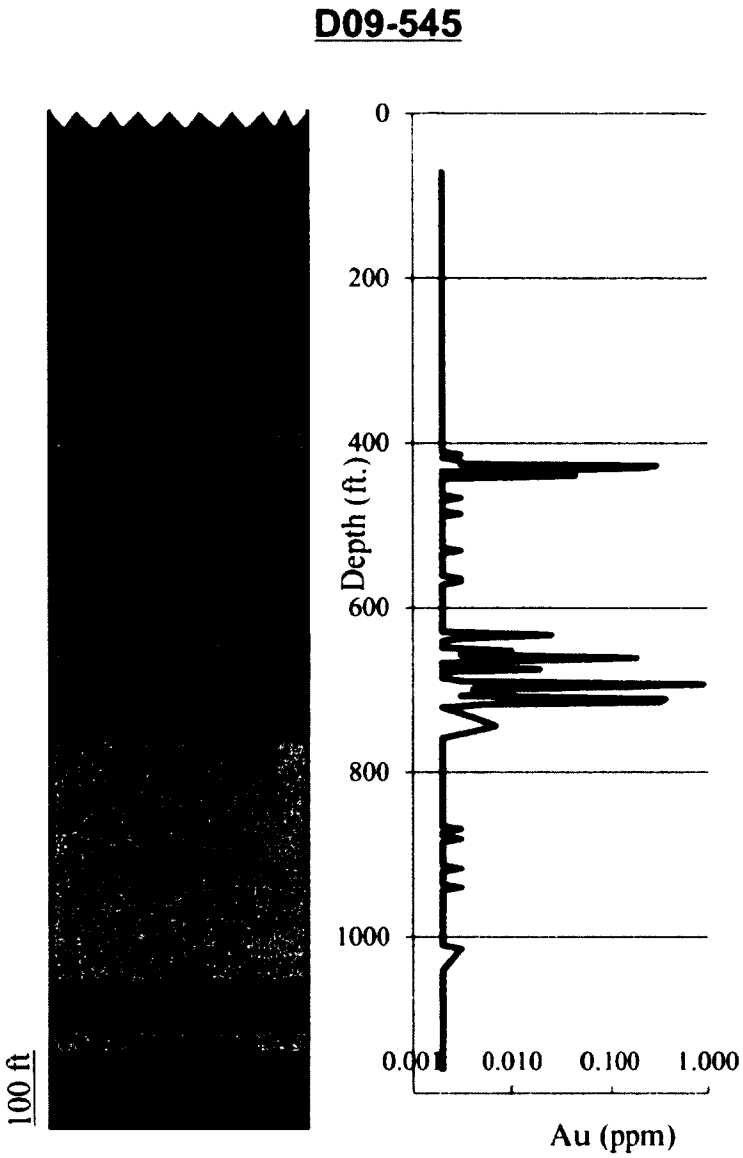

Figure 3.4. Graphic representation of drill hole D09-545. Log Au assay values on right. Schematic skarn pattern at 600 – 800 ft. indicates skarn interleaved with host units.

This zone consists of a mixture of contact metamorphosed volcanic rock and skarn and eventually turns into strictly skarn and then marble. The complex zone is shown simply as 'hornfels' on Fig. 3.4. The marble, intercalated with thin calc-silicate hornfels and pyroxene-rich skarn layers, extends to 650 feet (198 meters). A complex mixture of rock types (Fig. 3.5) occurs between 650 and 750 feet, shown diagrammatically as skarn overprinting hornfels and marble (Fig. 3.4).

A massive hornfels unit of varying composition extends from 750 feet to approximately 1050 feet. Rare garnet-rich skarn intervals (Fig. 3.5) were intercepted in this unit. Most of the rock is clearly altered biotite hornfels or calc-silicate hornfels. The intrusive rock intersected at the bottom is likely the Southwest pluton.

3.2.1.c Western Southwest Zone

The western part of the Southwest Zone has been entirely mined and backfilled and information about it is only available in drill core. Drill hole D07-404 (Fig. 3.7) represents this part of the deposit. This 54 foot (16 meters) hole was drilled underground down into marble from the uppermost part of the skarn. Based on other drill holes in the area, mineralized marble continues down for hundreds of feet. In other words, this part of the Southwest Zone is much thinner than the rest. The skarn mineralogy here is exclusively chlorite, phlogopite, plagioclase, calcite, and variable pyrrhotite; it lacks pyroxene. This section is a good example of misidentified mineralogy: the interval was logged as 'pyroxene skarn and marble' (due to the pale green color?), but in fact the higher grade parts are mostly phlogopite-rich skarn and the intervening lower grade

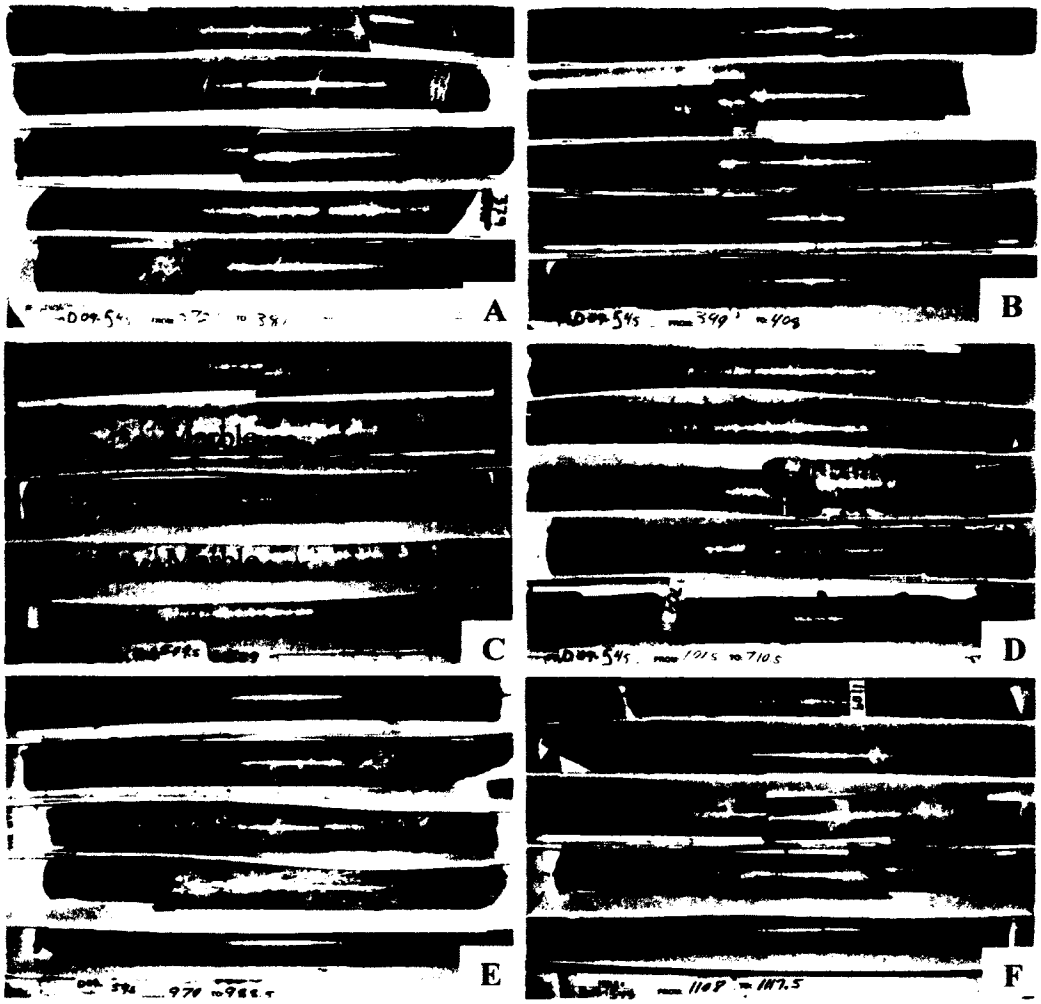

Figure 3.5 (a-f). Core photos of representative intervals for drill hole D09-545. A. Rocks interpreted as basalt flow with 1-5 mm hornblende phenocrysts. B. Basalt/marble contact. C. Marble with small bands of green mineral (phlogopite or pyroxene?). D. Transition with depth from calc-silicate hornfels into high grade pyrrhotite-chlorite-phlogopite-plagioclase low temperature assemblage. E. Classic example of biotite hornfels with intense stockwork veining and no mineralization. F. Biotite hornfels (first row) followed by calc-silicate (pyroxene) hornfels; distinguished by the pale color.

Figure 3.6. Photomicrograph of gold-bearing thin section from D07-404 at 12.5 ft. (3.8 m) Brown= phlogopite, green =chlorite, white= calcite, black=pyrrhotite.

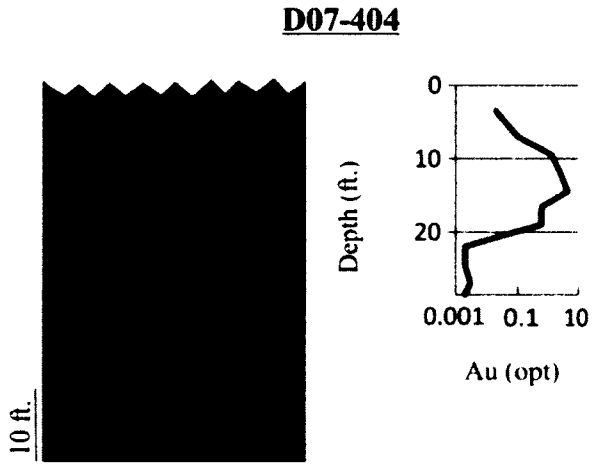

Figure 3.7 Graphic representation of drill hole D07-404. Log Au assay values on right. Underground drilling started at approximately the skarn/basalt contact. 10 ft. = 3 m.

material mostly marble. A thin section taken at 12.5 feet (3.8 meters) revealed the low temperature assemblage bearing abundant phlogopite (Fig. 3.6). The lower one-third of the skarn, while apparently indistinguishable in mineralogy, is low grade to barren, particularly at the marble front (Fig. 3.7) The hole ends at 54 feet (16 meters) in unaltered marble (Fig. 3.8).

3.3 Overall mineral occurrence and zoning in the Southwest Zone

I collected samples throughout the Southwest Zone from both drill core and underground exposures in order to record the spatial distribution of the major minerals (Fig. 3.9). Sample descriptions are given in Tables 3.2, 3.3 and 3.4. The skarn on the eastern side of the deposit was originally more garnet rich and in places contains abundant magnetite (Figure 3.10). The garnet-rich skarn has been extensively retrograded to epidote-dominant skarn in many places. The central and east-of-central region of the Southwest Zone typically hosts pyroxene-garnet skarn (Fig. 3.11), with the ratio of pyroxene to garnet increasing to the west. Pyroxene abundance continues to increase toward the west, then decreases in abundance relative to low temperature and retrograde assemblages near the North Lookout Fault and near the marble front (Fig. 3.12). From my data, the magnetite distribution seems erratic and not at all restricted to the eastern part of the Southwest Zone. Pyrrhotite seems to be more abundant along the marble front and otherwise shows no obvious pattern.

This distribution of silicate mineralogy (Fig. 3.9), when compared to a general skarn model (e.g. Fig. 1.4), suggests fluid movement from east to west across the

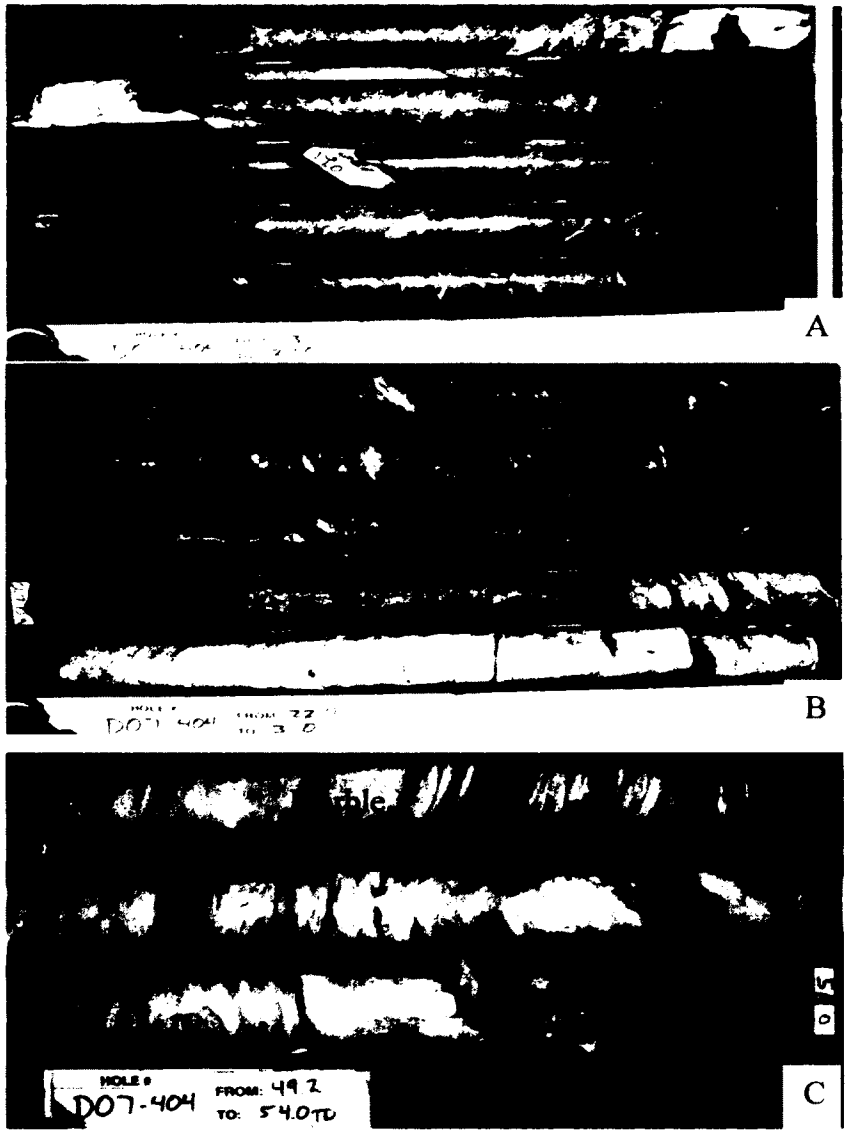

Figure 3.8. Core photos of representative intervals in D07-404. A- Mineralized portion of the low temperature assemblage. B- Marble contact (lower) with low temperature assemblage (higher). C- Unaltered marble. Green line marks the contact between skarn and marble.

Table 3.2 Modal mineralogy of skarn hand samples through the Southwest Zone.

Locations shown on Fig. 3.9.

Sample	Prograde		Retrograde		
	% Pyx	%Gar	% Amph	%Epi	% Chl
1	5-20%	5-20%	>50%	1-5%	
2	>50%	1-5%		1-5%	
3				>50%	5-20%
4	>50%		5-20%		
5	>50%		1-5%		
6				>50%	1-5%
7		1-5%	>50%		
8	>50%		1-5%		
9	>50%	<1%			
10		5-20%	>50%		
11	>50%	5-20%	5-20%		
12	>50%	1-5%	5-20%		
13		20-50%		>50%	
14	>50%	5-20%	5-20%	1-5%	
15	20-50%	5-20%	20-50%	<1%	
16		>50%	<1%	1-5%	
17		5-20%		>50%	
18	5-20%		1-5%	1-5%	
19			>50%	<1%	
20					
21					>50%
22				>50%	
23	>50%		5-20%	1-5%	1-5%
24	>50%	5-20%	5-20%	1-5%	
25	>50%	1-5%	20-50%		
26			>50%	<1%	1-5%
27	>50%	5-20%	1-5%	1-5%	
28	5-20%	5-20%	>50%		
29		20-50%	20-50%	20-50%	
30	20-50%	<1%	20-50%		
31	>50%	1-5%	5-20%		
32	>50%	5-20%	5-20%	1-5%	
33	>50%	1-5%	5-20%		
34	1-5%	>50%		5-20%	
35	>50%	5-20%	5-20%		
36		>50%		1-5%	
37		>50%		1-5%	1-5%
38		5-20%	>50%		
39	20-50%	20-50%	5-20%		1-5%

Table 3.3 Skarn hand sample descriptions.

Sample #	Comments
1	Original marble still present. Pyroxene almost all gone to amphibole (Ar-Ar dated hornblende.) Garnet present in small bands.
2	All samples are small, garnet in very small blebs actively being replaced by epidote. %Po on the lower end of 5-20%
3	Epidote dominant with patches of chlorite
4	Massive pyroxene going to amphibole
5	Massive pyroxene going to amphibole with minor pyrrhotite
6	Massive epidote, less sulfide.
7	Mostly amphibole after pyroxene with pyrrhotite strings and garnet blebs
8	Pyroxene dominant, locally going to amphibole, basically no sulfide
9	Pyroxene dominant with cross-cutting band of pyrrhotite and magnetite cutting. Very, very small blebs of garnet.
10	Pyroxene has all gone to amphibole (stilpnomelane?) 2% K 6%Ca, garnet against original calcite in small blebs.
11	Mostly pyroxene (going to amphibole and stilpnomelane visibly) and minor garnet, with sigmoidal texture in garnet.
12	Mostly pyroxene with about half the pyroxene going to amphibole, smaller samples have garnet bands but the big samples don't, mostly pyrrhotite for the sulfide with fine disseminated magnetite associated.
13	Dominantly epidote with some remnant garnet interstitially and as larger chucks along fractures.
14	Dominantly pyroxene, locally gone to amphibole.
15	Odd distribution of amphibole vs. pyroxene, individual samples are either all amphibole or all pyroxene, pyroxene samples have minor garnet
16	Garnet dominant, adjacent to epidote altered dike of something and an unaltered quartz porphyry dike.
17	Epidote dominant, very baked-looking with small patches of garnet.
18	Dominantly magnetite w/ original calcite and some pyroxene, pyroxene is interstitial to magnetite.
19	Dominantly pyroxene gone to amphibole w/ abundant pyrrhotite, some garnet.
20	Epidote retrograded after garnet.
21	Dominantly chlorite, biotite, plagioclase, and quartz. Low temperature assemblage +Au?
22	.5% Ti = endoskarn, advanced propylitic alteration, all epidote.
23	Massive magnetite with pyroxene, LOW T assemblage? Some samples are really soft... Biotite, chlorite, and calcite.
24	Garnet dominant with fairly intense retrograde alteration, magnetite>pyrrhotite>>chalcopyrite

Table 3.3 (continued) Skarn hand sample descriptions-continued.

Sample #	Comments
25	Pyroxene dominant with patchy retrograde alteration of pyroxene to amphibole
26	Pyroxene dominant but strongly retrograded to amphibole, accompanied by pyrrhotite
27	Pyroxene only slightly greater than garnet, minimal retrograde, remnant calcite, very little sulfide
28	Very retrograded pyroxene to amphibole, some samples contain garnet.
29	Some samples are mostly epidote and garnet and some are almost entirely amphibole... so not sure which was more dominant in that particular heading
30	Pyroxene mostly gone to amphibole w/ massive magnetite +lesser pyrrhotite adjacent original marble
31	Dominantly pyroxene with small zones of amphibole and patches of garnet
32	dominantly pyroxene with garnet veinlets
33	Epidote- after garnet- and pyroxene
34	Endoskarn against Buckhorn stock (.2%Ti, 190 Zr), garnet dominant against the endoskarn
35	Pyroxene dominant with abrupt contact between massive pyroxene and very sheared pyroxene/amphibole with sigmoidal garnets
36	Garnet dominant with abundant disseminated magnetite
37	Garnet dominant with a little chlorite along the tear fault in the East Ramp
38	Very retrograded with minor garnet present as bands and very abundant sulfide
39	Abrupt contact between pyroxene and garnet w/ amphibole at the contact, sulfide somewhat restricted to the pyroxene

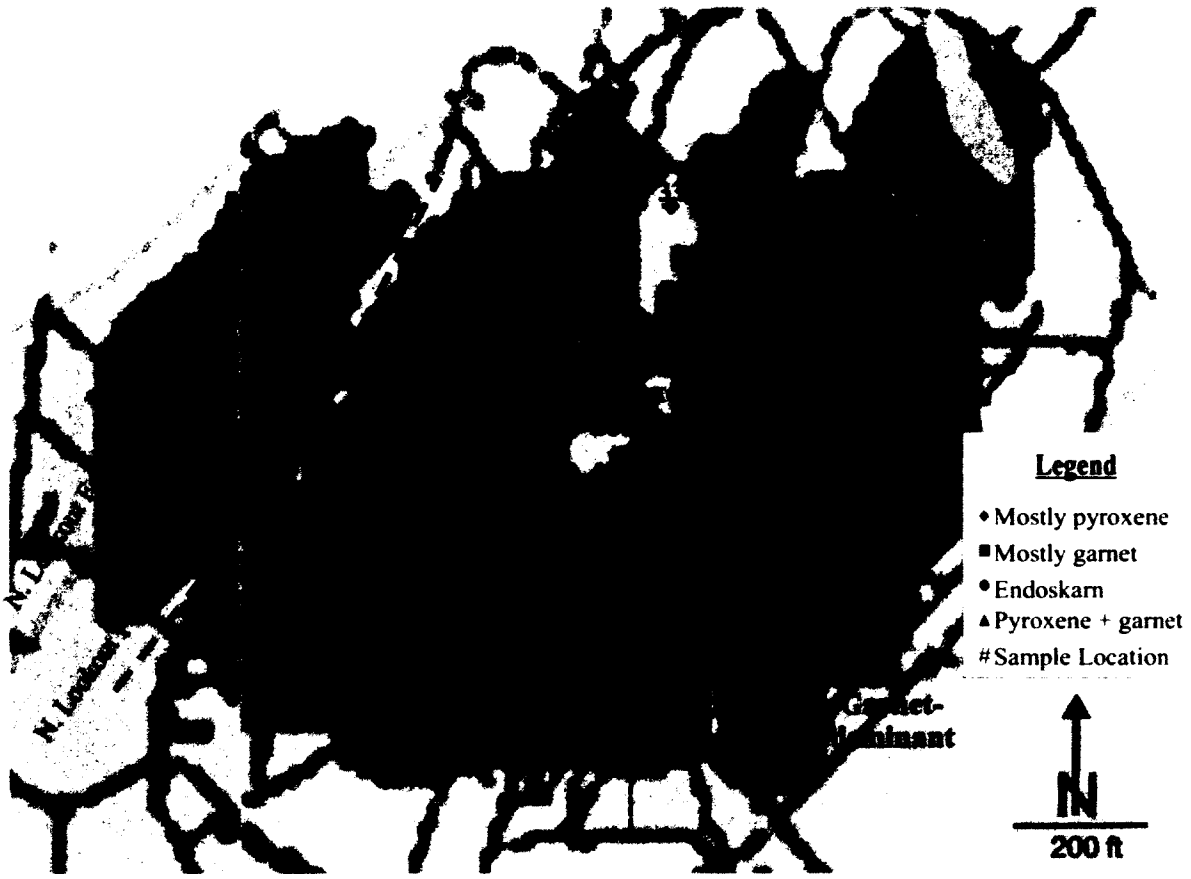

Figure 3.9. Distribution of silicate mineralogy in the Southwest Zone as exposed in underground headings. The numbers represent samples described in Tables 3.2 - 3.4. The underlying map is the surface geology with the underground ore body shown in brown; faults are shown in medium blue. Garnet-dominant skarn on the eastern side suggests a broad ESE to WNW zoning distinguished by the dashed hand-drawn contour lines. Garnet-endoskarn occurrence in the middle of the Southwest Zone is attributed to a cross-cutting dike and its influence, the dotted line around it represents the transition from rocks containing roughly proportionate amounts of garnet and pyroxene to rocks which are pyroxene dominant. 200 ft. is approximately 60 m.

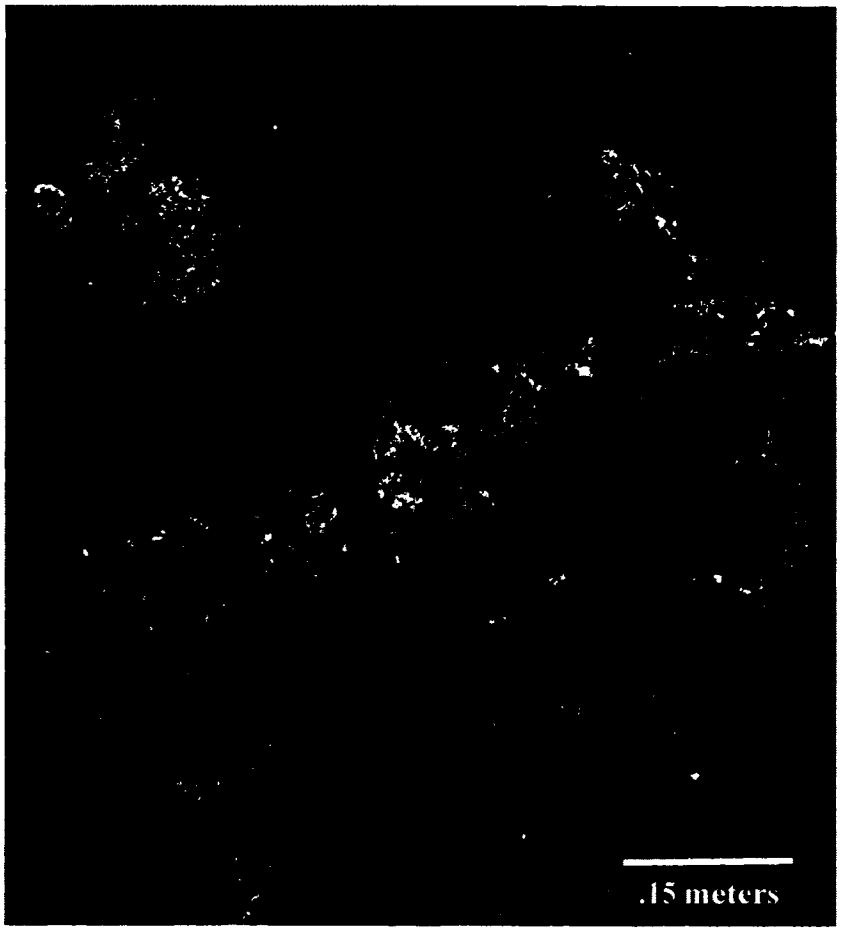

Figure 3.10. Garnet (red-brown)-magnetite (black) rich skarn. Photo taken from an underground heading in the eastern part of the Southwest Zone.

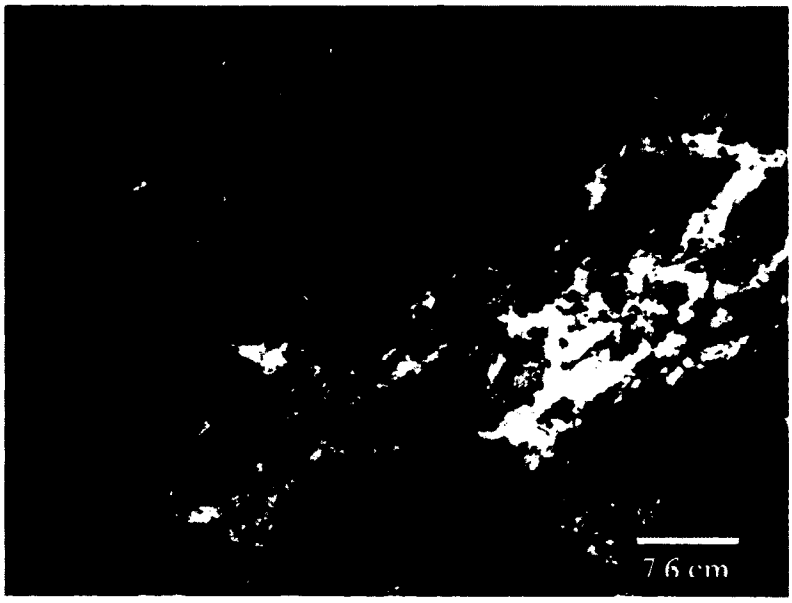

Figure 3.11. Exposure in the central Southwest Zone of garnet-pyroxene skarn. The garnet-rich bands might represent original Al-rich layers in marble.

Figure 3.12. Underground heading showing the "marble front"- skarn contact. Skarn here is pyrrhotite-rich skarn (dark brown) against white marble.

Southwest Zone. The vertical variation in mineralogy in D09-534 and D09-545 also suggests a vertical component to the fluid movement. This pattern suggests the fluid source (i.e., the source pluton) is at depth on the east side of the Southwest Zone, and that fluids ascended along the marble contact.

3.4 Gold Bowl (GB)

My detailed underground mapping in the Gold Bowl (Fig. 3.13) revealed no marble and complex relations between the various metamorphic units. I consequently interpret the original stratigraphy of the Gold Bowl to include hornfels generated from multiple protoliths (i.e., more than one host rock). At a minimum, there must have been Si-bearing calcareous rocks that generated calc-silicate hornfels and pelitic rocks that generated the biotite hornfels. The biotite hornfels is never altered to skarn but in a few places contains intense stockwork veining indicative of hydrothermal fluid movement. The area also contains rare layers of apparently volcanogenic sandstone (Fig. 3.13) with a composition equivalent to the overlying basaltic rocks. These layers proved impossible to distinguish from medium-grained igneous rocks underground. I labeled several bodies 'igneous looking' because, lacking hand samples, I can't be sure that they weren't volcaniclastic rocks. If these volcaniclastic rocks are indeed part of the basaltic unit, then the host sequence at Gold Bowl is either a basaltic unit (and thus, hosted in a different portion of the regional stratigraphy than the Southwest Zone skarn stratigraphy) or there are cryptic thrusts with interleaved older and younger rocks.

Systematic changes in orientation of thin calc-silicate bands in the hornfels units and of the gabbro sills reveals a pattern of broad, NW-plunging folds with wavelengths of several hundred feet. I noted faults, mostly oriented NNW or NNE, but found no slickenlines and rarely found measurable offsets. In the few cases where I found offsets, they were less than a foot (30 cm) with normal displacement. The high-angle, NE-trending faults are presumably normal faults that parallel the bounding graben (Fig. 1.11).

Intrusions I conclusively identified from chemical compositions in the Gold Bowl include Buckhorn pluton, marginal phase, Ti diorite, and gabbro. The latter—as well as several of the others—I recognized as sills rather than dikes. The gabbroic sills were likely part of a feeder zone for overlying basalt. The abundance of sill-like bodies in the Gold Bowl is in sharp contrast to the dikes in the Southwest Zone.

The lack of marble host rock at Gold Bowl makes skarn zoning problematic and necessarily different from that of the Southwest Zone. Skarn at Gold Bowl appears to have preferentially replaced more Ca-rich hornfels layers - in a few places witnessed as irregular garnet replacements (e.g., Fig. 3.14). More generally, the soot-covered underground exposures kept me from identifying skarn-hornfels relations.

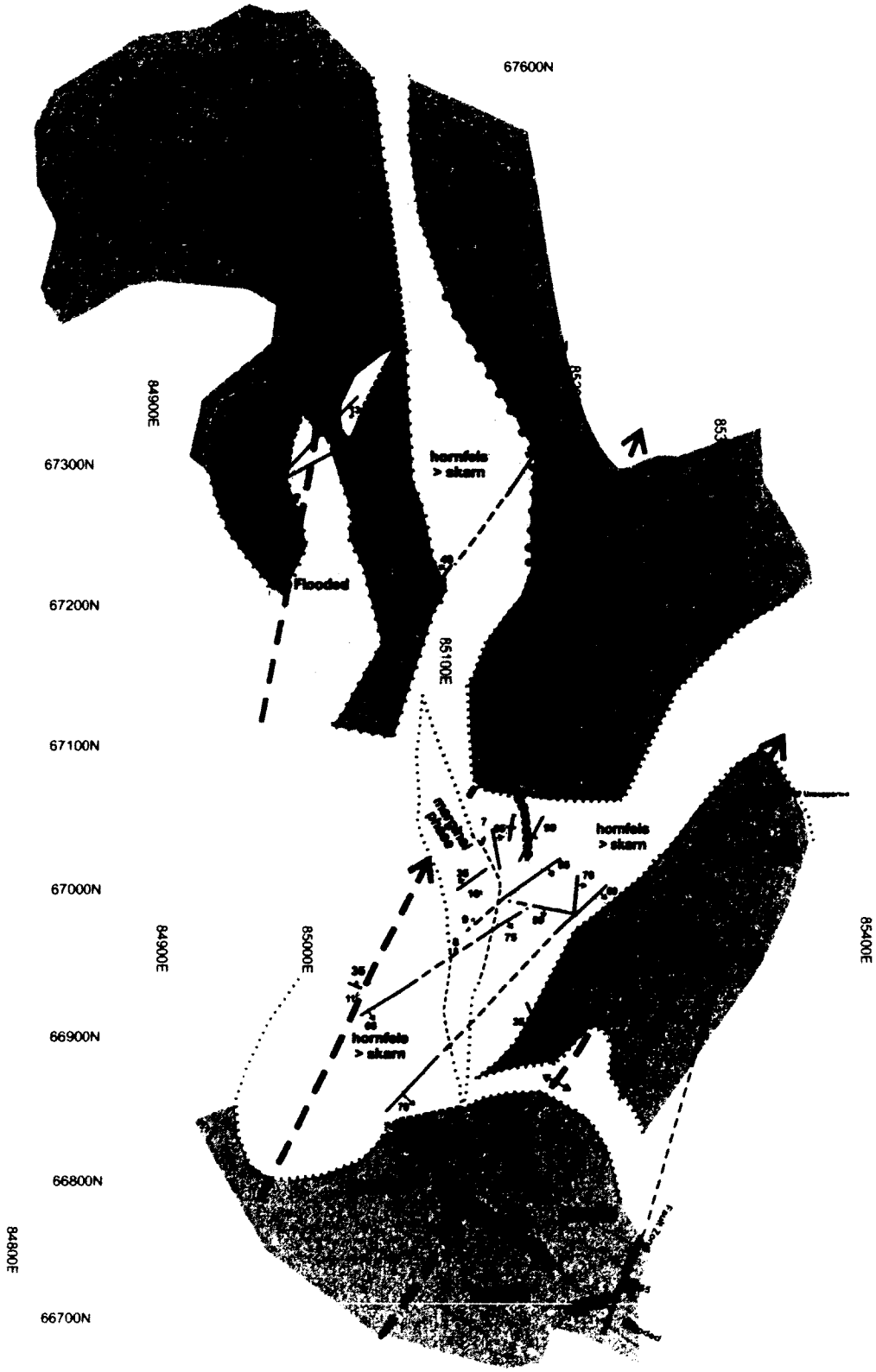

Figure 3.13a. Detailed underground map of the Gold Bowl workings. Legend follows.

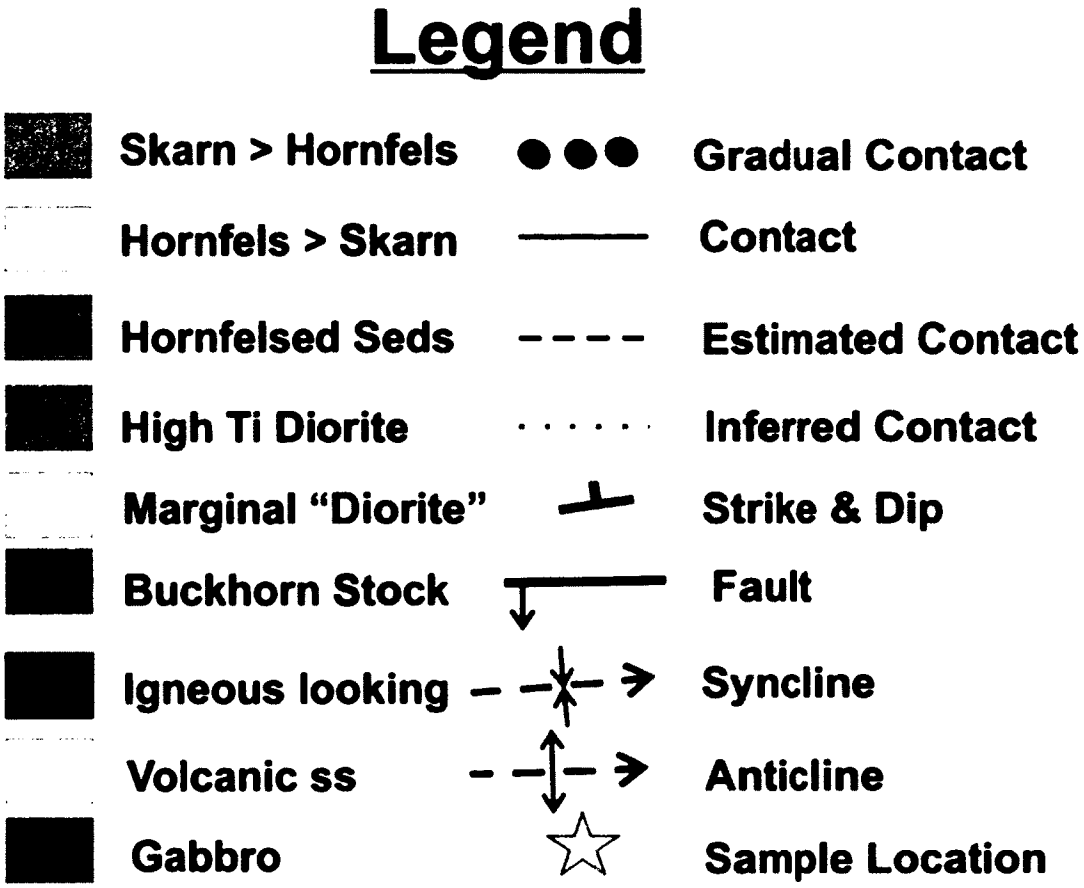

*Measured on layering within bedding or sills. Map grid is 100 feet (30 m.), state plane coordinates.

Figure 3.13b. Legend for underground map in Figure 3.13a.

Figure 3.14. Garnet skarn (outlined in black sharpie) replacing a calcareous hornfels. Magnet is 8 cm long. Photo taken in the Gold Bowl underground workings.

3.5 Elemental composition of the Buckhorn skarn

I performed bulk geochemical analyses on pulp samples from ore zones throughout the deposit. The analyses can be used to make distinctions between and support hypotheses concerning the three main portions of the Buckhorn deposit: the Gold Bowl, the Southwest Zone, and the recently delineated West Southwest Zone.

Table 3.5 summarizes the chemistry and highlights some important differences between Gold Bowl, Southwest Zone, and West Southwest Zone. Mapping in the Gold Bowl revealed no marble, and the mean and median values for wt % CaO for the Gold Bowl are, in fact, slightly lower than for the rest of the deposit. The western portion of the Southwest Zone includes a lower temperature assemblage of minerals which includes

Table 3.4 Descriptive statistics derived from XRF analysis of pulp samples from a representative suite of ore zones across the deposit.

GB (48 analyses)	Na_2O	MgO	Al_2O_3	SiO_2	P_2O_5	S	*Cl	K_2O	CaO	TiO_2	*V	*Cr	MnO	FeO	*Co	*Zr
Mean	1.50	3.80	9.84	41.6	0.24	2.00	0.04	0.39	21.3	0.72	0.02	0.01	0.39	17.3	0.01	0.01
Medium	0.27	3.31	9.17	41.2	0.21	0.31	0.02	0.11	22.9	0.67	0.02	0.01	0.37	15.4	0.01	0.01
Minimum	0.03	1.27	2.59	12.7	0.04	0.00	0.00	0.01	8.17	0.11	0.00	0.00	0.12	5.56	0.00	0.00
Maximum	7.28	7.53	16.7	55.1	0.66	16.3	0.27	2.07	39.8	1.45	0.07	0.04	0.77	53.2	0.09	0.03
SWZ (318 analyses)																
Mean	0.43	3.63	4.33	33.0	0.10	1.58	0.03	0.60	30.6	0.25	0.01	0.02	0.29	23.3	0.01	0.00
Medium	0.12	2.84	2.83	35.2	0.07	1.16	0.02	0.13	25.2	0.14	0.00	0.02	0.30	21.4	0.00	0.00
Minimum	0.01	0.25	0.13	1.03	0.00	0.00	0.00	0.00	4.19	0.00	0.00	0.00	0.01	0.75	0.00	0.00
Maximum	6.99	14.7	17.3	93.9	0.57	14.0	0.29	5.49	96.7	1.06	0.04	0.07	0.89	69.2	0.26	0.02
WSWZ (38 analyses)																
Mean	0.65	4.17	7.80	36.0	0.17	2.50	0.02	1.23	27.9	0.38	0.01	0.02	0.21	18.6	0.00	0.00
Medium	0.16	4.39	6.37	35.3	0.14	2.09	0.02	1.18	23.4	0.30	0.00	0.02	0.21	21.3	0.00	0.00
Minimum	0.01	1.14	1.35	7.65	0.02	0.13	0.00	0.07	7.03	0.04	0.00	0.00	0.07	2.39	0.00	0.00
Maximum	5.77	10.3	17.9	58.3	0.45	7.63	0.08	3.76	83.1	0.87	0.04	0.04	0.53	33.5	0.06	0.02

* indicates samples for which >20% of the analyses were below detection limits and instead recorded as half the lowest reported value (0.00 in this table means "<.01").

phlogopite; analyses from this portion of the deposit confirm this mineralogical change with notably higher K_2O.

The tables of correlation coefficients show striking patterns both within data sets (e.g., Southwest Zone) and also between data sets (e.g., Southwest Zone vs. Gold Bowl). One common and easy-to-understand correlation is between Ti and V: these elements behave similarly and commonly occur together, thus display strong correlations. One of the striking features is the difference in elemental correlations for Au among the three data sets.

Within the Gold Bowl Ti negatively correlates with Au and both S and Fe positively correlate (Table 3.6). Within the Southwest Zone no non-ore element appreciably correlates with Au (Table 3.7). Within the West Southwest Zone, Mn positively correlates with Au. I interpret these elemental relationships to indicate gold occurs frequently with pyrrhotite at Gold Bowl, occurs with a wide range of minerals in the Southwest Zone, and occurs with Mn-rich ('distal') silicates at West Southwest Zone.

Another striking feature is the common correlation of P with a variety of elements—Na, Al, Si, K, Ti, V—in both the Southwest Zone and West Southwest Zone data but no strong correlation between P and any element in the Gold Bowl data set. The

Table 3.5 Correlations between major elements by XRF analysis from ore intercepts in the Gold Bowl.

Gold Bowl																			
	Au	Na2O	MgO	Al2O3	SiO2	P2O5	S	*Cl	K_2O	CaO	TiO_2	*V	*Cr	MnO	FeO	*Co	*Rb	Sr	*Zr
Au (ppm)	1.00																		
Na2O	-0.27	1.00																	
MgO	-0.16	0.37	1.00																
Al2O3	-0.42	0.76	0.37	1.00															
SiO2	-0.40	0.69	0.48	0.72	1.00														
P2O5	-0.2	0.09	0.38	0.117	0.263	1.00													
S	0.51	-0.28	-0.4	-0.619	-0.78	-0.29	1.00												
Cl	-0.14	0.30	0.44	0.19	0.06	-0.09	0.08	1.00											
K2O	0.08	0.53	0.33	0.47	0.34	-0.19	-0.02	0.32	1.00										
CaO	0.01	-0.74	-0.35	-0.38	-0.34	0.01	-0.24	-0.50	-0.64	1.00									
TiO2	-0.43	0.70	0.45	0.80	0.64	0.28	-0.55	0.25	0.24	-0.35	1.00								
V	-0.32	0.59	0.59	0.69	0.55	0.14	-0.46	0.45	0.29	-0.39	0.79	1.00							
Cr	-0.26	-0.16	-0.30	0.05	-0.04	-0.27	-0.17	-0.21	-0.27	0.35	-0.11	-0.03	1.00						
MnO	-0.10	-0.70	-0.52	-0.42	-0.30	-0.08	-0.17	-0.41	-0.63	0.84	-0.45	-0.46	0.46	1.00					
FeO	0.42	-0.51	-0.42	-0.76	-0.88	-0.27	0.92	0.13	-0.18	-0.04	-0.67	-0.54	-0.11	0.08	1.00				
Co	0.31	-0.29	-0.21	-0.47	-0.49	-0.01	0.63	0.11	-0.18	-0.19	-0.37	-0.25	-0.29	-0.10	0.68	1.00			
Rb	0.09	0.41	0.31	0.41	0.24	-0.17	0.00	0.28	0.91	-0.54	0.13	0.24	-0.25	-0.49	-0.12	-0.12	1.00		
Sr	-0.11	0.13	0.18	0.44	0.26	0.31	-0.27	-0.09	0.09	-0.07	0.47	0.30	-0.31	-0.28	-0.32	-0.03	0.05	1.00	
Zr	-0.06	0.20	0.11	0.19	0.19	0.15	-0.16	0.16	-0.05	-0.15	0.28	0.17	-0.30	-0.18	-0.13	0.26	-0.09	0.20	1.00

Table 3.6 Correlations between major elements by XRF analysis from ore intercepts in the Southwest Zone.

Southwest Zone																			
	Au	**Na_2O**	**MgO**	**Al_2O_3**	**SiO_2**	**P_2O_5**	**S**	***Cl**	**K_2O**	**CaO**	**TiO_2**	***V**	***Cr**	**MnO**	**FeO**	***Co**	***Rb**	**Sr**	***Zr**
Au	1.00																		
Na_2O	-0.12	1.00																	
MgO	-0.03	-0.06	1.00																
Al_2O_3	-0.17	0.68	-0.03	1.00															
SiO_2	-0.01	0.48	0.02	0.54	1.00														
P_2O_5	-0.12	0.53	-0.11	0.83	0.53	1.00													
S	0.28	-0.20	-0.16	-0.19	0.00	-0.05	1.00												
Cl	0.13	-0.04	-0.08	0.08	0.08	0.08	0.25	1.00											
K_2O	-0.02	0.55	-0.03	0.74	0.38	0.49	-0.12	0.19	1.00										
CaO	-0.16	-0.30	0.08	-0.32	-0.72	-0.38	-0.26	-0.14	-0.25	1.00									
TiO_2	-0.13	0.52	-0.05	0.91	0.48	0.82	-0.18	0.12	0.69	-0.26	1.00								
V	-0.12	0.38	-0.06	0.72	0.37	0.67	-0.13	0.11	0.56	-0.22	0.74	1.00							
Cr	-0.05	0.01	-0.22	0.08	0.06	0.14	0.18	0.00	-0.05	-0.15	0.04	0.10	1.00						
MnO	-0.02	-0.19	-0.23	0.08	0.31	0.23	0.08	0.06	-0.11	-0.15	0.15	0.13	0.05	1.00					
FeO	0.21	-0.30	-0.21	-0.40	-0.16	-0.26	0.35	0.09	-0.32	-0.48	-0.39	-0.30	0.16	-0.09	1.00				
Co	-0.02	-0.07	-0.14	-0.09	-0.13	-0.05	0.05	-0.05	-0.10	-0.15	-0.11	-0.05	0.20	0.06	0.37	1.00			
Rb	0.00	0.10	0.04	0.26	0.09	0.16	-0.04	0.10	0.31	-0.06	0.27	0.13	-0.13	-0.03	-0.10	-0.04	1.00		
Sr	-0.22	0.04	0.19	0.15	-0.44	0.03	-0.28	-0.13	0.08	0.71	0.17	0.13	-0.15	-0.29	-0.54	-0.19	0.09	1.00	
Zr	0.17	-0.30	-0.22	-0.25	-0.13	0.05	0.47	0.19	-0.32	-0.16	-0.02	-0.11	-0.23	-0.02	0.39	-0.19	-0.71	-0.37	-0.30

negative correlation between Ca and P in the Southwest Zone indicates that the P is not derived from a phosphatic marble; rather, the correlations with Na, Al, Si, K, and Ti suggest that P is derived from a shale-rich or detrital component to the stratigraphy. The lack of a P correlation at Gold Bowl indicates a major difference in the stratigraphic host at Gold Bowl: the phosphatic shale component is simply absent. However, the Gold Bowl data do show strong Na-K-Al-Si-Ti-V correlations, presumably indicative of a shale (detrital) component, just a different one than in the Southwest Zone area. Thus, the Gold Bowl stratigraphy differs from that of Southwest Zone and West Southwest Zone not only in the scarcity of marble, but seemingly represents an entirely different package.

If the simple skarn formation model presented in the introduction is adequate for Buckhorn, then Ca (originally present as the calcite-rich host) ought to negatively correlate with those elements added from hydrothermal solution: Si, Fe, Mn, Au, S, etc. In fact, Ca negatively correlates with both Fe and Si in the Southwest Zone (Table 3.7) and West Southwest Zone (Table 3.8), and also negatively with Al, S, and P in the West Southwest Zone. In contrast, the Gold Bowl data show negative correlations of only Na and K with Ca, and—surprisingly—a very strong (0.8) positive correlation between Ca and Mn. One interpretation of this data—consistent with the core logging and mapping results shown—is that the original host rocks for the West Southwest Zone were marble-dominated, those in the Southwest Zone had a significant marble component, and there was little marble in the original Gold Bowl host rocks. The strong Ca-Mn correlation is

Table 3.7 Correlations between major elements by XRF analysis from ore intercepts in the West Southwest Zone.

West Southwest Zone																		
	Au	**Na_2O**	**MgO**	**Al_2O_3**	**SiO_2**	**P_2O_5**	**S**	***Cl**	**K_2O**	**CaO**	**TiO_2**	***V**	***Cr**	**MnO**	**FeO**	***Co**	***Rb**	**Sr**
Au	1.00																	
Na_2O	-0.18	1.00																
MgO	0.12	0.16	1.00															
Al_2O_3	-0.30	0.70	0.34	1.00														
SiO_2	-0.04	0.35	0.39	0.22	1.00													
P_2O_5	-0.21	0.77	0.57	0.85	0.39	1.00												
S	0.35	-0.12	0.22	-0.10	0.02	-0.04	1.00											
Cl	-0.06	-0.15	0.03	-0.10	0.14	-0.14	0.05	1.00										
K_2O	-0.22	0.29	0.10	0.67	0.00	0.46	-0.14	0.29	1.00									
CaO	-0.05	-0.38	-0.68	-0.48	-0.71	-0.58	-0.47	-0.21	-0.24	1.00								
TiO_2	-0.26	0.66	0.26	0.88	0.11	0.74	-0.13	0.03	0.64	-0.37	1.00							
V	-0.17	0.59	0.07	0.72	0.14	0.57	-0.13	-0.04	0.43	-0.30	0.69	1.00						
Cr	0.26	0.06	-0.14	0.00	0.00	-0.02	0.09	-0.03	-0.06	0.01	-0.15	0.08	1.00					
MnO	0.50	-0.36	0.31	-0.23	-0.05	-0.17	0.07	0.11	-0.10	-0.14	-0.18	-0.16	0.05	1.00				
FeO	0.20	-0.19	0.42	-0.06	0.05	-0.02	0.76	0.30	-0.04	-0.61	-0.08	-0.10	-0.03	0.39	1.00			
Co	-0.03	-0.03	0.15	-0.01	0.02	-0.01	0.20	0.00	-0.01	-0.19	0.06	0.02	-0.13	0.16	0.30	1.00		
Rb	-0.16	0.09	0.08	0.34	-0.08	0.16	-0.01	0.60	0.85	-0.23	0.39	0.22	-0.12	0.02	0.24	0.12	1.00	
Sr	-0.03	-0.19	-0.62	-0.29	-0.54	-0.45	-0.52	-0.15	-0.18	0.84	-0.21	-0.14	0.03	-0.01	-0.64	-0.13	-0.21	1.00

* Indicates samples for which > 20% of the analyses were below detection limits and instead recorded as half the lowest reported value.

frankly bizarre and suggests that the calcareous component, in the original Gold Bowl stratigraphy was also Mn-enriched.

Element correlations may also be used to define alteration, for example, a correlation between Na_2O and Al_2O_3 suggest the presence of albite (or albitic alteration) in a given analysis. Lithological distinctions, or alteration patterns, can then be correlated with gold values to define the preferential host units for a given portion of the Buckhorn deposit.

3.6 Pyroxene compositional zoning

3.6.1 General considerations

It is essential to understand the origin of the pyroxene and determine both lateral and vertical variations in order to incorporate useful clinopyroxene compositional data for interpretation of general hydrothermal fluid movement. I evaluated variation of skarn clinopyroxene compositions within single drill holes (Fig. 3.15), using my data combined with that of Gaspar (2005). These results show that an average skarn pyroxene analysis from one location in a drill hole is reasonably representative of skarn pyroxene compositions for the entire drill hole. Thus, for my purposes, there is no vertical variation in average skarn clinopyroxene compositions within the Southwest Zone.

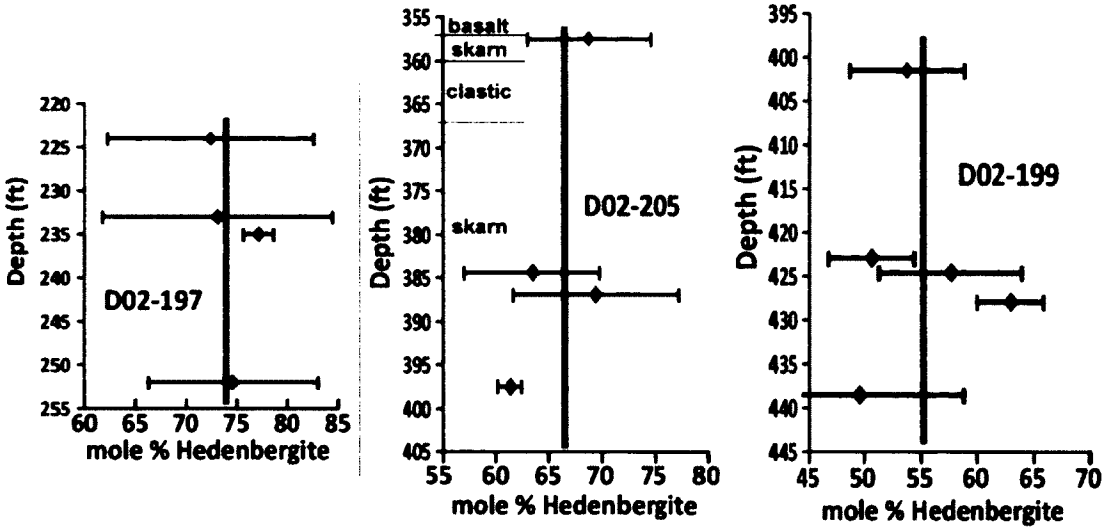

Figure 3.15. Statistical variation in clinopyroxene composition. Variation is with depth within three different drill holes in the Southwest Zone. Data from Gaspar (2005) and this study. Hole locations are from W (left) to E (right). Note progressive change from mean % Hd of 55 to 66 to 74. Intervals shown from left to right are 35 feet (11 m.), 50 feet (15 m.), and 50 feet (15 m.).

One complication is distinguishing truly metasomatic ("skarn") clinopyroxene from metamorphic clinopyroxene. The latter is present in metamorphosed impure carbonate rocks, which are especially abundant in the Gold Bowl area. Generally speaking, a 'metamorphic' clinopyroxene is tiny (< 100 microns), pale colored, and intergrown with quartz or other metamorphic minerals. Clots of such clinopyroxene can be surrounded, veined or replaced by coarser grained (> 0.5 mm), darker, euhedral clinopyroxene crystals, which are metasomatic. A plot of gold grade versus clinopyroxene composition (Fig. 3.16) highlights that low-iron pyroxene (≤ 50% Hd) is

always associated with low-Au grade intervals, and that pyroxenes with compositions of 65-78% Hd are generally gold-rich. This supports the need for using metasomatic clinopyroxene and not merely random clinopyroxenes compositions in tracking the pyroxene compositional zoning.

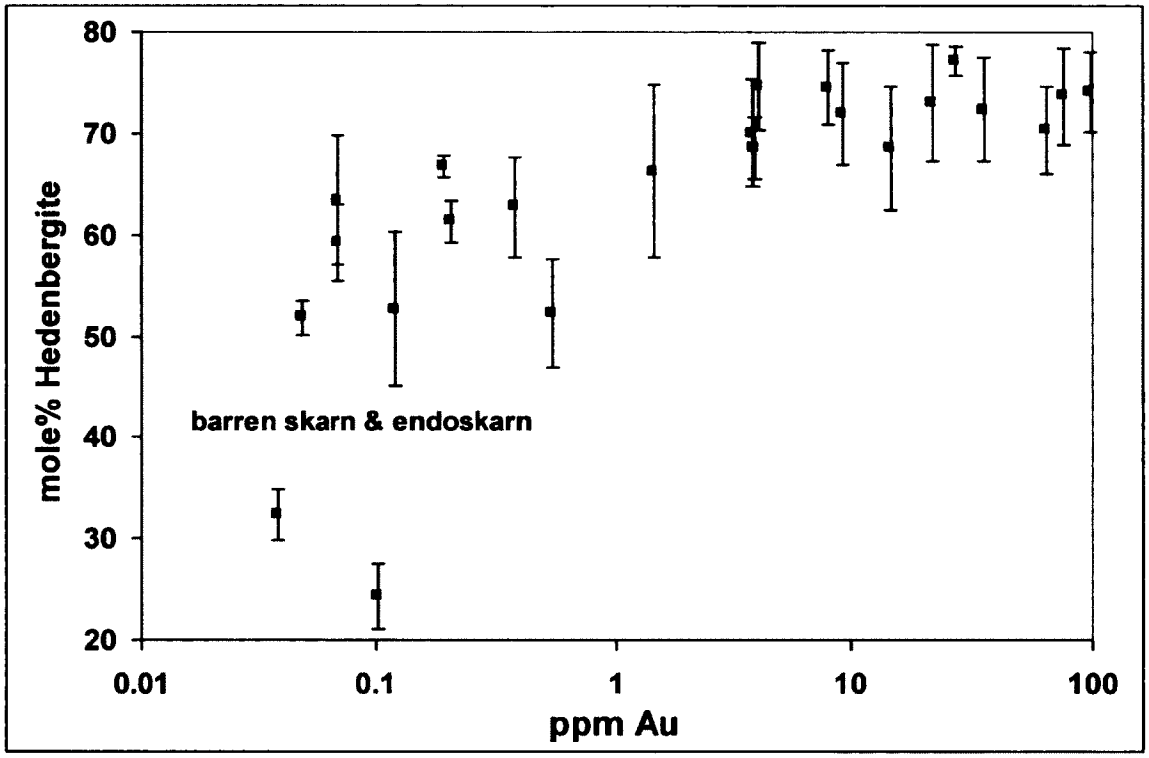

Figure 3.16. Relationship between mole % Hedenbergite in clinopyroxene and gold grade. Data from Gaspar (2005) and this study.

3.6.2 Pyroxene compositional zoning: Southwest Zone

Fig. 3.17 shows a systematic spatial variation in average clinopyroxene composition across the Southwest Zone of the Buckhorn deposit. The overall trend in clinopyroxene compositions is increasing Fe^{2+} content (% Hd) from east to west. There appear to be at least two distinct 'lobes,' one suggesting NW fluid movement along the northern part of the map and one suggesting east-west directed fluid flow through the center of the deposit. Post-mineralization quartz porphyry dikes have an orientation similar to the northern lobe, suggesting that joints were present and conducted some fluid movement. The lobe that traverses through the center of the deposit can be interpreted as a single lobe or two separate lobes.

In terms of overall fluid movement, these data suggest that the source of the fluids responsible for the formation of metasomatic (skarn) clinopyroxene is on the east side of the deposit (Fe^{2+} content increases from east to west). Fig. 3.16 shows a correlation between the amount of Fe in a clinopyroxene and gold grade, suggesting that the fluid responsible for forming the metasomatic clinopyroxenes was also responsible for gold deposition. Again the likely source of the mineralizing fluid was the east side of the Southwest Zone, in the general vicinity of the Southwest Pluton (Fig. 2.13).

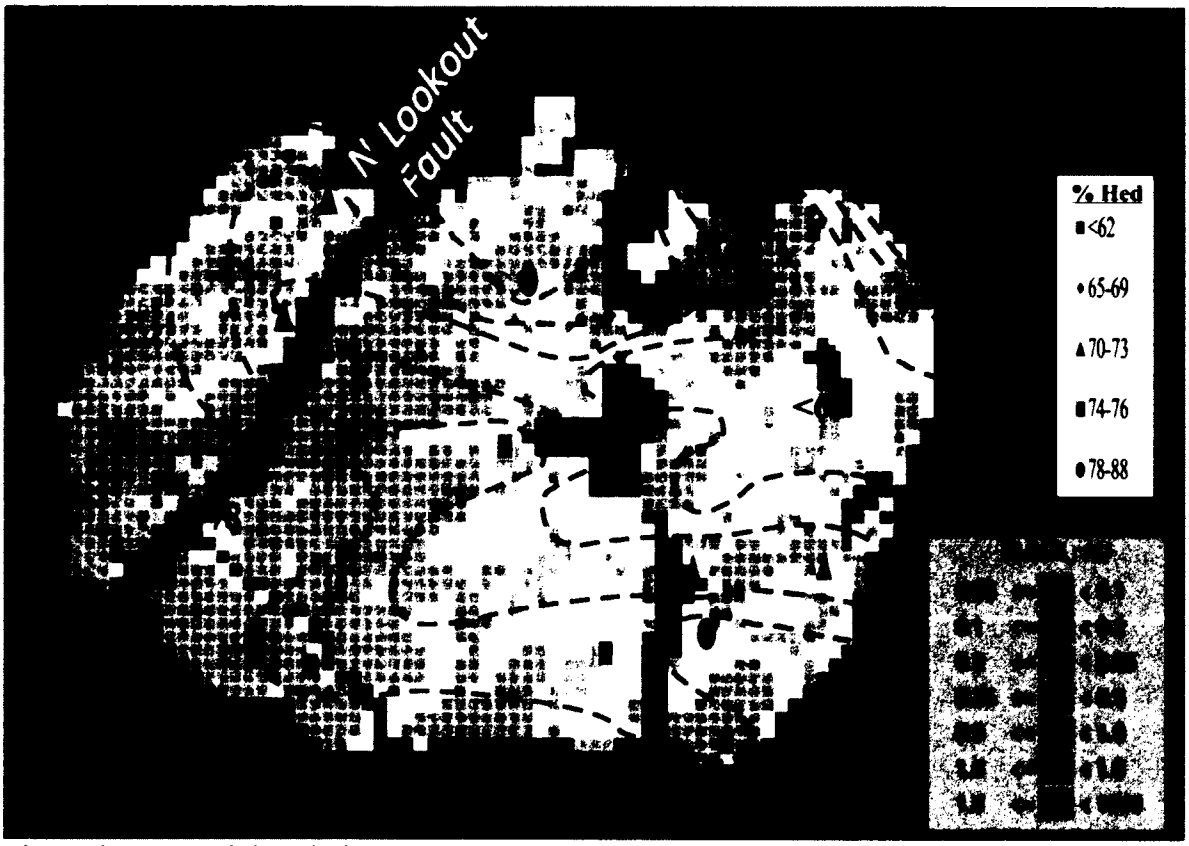

Figure 3.17. Spatial variation in clinopyroxene composition (mole % Hedenbergite) within the Southwest Zone. Average clinopyroxene composition determined by EMPA on at least ten points per sample, and then overlain on an ore grade map of the Southwest Zone. The black, dashed lines represent hand drawn contour lines of % Hedenbergite. The "BLOCK AU" legend refers to the underlying ore grade map; highest grades are pink and red, lower grades are blue to green. The left margin of the outlined body is at 48°75'N, 119°00' E.

3.7 Conclusion

A thorough examination of the mineralogy present in the Southwest Zone revealed an overall east to west trend of more garnet-rich skarn, to garnet and pyroxene-rich skarn, to pyroxene-rich skarn, to phlogopite-rich skarn. This sequential change in mineralogy reflects the change in fluid temperature and chemistry, indicating no major change in lithology exists within the Southwest Zone and that the fluids responsible for skarn formation were generated on the eastern portion of the deposit. Compositional zonation with metasomatic clinopyroxenes supports this conclusion.

The mineralogical distribution throughout the Gold Bowl is a stark contrast from that within the Southwest Zone. The amount of skarn present in Gold Bowl deposit is less than is present within the Southwest Zone. Instead it is supplemented with calc-silicate hornfels, suggesting both lithological variation and a lack of suitable host rock for skarn formation (i.e., marble). This lack of appropriate host rock makes both mineralogical and compositional zoning uninterpretable.

These contrasts suggests the two deposits are hosted in two different stratigraphic packages, highlighted by the presence of volcaniclastic rocks found solely in Gold Bowl. These differences also lend credence to the theory that Gold Bowl and Southwest Zone are two independent systems, with two independent sources (see Chapter 5).

4. Mineralization, metals, and metal zoning

4.1 Introduction

It is impossible to determine how the ore was deposited unless one knows something about the ore textural and mineralogical relationships. There is virtually no information about Buckhorn mineralization in the literature. Similarly, outside of some multi-element geochemistry for two Gold Bowl drill holes (Hickey, 1990), no multi-element information is available for the Buckhorn skarn. This makes it impossible to assess zoning or to compare it to other gold-bearing skarns. The purpose of this chapter is to provide information concerning the metals present at Buckhorn, their relationships to gold and to each other, and their relations to the various skarn stages.

4.2 Gold at Buckhorn

'Gold'—actually a gold-silver solid solution—is the ore mineral at Buckhorn. The key questions are: How does it occur? Where in the skarn does it occur? With what minerals does it occur? How does its composition vary in the deposit? I address these questions through examination of 17 gold-bearing samples from a variety of locations in the Buckhorn area (Fig. 4.1). Of these 17 locations, 12 were from the Southwest Zone, 4 from Gold Bowl, and one from an isolated skarn body west of the main mineralized area ('Mike's Skarn'; Fig. 1.11).

4.2.1 Gold-associated mineralogy

Petrographic examination of 12 gold-bearing samples (Tables 4.1-4.3) shows that gold is present with a variety of minerals and assemblages. These variable assemblages

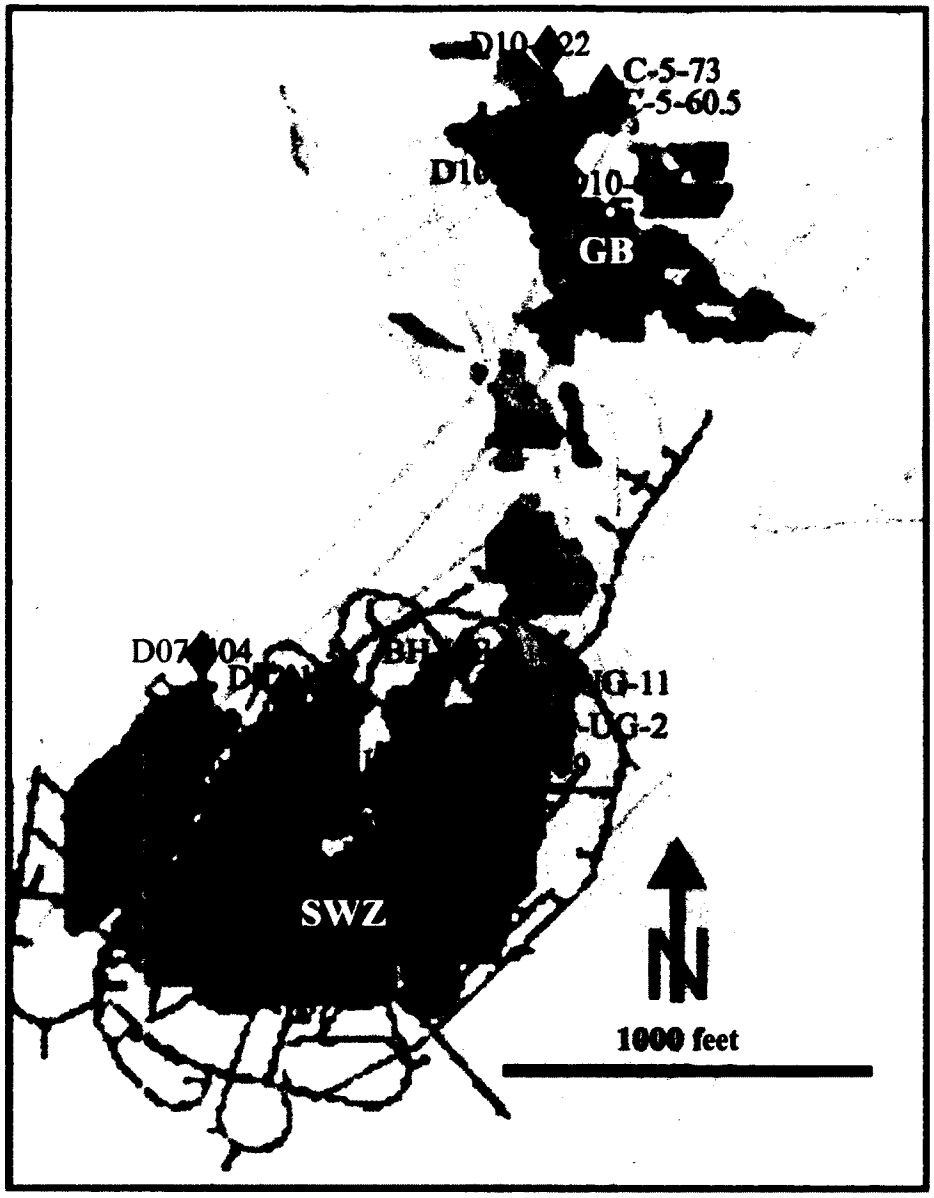

Figure 4.1. Location map for Au-bearing thin sections. GB=Gold Bowl. SWZ= Southwest Zone. Mike's Skarn sample is located approximately 4,000 ft. (1200 m) to the NW of D10-630. Scale bar is 300 meters. SWZ located at roughly 48°75'N, 119°00' E.

Table 4.1 Silicate mineralogy of Au-bearing thin sections.

*	Sample	Prograde			Retrograde				Low Temp		
		Pyx	Gar	Scap	Epi/Cz	Amph	Chl	Stilp	Bio	Qtz	Plag
P	BH-UG-8	>50%	1-5%			5-20%					
P	BH-UG-2	>50%									
P	D02-198-213.5	20-50%	20-50%			1-5%		>50%			
P/R	D10-622-159		>50%		20-50%						
P/R	BH-UG-11		20-50%		5-20%	20-50%		1-5%		1-5%	
P/R	C5-60.5	1-5%	20-50%		>50%		5-20%				
R	C5-73	1-5%	>50%		5-20%	<1%	5-20%				
R	D10-631-100.5	20-50%	1-5%	1-5%	20-50% cz		5-20%				
R	BH-UG-16		20-50%		1-5%	20-50%					
LT	D07-404-12.5						20-50%		20-50%	5-20%	5-20%
LT	D02-208-75				5-20% cz		5-20%		5-20%	20-50%	20-50%
LT	D09-545-692.5								20-50%	1-5%	5-20%

* P = Prograde, P/R = Prograde Au with retrograde minerals present, R = Retrograde, LT = Low temperature assemblages. Pyx = Pyroxene, Gar = Garnet, Scap = Scapolite, Epi = Epidote, Cz = clinozoisite, Amph = Amphibole, Chl = Chlorite, Stilp = Stilpnomelane, Bio = Biotite, Qtz = Quartz, and Plag = Plagioclase feldspar.

Table 4.2 Opaque mineralogy of Au-bearing thin sections.

*	Sample	Total % opaque	Opaque									
			Po	Cpy	Aspy	Moly	Gal	Marc	Mag	Bi	Bism	Au
P	BH-UG-8	25%	20-50%	5-20%						20-50%	20-50%	YES
P	BH-UG-2	<10%	>50%							20-50%	20-50%	YES
P	D02-198-213.5	30%	>50%	5-20%						5-20%	5-20%	YES
P/R	D10-622-159	15%	1-5%						>50%	5-20%		YES
P/R	BH-UG-11	25%	1-5%	1-5%			5-20%			20-50%	20-50%	YES
P/R	C5-60.5	35%	>50%	1-5%		1-5%				1-5%	1-5%	YES
R	C5-73	15%					1-5%			1-5%	>50%	YES
R	D10-631-100.5	>50%	>50%	1-5%	5-20%					1-5%		YES
R	BH-UG-16	40%	>50%	5-20%	5-20%					5-20%	1-5%	YES
LT	D07-404-12.5	<5%	>50%	5-20%					5-20%	5-20%		YES
LT	D02-208-75	50%	5-20%	1-5%				1-5%	>50%	5-20%	5-20%	YES
LT	D09-545-692.5	20%						1-5%	>50%	5-20%	5-20%	YES

* P = Prograde, P/R = Prograde Au with retrograde minerals present, R = Retrograde, LT = Low temperature assemblages. Po = Pyrrhotite, Cpy = Chalcopyrite, Aspy = Arsenopyrite, Moly = Molybdenite, Gal = Galena, Marc = Marcasite, Mag = Magnetite, Bi = Bismuth, Bism = Bismuthanite, and Au = Gold.

virtually require that the gold was deposited (and re-deposited?) over a wide range of temperature conditions.

Table 4.3 Summary sample descriptions of Au-bearing thin sections.

BH-UG-8	Sulfide replaces carbonate and pyroxene and not associated w/ retrograde; bismuth-bismuthinite-gold grains are associated with un-retrograded pyroxene independent of sulfide
BH-UG-2	Au occurs in pyroxene, which displays NO retrograde alteration, Au not associated with sulfides. (Chalcopyrite only associated with pyrrhotite), carbonate replaced by sulfide
D02-198 213.5 ft.	All Au present interstitial to magnetite and/or adjacent to primary prograde assemblages.
D10-622-159	Au in calcite near well-formed, non-retrograded pyroxene. Mostly consists of garnet locally retrograded to epidote/chlorite. Local conversion of Bi° to Bi_2S_3
BH-UG-11	Moderate retrograde of garnet (some remnant) to epidote; abundant amphibole presumably after pyroxene. Au in retrograde assemblage minerals with Bi° locally converted to B_2S_3
C-5-60.5	Bismuth, bismuthinite, and gold all together in fractures in epidote, slide is almost completely epidote after garnet; Au is in both garnet and epidote, suggesting that it was originally deposited in garnet that was later retrograded into epidote
C-5-73	Dominantly garnet/ pyroxene skarn with garnet>> pyroxene, scattered remnant pyroxene, local retrograde of garnet to epidote, chlorite psuedomorphs garnet. Epidote-calcite filled fractures contain Bi°-Bi_2S_3-Au, so Au likely part of retrograde assemblage
D10-631-100.7	Sphene, very large, well formed clinozoisite and low-Fe pyroxenes with interstitial chlorite; Au in calcite near clinozoisite; Hi Ti-Al= metasomatically altered hornfels (either pyroxene/garnet or pyroxene/epidote). MoS_2 replaces both clinozoisite and clinopyroxene, Au replaces calcite
BH-UG-16	Au in amphibole; pyroxene completely retrograded but garnets are only modestly retrograded into epidote; Au not associated with sulfide
D07-404-12.5	West of NLF, notably less bismuth minerals. Sphene in chlorite rich zones (suggesting that chlorite replaced a siltier layer in the marble-- higher Ti and Al), sulfide clearly replaces the carbonate portion of the slide and not the chlorite.
D02-208-75	Low temperature assemblage— biotite-chlorite-plagioclase-quartz. No evidence for replacement of higher-T minerals.
D09-545-692.5	Au in arsenopyrite suggests that the gold was deposited before the arsenopyrite, Au is also present in calcite + biotite, no (?) or very little bismuthinite

Samples marked 'P' (Table 4.1) contain gold grains in or adjacent to pyroxene grains, with no obvious retrograde minerals (refer to Chapter 1) between gold and the pyroxene (Fig. 4.2). The most likely interpretation of this texture is that gold either

precipitated with pyroxene or—if later—at conditions where pyroxene was still a stable mineral. In either case, this requires gold deposition with prograde alteration.

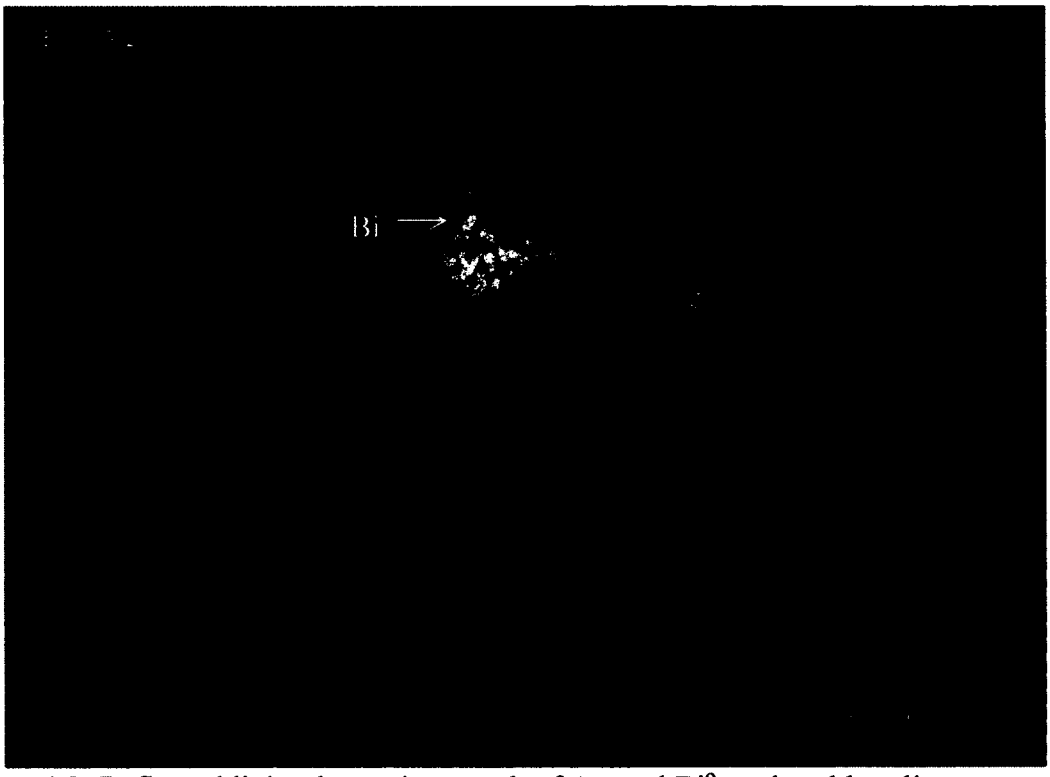

Figure 4.2. Reflected light photomicrograph of Au and Bi^{o} enclosed by clinopyroxene.

The sulfide/oxide assemblage which seems to be most commonly associated with prograde deposition is dominantly pyrrhotite ± chalcopyrite. Local magnetite-rich zones occur on the far east and far west regions of the Southwest Zone and more sporadically throughout the Gold Bowl. Where present, magnetite commonly accompanies the prograde assemblage (Fig. 4.3). Gold grains within the prograde assemblage appear to be most closely associated with native bismuth, which commonly has variable amounts of

bismuthinite formed around its rim. Overall, in the prograde assemblage, the amount of native bismuth is considerably greater than bismuthinite (Bi_2S_3).

Figure 4.3. Reflected light photomicrograph of Au and adjacent Bi^0. Bismuth was partially replaced by bismuthinite and is surrounded by magnetite (medium grey).

This close association of gold with native bismuth is logically explained by the presence of maldonite (Au_2Bi) in two of the thin sections containing an exclusively prograde assemblage. Maldonite is not a particularly stable mineral and decomposes into almost pure Au (fineness = 999) and native bismuth. Fluid evolution apparently adds sulfur (and modifies the oxidation state) to add bismuthinite to the assemblage.

Mineralization which is deposited during retrograde alteration ('R' in tables 4.1-4.3) of the prograde skarn assemblage can be identified by several different characteristics. Au is found interstitial to retrograde minerals (Table 4.3; Figs.4.4, 4.5), which include epidote, clinozoisite, amphibole (generally actinolite ± hornblende), chlorite (Table 4.1) and (or) their related by-products (quartz and calcite) from the retrograde reaction (section 1.3). By-product calcite forms in small, fine-grained, anhedral masses interstitial to retrograde minerals and is significantly different in shape and size from calcite in veins or marble, which is coarser-grained.

Figure 4.4. Transmitted photomicrograph of Au (opaque) surrounded by a clearly retrograde (actinolite-rich) assemblage.

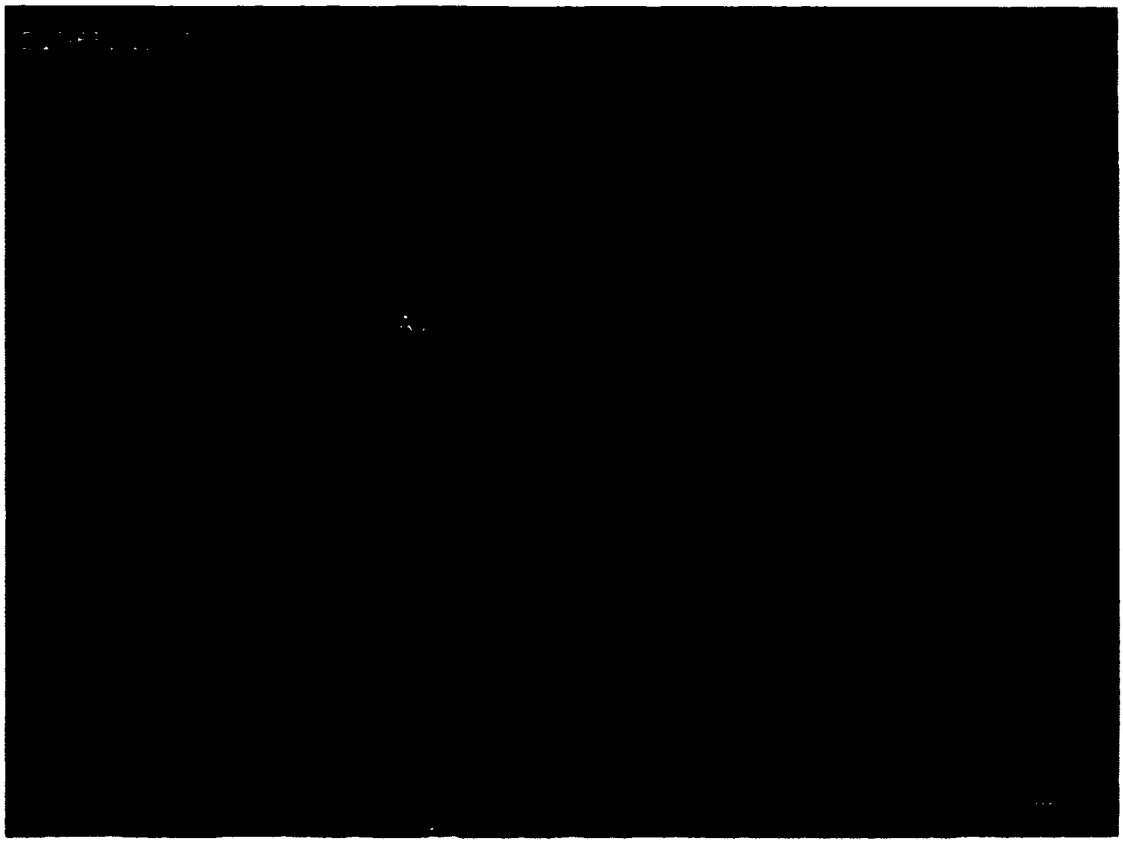

Figure 4.5. Transmitted light photomicrograph of Au (opaque) surrounded by a clearly retrograde assemblage (clz = clinozoisite).

The retrograde assemblage seems to incorporate the same suite of opaque minerals, namely pyrrhotite, magnetite, bismuth, and bismuthinite, as seen with prograde-only assemblages. The most obvious difference is a change from $Bi^{o} > Bi_2S_3$ (prograde) to $Bi_2S_3 >> Bi^{o}$. In other words, retrograde alteration apparently was associated with an increase in fS_2 in the system. Any maldonite still present from prograde deposition would be converted to Au + bismuthinite: $2Au_2Bi + 3/2S_2 = 4Au + Bi_2S_3$. In both assemblages,

pyrrhotite is locally converted into marcasite (most likely a supergene weathering reaction), which displays a classic "bird's eye" texture.

Some assemblages are ambiguous; these contain gold and both prograde and retrograde assemblages. Gold which was deposited with the prograde assemblage may have later experienced some varying degree of retrograde alteration or redistribution. Several samples examined exemplified this problem (Tables 4.1-4.3, marked 'P/R'). Many of the samples containing both retrograde and prograde silicate assemblages contain gold that is surrounded by a retrograde mineral (e.g., Fig. 4.6; Table 4.3). In another case, gold replaces calcite near unaltered pyroxene with retrograde phases elsewhere in the slide. The first is truly ambiguous; the second is most compatible with gold deposited while pyroxene was stable (at least late in 'prograde' time).

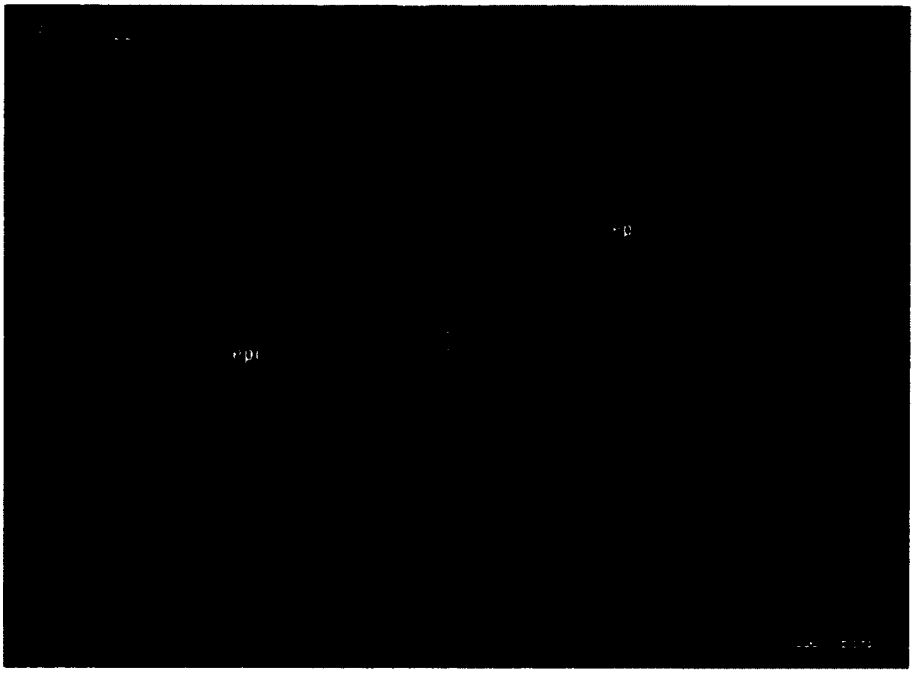

Figure 4.6. Gold and bismuthinite encased in epidote.

The final type of gold occurrence noted in this study is associated with a previously unrecognized low-temperature assemblage. To date, this assemblage has only been noted on the western half of the Southwest Zone, at variable depths, and is pervasive in the westernmost part of the Southwest Zone. Its typically green color, in hand sample, caused it to be classified as part of the pyroxene skarn assemblage, and only petrographic examination and XRD analysis highlighted its existence. The silicate assemblage associated with this type of gold deposition includes chlorite, phlogopite, and calcite ± plagioclase and quartz (Table 4.1, 4.3; Figs. 3.6, 4.7). The opaque mineralogy seems to vary depending on the sample location, but includes pyrrhotite, magnetite, native bismuth, and bismuthinite (Table 4.2). I have not observed phlogopite replacing any prograde or retrograde assemblage but only see it as a replacement of marble. I consequently interpret this assemblage to occur at the same temperature range (and time) as retrograde alteration, but as a direct replacement of marble that never contained prograde minerals. Gold is sporadically associated with this assemblage (e.g. Fig. 3.7), and I do not know whether this gold was leached from prograde skarn and re-deposited in altered marble or represents new gold brought into the skarn.

Figure 4.7. Transmitted and reflected light photomicrograph sample D02-208-75'. Shows the low temperature Au deposition assemblage of calcite, plagioclase and biotite. Gold grains (Au) are surrounded by black = gold below the surface of the thin section. Such gold neither reflects nor transmits light, hence it is 'black'.

4.2.2 Gold compositions

I analyzed 24 different gold grains from 16 separate locations in the Buckhorn area by quantitative microprobe analysis for Au, Ag, and Hg (Table 4.4). Fineness values (1000*wt % Au/ (wt % Au + Ag)) vary tremendously—from nearly 1000 (pure gold) to nearly 600—and show neither obvious patterns in plan view nor simple patterns with respect to the associated mineral assemblage (e.g., prograde vs. retrograde—Fig. 4.8). However, gold associated with prograde alteration is EXCLUSIVELY high

fineness (900-1000, Fig. 4.8), whereas that associated with lower temperature assemblages includes both low and high fineness. It is conceivable that all the gold of high fineness was deposited with prograde alteration and remobilized or else that newly-introduced gold has lower fineness.

Table 4.4 EMPA-derived gold fineness data, Buckhorn deposit

Sample	Avg. Fineness	Std Dev.	# Analysis
BH-UG-8.1	922	8	7
BH-UG-2	857	93	8
D02-198-213.5.1	933	45	7
D10-622-159	684	77	8
BH-UG-11	709	76	22
C-5-60.5	804	10	7
C-5-73	793	5	12
BH-UG-16	924	0.5	8
D07-404-12.5	913	3	12
D02-208-75	907	2	4
D09-545-692.5	613	4	2
D02-199-430	873	11	4
D10-630-100.7	823	4	5

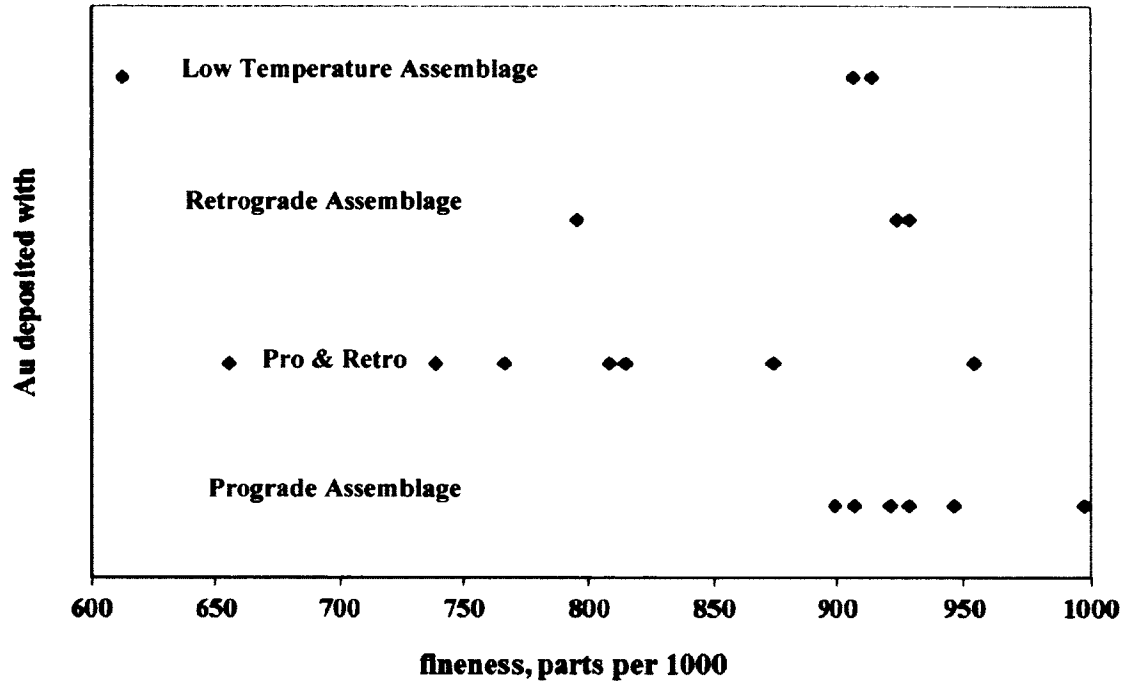

Figure 4.8. Silicate assemblage compared to gold fineness, Buckhorn deposit.

Buckhorn gold contains very low Hg (Fig. 4.9). However, the Hg content varies with fineness and with patterns that distinguish Southwest Zone from Gold Bowl gold. Gold from Gold Bowl is typically of lower fineness and contains less Hg for a given fineness than gold from Southwest Zone (Fig. 4.9). These distinctly different compositional patterns suggest the gold in these two deposits is of different origins.

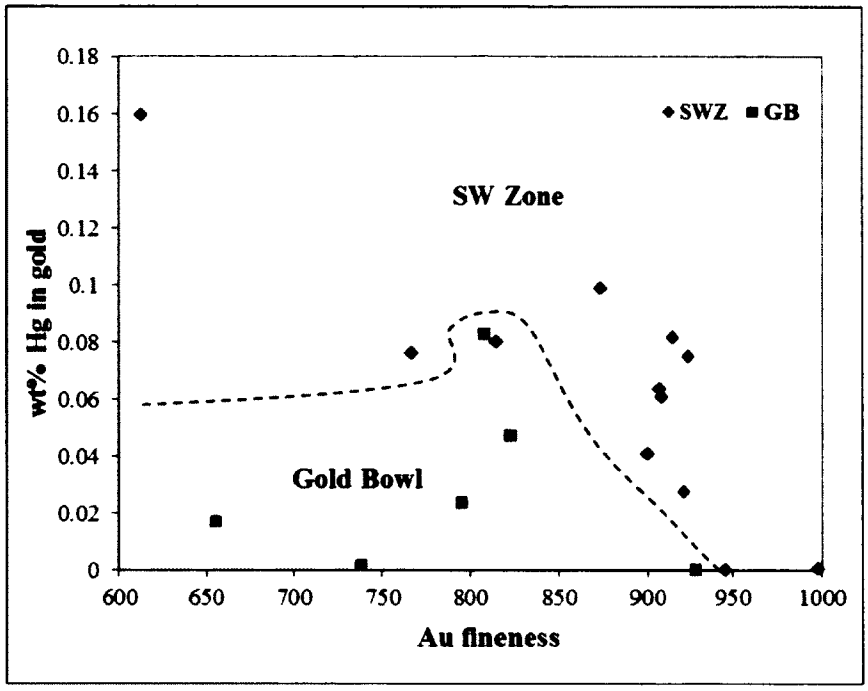

Figure 4.9. Contrast in gold compositions between Southwest Zone and Gold Bowl.

4.3 Metal values

I analyzed several hundred mineralized pulps, mostly from Au-rich (Au > 1 ppm) intercepts, by quantitative XRF for a suite of metals: Cu, As, Ag, Te, Bi, W, Mo, Pb, Zn, Sb, and Ni (Table 4.5). I also analyzed the pulps by IQ+ for major elements, including sulfur. In analyzing this data, I have broken the Buckhorn deposit into four sub-parts, (main Southwest Zone, western Southwest Zone, Gold Bowl, and north of Gold Bowl) based on mineralogical and host rock differences I have documented in Chapters 3 and 4. It is worth noting that the pulps from the area north of Gold Bowl were all low in Au (Table 4.5); for the others the mean, median, and maximum gold concentrations are all of

comparable values. However, even if the north-of-Gold Bowl group isn't comparable to the others, removing it from the Gold Bowl group makes that group more comparable to the others.

Table 4.5 Summary statistics for metals in the Buckhorn Deposit. All values in ppm. Unusually high values are shown in bold and underlined; unusually low values shown in italics and underlined.

	Cu	As	Ag	Te	Bi	Au	W	Mo	Pb	Zn	Sb	Ni
Southwest Zone (318 analyses)												
Mean	632	275	14	15	901	26	21	25	46	97	8	37
Median	366	28	10	6	84	6	13	3	11	77	6	23
Maximum	3946	5975	299	178	20309	336	1653	976	1690	689	296	1729
Minimum	0	0	0	0	0	0.1	0	0	0	1	0	0
W Southwest Zone (38 analyses)												
Mean	735	*127*	11	12	*61*	11	14	50	26	89	6	28
Median	717	*7*	10	3	*14*	0.45	11	14	20	97	6	29
Maximum	2306	3647	28	102	664	117	137	488	96	146	18	78
Minimum	5	0	0	0	3	0.03	0	1	6	20	0	8
Gold Bowl (48 analyses)												
Mean	*329*	207	11	20	2066	20	18	15	**159**	195	10	40
Median	*49*	**66**	*0.5*	8	**223**	5.7	14	5	**42**	112	8	23
Maximum	2033	1702	102	118	14195	235	146	205	3500	3441	57	351
Minimum	5	9	0	0	0	0.07	0	1	1	**48**	0	14
N Gold Bowl (38 analyses)												
Mean	1353	33	12	8	108	*5*	30	5	98	194	9	42
Median	414	13	11	2	8	*0.07*	14	5	37	120	10	23
Maximum	15306	162	40	250	2431	170	305	13	1244	1540	22	705
Minimum	2	1	0	0	4	0.07	6	1	7	51	0	13

Metal concentrations in the pulps vary wildly, as indicated by the range between minimum and maximum values (Table 4.5). Given that, 'mean' concentration can be

strongly weighted by a few very high concentrations and be less indicative of the 'average' than the median concentration. I am more confident in apparent differences between different sub-groups where both median and mean concentrations are anomalously high or low. Such is the case for many. Based on such criteria, the Western Southwest Zone contains the lowest As and Bi concentrations. In contrast Gold Bowl contains the lowest Cu and Ag and the highest As, Bi, and Pb concentrations (Table 4.5). For the elements Te, W, Zn, Sb, Cu, Mo, and Ni, differences in the mean and median concentrations among the groups are unclear. These major elemental contrasts again point to significant differences between main Southwest Zone (proximal: dominantly prograde replacement of marble) and western Southwest Zone (distal: dominated by hydrosilicate replacement of marble) and between Southwest Zone (marble hosted) and Gold Bowl (hornfels hosted). However, the relative elemental concentrations at Gold Bowl seemingly are compatible with it being 'distal' to Southwest Zone, by virtue of higher As and Pb.

The correlations between these different metals, and notably their correlations with gold, also vary tremendously between the different parts of the deposit (Tables 4.6-4.8) and presumably reflect differences in ore element mineralogy and mineral associations. (In these tables, r^2 values > .4 are bold and those > .75 are underlined.) In all cases Au correlates strongly with Te (r^2 = .80 to .90), despite the absence of an Au-Te mineral in the deposit. This is, in fact, the only consistent metal correlation at Buckhorn!

Table 4.6 Elemental correlation coefficients for Gold Bowl mineralized pulps. R^2 values greater than .4 are bold, those greater than .75 are underlined.

Gold Bowl												
(ppm)	**Cu**	**As**	***Ag**	**Te**	**Bi**	**Au**	**W**	**Mo**	**Pb**	**Zn**	***Sb**	**Ni**
Cu	1.00											
As	**0.42**	1.00										
Ag*	0.07	0.15	1.00									
Te	**0.49**	**0.44**	0.14	1.00								
Bi	**0.48**	**0.76**	0.16	**0.59**	1.00							
Au	**0.62**	**0.42**	0.12	**0.80**	0.39	1.00						
W	**0.53**	**0.79**	0.13	**0.42**	**0.78**	0.40	1.00					
Mo	**0.61**	0.20	-0.05	**0.52**	0.21	**0.72**	0.29	1.00				
Pb	-0.07	-0.03	**0.70**	-0.01	-0.04	0.00	-0.05	-0.07	1.00			
Zn	**0.43**	0.28	-0.08	0.13	**0.50**	-0.04	0.22	0.32	-0.05	1.00		
Sb*	-0.22	-0.25	-0.10	-0.38	-0.38	-0.27	-0.24	-0.08	-0.01	-0.12	1.00	
Ni	0.32	0.12	-0.03	0.11	0.22	0.08	0.24	0.02	-0.06	-0.06	-0.20	1.00

*Many values for these elements were below detection and were assigned a value of one-half the detection limit; statistics for these are of lower certainty.

Table 4.7 Elemental correlation coefficients for Southwest Zone mineralized pulps. R^2 values greater than .4 are bold, those greater than .75 are underlined.

Southwest Zone												
(ppm)	Cu	As	*Ag	Te	Bi	Au	W	Mo	Pb	Zn	*Sb	Ni
Cu	1.00											
As	0.00	1.00										
Ag*	-0.05	0.05	1.00									
Te	0.17	0.00	0.07	1.00								
Bi	-0.03	0.36	0.02	0.20	1.00							
Au	0.11	-0.04	0.04	**0.86**	0.13	1.00						
W	0.14	0.03	-0.04	0.00	0.05	-0.01	1.00					
Mo	0.18	-0.02	0.18	0.04	-0.06	0.01	-0.02	1.00				
Pb	-0.01	0.15	0.52	0.15	0.11	0.00	-0.01	0.14	1.00			
Zn	0.31	0.34	**0.47**	0.11	0.30	0.02	-0.01	0.22	**0.50**	1.00		
Sb*	-0.04	0.13	**0.84**	-0.02	0.00	-0.05	0.00	0.25	**0.55**	**0.51**	1.00	
Ni	0.25	**0.44**	-0.07	0.07	0.05	0.02	0.02	0.02	0.03	0.02	-0.04	1.00

Table 4.8 Elemental correlation coefficients Western Southwest Zone mineralized pulps. R^2 values greater than .4 are bold, those greater than .75 are underlined.

West Southwest Zone												
(ppm)	Cu	As	*Ag	Te	Bi	Au	W	Mo	Pb	Zn	*Sb	Ni
Cu	1.00											
As	-0.13	1.00										
Ag*	**-0.65**	0.26	1.00									
Te	0.17	**0.71**	0.11	1.00								
Bi	0.15	**0.80**	0.14	**0.97**	1.00							
Au	0.17	**0.54**	0.17	**0.90**	**0.86**	1.00						
W	-0.05	-0.02	-0.07	0.01	-0.01	0.02	1.00					
Mo	0.23	**0.72**	0.08	0.90	0.90	**0.86**	0.04	1.00				
Pb	-0.26	0.33	0.35	0.15	0.27	0.18	0.11	0.14	1.00			
Zn	0.50	-0.26	-0.59	-0.02	-0.10	-0.03	0.01	-0.01	**-0.42**	1.00		
Sb*	-0.23	0.00	0.29	0.02	0.06	0.11	0.13	0.00	0.29	-0.19	1.00	
Ni	**0.79**	-0.12	**-0.48**	0.08	0.04	0.12	-0.04	0.25	-0.31	**0.60**	-0.10	1.00

Mineralized samples from the Southwest Zone are notable in that few metals correlate very well (Table 4.7). The only additional strong correlation is between Ag and Sb (r^2 = .84). Other weakly correlated metals include Ag-Zn, Pb-Zn, Pb-Sb, and Zn-Sb. In other words, the elements Ag, Pb, Zn, and Sb frequently occur together in the Southwest Zone.

The western Southwest Zone, in contrast, displays many significant elemental correlations (Table 4.8). Most notably, the group Au-Bi-Te have the highest correlations seen at Buckhorn (r^2 = .86-.97), perhaps indicating a single stage of gold deposition with hydrosilicate replacements of marble there. Other notable positive correlations are of As with Bi and Te, Cu with Ni, and especially Au with Mo (r^2 = 0.86). Strong negative correlations include Cu-Ag, Ni-Ag, and Pb-Zn (Table 4.8). As with the distinctive metal concentrations in the western Southwest Zone (Table 4.5), the distinctive metal correlations are potentially related to lower-temperature metal deposition by direct reaction with calcite.

Metal correlations from the Gold Bowl samples show yet different patterns (Fig. 4.6). First, gold correlates moderately well with both Mo (r^2 =.72) and W (r^2 = .62). W also correlates strongly with Bi and As (r^2 = 0.78 and 0.79, respectively), not seen in any other part of Buckhorn. In turn, As also correlates well with Bi (r^2 = .76). In other words the group W-Bi-As seems characteristic of Gold Bowl. Finally, the expected strong correlation between Pb and Ag—so often the case in many deposits—is only true for Gold Bowl (Table 4.6)

In sum, the combination of metal concentrations and metal correlations points to important differences between the main Southwest Zone, the western Southwest Zone, and Gold Bowl. Differences between the former two can be ascribed to differences in temperature of major mineral deposition, with exclusively lower-temperature deposition at western Southwest Zone. On the other hand, the higher concentrations of the more soluble element (Pb) and lower concentrations of the less soluble element (Cu) point to Gold Bowl as 'distal.' But, distal to what? Major differences in metals and metal correlations between Gold Bowl and western Southwest Zone suggest that Gold Bowl is not distal to the Southwest Zone. The variation in bulk metal distribution between the Gold Bowl and the Southwest Zone (Table 4.5) in and of itself is interesting because the metal assemblage present within the Gold Bowl is dominated by higher solubility metals. Seemingly, Gold Bowl is distal to a different hydrothermal system.

4.4 Metal zoning

Metal ratio zonation between elements with different established solubilities can be used to indicate fluid flow direction and help define a source. Metals commonly used in other research of a similar nature include Cu, Pb, and Au (e.g., Fig. 1.4). However, the uniquely poor Bi-Au correlation (r^2= 0.13) in the Southwest Zone of Buckhorn encouraged me to evaluate variations in its ratio to Au in addition to more standard ratios involving Au, Cu, and Pb. In all cases, the much larger data set I possess for Southwest Zone than for Gold Bowl makes zoning patterns for the former much more certain.

4.4.1 Bi/Au

Bi/Au ratios at Buckhorn (Fig. 4.10) are not only uniquely higher than Bi/Au ratios recorded for other plutonic-related Au systems (e.g., Flannigan et al., 2000), they also vary dramatically. The Bi/Au ratios for the deposit as a whole range between 1 and >200. When plotted spatially (Fig. 4.10) the Southwest Zone and the Gold Bowl show markedly different trends.

The Southwest Zone shows lower Bi/Au ratios as a SE-NW oriented horseshoe surrounding higher values on three sides. Highest Bi/Au ratios are in the center (Fig. 4.10). This trend is decidedly different from the distribution of Bi/Au ratios within the Gold Bowl, where there is an overall decrease in Bi/Au from N to S. Depending on the fluid conditions, Bi is marginally less soluble than Au (Barnes, 1979) and therefore is expected to be deposited before Au; hence, increasing distance from the source should correspond to lower Bi/Au ratios. Consequently, the Gold Bowl and Southwest Zone show different overall trends in fluid direction, suggesting mineralizing fluid for the two portions of the deposit traveled from two different directions. Based on this interpretation, either the Southwest Zone and Gold Bowl were derived from two separate sources, or a single source intrusion utilized two completely different fluid pathways into the Buckhorn host rocks.

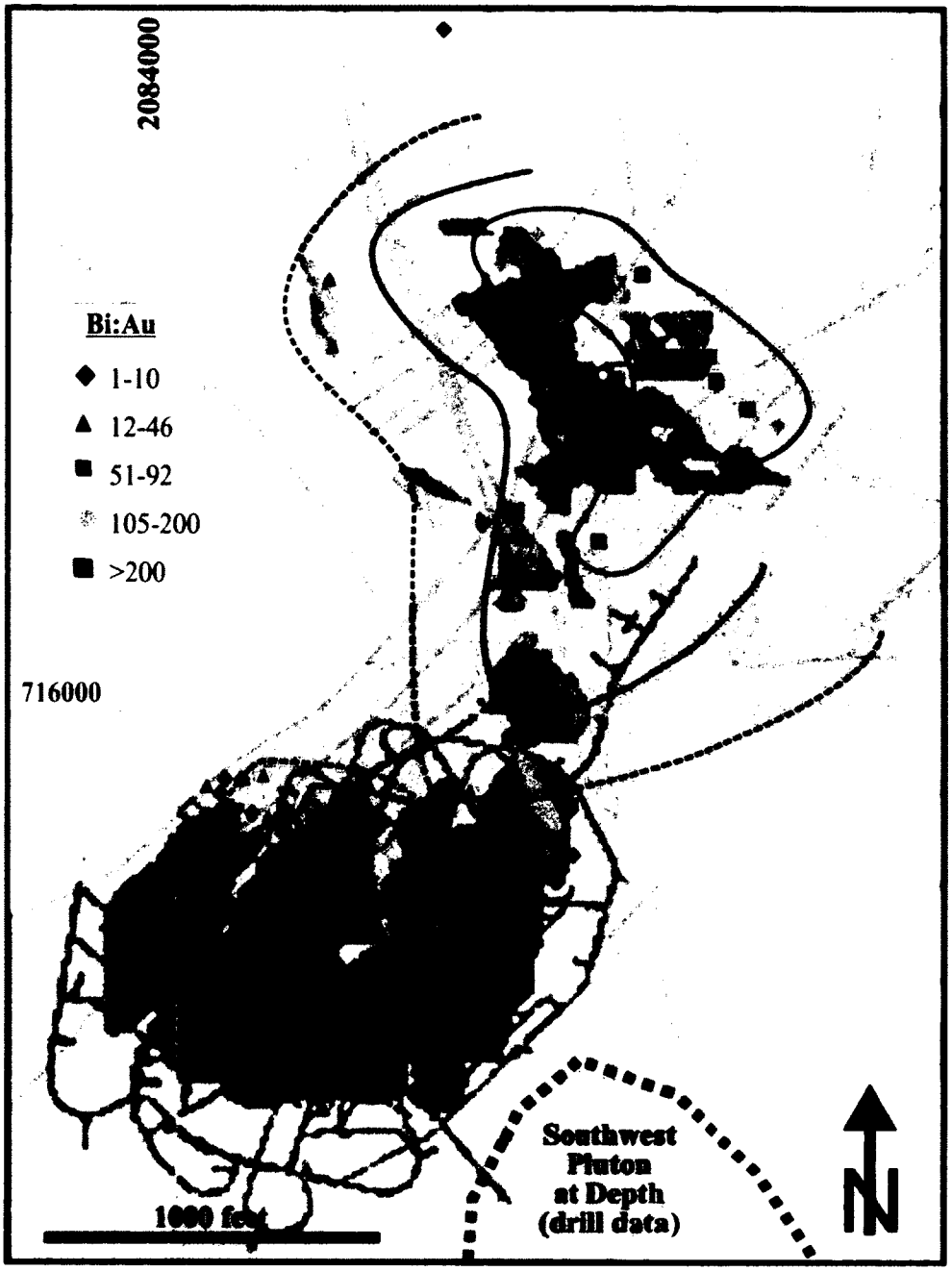

Figure 4.10. Bi/Au distribution throughout the Buckhorn deposit. Values and contours are overlain on a general geology map (Fig. 1.11). Colored lines are hand drawn contour lines separating different Bi/Au ratios. Scale bar is 300 meters.

4.4.2 Cu/Au

The distribution of Cu/Au ratios for the Buckhorn deposit (Fig. 4.11) shows reasonably straightforward patterns for Southwest Zone and less so for Gold Bowl. Cu/Au ratios at Southwest Zone are highest (>500) along the east side with a lobe of moderate ratios (30-100) along the northern portion of the deposit. Outside of the 'lobe' the ratios are <30 and <9 on the margins. The trend in the Gold Bowl is exactly opposite (Fig. 4.11): Cu/Au values decrease from west (>500) to east (<100).

Cu distribution relative to gold in Au skarn systems has been well characterized (Fig. 1.3). Copper is generally deposited closer to the source, decreasing with distance, and as Cu values drop off, Au values increase (Myers and Meinert, 1991). The E-W decrease in Cu/Au within the Southwest Zone suggests that the mineralizing fluid originated on the eastern side and traveled westward. The Cu/Au distribution in the Gold Bowl shows an opposite trend, suggesting instead the mineralizing fluid originated in the western region and migrated east.

4.4.3 Cu/Pb

Pb solubility is significantly greater than that of Cu (Barnes, 1979), so with increasing distance from a hydrothermal source, Pb concentrations should increase and generate elevated Pb/Cu ratios. The actual distribution of Cu/Pb ratios throughout the Buckhorn deposit (Fig. 4.12) again shows a relatively simple pattern for Southwest Zone and a complex one for Gold Bowl. Cu/Pb ratios in the Southwest Zone show the

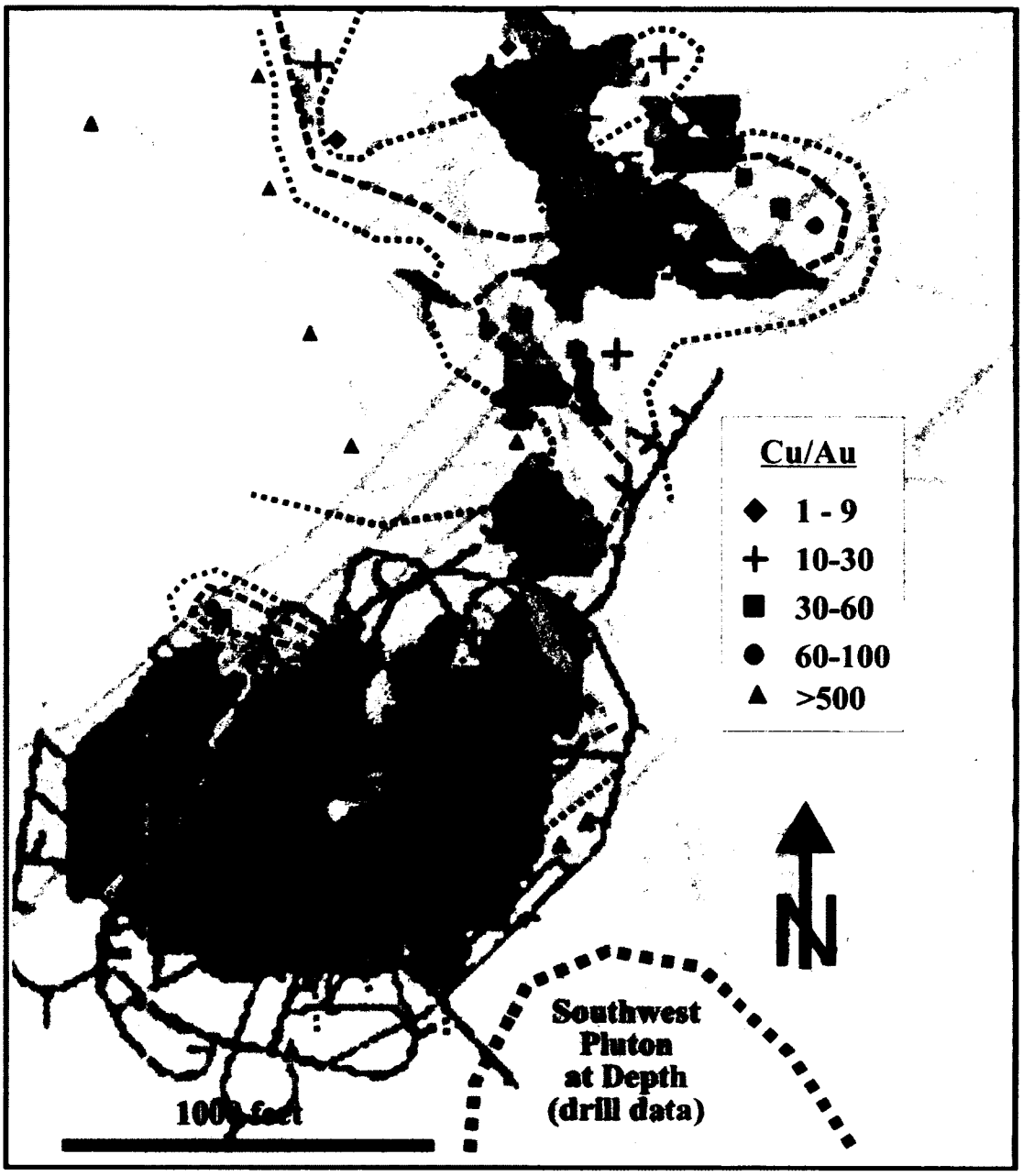

Figure 4.11. Cu/Au distribution throughout the Buckhorn deposit. Values and contours are overlain on a general geology map, as in Fig. 4.10. Colored lines are hand drawn contour lines separating different Cu/Au ratios. Scale bar is 300 meters.

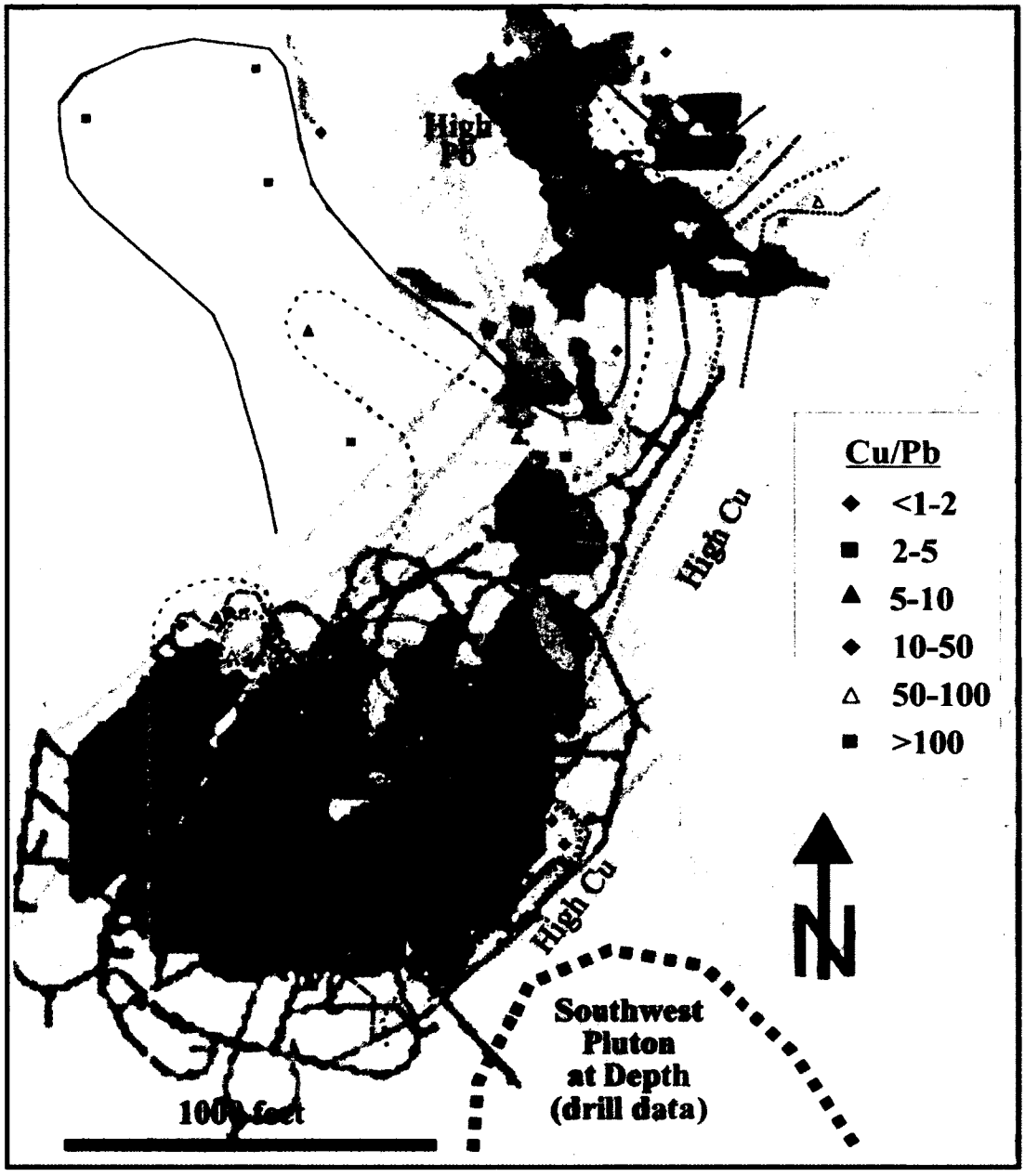

Figure 4.12. Cu/Pb distribution throughout the Buckhorn deposit. Values and contours are overlain on a general geology map, as in Fig. 4.10. Colored lines are hand drawn contour lines separating different Cu/Pb ratios. Scale bar is 300 meters.

same pattern as the Cu/Au: higher Cu/Pb ratios on the east side and a lobe extending through the northern third, and decreasing ratios with distance west. Cu/Pb on the east side are >10 and those on the west side (outside of the lobe) are <2. The Cu/Pb distribution in the Gold Bowl, on the other hand, displays an inverse relationship to the Cu/Au distribution, with higher Cu/Pb ratios (>50) on the eastern half and a decrease with distance west, with the lowest ratios (<1-5) on the west.

In sum, distribution of Cu/Pb, Cu/Au, and Bi/Au ratios in the Southwest Zone are all compatible with a broad pattern of east to west fluid movement. This makes an intrusion to the east of the Southwest Zone (e.g., the SW pluton, Figs. 4.10-4.12) the likely source of mineralization.

In contrast, the pattern of metal ratios in the Gold Bowl is not simple. Cu/Pb, Cu/Au, and Bi/Au all suggest different patterns of fluid flow: E→W, W→E, and N→S, respectively (Figs. 4.10-4.12). That is, the metal distribution patterns in the Gold Bowl show no easily interpretable results regarding the source of the fluid. I noted earlier that based on overall lower Cu and higher Pb at Gold Bowl, the Gold Bowl could potentially be the distal portion of the Southwest Zone. Ironically, not one set of metal ratios suggests that is the case (Figs. 4.10-4.12). If the Gold Bowl is not the distal portion of the Southwest Zone, then it is most likely part of an unrelated system, that is, it has a different source.

4.5 Geochronology

Since both known Eocene and Jurassic intrusions are near the Buckhorn deposit, and regionally both Jurassic Au skarns and Eocene epithermal deposits occur (Fig. 1.1), the gold at Buckhorn has been variably considered Eocene, Jurassic, or both. Cross-cutting relationships of the quartz porphyry dikes suggest the skarn itself is older than about 163 Ma, i.e., Jurassic. The dikes cut the skarn and marble without affecting either (Section 2.5, Figs. 2.16 and 2.17), indicating they are younger than, and unrelated to, the skarn, although they may be responsible for localized remobilization or re-concentration of gold.

The most effective way to date the mineralization is to find a datable mineral intimately intergrown with gold. In a skarn system, the most datable mineral is likely a potassium-bearing silicate: hornblende, biotite, stilpnomelane, or scapolite. Of these, scapolite is exceedingly rare; I've identified it in one thin section. However, there are several complicating factors in Ar-Ar dating a mineral in this setting. In particular the abundance of Eocene dikes, plutons, and volcanic rocks makes re-setting of the K-Ar systematics likely. Furthermore, finding a sample containing considerable potassium-rich minerals intergrown with gold has not been easy.

I made three attempts to date the mineralization at Buckhorn. (1) I used a sample of stilpnomelane intergrown with gold. Despite its high K content stilpnomelane is not a mineral commonly used for K-Ar or $^{40}Ar/^{39}Ar$ dating, although I have found no explanation for this in the literature. The $^{40}Ar/^{39}Ar$ spectrum for this mineral showed

ages 'stepping up' to Eocene age, but this spectrum indicated the mineral had leaked considerable Ar since the Eocene (60% Ar loss). I conclude (in retrospect) that stilpnomelane is not used for radiometric dating because it too readily leaks Ar and thus does not yield reliable radiometric ages. However, the sample does confirm the presence of Eocene heating in the region.

(2) I attempted to date actinolite from the Southwest Zone (sample BH-UG-16) intergrown with gold, but its low K content and high Ca/K ratio precluded a usable age. Perhaps in retrospect I should have gone for biotite instead, despite the ease of thermally resetting the Ar systematics of biotite.

(3) Finally, I sampled a hornblende from 'Mike's Skarn,' a small skarn body slightly NW of the Gold Bowl (Fig. 1.3). The surface outcrop of the skarn here is small and drilling revealed it to have no significant depth. However, it is a sufficient distance from the known Eocene intrusions to be safe from the interference of Ar resetting. The mean weighted plateau age from this hornblende sample indicates a mineralization age of approximately 169 Ma (UAF Geochronology Laboratory, unpub. data). This age indicates that mineralizing fluids (and not merely the skarn-forming fluids) at Mike's Skarn were related to the Jurassic intrusions. However, because Mike's Skarn is not one of the larger deposits of the Buckhorn area, I cannot be certain that all the mineralization at Buckhorn is Jurassic.

5. Conclusions and discussion

In this study, I have presented extensive data concerning the Buckhorn gold skarns, including the type, nature, and distribution of igneous rocks, the distribution and composition of the silicate mineralogy within the skarns, and the concentrations and distributions of metals across the deposits. This section is devoted to placing all the puzzle pieces together into a viable interpretation of the skarn's origin.

The complex intrusive history in the area has fostered extensive debate about the timing of the mineralization relative to the timing of skarn formation and relative to the different suites of intrusions. I tried Ar-Ar dating of potassium bearing minerals intergrown with gold as a clue for timing of mineralization. The dating of minerals selected for their gold association in the Southwest Zone was inconclusive as neither actinolite nor stilpnomelane are ideal minerals for Ar^{40}/Ar^{39} dating and both display Eocene resets. A sample of hornblende intimately intergrown with gold from Mike's Skarn, a small body to the NW of the Gold Bowl (Fig. 1.11), however, returned an age of ~168 Ma, suggesting that skarn-related gold mineralization in the area occurred in the Jurassic and not the Eocene.

The trouble with pinning the mineralizing event to a specific intrusion has been which one to pin it to. I have established that intrusions in the Buckhorn area include the Buckhorn pluton and its early crystallizing 'Marginal phase,' the Southwest pluton and its early crystallizing 'Ti Diorite' phase, quartz porphyry dikes, granodiorite dikes, the Roosevelt Granite, and andesitic Eocene dikes. The first seven are likely Jurassic, based on a combination of U-Pb zircon dating and some field relations. The only way to

correlate skarn formation with one of these intrusions is to determine their spatial distribution relative to the hydrothermal fluid flow indicators present within the skarn system itself.

Determining the spatial distribution of the igneous bodies required finding a reliable and consistent way to distinguish between them. The quartz porphyry dikes are easily recognizable and cut but do not alter both marble and skarn (Figs. 2.16, 2.17), showing that they intruded after skarn formation. The remaining intrusions, where feasible, were distinguished by immobile element concentrations. Determining the extent of each then became an exercise in selectively re-logging drill core and re-mapping the surface.

Zoning within the Southwest Zone proved to be both consistent and conclusive. Zoning displayed by the silicate mineralogy, including the low- temperature assemblage, suggests fluid moved both vertically and westward. Skarn found at depth within the eastern Southwest Zone tends to be garnet rich (pyroxene-rich with elevation) and the amount of garnet and skarn decreases with distance west (Fig. 3.9). The east side of the Southwest Zone has a higher garnet to pyroxene ratio (Fig. 3.9). I propose that this is due to skarn formation closer to the fluid source. It is also possible that this portion of the deposit originally contained less marble and the hypothetical hornfels-dominated package was more easily turned into garnet-rich rock. If this latter possibility is true, then the proposed decrease in proportion of pre-skarn marble could be due to stratigraphic or structural causes.

Zoning within the pyroxene-rich portion of the Southwest Zone supports east to west fluid movement, as clinopyroxenes became more Fe rich with distance westward, suggesting a source location on the east side (Fig. 3.17). Metal zoning of each of the three ratios employed (Bi/Au, Cu/Au, and Cu/Pb; Figs. 4.10, 4.11, 4.12) are all consistent with this pattern. Based on analogies with other skarns (e.g., Fortitude, Fig. 1.3) Cu/Au and Cu/Pb decrease drastically with distance from the hydrothermal source. I know of no other deposit that displays the tremendous variations in Bi:Au seen in the Southwest Zone, but the regular pattern of changes in ratio (it goes up and then down with distance west) is consistent with the east to west zoning model.

Hydrothermal fluid movement indicators within the Southwest Zone suggest a source on the east side of the deposit (e.g., Figs. 3.9, 3.17, 4.10, 4.11, and 4.12), in the general vicinity of the historic Roosevelt Mine. Surface mapping and logging show that all the intrusions of the Buckhorn area are present in the Roosevelt mine area, if only as dikes (Fig. 2.15). The Southwest pluton occurs at the surface in that area as small, sporadic sub-crops, but it is present at depth. Drilling reveals Ti Diorite at approximately 400 feet (120 meters) below the surface (Fig. 5.1).

Of the igneous phases known in the area, the Roosevelt Granite can be excluded from consideration based on the limited age constraints and its lack of hydrothermal alteration, leaving the Buckhorn pluton and the Southwest pluton (and their respective early crystallizing phases). In considering the characteristics of both intrusions, the Southwest pluton is the most likely causative pluton. The sheer size of the Buckhorn

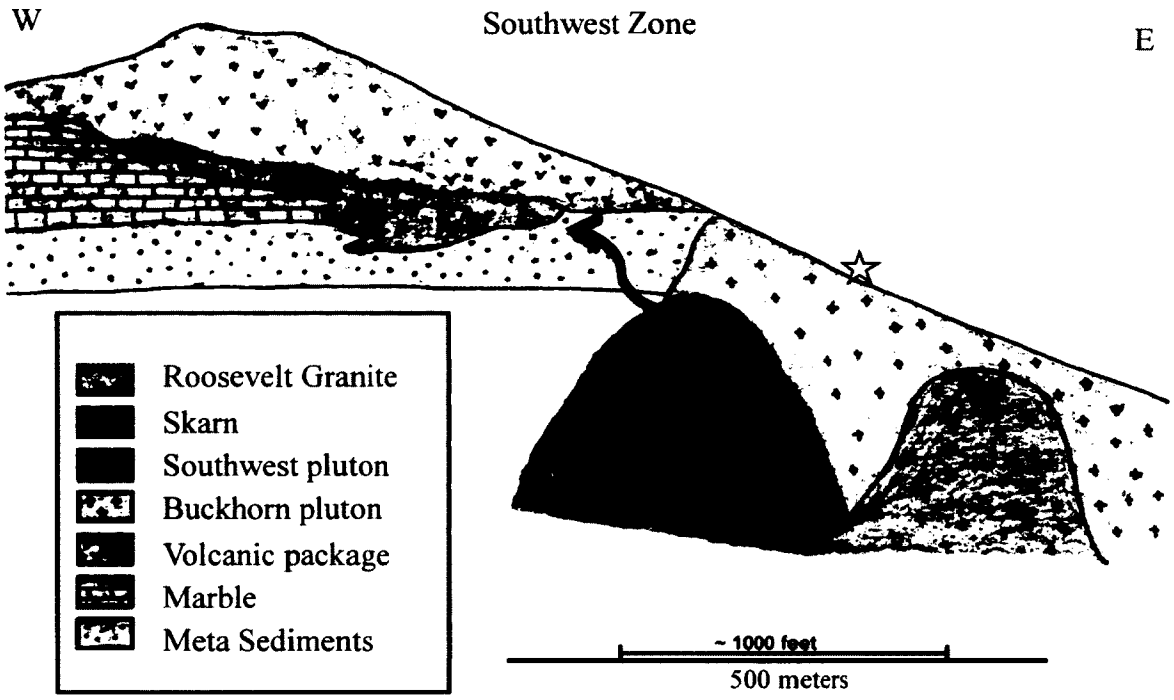

Figure 5.1. Cartoon cross section of the proposed relationship between intrusive rocks and skarn in the Southwest Zone area. Yellow star demarcates approximate location of historic Roosevelt Mine. Black arrows show schematic fluid movement out of the SW pluton and into the Southwest Zone.

pluton (as exposed on the surface, Figs; 5.2, 5.3) suggests an enormous portion of the body has already been eroded away. If the Buckhorn pluton was the source pluton, then an enormous body of skarn would have formed above the pluton and already been eroded away. Certainly this is the case with most large skarns: they are located above a major pluton or at least near its apex (Robb, 2010). Alternatively it could suggest that the bulk of fluid from the pluton migrated laterally (and not vertically) at depth—and through the impermeable cap of marginal phase (Figs. 5.2, 5.3). It is conceivable, for example, that the small massive magnetite bodies present at the Magnetite and Roosevelt mines (Fig. 1.5) are related to the immediately adjacent marginal phase of the Buckhorn pluton.

Disregarding the physical problems of channeling large amounts of fluid laterally (instead of vertically), the intrusion, at best, displays only propylitic alteration. Surely high-temperature fluids migrating though a pluton would leave behind potassic or other feldspathic alteration. Some variety of feldspathic alteration is required by change in fluid temperature when the fluid is of a constant composition and it is a two feldspar system (Barnes et al., 1979). In contrast, I have neither seen nor read of higher-temperature alteration in the Buckhorn pluton.

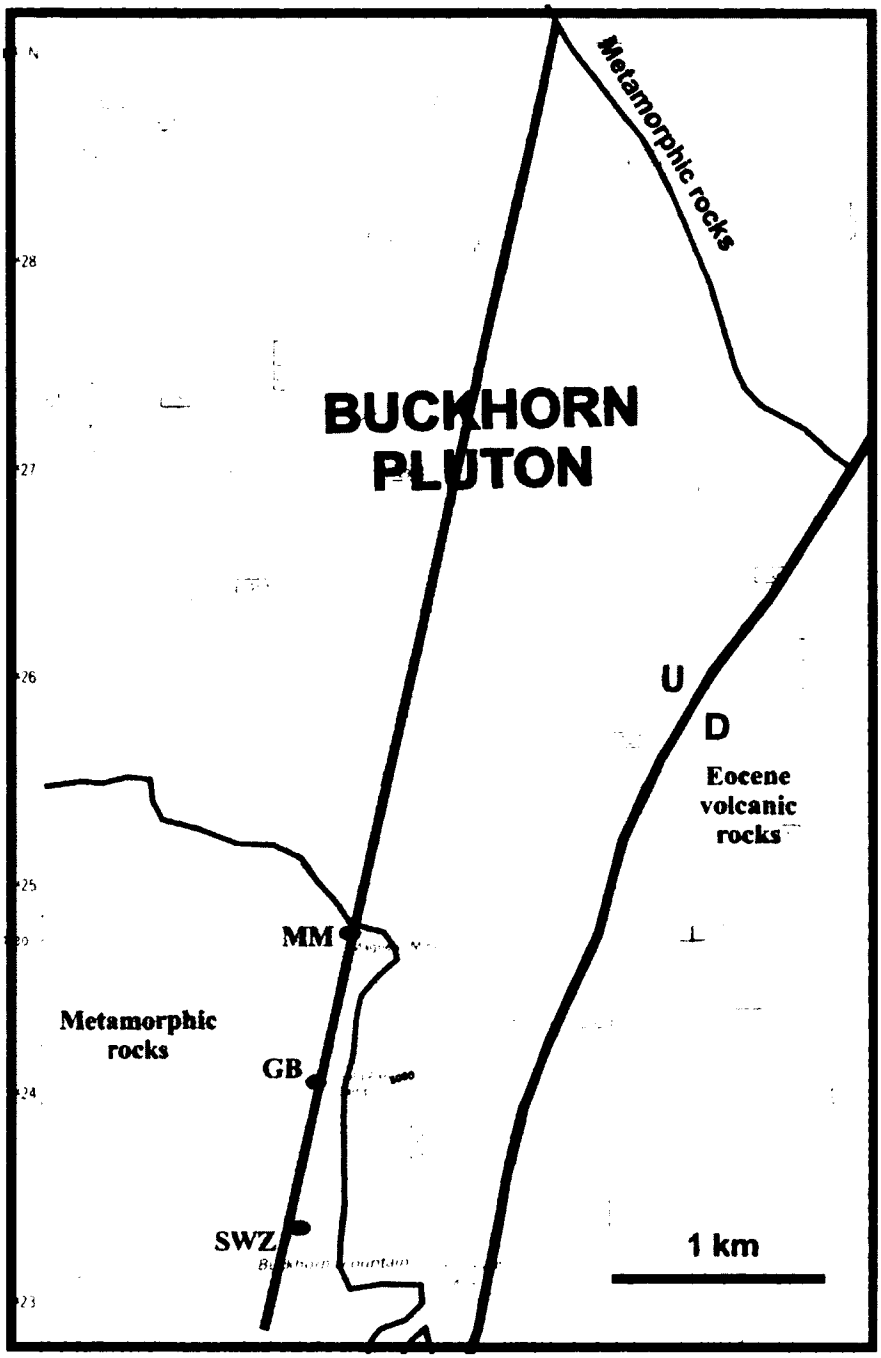

Fig. 5.2. Location of cartoon cross-section in Fig. 5.3. SWZ= Southwest Zone, GB= Gold Bowl, MM= Magnetic Mine. Geology simplified from Pearson (1967).

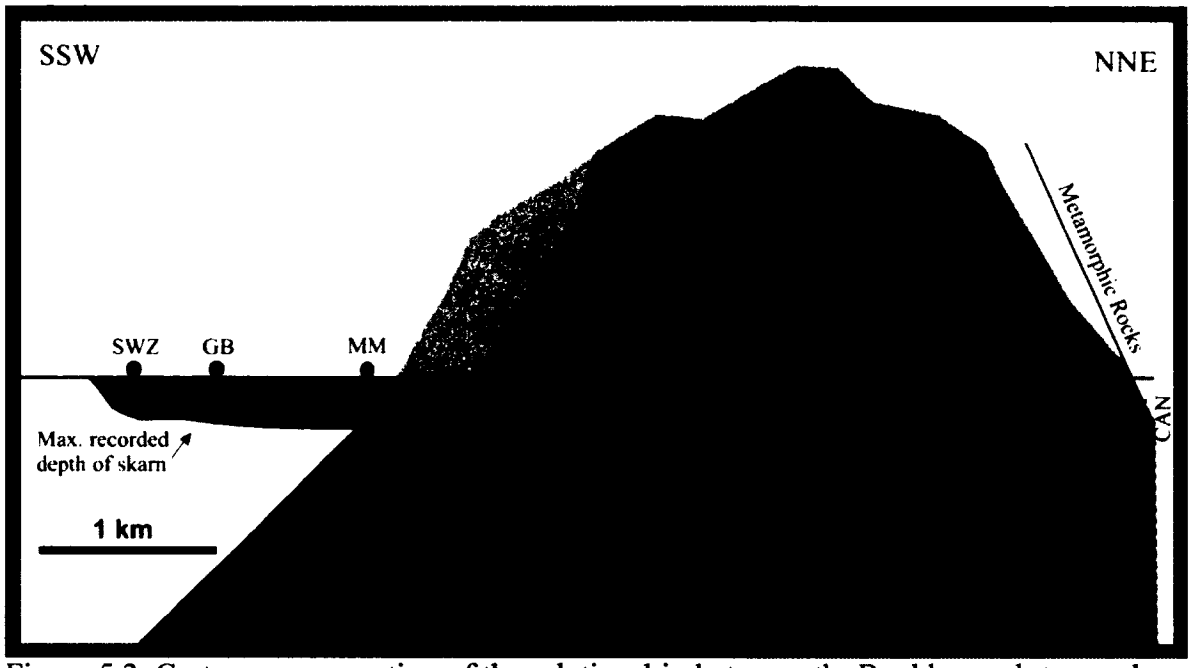

Figure 5.3. Cartoon cross-section of the relationship between the Buckhorn pluton and the Southwest Zone (SWZ), Gold Bowl (GB), and Magnetic Mine (MM). No vertical exaggeration.

The Southwest pluton, by contrast, has an extremely limited surface exposure, but fairly extensive subsurface appearances, as revealed in drill core (Fig. 2.13). The pluton is in an ideal location to be responsible for causing the silicate, compositional, and metal zoning patterns present, based on its spatial and vertical position (Fig. 5.1). Additionally, this pluton displays evidence of high-temperature hydrothermal alteration. The early crystallizing phase (Ti Diorite) contains potassium feldspar veinlets (Fig. 2.10), reminiscent of "A veinlets" of porphyry Cu systems, and intense albitic alteration (Na-enrichment). The Southwest pluton also has a highly variable magnetic susceptibility,

suggesting secondary magnetite. This is another relatively high-temperature hydrothermal alteration mineral.

The age of the Southwest pluton is unknown, but indirect evidence suggests it is Jurassic. The Southwest pluton is cut by the Roosevelt Granite (surface), it cuts the Buckhorn pluton (drill core) and is cut by a quartz-porphyry-like dike. Given the amount of overall alteration present in the Southwest pluton relative to the Roosevelt Granite and these cross-cutting relations, the Southwest pluton is most likely Jurassic. In sum, the evidence and the constraints discussed in the previous chapters and summarized above suggests that the Southwest pluton (below and to the east of the Southwest Zone) is responsible for gold mineralization in the Southwest Zone (Fig. 5.1).

The recognition of the Southwest pluton as the pluton responsible for gold mineralization within the Southwest Zone provides a potential exploration tool. A proper re-examination of the igneous intercepts (both in drill core and in outcrop) to determine the on-site distribution of this intrusion could potentially open up new target areas. On a regional exploration scale, the logical next step in using this information is a geophysical investigation of the Southwest pluton and its Ti Diorite margin. A geophysical signature of the pluton would allow for easier identification of the same intrusive body in the region. As this body is associated with gold deposition, its periphery would be a good place to focus some rudimentary exploration geology.

No previous workers have drawn any conclusions concerning the nature of the relationship between the Gold Bowl and the Southwest Zone—or if it is related to the

Southwest Zone at all. Certainly the higher Hg present in Gold Bowl gold (for a given Ag content, Fig. 4.9) suggests Gold Bowl is a completely different system. Major contrasts in elements present and in elemental correlations (Tables 4.6, 4.7) between the Southwest Zone and Gold Bowl also hint that the two are unrelated. Unfortunately, some methods I used to determine direction of fluid movement in the Southwest Zone are not applicable for the Gold Bowl. The Gold Bowl seemingly lacks the appropriate host rock (limestone or marble) for forming the simple silicate zoning expected in a skarn system. Instead the host lithologies are mostly aluminum-rich calcareous hornfels (Fig. 3.13), with little, if any, pure marble. Further, since the amount of purely metasomatic pyroxene present in the Gold Bowl is apparently small, the limited pyroxene compositional data available show no discernible pattern.

Metal zoning in the Gold Bowl is similarly problematic, in part because I lack sufficient data for reliable contouring. The data I do have (Figs. 4.10, 4.11, 4.12) suggest a different direction of fluid flow for each ratio: N→S (Bi/Au), W→E (Cu/Au), and E→W (Cu/Pb). While the patterns within the Gold Bowl may be a little obscure as a result of the limited data, the elevated Cu/Au ratios along the western margin are clearly different from the Southwest Zone. In contrast, the Cu/Pb ratios for both the Gold Bowl and the Southwest Zone are strikingly higher along the eastern edges of the deposits.

The Gold Bowl also displays elevated concentrations (Table 4.5) of more soluble elements (higher mean and median values for Pb, Zn, and Sb) relative to the Southwest Zone (Table 4.5: higher mean and median Cu, As, W, Mo, and Ni), which suggests it is a

distal portion of SOME deposit. However, NONE of the metal ratio zoning patterns suggests a S→N fluid movement, and no physical evidence of fluid flow (such as stockwork veining in hornfels) between the Southwest Zone and Gold Bowl has been documented. If the Gold Bowl cross-section (Fig. 1.9) is representative, then the magnetite→ garnet zoning suggests a source below and NE of that deposit. While not totally conclusive, this lack of interpretable metal distribution and ratio pattern and lack of veining between the Gold Bowl and Southwest Zone suggest that these are in fact two different systems, related only by spatial proximity. It is possible, for example, that a different pluton - similar in size and geometry to the SW pluton - underlies the Gold Bowl area. Finally, some geologic maps (e.g., Fig. 1.11) show one or more major faults between the Southwest Zone and Gold Bowl: the present spatial proximity might be in part structural.

The source of the mineralization within the Gold Bowl remains ambiguous. A wide variety of intrusions are present within the Gold Bowl, including the Buckhorn pluton, marginal phase, Ti Diorite, gabbro feeder dikes, and an assortment of other un-analyzed intrusions. The focus of this study was the Southwest Zone, and further investigation would be needed to form a better interpretation of the Gold Bowl and its source. The first step in investigating the nature of the Gold Bowl would be to provide much more complete sampling for metal ratios. To better understand the relationship between the Gold Bowl and the Southwest Zone, I recommend selecting a K-bearing mineral from both portions that would be more appropriate for $^{40}Ar/^{39}Ar$ dating and is directly intergrown with gold.

References

Atkinson, W.W., and Einaudi, M.T., 1978, Skarn formation and mineralization in the contact aureole at Carr Fork, Bingham, Utah: Econ. Geol., v. 73, p. 1326-1365.

Barnes, H.L., 1979, Geochemistry of hydrothermal ore deposits: Solubilities of ore minerals, The Pennsylvania State University Ore Deposit Research Section, University Park, Pennsylvania, ed. 2., p. 405 – 460.

Barnes, H.L., Rose, A.W., Burt, D.M., 1979, Geochemistry of hydrothermal ore deposits: Hydrothermal Alteration, The Pennsylvania State University Ore Deposit Research Section, University Park, Pennsylvania, ed. 2., p. 173 – 202.

Cheney, E.S., Rasmussen, M.G., Miller, M.G. 1994, Major Faults, Stratigraphy, and Identity of Quesnellia in Washington and Adjacent British Columbia: Washington Division of Geology and Earth Resources Bulletin, vol. 80, p. 49 - 71.

Einaudi M.T., & Burt D.M., 1982. Introduction, terminology, classification and composition of skarn deposits. Economic Geology, 77, pp. 745–754.

Einaudi, M.T., Meinert, L.D., Newberry, R.J., 1981, Skarn deposits. In 75th Anniversary Volume, 1906-1980, Economic Geology, in B.J. Skinner, ed., Economic Geology Publishing Co. p. 317 - 391.

Ettlinger, A.D., Meinert, L.D., and Ray, G.E., 1992, Skarn evolution and hydrothermal fluid characteristics in the Nickel Plate deposit, Hedley District, British Columbia. Economic Geology, Vol. 87, p. 1541 - 1565.

Evans, A.M., 1987, An Introduction to Ore Geology, Blackwell Science Ltd., Ed. 2,

Flanigan, B., Freeman, C., Newberry, R., McCoy, D., Hart, C., 2000, Exploration models for mid and late cretaceous Intrusion-related gold deposits in Alaska and the Yukon Territory, Canada, in Geology and Ore Deposits 2000: The Great Basin and Beyond, Geological Society of Nevada, p. 138 - 157.

Gaspar, L.M.G.G., 2005, The Crown Jewel gold skarn deposit: Unpublished Ph.D. thesis, Pullman, Washington, USA, Washington State University, p. 346.

Hickey III, R.J., 1990, The Geology of the Buckhorn Mountain Gold Skarn, Okanogan County, Washington: Unpublished M.S. thesis, Pullman, Washington, USA, Washington State University.

Hickey III, R.J., 1992, The Buckhorn Mountain (Crown Jewel) gold skarn deposit, Okanogan County, Washington. Economic Geology, Vol. 87, p. 125 - 141.

Klaus K.E. Neuendorf, James P. Mehl, Jr., and Jackson, J.A., 2011, Glossary of Geology, American Geosciences Institute, Ed. 5.

Le Bas, M.J., & Streckeisen, A.L., 1991, The IUGS Systematics of Igneous Rocks, Journal of the Geological Society, London, Vol. 148, p. 825 – 833.

Le Maitre, R.W., ed. 2002, Igneous Rocks: A classification and Glossary of Terms, 2d. ed. Cambridge: Cambridge University Press.

Lough, T.A., Freeman, L.K., Elliot, B.A., Griesel, G.A., Newberry, R.J., and Szumigala, D.J., 2012, Geochemical, major-oxide, trace-element, and carbon data from rocks collected in 2011 in the Moran area, Tanana and Melozitna quadrangles, Alaska; Data File 2011-4 v.2, p. 176.

Lyons, P.C., 1971, Staining of feldspars on rock-slab surfaces for modal analysis. Short Communications: Mineralogical Magazine, Vol. 38, p.519 - 519.

McMillen, D.D., 1979, The Structure and Economic Geology of Buckhorn Mountain, Okanogan County, Washington: Unpublished Ph.D. thesis, Seattle, Washington, USA, University of Washington.

Meinert, L.D., 1983, Variability of skarn deposits - Guides to exploration: in Boardman, S.J., ed., Revolution in the Earth Sciences, Kendall-Hunt Publishing Co., p. 301-316.

Meinert, L.D., 1992, Skarns and Skarn Deposits: Geoscience Canada, V. 19, p. 1-23,145-162.

Meinert, L.D., 1997, Application of skarn deposit zonation models to mineral exploration. Expl. and Mining Geol. 6, 185-208.

Meinert, L.D., Newberry, R.J., and Einaudi, M.T., 1980, An overview of W, Cu, and Zn-bearing skarns in Western North America: in Mineral Deposits of the Pacific Northwest, Field C., and Silberman, M., eds., U.S. Geological Survey Open File Report 81-355, p. 303-327.

Meinert, L.D., Dipple, G.M., and Nicolescu, S., 2005, World Skarn Deposits: in Hedenquist, J.W., Thompson, Economic Geologists, Littleton, Colorado, p. 299 – 336.

Mutschler, F.E., Rougon, D.J., Lavin, O.P., and Hughes, R.D., 1981, Petros – A data bank of major element chemical analyses of igneous rocks for research and teaching (Version 6.1): Boulder, Colorado, NOAA – National Geophysical and Solar-Terrestrial Data Center.

Myers, G.L. and Meinert, L.D., 1991, Alteration, Mineralization, and Gold Distribution in the Fortitude Gold Skarn, in Geology and Ore Deposits of the Great Basin: Symposium Proceedings, Geological Society of Nevada, Vol. 1, p. 407 - 417.

Newberry, R.J., 1982, Tungsten-bearing skarns of the Sierra Nevada I. The Pine Creek Mine, California, Economic Geology, v. 77, p. 823-844.

Newberry, R.J., 1998, W & Sn Skarn Deposits: A 1998 Status Report, in D.R. Lentz, ed., Mineralized Intrusion-related skarn systems, Mineralogical Assoc. Canada Short Course Notes, Vol. 26, p. 289-336.

Newberry, R.J., Mrozek, S.A., Perttu, B.K., Broman, B., Wagner, K., and Lessard, R., 2010, Yet still ANOTHER look at the Nixon Fork Au-Cu-Ag Skarn, SW Alaska: Alaska Miners Association Spring Meeting, Abstracts with Program, p. 12-15.

Pearson, R.C., 1967, Geologic Map of the Bodie Mountain Quadrangle Ferry and Okanogan Counties, Washington, U.S. Geological Survey, GQ 636.

Potts, P.S., 1987. A Handbook of Silicate Rock Analysis: Glasgow, Blackie. p. 622.

Ray, G.E., 2006, A Review of Skarns and Skarn-deposits in the Canadian Cordillera, Geofile 2007, British Columbia Geological Survey, Ministry of Energy, Mines and Petroleum Resources.

Ray, G.E., 2009, Summary Report on a Second Visit to the Buckhorn Mine Area, Okanogan County, WA, USA, unpublished Kinross report.

Ray, G.E. and Dawson, G.L., 1994, The Geology and Mineral Deposits of the Hedley Gold Skarn District, Southern British Columbia; B.C. Ministry of Energy, Mines and Petroleum Resources, Bulletin 87, p. 156.

Ray, G.E., Ettlinger, A.D., Meinert, L.D., 1990, Gold skarns: their distribution, characteristics and problems in classification. B.C. Ministry of Energy, Mines and Petroleum Resources, Paper 1990-1, p. 237-246.

Ray, G.E., Dawson, G.L., Ettlinger, A.D., 1992, A Geological Overview of the Hedley Gold Skarn District British Columbia (92H). Geological Fieldwork: B.C. Geological Survey Branch, p. 275.

Robb, L., 2010, Introduction to Ore Forming Processes, Blackwell Publishing, Oxford, UK

Streckeisen, A. L. & Le Maitre, R. W. 1979. A chemical approximation to the modal QAPF classification of the igneous rocks. Neues Jahrbuch für Mineralogie, Abhandlungen, 136, 169 - 206.

Table A1-1. Clinopyroxene Electron Microprobe (EMP) routine

Beam conditions for all elements								
Kilovolts	15							
Current	10							
Size	1							
Magnification	1000							
Analytical Conditions								
Element	Silica	Manganese	Sodium	Magnesium	Calcium	Aluminum	Iron	Potassium
Element Symbol	Si	Mn	Na	Mg	Ca	Al	Fe	K
X-Ray	ka	ka	ka	ka	ka	ka	ka	ka
Crystal	TAP	LIF	TAP	TAP	PET	TAP	LIF	PET
Spectrometer	4	3	2	2	1	4	3	1
On Peak Position	27840	52282	46310	38463	38388	32527	48150	42760
High Background Position	28840	52782	47160	39463	38888	33427	48600	43459
Low Background Position	26840	51782	45460	37363	37888	31627	47700	42060
Count Times								
On Peak	10	10	10	10	10	10	10	10
High Background	5	5	5	5	5	5	5	5
Low Background	5	5	5	5	5	5	5	5

Table A1-2. Gold Electron Microprobe (EMP) routine.

Beam conditions for all elements			
Kilovolts	25		
Current	20		
Size	5		
Magnification	1000		
Analytical Conditions			
Element	Gold	Silver	Mercury
Element Symbol	Au	Ag	Hg
X-Ray	la	la	la
Crystal	LIF	PET	LIF
Spectrometer	3	2	1
On Peak Position	31795	47493	30848
High Background Position	32422	48156	30212
Low Background Position	31167	46829	30212
Count Times			
On Peak	10	10	10
High Background	5	5	0
Low Background	5	5	10

Table A1-3. XRF Analytical conditions for pressed pellet trace element analysis

Analytical Conditions														
Element		Cu	As	Ag	Te	Bi	Au	Rh	W	Mo	Pb	Zn	Sb	Ni
X-ray Line		ka	ka	ka	ka	la	la	ka-C	la	ka	lb2	ka	ka	ka
Cyrstal		LiF 220	LiF 220	LiF 220	LiF 220	LiF 220	LiF 220	LiF 220	LiF 220	LiF 220	LiF 220	LiF 200	LiF 220	LiF 220
Collimator		150 µm	150 µm	150 µm	150 µm	150 µm	150 µm	150 µm	150 µm	150 µm	150 µm	150 µm	150 µm	150 µm
Detector		Flow	Scint.	Scint.	Scint.	Scint.	Scint.	Scint.	Flow	Scint.	Scint.	Scint.	Scint.	Flow
Tube Filter						None						Al**	None	
kV		60	60	60	60	60	60	60	60	60	60	60	60	60
mA		66	66	66	66	66	66	66	66	66	66	66	66	66
Angle	(°2T)	65.567	43.586	22.651	18.223	47.351	53.248	26.200	62.47	28.839	40.360	41.775	19.002	71.289
Offset Bg 1	(°2T)	1.103	0.357	-0.300	-0.317	0.847	-0.359	-0.808	-0.447	-0.549	0.750	-0.850	-0.287	-0.611
Offset Bg 2	(°2T)	-0.905	-0.342		0.417	-0.913		1.184	1.019	0.653		0.688	0.395	0.888
PHID*	LL	39	33	33	30	23	27	29	41	30	31	30	29	40
PHID*	UL	60	69	64	60	73	68	69	61	65	66	68	61	66
Count Times														
Peak		20	120	100	100	246	238	8	98	12	40	10	30	30
Background 1		2	60	68	50	22	156	4	18	4	40	None	16	10
Background 2		3	60	None	50	16	None	4	8	4	None	None	16	10
Background 1 Factor		0.451	0.489	1	0.568	0.519	1	0.594	0.695	0.543	1	1	0.579	0.593
Background 2 Factor		0.549	0.511		0.432	0.481		0.406	0.305	0.457			0.421	0.407

*Pulse height descriminator, LL = lwer limit, UL = upper limit, **Aluminum filter (200 µm), Flow = Flow porportional, Scint. = scintillator counter, Bg = background, Cu = copper, As = Arsenic, Ag = Silver, Te = Tellurium, Bi = Bismuth, Au = Gold, Rh = Rhodium compton, W = Tungsten, Mo = Molybdenum, Pb = Lead, Zn = Zinc, Sb = Antimony, Ni = Nickel, °2T = 2 Theta

Table A1-4. Correction coefficients* for the XRF routine detailed in Table A1-3

Element	Cu	As	Ag	Te	Bi	Au	W	Mo	Pb	Zn	Ni	Rh5Bg1
	Lo (C)	Lo (C)	Lo (C)	Lo (C)	Lo (C)	Lo (C)	Lo (C)	Lo (C)	Lo (C)	Lo (C)	Lo (C)	Lo (R)
Cu										0.0088		
As					0.0031				0.0007			
Ag					-0.0007			-0.013		-0.0003		r.231541
Te										-0.0001		
Bi		-0.003				0.0985	-0.005		-0.006	0.0004		
Au							0.0724			0.0016		
W	0.00008				-0.0007				-0.002	-0.0012	-0.055	
Mo												
Pb		-0.0009			0.0116		-0.0001					
Zn	0.0082				-0.007		0.0035		0.001			
Sb			-0.163	0.1646	0.0016					-0.0025		
Ni												

*all data for a given sample ratioed to counts for the Rh compton peak in that sample. Lo(C)= line overlap correction using calculated concntration of the interfering element, 'Lo(R)= line overlap correction using the counts/per second (rate) of the interfering peak, Cu = Copper, As = Arsenic, Ag = Silver, Te = Tellurium, Bi = Bismith, Au = Gold, W = Tungsten, Mo = Molybdenum, Pb = Lead, Zn = Zinc, Sb = Antimony, Ni = Nickel.

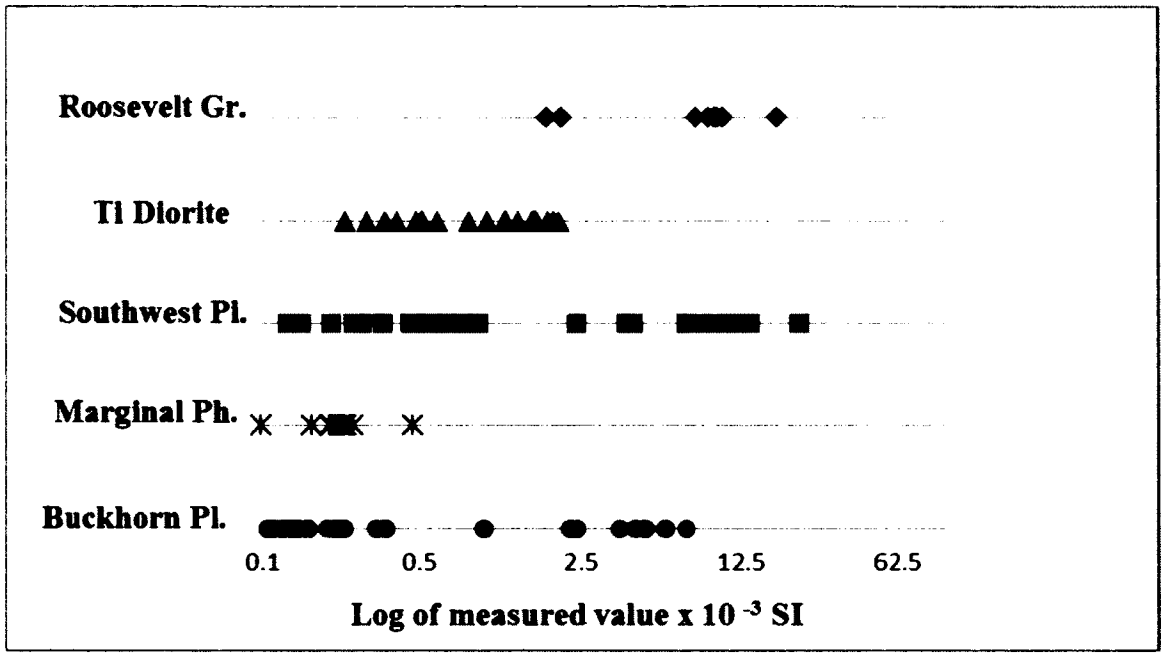

*Magnetic susceptibility values on stained and un-stained rock slabs plotted on a log scale. Pl. = pluton. Ph. = phase. Gr = granite.

Figure A-2.1. Magnetic susceptibility by igneous rock type.

Table A2-1. Buckhorn pluton compositions (surface samples) by XRF.

SAMPLE	SiO_2	Al_2O_3	CaO	FeO	K_2O	MgO	MnO	Na_2O	P_2O_5	TiO_2
	weight percent oxide									
357	66.8	15.2	5.0	3.3	0.8	2.1	0.1	5.9	0.3	0.5
361	67.6	15.4	4.1	3.4	3.8	1.2	0.1	3.3	0.2	0.5
361	67.6	15.4	4.1	3.4	3.8	1.2	0.1	3.3	0.2	0.5
382	68.6	15.1	4.0	3.0	3.7	1.2	0.1	3.6	0.2	0.4
383	69.7	15.3	4.5	1.2	0.8	1.4	0.0	6.2	0.3	0.3
384	65.2	17.1	5.5	2.0	2.8	1.8	0.0	4.6	0.3	0.4
385	67.4	15.8	4.6	3.2	3.2	1.3	0.1	3.5	0.2	0.4
387	67.4	15.7	3.6	3.8	3.9	1.3	0.1	3.2	0.3	0.5
388	67.0	15.9	4.4	3.5	3.2	1.3	0.1	3.8	0.3	0.4
392	69.0	15.1	4.1	3.2	2.6	1.1	0.1	3.9	0.3	0.4
393	69.8	15.5	4.3	2.4	1.8	0.9	0.0	4.5	0.2	0.3
394	68.5	15.5	4.2	2.9	2.9	1.1	0.1	4.0	0.2	0.3
395	68.4	15.9	3.3	2.8	2.3	1.2	0.0	5.2	0.3	0.3
396	65.2	16.5	4.4	3.6	3.6	1.5	0.1	4.1	0.3	0.5
397	66.2	15.9	4.7	3.7	2.6	1.2	0.0	4.5	0.3	0.4
399	66.0	16.0	4.7	3.0	2.5	2.1	0.1	4.6	0.3	0.6
400	66.4	16.2	4.6	2.7	2.4	1.8	0.0	4.7	0.4	0.5
401	67.1	15.6	4.2	3.5	3.7	1.4	0.1	3.4	0.2	0.5
402	67.0	16.0	4.3	3.5	3.6	1.2	0.1	3.3	0.3	0.5
404	66.4	16.0	4.4	2.7	2.7	1.9	0.0	4.5	0.3	0.6
BS048	67.7	15.0	4.2	3.7	3.2	1.5	0.1	3.6	0.3	0.5
BS058	67.3	16.3	4.9	1.5	2.1	1.3	0.0	5.8	0.2	0.3
BS059	63.7	15.7	4.7	5.0	3.2	1.9	0.1	4.4	0.4	0.6
BS076	65.0	16.1	4.7	3.5	2.4	2.4	0.1	4.5	0.3	0.6
CF1	67.1	15.3	4.1	3.1	3.1	1.8	0.1	4.3	0.3	0.5
CF10	66.8	15.7	4.5	3.3	2.6	1.5	0.1	4.5	0.3	0.5
CF17	66.9	15.9	3.5	3.8	3.7	1.5	0.0	3.6	0.3	0.5
CF17	66.9	15.9	3.5	3.8	3.7	1.5	0.0	3.6	0.3	0.5
CF22	69.0	15.9	3.7	1.9	2.7	0.8	0.0	5.1	0.2	0.4
CF3	66.5	15.4	4.5	3.1	2.9	2.1	0.1	4.1	0.4	0.6
CF31	66.5	16.2	4.2	3.3	3.8	1.5	0.1	3.6	0.2	0.4
CF32	66.0	16.2	7.2	2.2	1.1	1.5	0.0	4.9	0.3	0.4
CF33	66.5	16.0	5.4	2.2	2.4	1.7	0.0	5.0	0.3	0.4
CF36	63.5	17.0	5.4	3.1	3.1	1.8	0.1	4.8	0.3	0.5
CF38	68.7	15.1	4.0	3.2	3.2	1.2	0.1	3.7	0.3	0.4
CF3C	66.5	15.5	4.3	3.9	4.3	1.1	0.1	3.5	0.3	0.4
CF54	65.4	16.3	4.6	3.3	3.8	1.3	0.1	4.2	0.2	0.5
CF58	66.0	16.0	4.4	2.8	2.6	2.3	0.1	4.6	0.3	0.6
CF5A	66.0	15.1	5.1	3.5	3.1	1.8	0.1	4.3	0.3	0.4
CF5C	64.4	16.2	5.5	3.4	4.1	1.5	0.1	3.8	0.3	0.4
CF7	66.7	15.8	4.0	2.6	3.4	1.9	0.0	4.2	0.3	0.5
CF8	66.3	15.9	4.3	2.7	3.4	1.9	0.0	4.2	0.3	0.5

Table A2-1 continued. Buckhorn pluton compositions (surface samples) by XRF.

SAMPLE	Rb	Sr	Y	Zr	Nb
	parts per million				
357	25	532	17	155	13
361	99	186	14	123	11
361	99	186	14	123	11
382	101	618	15	126	10
383	36	704	13	111	10
384	74	774	14	132	11
385	101	720	12	94	9
387	110	523	16	130	11
388	108	681	17	118	11
392	76	651	14	131	12
393	71	870	10	108	11
394	73	652	7	86	6
395	96	639	14	146	11
396	108	702	17	119	12
397	110	683	17	160	13
399	65	912	13	137	9
400	77	948	11	127	8
401	131	616	17	122	11
402	128	719	19	124	11
404	70	964	13	153	11
BS048	105	-	18	121	12
BS058	64	-	14	107	11
BS059	129	-	20	125	12
BS076	62	928	13	141	9
CF1	124	905	15	155	11
CF10	87	787	18	120	12
CF17	125	524	20	124	11
CF17	125	524	20	124	11
CF22	96	546	24	190	16
CF3	93	936	15	164	12
CF31	107	579	16	130	12
CF32	26	717	16	126	11
CF33	54	686	15	122	11
CF36	95	664	18	162	12
CF38	112	795	17	110	10
CF3C	145	614	22	162	13
CF54	107	531	15	109	10
CF58	87	918	14	143	10
CF5A	77	488	15	129	10
CF5C	102	610	16	117	9
CF7	93	996	15	167	14
CF8	84	990	15	179	13

Table A2-1 continued. Buckhorn pluton compositions (drill core samples) by XRF.

SAMPLE	Depth	SiO_2	Al_2O_3	CaO	FeO	K_2O	MgO	MnO	Na_2O	P_2O_5	TiO_2
	(feet)	weight percent oxide									
D07-309	82	65.2	16.4	4.2	2.3	3.5	1.8	0.0	5.1	0.2	0.4
D07-371	352	64.4	15.8	6.5	2.5	3.3	1.7	0.1	4.5	0.3	0.5
D07-371	89	69.8	14.2	4.6	1.7	1.9	1.3	0.0	5.5	0.2	0.4
D07-378	704	65.5	15.8	4.4	3.7	4.2	1.6	0.1	3.6	0.3	0.5
D07-378	716	65.1	15.7	4.8	4.1	3.2	1.6	0.1	4.1	0.4	0.5
D07-405	540	69.2	14.6	2.0	2.4	4.3	1.4	0.1	5.0	0.4	0.4
D07-405	814	66.5	15.8	2.8	2.7	4.9	1.6	0.0	4.2	0.3	0.6
D07-407	341	63.4	16.1	5.1	4.2	2.7	2.6	0.1	4.2	0.4	0.7
D07-407	794	75.6	12.9	1.3	1.0	4.2	0.4	0.0	4.0	0.1	0.2
D07-407	846	61.8	16.5	5.6	4.7	2.2	2.7	0.1	4.6	0.5	0.8
D08-448	10	66.0	16.0	3.6	2.6	1.7	1.6	0.0	7.5	0.3	0.4
D08-453	1048	68.8	16.8	3.5	0.7	0.3	0.5	0.0	8.7	0.1	0.4
D09-511	101	63.4	17.3	6.2	1.3	3.4	1.6	0.0	5.9	0.2	0.3
D09-511	1311	67.4	15.1	4.3	3.7	3.2	1.6	0.1	3.5	0.3	0.5
D09-512	1049	67.6	15.6	3.3	3.2	2.8	1.7	0.1	4.9	0.2	0.4
D09-512	1280	67.2	15.2	4.8	3.8	2.8	1.4	0.1	3.7	0.3	0.5
D09-514	966	67.2	16.0	4.0	3.1	3.6	1.3	0.0	4.0	0.2	0.4
D09-515	745	68.9	15.4	2.9	2.6	3.3	1.2	0.0	4.7	0.3	0.4
D09-515	898	68.9	15.1	3.7	2.8	3.3	1.2	0.1	4.1	0.2	0.3
D09-516	179	67.3	16.8	3.2	0.8	3.8	1.0	0.0	6.6	0.2	0.2
D09-516	237	68.0	16.2	3.5	1.2	2.8	1.1	0.0	6.2	0.2	0.2
D09-516	845	63.5	16.9	5.9	2.4	3.5	1.9	0.0	4.9	0.3	0.4
D09-536	1022	64.5	6.9	12.3	9.9	0.1	4.6	0.3	0.3	0.2	0.5
D09-541	275	67.9	15.7	3.3	2.7	1.9	2.1	0.0	4.8	0.3	0.5
D10-587	1263	66.8	15.6	4.1	3.5	3.6	1.5	0.1	3.9	0.2	0.5
D10-587	346	61.9	17.4	5.9	3.8	1.9	2.7	0.1	4.9	0.4	0.6
D10-587	932	70.6	15.0	3.2	1.9	2.8	1.1	0.0	4.4	0.2	0.4
D10-721	1281	65.0	16.6	4.9	2.8	3.2	1.0	0.1	5.2	0.2	0.4
D10-725	167	64.3	16.7	5.4	1.6	3.6	1.7	0.1	5.6	0.3	0.4
D10-725	779	64.3	15.7	5.8	3.9	2.5	1.5	0.1	5.4	0.3	0.5
D11-795	753	67.0	15.5	4.1	3.1	1.8	1.7	0.1	5.7	0.2	0.4
D11-842	770	65.9	15.6	4.5	4.1	3.5	1.5	0.1	3.7	0.3	0.5
D92-162	186	68.7	15.2	3.9	2.9	4.1	1.0	0.0	3.2	0.2	0.4

Table A2-1 continued. Buckhorn pluton compositions (drill core samples) by XRF.

SAMPLE	Depth	Rb	Sr	Y	Zr	Nb
	(feet)	parts per million				
D07-309	82	97	590	21	148	13
D07-371	352	81	630	21	158	14
D07-371	89	82	467	13	121	11
D07-378	704	120	-	17	106	10
D07-378	716	96	-	18	122	11
D07-405	540	137	-	10	130	12
D07-405	814	191	-	14	194	21
D07-407	341	76	-	16	178	12
D07-407	794	113	-	6	76	9
D07-407	846	63	-	16	166	9
D08-448	10	71	324	19	161	12
D08-453	1048	11	344	14	104	3
D09-511	101	124	650	19	130	10
D09-511	1311	95	-	15	108	10
D09-512	1049	93	771	15	100	12
D09-512	1280	83	797	15	101	11
D09-514	966	114	701	13	102	10
D09-515	745	92	-	17	109	11
D09-515	898	109	-	12	88	9
D09-516	179	111	472	14	127	11
D09-516	237	83	-	11	116	10
D09-516	845	80	-	14	128	11
D09-536	1022	2	244	22	94	5
D09-541	275	65	434	21	164	14
D10-587	1263	131	603	20	167	13
D10-587	346	56	-	15	105	8
D10-587	932	106	475	14	165	13
D10-721	1281	51	325	21	75	3
D10-725	167	100	491	20	153	14
D10-725	779	95	485	21	145	11
D11-795	753	85	-	14	131	11
D11-842	770	131	792	17	122	12
D92-162	186	130	662	18	104	10

- Indicates sample values below analytical detection.

Table A2-2. Marginal phase compositions by XRF.

SAMPLE	Depth	SiO_2	Al_2O_3	CaO	FeO	K_2O	MgO	MnO	Na_2O	P_2O_5	TiO_2
	(feet)	weight percent oxide									
362		60.2	17.8	4.7	5.0	1.4	2.3	0.1	7.3	0.5	0.4
363		63.0	17.6	3.9	3.4	1.7	1.7	0.1	7.6	0.3	0.3
366		61.0	17.1	7.5	3.2	1.5	3.0	0.1	4.9	0.3	0.4
367		60.9	20.5	5.2	3.0	3.1	3.5	0.1	2.3	0.3	0.4
368		55.4	16.4	7.6	9.8	0.1	4.0	0.2	5.4	0.2	0.8
380C		60.5	16.6	5.7	5.3	3.9	2.3	0.1	4.2	0.4	0.6
BS060MD		57.8	16.4	6.7	6.4	3.7	3.5	0.1	4.0	0.5	0.6
BS064MD		60.2	18.1	4.8	5.0	1.4	2.3	0.1	7.2	0.3	0.4
CF13		56.2	18.2	12.0	3.1	0.1	3.1	0.1	6.0	0.4	0.7
CF41		57.3	18.7	9.7	2.5	3.4	2.4	0.1	4.6	0.4	0.5
CF55		56.4	18.2	9.2	4.4	2.2	2.7	0.1	5.4	0.3	0.7
CF57		62.2	17.3	5.3	4.0	3.4	1.6	0.1	4.9	0.3	0.5
D08-426	867	56.1	18.8	8.2	4.2	3.9	2.6	0.1	4.2	0.5	0.6
D08-479	1091	55.7	13.9	14.3	9.2	0.1	2.4	0.3	3.0	0.2	0.6
D09-511	514	56.8	16.5	7.0	6.7	3.5	3.6	0.2	4.2	0.5	0.7
D09-512	1045	57.5	15.9	6.8	7.3	3.2	4.0	0.1	3.8	0.5	0.7
D09-512	412	56.5	15.3	10.5	6.6	3.0	4.7	0.2	1.7	0.5	0.8
D09-514	150	57.0	16.5	7.0	7.0	3.7	3.5	0.1	3.9	0.5	0.6
D09-514	464	57.6	15.4	7.3	8.1	2.9	4.2	0.1	2.5	0.5	0.7
D09-516	657	58.5	15.8	6.5	7.2	3.1	3.2	0.1	3.9	0.5	0.7
D09-516	669	55.6	18.2	4.8	7.8	3.6	3.9	0.1	5.2	0.6	0.8
D09-516	793	55.4	16.8	7.2	7.7	2.7	4.1	0.1	4.4	0.5	0.8
D09-518	887	59.0	18.3	4.4	7.3	2.3	2.5	0.1	4.5	0.2	0.7
D09-536	812	60.8	7.6	16.7	8.4	0.1	4.4	0.2	0.7	0.5	0.5
D10-560	70	57.9	17.4	8.7	3.2	2.1	2.2	0.1	7.1	0.4	0.5
D10-560	76.5	57.0	18.5	5.8	4.9	1.8	3.9	0.0	7.0	0.5	0.5
D10-582	432	59.7	17.8	5.7	5.1	3.0	2.5	0.1	4.1	0.5	0.6
D10-582	458	57.0	18.8	6.2	5.5	3.6	2.4	0.1	4.0	0.5	0.6
D10-582	536	58.7	18.1	6.6	5.5	2.7	2.3	0.1	4.3	0.6	0.6
D10-583	1090	58.5	18.9	7.9	2.3	3.7	2.3	0.1	5.2	0.4	0.5
D10-583	1152	57.6	19.3	9.9	2.2	0.5	2.1	0.1	7.2	0.5	0.4
D10-587	592	60.7	17.7	6.4	4.8	3.0	1.5	0.1	4.5	0.2	0.4
D10-713	429	60.0	18.0	5.9	4.8	3.0	2.3	0.1	4.0	0.5	0.5
D10-721	38	59.4	18.5	6.0	2.8	3.8	1.7	0.0	6.4	0.4	0.5
D10-725	79	60.1	17.4	7.0	2.9	0.5	2.1	0.1	9.1	0.3	0.5
G.R. T.L. E.D.		54.4	18.1	9.5	6.2	0.7	4.4	0.1	5.6	0.2	0.6
J.E.038		56.0	17.8	6.1	7.5	0.4	3.7	0.2	7.5	0.2	0.6
MD-IGN-1		58.6	15.9	5.2	7.6	0.6	5.9	0.2	4.7	0.3	0.7

Table A2-2. Marginal phase compositions by XRF.

SAMPLE	Depth	Rb	Sr	Y	Zr	Nb
	(feet)	parts per million				
362		36	587	10	72	5
363		36	584	9	71	6
366		41	775	8	40	4
367		95	560	7	66	5
368		0	648	21	74	3
380C		122	816	19	111	12
BS060MD		120	-	21	93	10
BS064MD		41	-	9	72	5
CF13		1	638	23	141	12
CF41		68	783	20	115	9
CF55		55	636	24	145	12
CF57		118	785	20	114	13
D08-426	867	92	591	21	106	9
D08-479	1091	2	390	32	60	2
D09-511	514	111	-	21	89	10
D09-512	1045	117	894	23	93	11
D09-512	412	87	418	20	91	11
D09-514	150	106	-	20	43	6
D09-514	464	125	-	23	42	9
D09-516	657	103	988	21	56	9
D09-516	669	151	651	25	87	12
D09-516	793	79	-	20	51	8
D09-518	887	50	1210	27	119	4
D09-536	812	1	397	14	58	2
D10-560	70	53	-	14	77	6
D10-560	76.5	94	-	16	83	6
D10-582	432	94	-	21	110	9
D10-582	458	83	846	19	101	10
D10-582	536	102	-	20	98	9
D10-583	1090	82	511	17	114	9
D10-583	1152	13	559	16	108	9
D10-587	592	66	364	32	94	3
D10-713	429	97	-	17	117	9
D10-721	38	120	698	24	169	14
D10-725	79	15	595	19	145	12
G.R. T.L. E.D.		51	-	14	54	2
J.E.038		5	-	18	66	3
MD-IGN-1		14	-	17	50	3

Table A2-3. Southwest pluton compositions by XRF.

SAMPLE	Depth (feet)	SiO_2	Al_2O_3	CaO	FeO	K_2O	MgO	MnO	Na_2O	P_2O_5	TiO_2
		weight percent oxide									
389		58.0	15.5	8.2	5.7	2.6	2.4	0.1	4.0	0.5	1.0
390		64.1	15.0	3.8	6.1	3.4	1.8	0.1	3.8	0.6	0.8
391		64.1	16.2	4.7	4.3	2.6	2.1	0.1	4.5	0.4	0.8
398		60.3	16.7	5.9	4.5	2.8	3.5	0.1	4.4	0.5	0.9
CF2		63.0	15.2	5.0	4.4	3.6	3.2	0.1	3.6	0.5	0.9
CF46		63.4	15.2	4.9	4.2	3.6	3.0	0.1	3.7	0.5	0.8
CF50		63.4	16.5	5.4	3.1	3.6	2.1	0.1	4.5	0.4	0.6
D07-306	115	61.0	15.3	5.3	5.1	3.9	3.5	0.1	3.6	0.7	0.9
D07-306	53	57.6	15.2	5.1	7.1	3.9	5.5	0.1	2.6	1.0	1.3
D07-320	134	62.6	15.3	5.0	4.7	3.5	3.4	0.1	3.6	0.6	0.9
D07-371	516	61.6	15.6	6.7	4.5	1.8	3.6	0.1	4.3	0.4	0.9
D07-407	562	62.3	15.2	5.6	5.0	2.9	3.2	0.1	3.8	0.5	0.8
D07-408	852	61.7	16.3	5.5	4.5	2.8	2.8	0.1	4.2	0.6	0.9
D09-519	193	61.5	14.0	6.0	8.4	1.1	1.4	0.2	5.4	0.5	0.9
D09-528	317	60.6	15.9	5.3	5.1	2.7	3.3	0.1	4.8	0.7	0.9
D09-551	349	60.0	16.1	6.0	6.2	2.2	3.9	0.1	3.8	0.5	0.9
D10-581	697	60.1	15.9	5.4	4.1	4.4	3.8	0.1	3.2	0.8	0.9
D10-583	112	62.3	15.8	4.5	4.7	3.4	3.3	0.1	4.0	0.6	0.8
D10-583	283	60.9	16.5	5.7	5.1	2.5	3.4	0.1	4.1	0.4	0.8
D10-584	737	60.0	16.2	4.9	5.8	2.2	3.1	0.1	5.4	0.6	1.3
D10-587	710	60.3	16.2	6.0	5.6	2.6	3.3	0.1	4.0	0.7	0.9
D10-587	894	64.5	16.2	3.6	2.6	3.3	3.3	0.0	3.9	0.4	1.0
D10-588	522	64.5	14.9	5.2	4.0	2.8	1.9	0.1	4.7	0.4	0.8
D10-589	361	61.8	16.3	5.7	4.2	3.0	3.3	0.1	4.1	0.5	0.8
D10-589	478	64.5	15.9	4.6	3.9	3.3	2.0	0.1	4.4	0.4	0.7
D10-590	966	63.0	16.3	6.1	4.2	2.7	2.3	0.1	3.9	0.3	0.7
D10-590	968	61.8	16.6	6.6	4.5	2.6	2.6	0.1	3.9	0.3	0.8
D10-634	116	65.0	15.9	4.4	3.9	3.1	2.0	0.1	4.2	0.3	0.7
D10-634	193	61.8	15.8	3.1	6.3	2.7	2.6	0.1	5.5	0.6	1.3
D10-636	936	60.0	17.1	6.1	4.9	2.7	3.4	0.1	4.1	0.5	0.9
D10-721	1520	60.1	14.9	6.3	5.3	3.8	3.5	0.1	3.7	0.8	0.9
D10-721	783	60.7	16.6	6.0	5.3	2.2	3.2	0.1	4.1	0.5	0.8
D10-721	845	60.3	16.9	6.2	5.2	2.5	3.2	0.1	3.9	0.4	0.8
D10-726	375	59.4	15.1	5.4	6.8	3.0	3.7	0.1	4.4	0.7	1.1
D10-729	451	61.4	14.2	3.4	9.5	2.6	1.7	0.2	5.0	0.5	1.1
D11-796	730	59.2	15.9	5.0	5.6	3.2	2.8	0.1	5.4	0.6	1.2
D11-836	16	56.7	16.5	6.8	7.5	2.3	5.8	0.1	2.7	0.3	1.0

Table A2-4 continued. Ti diorite compositions by XRF.

SAMPLE	Depth (feet)	SiO_2	Al_2O_3	CaO	FeO	K_2O	MgO	MnO	Na_2O	P_2O_5	TiO_2
		weight percent oxide									
354		46.4	17.3	15.2	11.0	0.6	6.0	0.1	2.1	0.0	1.1
378		47.9	17.9	10.2	10.5	2.3	7.0	0.2	1.6	0.3	1.4
CF53		51.6	16.5	9.0	9.7	1.0	5.2	0.2	4.9	0.2	1.4
D07-370	177	48.6	20.6	8.2	7.7	3.6	6.3	0.2	2.7	0.2	1.0
D07-371	69	52.4	16.4	15.8	4.1	0.1	3.6	0.1	5.6	0.3	1.3
D07-407	436	53.3	16.8	8.8	8.9	0.3	3.1	0.2	5.9	0.5	1.7
D08-418	447	53.0	15.8	8.3	9.3	0.6	3.7	0.1	6.3	0.4	1.7
D08-418	740	55.1	16.4	10.4	5.5	0.3	2.8	0.1	7.1	0.4	1.4
D08-418	912	53.9	18.2	6.6	7.3	1.5	3.7	0.1	6.8	0.2	1.1
D08-421	369	54.7	14.4	7.8	9.7	0.9	3.6	0.2	6.4	0.3	1.7
D08-453	600	55.2	15.4	6.3	9.4	1.2	2.9	0.1	6.8	0.5	1.6
D08-453	652	54.3	15.4	6.4	9.9	1.3	3.3	0.1	6.7	0.5	1.7
D08-453	686	54.0	16.1	8.2	8.4	0.4	3.2	0.1	6.9	0.5	1.6
D08-479	106	50.3	17.4	12.2	8.2	0.4	3.2	0.1	6.1	0.2	1.2
D08-479	678	53.2	18.9	7.7	7.1	1.5	3.7	0.1	6.2	0.2	1.0
D09-512	115	52.8	16.6	6.9	9.8	1.1	3.6	0.1	6.4	0.5	1.6
D09-512	150	53.3	16.2	6.0	10.4	1.9	4.1	0.2	5.4	0.4	1.7
D09-515	97	55.3	14.1	5.6	12.0	1.2	6.3	0.2	4.8	0.7	1.7
D09-517	133	52.4	17.2	7.2	9.8	1.3	3.9	0.2	6.2	0.2	1.1
D09-518	107	51.9	17.0	6.7	10.6	1.5	4.0	0.2	6.1	0.3	1.2
D09-518	124	56.2	14.8	4.9	10.8	1.8	2.9	0.2	6.2	0.4	1.2
D09-518	220	51.9	14.8	6.4	13.4	1.4	3.5	0.2	5.9	0.4	1.6
D09-538	1003	53.8	18.2	3.3	9.0	1.7	4.5	0.1	7.2	0.2	1.1
D09-538	1005	53.7	18.2	3.9	8.9	2.3	4.4	0.1	6.8	0.3	1.2
D09-538	1095	51.5	18.8	8.2	8.9	1.2	3.8	0.1	5.6	0.2	1.0
D09-538	684	53.5	18.3	6.6	7.9	1.4	3.6	0.1	6.7	0.2	1.0
D09-541	675	54.2	16.2	10.0	6.6	0.3	4.1	0.1	6.1	0.2	1.1
D09-542	903	53.2	19.0	6.1	8.5	1.5	3.5	0.1	6.7	0.2	0.9
D09-544	642	52.5	18.7	6.6	7.9	1.4	3.6	0.1	6.6	0.2	0.9
D09-544	848	52.8	17.7	10.7	7.4	0.7	3.6	0.1	5.5	0.2	1.0
D09-547	484	52.9	17.7	8.9	7.3	0.9	3.7	0.1	6.2	0.2	1.1

Table A2-4 continued. Ti diorite compositions by XRF.

Sample	Depth (feet)	SiO_2	Al_2O_3	CaO	FeO	K_2O	MgO	MnO	Na_2O	P_2O_5	TiO_2
		weight percent oxide									
D09-549	378	53.7	15.9	9.4	7.8	0.4	3.5	0.1	6.4	0.4	1.6
D09-549	512	53.9	18.4	6.0	7.3	1.0	3.9	0.1	7.2	0.2	0.9
D09-549	520	55.6	17.8	7.0	6.6	0.9	3.6	0.1	7.0	0.2	0.8
D09-549	709	53.6	16.1	6.7	9.5	1.2	3.9	0.2	6.6	0.4	1.5
D09-549	809	51.8	18.6	7.7	9.1	1.6	3.5	0.1	5.9	0.2	1.1
D09-552	706	54.9	17.7	6.5	7.1	0.8	3.4	0.1	7.3	0.2	1.0
D09-552	926	53.5	17.5	6.5	8.3	1.5	4.1	0.1	6.6	0.2	1.1
D09-562	926	53.5	17.6	6.2	8.2	1.7	4.1	0.1	6.8	0.2	1.1
D10-581	1129	54.9	17.5	4.9	8.9	1.8	3.1	0.1	7.0	0.2	1.2
D10-581	1225	54.0	17.4	7.0	8.6	0.7	3.6	0.2	6.8	0.2	1.2
D10-582	368	53.2	16.0	9.4	7.2	2.7	5.0	0.1	3.4	0.5	1.0
D10-583	650	52.1	16.4	10.3	8.0	2.0	5.1	0.1	3.7	0.4	1.0
D10-587	412	54.1	18.5	8.8	8.1	0.7	2.9	0.2	5.0	0.3	1.1
D10-589	1156	52.6	18.5	7.7	9.4	1.2	3.6	0.2	4.9	0.2	1.3
D10-589	639	55.5	16.8	5.1	7.7	1.4	3.3	0.1	7.5	0.2	1.4
D10-635	645	52.2	18.4	11.2	6.7	0.9	3.7	0.1	4.9	0.2	1.0
D10-636	947	52.8	15.0	8.5	8.0	1.9	7.1	0.1	3.7	0.9	1.6
D10-637	1559	52.1	16.2	5.5	11.2	2.1	5.7	0.2	4.6	0.5	1.8
D10-725	1222	54.8	16.4	7.9	7.4	0.5	3.5	0.1	7.1	0.4	1.5
D10-729	502	55.0	15.1	5.7	11.5	1.1	2.7	0.2	6.4	0.4	1.4
D11-795	466	54.1	16.8	6.9	8.4	1.2	3.3	0.1	6.8	0.4	1.3
J.E.037		50.8	16.7	7.6	12.2	0.2	4.7	0.2	6.1	0.2	1.1

Table A2-4 continued. Ti diorite compositions by XRF

SAMPLE	Depth (feet)	Rb	Sr	Y	Zr	Nb
		parts per million				
354		23	794	29	97	6
378		126	274	34	114	3
CF53		52	483	28	113	4
D07-370	177	190	405	26	78	3
D07-371	69	1	656	27	103	4
D07-407	436	8	358	32	137	6
D08-418	447	38	454	40	159	4
D08-418	740	9	548	39	190	5
D08-418	912	101	-	25	94	4
D08-421	369	36	394	32	137	4
D08-453	600	51	414	41	172	5
D08-453	652	55	-	40	148	5
D08-453	686	12	-	38	141	4
D08-479	106	18	596	28	86	3
D08-479	678	93	658	24	84	3
D09-512	115	54	-	40	160	4
D09-512	150	97	-	39	147	4
D09-515	97	86	203	37	117	5
D09-517	133	47	644	24	82	3
D09-518	107	66	-	26	88	3
D09-518	124	84	-	37	183	5
D09-518	220	73	405	33	130	4
D09-538	1003	88	319	20	100	3
D09-538	1005	129	442	24	97	3
D09-538	1095	50	-	24	83	3
D09-538	684	74	676	24	88	3
D09-541	675	14	372	23	98	3
D09-542	903	66	-	22	82	3
D09-544	642	65	-	25	87	4
D09-544	848	35	689	24	94	3
D09-547	484	57	548	25	87	4

- Indicates samples analyte values below detection limit.

Table A2-4 continued. Ti diorite compositions by XRF.

SAMPLE	Depth (feet)	Rb	Sr	Y	Zr	Nb
		parts per million				
D09-549	378	12	428	40	177	5
D09-549	512	41	-	20	84	3
D09-549	520	45	-	19	67	3
D09-549	709	61	318	36	160	4
D09-549	809	69	822	20	70	3
D09-552	706	33	-	21	85	3
D09-552	926	105	288	24	95	4
D09-562	926	120	297	25	92	3
D10-581	1129	71	321	28	115	4
D10-581	1225	27	415	21	93	3
D10-582	368	74	-	21	95	7
D10-583	650	62	813	22	85	8
D10-587	412	23	-	27	125	4
D10-589	1156	51	432	29	108	4
D10-589	639	57	218	27	138	3
D10-635	645	33	595	26	94	3
D10-636	947	53	911	29	131	16
D10-637	1559	109	496	40	152	4
D10-725	1222	17	-	33	157	4
D10-729	502	43	-	36	146	5
D11-795	466	64	-	36	168	4
J.E.037		2	-	17	55	3

- Indicates sample's analyte values below detection limit.

Table A2-5. Volcanic rock compositions by XRF.

Sample	Depth (feet)	SiO_2	Al_2O_3	CaO	FeO	K_2O	MgO	MnO	Na_2O	P_2O_5	TiO_2
		weight percent oxide									
D07-299	76	52.8	16.7	11.2	8.0	1.0	4.0	0.2	5.1	0.2	0.7
D07-302	5	52.3	15.4	10.7	9.8	0.5	4.4	0.2	5.3	0.4	0.7
D07-306	20	50.1	17.0	12.5	9.7	0.5	4.5	0.2	4.1	0.4	0.8
D07-315	121	51.8	17.0	9.8	9.0	0.8	4.5	0.2	5.5	0.4	0.8
D07-315	62	52.5	19.1	9.3	6.9	1.0	3.8	0.1	5.9	0.4	0.6
D07-371	149	52.4	17.9	15.8	3.1	0.2	4.9	0.1	4.2	0.2	0.9
D07-390	253	54.0	16.9	8.5	6.7	0.8	5.2	0.1	5.7	0.4	0.7
D08-414	206	51.2	17.2	10.5	8.1	1.2	6.2	0.1	4.0	0.5	0.6
D08-421	227	48.4	16.7	11.8	9.3	0.4	4.8	0.2	6.3	0.4	0.9
D08-426	679	53.8	18.8	10.5	5.5	0.5	4.0	0.1	5.5	0.2	0.9
D08-448	33	49.9	18.0	7.8	10.3	2.7	5.5	0.1	4.4	0.4	0.8
D08-449	27	52.0	17.4	9.1	9.6	1.3	4.3	0.2	4.6	0.4	0.6
D08-477	83	51.6	17.7	11.1	8.3	1.0	4.1	0.1	4.5	0.6	0.7
D09-491	14	51.4	18.3	5.0	9.2	3.5	6.2	0.1	4.9	0.3	0.6
D09-491	40	51.2	20.4	5.0	8.7	1.5	7.3	0.1	4.5	0.4	0.7
D09-493	37	51.8	16.5	11.2	8.5	1.6	5.2	0.1	3.1	0.5	0.8
D09-524	223	48.2	17.4	8.9	9.6	2.5	9.0	0.1	2.0	0.2	0.6
D09-527	188	48.4	17.8	9.4	10.8	0.9	7.5	0.2	3.7	0.3	0.6
D09-528	344	52.0	16.3	10.1	7.9	0.5	6.7	0.1	4.7	0.3	0.7
D09-547	79	52.8	18.4	7.1	8.7	1.3	3.7	0.1	6.4	0.2	0.9
D09-551	26	51.7	18.2	11.6	6.9	1.3	5.0	0.1	3.5	0.3	0.8
D10-568	84	51.9	17.4	12.3	6.6	2.6	5.1	0.2	2.2	0.5	0.7
D10-584	413	45.9	16.3	17.9	6.7	2.0	2.5	0.1	4.3	0.3	0.8
D10-584	810	50.4	17.3	9.4	10.3	0.8	3.8	0.2	6.3	0.3	0.9
D10-584	851	53.3	17.0	6.6		0.3	3.9	10.2	7.2	0.2	0.9
D10-588	97	48.4	18.1	10.7	11.0	1.1	6.2	0.2	2.8	0.3	0.8
D10-589	139	51.3	18.5	10.1	7.3	1.5	5.2	0.1	3.9	0.3	0.5
D10-590	944	51.8	19.2	8.2	8.2	1.6	4.0	0.1	5.5	0.2	0.9
D10-721	209	51.7	14.6	10.1	10.0	1.2	6.7	0.1	3.7	0.3	0.6
D10-725	394	52.2	16.7	9.5	9.5	1.0	5.8	0.2	3.3	0.5	0.8
D10-725	534	49.4	16.1	14.0	9.6	0.7	5.3	0.2	3.0	0.4	0.7
D11-834	630	53.3	19.2	8.8	6.5	0.8	3.3	0.1	5.8	0.2	0.9

Table A2-5 continued. Volcanic rock compositions by XRF.

Sample	SiO_2	Al_2O_3	CaO	FeO	K_2O	MgO	MnO	Na_2O	P_2O_5	TiO_2
	weight percent oxide									
405	52.8	19.8	7.9	7.3	0.7	3.4	0.1	6.4	0.5	0.7
358	52.7	14.1	9.5	9.9	0.2	7.5	0.2	4.8	0.2	0.9
364	53.8	16.4	7.8	8.7	0.8	6.6	0.1	4.2	0.5	0.8
374	48.7	21.3	9.5	7.8	2.8	6.8	0.1	1.7	0.1	0.9
CF25	48.4	16.4	15.1	9.3	0.6	5.8	0.2	2.4	0.5	0.7
CF27	52.5	18.0	10.1	7.7	0.7	3.8	0.1	5.4	0.5	0.7
CF28	50.0	16.3	14.6	7.9	0.5	6.0	0.1	3.1	0.5	0.7
CF47	50.6	17.0	9.4	11.0	2.0	4.8	0.1	3.5	0.3	0.9
J.E.033	53.2	16.9	7.3	10.0	0.6	4.2	0.2	6.4	0.2	0.7
J.E.035	50.7	17.0	9.0	10.4	0.1	5.4	0.2	6.2	0.2	0.7
J.E.036	51.8	18.0	6.8	10.5	0.8	5.1	0.2	5.8	0.2	0.7
J.E.039	52.6	18.7	8.1	8.6	0.3	4.6	0.2	6.3	0.2	0.5

Table A2-5 continued. Volcanic rock compositions by XRF.

Sample	Depth (feet)	Rb	Sr	Y	Zr	Nb
		parts per million				
D07-299	76	45	442	15	68	3
D07-302	5	19	405	14	55	4
D07-306	20	16	533	15	37	2
D07-315	121	37	691	19	50	3
D07-315	62	47	1201	16	41	3
D07-371	149	7	687	19	64	3
D07-390	253	49	-	17	44	3
D08-414	206	60	-	18	39	4
D08-421	227	20	-	15	55	3
D08-426	679	27	690	19	76	3
D08-448	33	166	621	25	41	3
D08-449	27	70	659	19	41	3
D08-477	83	55	-	20	53	5
D09-491	14	287	-	26	40	2
D09-491	40	105	-	15	47	2
D09-493	37	80	-	21	53	3
D09-524	223	135	-	17	34	2
D09-527	188	58	-	18	28	2
D09-528	344	31	-	15	45	3
D09-547	79	62	528	24	94	3
D09-551	26	66	699	17	54	3
D10-568	84	77	-	20	48	2
D10-584	413	53	598	17	49	2
D10-584	810	13	468	20	71	2
D10-584	851	6	346	15	66	3
D10-588	97	60	678	18	33	3
D10-589	139	61	575	14	31	3
D10-590	944	72	492	17	70	3
D10-721	209	84	503	16	38	2
D10-725	394	60	669	20	47	3
D10-725	534	19	612	15	42	3
D11-834	630	37	404	20	92	3

- Indicates sample's analyte value below detection limit.

Table A2-5 continued. Volcanic rock compositions by XRF.

Sample	Rb	Sr	Y	Zr	Nb
	parts per million				
405	34	1008	21	41	3
358	3	280	20	59	3
364	17	372	19	48	2
374	150	376	26	76	2
CF25	12	757	17	36	3
CF27	22	818	18	42	3
CF28	22	727	17	31	3
CF47	111	683	18	41	2
J.E.033	19	-	17	65	3
J.E.035	0.2	-	13	45	2
J.E.036	16	-	15	56	2
J.E.039	5	-	15	52	3

- Indicates sample's analyte below detection limit.

Table A3-1. Clinopyroxene compositions by microprobe analysis.

Sample ID	Depth (ft.)	SiO_2	MnO	Na_2O	MgO	CaO	Al_2O_3	FeO	K_2O	Total	%Hd
11RN346	UG	50.51	0.29	0.06	7.66	20.39	0.59	20.57	0.03	100.10	0.60
		49.35	0.41	0.08	6.91	21.50	0.26	17.91	0.03	96.45	0.58
		49.52	0.30	0.01	6.45	21.78	0.13	18.75	0.02	96.97	0.61
		49.66	0.46	0.08	7.43	20.78	0.18	17.57	0.00	96.14	0.56
		50.43	0.27	0.05	8.26	22.29	0.22	16.17	0.00	97.69	0.52
		49.70	0.34	0.07	8.45	21.17	0.29	15.93	0.00	95.97	0.51
		22.74	0.18	0.10	4.51	37.65	0.36	9.03	0.01	74.59	0.52
		28.87	0.39	0.07	5.37	34.47	0.60	11.54	0.00	81.29	0.54
		33.24	0.30	0.05	5.25	24.92	0.14	11.32	0.00	75.21	0.54
		50.29	0.50	0.12	7.16	22.01	0.39	18.42	0.04	98.93	0.58
		49.89	0.32	0.08	6.52	21.68	0.72	21.02	0.10	100.34	0.64
		47.94	0.15	0.12	6.59	18.05	0.75	22.65	0.07	96.32	0.66
		50.59	0.35	0.14	7.29	21.61	0.42	18.53	0.04	98.97	0.58
		50.21	0.24	0.08	7.28	22.40	0.11	18.68	0.00	98.98	0.59
BH-UG-11	UG	50.11	0.58	0.01	3.13	23.43	0.18	24.21	0.03	101.68	0.80
		49.98	0.68	0.08	3.94	23.43	0.21	23.29	0.01	101.62	0.75
		49.83	0.59	0.12	3.27	23.51	0.32	24.32	0.00	101.96	0.79
		49.86	0.50	0.09	2.35	23.08	0.16	23.90	0.00	99.94	0.84
		36.50	0.35	0.10	-0.02	33.95	7.52	18.22	0.02	96.63	0.98
		36.94	0.49	0.02	0.09	34.02	7.37	19.58	0.03	98.54	0.97
		36.50	0.41	0.00	0.02	34.10	7.84	17.38	0.01	96.24	0.97
		44.72	0.36	0.11	3.01	24.81	2.60	20.49	0.00	96.13	0.78
		47.84	0.43	0.27	3.04	23.38	0.63	23.76	0.00	99.32	0.80
		50.04	0.23	0.18	3.43	22.96	0.45	24.17	0.00	101.44	0.79
		50.63	0.60	0.25	5.69	23.62	0.82	19.97	0.02	101.60	0.65
		50.21	0.46	0.17	5.02	23.10	0.23	20.70	0.02	99.92	0.69
BH-UG-13	UG	48.43	0.59	0.18	6.19	21.99	0.89	16.82	0.03	95.12	0.59
		48.99	0.59	0.25	6.22	21.45	1.22	18.23	0.00	96.95	0.61
		50.31	1.19	0.03	3.54	22.10	0.10	22.31	0.06	99.63	0.75
		49.20	0.77	0.06	3.46	22.52	0.16	22.28	0.00	98.46	0.76
		58.52	0.81	0.05	2.78	19.02	0.17	18.04	0.00	99.39	0.76
		48.83	0.82	0.11	3.01	22.88	0.06	23.49	0.00	99.18	0.79
		47.59	0.68	0.05	2.24	22.23	9.91	16.47	0.02	99.19	0.78
		51.33	0.81	0.03	3.79	22.53	0.13	21.38	0.02	100.0	0.74
		45.05	0.86	0.05	2.56	22.61	6.56	19.03	0.00	96.71	0.78
		50.62	0.68	0.20	7.24	23.63	0.90	16.13	0.00	99.39	0.54
		50.28	1.58	0.06	5.07	23.71	0.08	19.55	0.01	100.3	0.65
		50.82	1.64	0.08	5.76	23.27	0.07	17.80	0.00	99.45	0.60

Table A3-1 continued. Clinopyroxene compositions by microprobe analysis.

Sample ID	Depth (ft.)	SiO_2	MnO	Na_2O	MgO	CaO	Al_2O_3	FeO	K_2O	Total	%Hd
BH-UG-14	UG	49.94	0.39	0.27	4.69	22.97	0.11	22.28	0.02	100.7	0.72
		50.55	0.26	0.21	4.58	22.27	0.28	22.03	0.01	100.2	0.72
		50.76	0.51	0.16	4.81	23.64	0.09	21.45	0.00	101.4	0.70
		50.58	0.40	0.14	3.73	22.87	0.07	23.80	0.01	101.6	0.77
		47.06	0.34	0.46	5.08	13.71	3.94	27.59	0.46	98.64	0.75
		50.95	0.38	0.28	4.98	22.76	0.11	21.55	0.00	101.0	0.70
		51.16	0.43	0.29	5.03	22.65	0.10	21.81	0.01	101.5	0.70
		50.28	0.60	0.23	4.41	23.03	0.01	22.40	0.00	100.9	0.73
		50.28	0.51	0.18	4.41	23.08	0.08	22.19	0.00	100.7	0.73
		49.95	0.52	0.15	3.41	22.96	0.37	24.45	0.00	101.8	0.79
		50.85	0.37	0.20	4.67	23.27	0.12	22.53	0.01	102.0	0.72
		49.75	0.26	0.22	3.77	22.99	0.15	23.10	0.04	100.3	0.77
		48.06	0.47	0.15	2.60	22.82	1.20	23.94	0.00	99.22	0.82
		48.08	0.52	0.17	2.70	23.25	1.33	24.59	0.00	100.6	0.82
		48.27	0.42	0.17	2.66	22.85	1.07	24.49	0.02	99.95	0.83
BH-UG-15	UG	49.60	0.65	0.11	3.27	22.16	0.37	24.17	0.02	100.3	0.79
		49.33	0.61	0.12	2.16	22.92	0.52	25.58	0.00	101.2	0.85
		49.23	0.57	0.14	2.34	22.94	0.88	25.77	0.01	101.9	0.84
		14.08	0.45	0.10	0.50	43.21	0.12	7.66	0.00	66.10	0.85
		33.73	0.51	0.05	1.61	31.80	0.26	18.69	0.05	86.70	0.85
		48.94	0.52	0.14	2.30	22.87	0.57	25.10	0.00	100.4	0.84
		49.43	0.47	0.15	2.11	23.11	0.78	25.64	0.01	101.7	0.86
		49.94	0.67	0.19	2.51	22.97	0.36	25.18	0.00	101.8	0.83
		50.02	0.47	0.19	2.98	23.38	0.34	24.49	0.00	101.8	0.81
		49.31	0.53	0.16	2.53	23.06	0.38	24.46	0.02	100.5	0.83
BH-UG-2	UG	49.01	0.42	0.20	2.41	22.62	0.62	25.42	0.03	100.7	0.84
		50.31	0.21	0.32	6.72	22.85	1.25	18.51	-0.01	100.2	0.60
		50.58	0.53	0.19	6.87	22.98	0.63	18.25	-0.01	100.0	0.59
		49.44	0.22	0.15	4.20	23.20	0.52	22.29	0.02	100.0	0.74
		50.17	0.60	0.11	5.05	23.07	0.39	21.88	-0.01	101.2	0.69
		49.70	0.55	0.07	3.88	23.06	0.66	23.26	0.01	101.2	0.76
		49.85	0.65	0.01	4.13	23.25	0.51	22.88	-0.01	101.3	0.74
		49.30	0.41	0.06	4.31	23.36	0.65	22.35	0.03	100.5	0.73
		49.36	0.51	0.11	4.86	22.25	0.64	22.18	0.06	99.97	0.71
		49.69	0.68	0.16	3.80	23.17	0.68	23.88	-0.01	102.1	0.76
		49.43	0.37	0.09	4.39	21.74	1.13	20.85	0.64	98.63	0.72
		50.77	0.36	0.41	7.34	22.75	1.58	17.24	0.02	100.5	0.56
		49.44	0.52	0.19	5.80	22.90	0.84	20.19	0.02	99.89	0.65
		50.89	0.27	0.40	7.88	23.16	0.92	17.05	-0.01	100.6	0.54
		50.51	0.40	0.38	7.96	22.86	0.99	16.83	-0.01	99.92	0.54
		48.72	0.37	0.28	6.56	21.28	2.03	19.92	0.15	99.31	0.62
		49.65	0.38	0.25	5.99	22.35	1.14	19.68	0.00	99.44	0.64

Table A3-1 continued. Clinopyroxene compositions by microprobe analysis.

Sample ID	Depth (ft.)	SiO_2	MnO	Na_2O	MgO	CaO	Al_2O_3	FeO	K_2O	Total	%Hd
BH-UG-24	UG	50.64	0.58	0.11	5.34	22.41	0.24	21.47	0.01	100.8	0.68
		48.54	0.61	0.08	5.06	22.21	0.07	20.43	0.01	97.03	0.68
		48.46	0.53	0.14	4.80	21.44	0.02	21.26	-0.01	96.64	0.70
		50.37	0.30	0.14	4.97	22.87	0.22	21.03	-0.01	99.87	0.70
		50.43	0.57	0.08	4.82	22.85	0.07	20.76	0.00	99.58	0.69
		50.41	0.52	0.11	5.35	23.55	0.08	20.50	0.01	100.5	0.67
		50.91	0.52	0.13	5.08	22.93	0.23	20.90	0.01	100.7	0.69
		50.18	0.56	0.11	5.02	22.96	0.31	20.97	0.03	100.1	0.69
		50.59	0.55	0.16	5.04	22.95	0.21	20.38	-0.01	99.87	0.68
		50.46	0.31	0.05	5.44	22.83	0.29	20.76	0.02	100.2	0.67
		50.48	0.37	0.16	4.86	23.03	0.35	21.04	-0.01	100.3	0.70
		51.33	0.55	0.00	6.45	23.77	0.02	17.97	0.01	100.1	0.60
		50.83	0.48	0.01	5.99	23.86	0.01	19.71	-0.02	100.9	0.64
		50.92	0.57	0.08	6.18	23.77	-0.05	19.68	0.00	101.1	0.63
		50.89	0.74	0.00	5.50	23.40	0.00	20.43	0.00	101.0	0.66
		50.60	0.28	0.04	5.72	23.26	0.01	19.69	-0.01	99.60	0.65
BH-UG-6	UG	49.61	0.73	0.03	2.74	22.81	0.22	24.04	0.00	100.2	0.81
		49.28	0.48	0.09	3.67	22.69	0.13	22.61	0.02	98.98	0.76
		50.05	0.18	0.08	4.56	23.18	0.29	22.05	0.02	100.4	0.73
		49.55	0.20	0.10	4.59	23.38	0.99	21.23	0.01	100.0	0.72
		49.25	0.21	0.12	6.19	18.95	0.92	20.69	0.17	96.49	0.65
		50.13	0.32	0.04	4.44	22.93	0.86	22.24	-0.02	100.9	0.73
		49.11	0.21	0.18	1.97	23.01	0.25	26.44	-0.01	101.2	0.88
		49.31	0.74	0.00	2.55	23.34	0.14	24.75	-0.02	100.8	0.82
		50.24	0.24	0.10	4.32	23.28	0.30	22.41	-0.02	100.9	0.74
		50.90	0.20	0.31	6.09	23.21	1.28	18.16	0.01	100.2	0.62
		49.70	0.38	0.09	3.24	22.93	0.30	23.87	-0.01	100.5	0.79
		50.35	0.41	0.06	3.59	22.96	0.30	23.28	-0.02	100.9	0.77
		50.93	0.36	0.18	5.97	21.54	0.65	19.70	0.01	99.35	0.64
		50.20	0.21	0.41	6.14	23.27	1.53	18.87	0.00	100.6	0.63
		50.13	0.10	0.40	5.90	23.04	1.85	17.93	-0.03	99.32	0.63
		50.54	0.35	0.06	6.13	23.23	0.79	18.59	-0.01	99.69	0.62
		50.10	0.25	0.16	6.39	23.44	0.73	19.23	-0.01	100.3	0.62
		50.14	0.18	0.22	6.00	23.57	0.82	19.69	0.02	100.6	0.64
		50.96	0.22	0.21	5.96	23.17	0.79	19.68	0.00	101.0	0.64
		50.99	0.21	0.15	6.81	23.40	0.78	18.69	-0.02	101.0	0.60
BH-UG-8	UG	51.30	0.47	0.06	8.18	23.63	0.13	15.90	0.02	99.69	0.51
		50.27	0.43	0.23	6.94	23.52	0.36	17.41	0.02	99.19	0.58
		51.32	0.32	0.13	8.27	23.54	-0.01	15.59	0.01	99.16	0.51
		51.37	0.23	0.11	8.47	23.29	0.14	14.09	-0.01	97.70	0.48
		50.81	0.36	0.15	7.11	23.55	0.25	16.36	0.00	98.61	0.56
		50.88	0.27	0.12	7.28	23.57	0.20	17.59	0.04	99.95	0.57
		51.30	0.46	0.11	7.67	23.09	0.09	16.52	-0.02	99.22	0.54
		51.08	0.29	0.11	7.20	22.69	0.19	17.48	0.01	99.02	0.57

Table A3-1 continued. Clinopyroxene compositions by microprobe analysis.

Sample ID	Depth (ft.)	SiO_2	MnO	Na_2O	MgO	CaO	Al_2O_3	FeO	K_2O	Total	%Hd
BH-UG-8	UG	51.41	0.32	0.11	8.29	23.63	0.63	15.50	0.00	99.90	0.51
		51.17	0.31	0.17	7.40	23.32	0.46	16.78	0.02	99.63	0.55
		51.49	0.15	0.16	8.74	22.69	0.11	15.18	0.02	98.52	0.49
		51.25	0.29	0.14	8.22	23.25	0.09	15.77	0.03	99.04	0.51
		51.57	0.44	0.10	9.13	22.75	0.49	14.41	0.00	98.90	0.46
		49.97	0.24	0.09	6.83	22.99	0.63	17.92	0.01	98.68	0.59
		51.61	0.30	0.07	7.13	22.89	0.31	17.55	0.03	99.89	0.57
		50.54	0.45	0.12	7.58	23.28	1.00	16.11	0.02	99.10	0.54
		16.85	0.11	0.11	2.44	39.92	1.20	6.57	0.11	67.31	0.60
		47.65	0.39	0.10	7.74	25.57	0.25	15.64	0.00	97.35	0.52
		51.47	0.38	0.20	7.51	23.37	0.29	16.57	0.00	99.79	0.55
		51.51	0.39	0.14	7.42	23.34	0.25	16.81	-0.02	99.85	0.55
		50.34	0.28	0.13	7.39	23.51	0.18	16.80	0.05	98.67	0.56
		50.93	0.33	0.19	6.79	22.86	0.25	18.51	0.03	99.89	0.60
		51.99	0.33	0.06	8.49	23.67	0.02	14.92	0.00	99.48	0.49
		50.83	0.30	0.24	6.93	23.42	0.36	17.62	0.01	99.72	0.58
BH-UG-9	UG	49.86	0.40	0.25	5.34	23.12	0.25	19.87	0.00	99.09	0.67
		49.92	0.53	0.06	4.20	22.96	0.27	21.84	0.02	99.80	0.73
		50.01	0.37	0.17	6.62	23.15	0.62	18.86	-0.02	99.78	0.61
		49.54	0.51	0.13	4.06	22.96	0.23	22.26	-0.01	99.68	0.74
		50.68	0.78	0.10	4.38	22.95	0.10	21.93	0.01	100.9	0.72
		50.82	0.82	0.17	4.44	22.94	0.14	22.20	-0.03	101.5	0.72
		50.24	0.38	0.19	5.95	22.95	0.43	19.10	0.00	99.25	0.63
		48.69	0.34	0.21	6.10	22.33	0.37	18.77	-0.01	96.81	0.63
		48.55	0.34	0.19	6.18	22.36	0.30	18.21	0.00	96.14	0.62
		49.75	0.66	0.07	3.31	22.95	0.19	23.34	0.00	100.3	0.78
		51.35	0.28	0.14	6.24	23.08	0.28	18.69	0.01	100.1	0.62
		49.68	0.41	0.11	5.59	23.41	0.21	20.12	0.02	99.54	0.66
		50.07	0.42	0.10	3.68	22.63	0.31	22.86	0.00	100.1	0.77
		49.35	0.59	0.11	3.76	23.08	0.59	23.01	0.00	100.5	0.76
		49.96	0.66	0.10	4.92	23.02	0.31	20.48	0.05	99.51	0.68
		49.96	0.40	0.10	4.23	23.38	0.27	21.92	-0.02	100.2	0.73
		50.10	0.46	0.07	4.25	22.95	0.27	21.96	0.01	100.1	0.73
		47.08	0.46	0.08	3.79	21.90	0.34	21.99	0.03	95.67	0.75
		49.69	0.46	0.09	3.42	23.21	0.32	22.95	0.00	100.1	0.78
		49.41	0.52	0.02	3.08	23.14	0.37	24.34	-0.02	100.9	0.80
		49.45	0.45	0.18	3.58	22.70	0.28	22.83	-0.03	99.44	0.77
		49.44	0.38	0.10	4.07	23.05	0.50	21.30	-0.01	98.82	0.74
		50.56	0.38	0.07	3.54	22.79	0.41	22.79	0.00	100.5	0.77
		49.51	0.32	0.07	3.50	23.07	0.45	22.57	-0.01	99.47	0.77
		49.09	0.37	0.13	4.39	22.95	1.26	21.80	0.03	100.0	0.73
		49.71	0.62	0.14	4.04	23.04	0.44	21.73	0.04	99.74	0.74
		50.25	0.67	0.24	4.90	22.87	0.24	21.07	0.00	100.2	0.69
		38.90	0.34	0.10	2.76	16.49	0.55	17.87	0.08	77.08	0.77

Table A3-1 continued. Clinopyroxene compositions by microprobe analysis.

Sample ID	Depth (ft.)	SiO_2	MnO	Na_2O	MgO	CaO	Al_2O_3	FeO	K_2O	Total	%Hd
BH-UG-9	UG	50.34	0.27	0.12	5.69	22.96	0.58	19.45	0.00	99.40	0.65
		49.90	0.78	0.15	2.53	22.71	0.14	24.03	0.00	100.3	0.82
		49.86	0.38	0.15	4.76	22.90	0.45	21.16	0.02	99.68	0.70
		50.12	0.40	0.22	5.49	23.06	0.73	19.73	0.00	99.74	0.66
		50.11	0.34	0.05	5.32	23.06	0.37	19.86	0.02	99.14	0.67
		48.41	0.27	0.11	3.69	22.45	0.30	22.49	0.01	97.72	0.77
		50.60	0.35	0.10	6.33	23.33	0.34	19.03	-0.01	100.1	0.62
C-5	60.5	52.40	0.21	0.06	11.96	24.94	1.42	9.38	0.00	100.4	0.30
		53.79	0.22	-0.04	11.76	25.26	0.23	10.84	0.00	102.1	0.34
		53.28	0.14	0.02	12.86	25.18	1.04	8.63	-0.01	101.1	0.27
		52.80	0.14	0.02	12.85	25.27	1.48	8.30	0.00	100.9	0.26
		52.36	0.38	-0.01	10.59	24.60	0.93	11.61	-0.04	100.4	0.38
		52.58	0.20	0.04	12.30	24.69	1.19	9.61	0.46	101.1	0.30
		52.89	0.29	0.00	10.98	25.00	0.53	11.57	0.03	101.3	0.37
		58.25	0.55	0.06	7.04	20.25	0.13	13.78	-0.01	100.1	0.51
		53.01	0.22	0.00	11.27	24.87	0.82	11.57	0.02	101.8	0.36
		52.50	0.35	0.01	11.18	24.65	0.77	10.37	0.02	99.84	0.34
		53.12	0.40	0.02	12.23	24.91	0.88	9.74	0.00	101.3	0.31
		52.69	0.34	0.03	12.29	24.91	0.95	9.59	-0.01	100.8	0.30
		50.29	0.18	0.02	11.41	24.48	0.63	11.49	0.02	98.53	0.36
		53.23	0.21	0.10	11.46	24.64	0.51	10.98	-0.01	101.1	0.35
C-5	73.1	50.18	0.54	0.07	6.31	23.25	0.12	18.32	0.03	98.83	0.61
		51.72	0.55	0.05	6.53	23.57	0.11	20.22	0.03	102.8	0.62
		50.51	0.54	0.07	5.64	23.46	0.10	19.79	0.01	100.1	0.65
		50.41	0.67	0.12	5.72	22.94	0.15	19.13	-0.01	99.14	0.64
		51.01	0.39	0.11	7.39	23.81	0.36	17.52	0.01	100.6	0.56
		49.64	0.47	0.14	7.80	23.10	0.54	16.45	0.04	98.18	0.53
		51.33	1.02	0.25	6.86	23.48	0.14	17.74	-0.02	100.8	0.57
		51.64	1.03	0.29	6.48	23.30	0.26	18.34	0.01	101.3	0.59
		51.72	0.95	0.22	7.06	23.54	0.16	18.33	0.02	102.0	0.57
		51.69	1.15	0.18	7.32	23.64	0.10	17.90	0.01	102.0	0.56
		51.63	0.85	0.22	6.93	23.10	0.07	17.54	0.02	100.4	0.57
		35.35	0.09	0.00	0.04	32.97	0.39	29.11	0.03	97.97	0.99
		35.72	0.08	-0.03	0.06	32.69	0.13	27.45	-0.02	96.08	0.99
		53.48	0.18	-0.03	13.24	24.94	0.43	8.43	-0.02	100.6	0.26
		53.30	0.42	0.03	12.79	24.76	0.43	8.60	-0.05	100.3	0.27
		53.33	0.19	0.04	13.46	24.91	0.48	6.69	-0.01	99.08	0.22
		51.10	0.55	0.14	7.98	23.89	0.32	16.68	0.00	100.7	0.53
D02-198	208.3	34.13	0.51	0.16	3.27	22.10	0.35	20.04	0.10	80.66	0.76
		47.54	0.36	0.12	3.31	21.57	0.60	21.92	0.00	95.43	0.78
		46.62	0.40	0.09	4.13	20.87	0.46	20.50	0.00	93.08	0.72
		46.12	0.45	0.11	5.08	21.80	0.03	19.34	0.03	92.96	0.67
		45.73	0.38	0.12	4.60	21.49	0.09	19.55	0.01	91.96	0.69

Table A3-1 continued. Clinopyroxene compositions by microprobe analysis.

Sample ID	Depth (ft.)	SiO_2	MnO	Na_2O	MgO	CaO	Al_2O_3	FeO	K_2O	Total	%Hd
D02-201	122.3	48.89	0.44	0.17	6.08	22.77	0.40	20.51	0.01	99.26	0.65
		50.19	0.70	0.05	4.79	23.02	0.00	20.83	0.01	99.56	0.69
		50.47	0.50	0.15	5.42	23.57	0.05	19.45	0.02	99.63	0.66
		50.11	0.56	0.14	4.88	22.98	0.08	20.97	0.00	99.71	0.69
		50.81	0.73	0.10	5.01	23.23	0.10	21.84	-0.01	101.8	0.69
		49.59	0.33	0.17	4.69	22.67	0.22	21.16	-0.01	98.81	0.71
		50.03	0.71	0.03	4.83	22.90	0.03	20.76	0.01	99.29	0.69
D02-207	140	47.92	0.51	0.23	4.15	21.51	0.41	19.68	0.00	94.42	0.71
		47.51	0.21	0.12	3.80	21.16	0.23	19.27	0.01	92.33	0.73
		47.04	0.23	0.28	4.04	20.63	0.16	19.49	0.01	91.89	0.72
		47.77	0.25	0.19	3.77	21.31	0.27	18.69	0.00	92.25	0.73
		47.09	0.19	0.18	4.26	19.91	0.15	20.32	0.00	92.10	0.72
		46.90	0.30	0.08	3.34	20.69	0.29	20.68	-0.03	92.25	0.77
		47.84	0.23	0.27	4.39	20.94	0.12	18.32	0.02	92.13	0.69
		47.11	0.40	0.21	4.42	20.58	0.18	19.86	0.02	92.80	0.71
		47.55	0.45	0.11	3.63	20.93	0.34	19.93	0.02	92.96	0.74
		47.60	0.42	0.10	3.72	21.75	0.23	18.85	0.02	92.69	0.73
		47.41	0.43	0.10	4.09	20.64	0.13	18.94	-0.01	91.74	0.71
		46.99	0.27	0.28	4.99	20.17	0.12	19.46	0.03	92.32	0.68
		47.89	0.41	0.24	4.34	21.62	0.22	18.77	-0.01	93.47	0.70
		48.55	0.35	0.15	4.31	21.49	0.09	18.92	0.01	93.86	0.70
		47.79	0.19	0.25	5.85	20.45	0.05	16.15	0.03	90.77	0.60
		47.10	0.29	0.20	4.66	20.87	0.18	18.89	0.00	92.21	0.69
D02-208	119	49.49	0.59	0.09	4.17	22.61	0.31	21.58	-0.01	98.84	0.73
		50.75	0.47	0.13	6.88	22.71	0.22	18.18	0.03	99.37	0.59
		50.72	0.23	0.15	7.34	22.79	0.27	17.43	0.02	98.95	0.57
		50.27	0.46	0.21	6.15	22.51	0.40	18.77	0.03	98.79	0.62
		50.65	0.45	0.09	6.58	23.21	0.26	18.65	-0.02	99.87	0.60
		49.48	0.32	0.09	3.11	23.00	0.10	24.63	-0.02	100.7	0.81
		49.09	0.34	0.11	1.94	22.84	0.04	26.81	0.00	101.2	0.88
		50.91	0.45	0.08	5.96	22.60	0.18	19.03	0.02	99.22	0.63
		50.86	0.53	0.16	5.62	22.81	0.56	19.33	-0.03	99.83	0.65
		50.48	0.52	0.17	5.65	22.62	0.28	19.96	0.01	99.69	0.65
		51.08	0.54	0.16	6.16	22.50	0.16	18.66	0.01	99.27	0.62
		50.25	0.39	0.12	6.38	21.97	0.30	19.60	-0.02	98.99	0.62
		50.72	0.50	0.14	6.15	22.78	0.15	19.13	0.00	99.57	0.63
		50.41	0.33	0.08	6.64	23.17	0.25	18.66	0.03	99.56	0.61
		50.50	0.32	0.22	6.21	22.49	0.45	18.09	0.01	98.29	0.61
D02-208	127	49.13	0.43	0.20	4.41	22.69	0.30	21.20	0.01	98.36	0.72
		50.83	0.53	0.08	5.98	23.23	0.05	19.32	0.00	100.0	0.63
		50.82	0.65	0.09	5.77	23.10	0.08	20.38	0.01	100.9	0.65
		50.13	0.70	0.06	5.59	23.26	0.13	19.33	0.01	99.21	0.64
		49.94	0.48	0.19	4.84	23.01	0.25	20.82	-0.01	99.51	0.70
		50.72	0.57	0.00	6.15	23.23	0.08	19.16	0.01	99.91	0.62

Table A3-1 continued. Clinopyroxene compositions by microprobe analysis.

Sample ID	Depth (ft.)	SiO_2	MnO	Na_2O	MgO	CaO	Al_2O_3	FeO	K_2O	Total	%Hd
D02-208	127	50.32	0.71	0.11	5.44	22.95	0.17	19.33	0.01	99.03	0.65
		50.50	0.66	0.09	6.03	22.21	0.03	18.22	-0.01	97.72	0.61
		50.51	0.67	0.11	6.14	23.19	0.12	18.46	-0.02	99.17	0.61
		51.15	0.55	0.08	6.20	23.38	0.03	18.90	0.01	100.3	0.62
		50.11	0.44	0.15	4.90	22.87	0.20	19.85	0.03	98.55	0.68
		49.93	0.40	0.19	4.47	22.41	0.30	22.04	0.01	99.73	0.72
		50.90	0.49	0.10	6.88	23.21	0.15	18.02	-0.01	99.73	0.59
		50.26	0.57	0.12	5.15	23.20	0.09	20.53	0.00	99.93	0.68
D06-270	271	50.40	0.21	0.22	4.51	23.04	0.34	22.43	0.00	101.1	0.73
		51.05	0.48	0.18	4.49	22.85	0.17	23.29	0.02	102.5	0.73
		50.50	0.20	0.24	5.41	22.19	0.67	20.98	0.03	100.2	0.68
		51.62	0.34	0.33	5.69	22.34	0.10	20.11	-0.02	100.5	0.66
		50.94	0.27	0.23	5.70	22.89	0.03	19.84	-0.02	99.87	0.66
		50.79	0.38	0.25	5.12	22.84	0.14	22.19	0.02	101.7	0.70
		50.64	0.40	0.27	4.93	22.80	0.08	21.18	0.01	100.3	0.70
		36.72	0.83	-0.04	0.01	32.47	3.79	25.27	0.01	99.06	0.97
		36.39	0.70	0.03	0.01	32.41	4.13	25.41	-0.01	99.07	0.97
		36.21	0.28	-0.02	0.02	32.78	1.30	27.90	0.00	98.48	0.99
		36.19	0.32	0.04	0.01	33.05	1.60	28.23	0.02	99.45	0.99
		36.36	0.11	0.06	0.03	33.02	1.22	28.47	-0.01	99.27	0.99
		49.73	0.54	0.20	4.49	21.27	0.80	24.57	0.09	101.7	0.74
		49.41	0.31	0.13	3.41	22.83	0.41	23.69	0.03	100.2	0.79
		50.44	0.49	0.12	4.09	23.04	0.23	23.64	-0.02	102.0	0.75
		49.83	0.57	0.11	3.38	22.76	0.32	24.53	0.02	101.5	0.79
		50.59	0.39	0.16	4.69	23.38	0.22	21.55	-0.01	101.0	0.71
		50.63	0.48	0.11	3.71	22.92	0.29	23.48	0.02	101.7	0.77
		50.87	0.26	0.18	4.58	22.93	0.23	21.72	-0.01	100.8	0.72
		50.15	0.42	0.13	3.80	23.31	0.31	22.87	0.03	101.0	0.76
		50.08	0.29	0.13	4.05	22.91	0.32	23.32	0.03	101.1	0.76
		50.26	0.52	0.15	3.45	22.67	0.23	24.10	-0.02	101.4	0.78
D10-622	159	52.25	0.89	-0.01	7.56	24.45	0.11	16.01	0.01	101.3	0.53
		52.10	0.83	0.02	7.87	25.00	0.17	15.26	0.01	101.3	0.51
		52.05	0.81	0.02	8.17	24.26	0.08	14.95	-0.01	100.3	0.49
		51.90	0.91	-0.01	7.79	24.47	0.10	15.65	-0.01	100.8	0.51
		50.92	0.43	0.08	5.57	24.16	0.16	20.17	-0.01	101.5	0.66
		51.04	0.38	0.05	5.66	24.04	0.27	19.94	0.02	101.4	0.66
		50.32	0.52	0.09	5.17	23.83	0.21	20.23	0.01	100.4	0.67
		50.23	0.70	0.03	4.22	23.61	0.04	21.78	0.01	100.6	0.73
		51.49	0.42	0.07	5.10	24.27	0.10	20.38	0.01	101.8	0.68
		50.40	0.35	0.07	4.66	23.87	0.13	19.97	-0.01	99.46	0.70
		50.89	0.55	0.13	4.51	23.55	0.15	21.82	-0.01	101.6	0.72
		50.64	0.42	0.08	4.52	23.95	0.12	22.59	0.01	102.3	0.73
		51.37	0.58	0.04	4.90	23.64	0.15	21.33	0.03	102.0	0.70
		50.43	0.62	0.04	3.84	23.68	0.07	22.12	-0.03	100.8	0.75

Table A3-1 continued. Clinopyroxene compositions by microprobe analysis.

Sample ID	Depth (ft.)	SiO_2	MnO	Na_2O	MgO	CaO	Al_2O_3	FeO	K_2O	Total	%Hd
D10-622	159	51.09	0.72	0.08	3.57	23.77	0.07	23.13	0.01	102.4	0.77
		50.54	0.61	0.08	4.33	24.32	0.07	21.58	-0.02	101.5	0.72
		50.09	0.78	0.10	4.20	23.32	0.06	21.89	-0.01	100.4	0.73
		50.84	0.45	0.00	5.27	23.79	0.14	20.49	0.00	101.0	0.68
		50.32	0.48	0.09	4.18	23.49	0.16	23.02	-0.01	101.7	0.74
		50.23	0.40	0.05	3.69	23.32	0.15	23.87	-0.02	101.7	0.77
		50.30	0.34	0.08	3.64	23.42	0.19	24.38	0.01	102.4	0.78
		50.87	0.55	0.01	4.60	23.79	0.22	22.22	0.01	102.3	0.72
		50.36	0.51	0.19	4.73	23.23	0.54	22.39	-0.02	101.9	0.71
		51.14	1.14	0.05	5.81	23.66	0.08	19.01	0.05	100.9	0.62
D10-622	163	50.23	0.99	0.15	6.09	23.19	0.25	19.31	0.05	100.3	0.62
		35.07	1.05	0.13	3.94	28.81	0.26	13.17	0.09	82.52	0.62
		50.19	1.40	0.14	5.37	23.37	0.17	19.84	-0.01	100.5	0.64
		50.86	1.70	0.11	5.37	23.68	0.08	19.33	-0.04	101.1	0.63
	Hornfels	52.85	0.35	0.08	11.55	24.35	0.23	10.71	-0.01	100.1	0.34
	Hornfels	52.45	0.31	-0.02	13.11	25.32	0.96	6.85	-0.02	98.97	0.22
	Hornfels	52.15	0.21	0.03	12.03	24.94	0.67	8.88	-0.01	98.90	0.29
	Hornfels	52.52	0.33	-0.01	12.54	24.94	0.28	8.45	0.04	99.08	0.27
	Hornfels	53.14	0.11	0.11	12.53	24.67	0.48	8.61	0.02	99.66	0.28
	Hornfels	52.78	0.36	0.08	12.82	24.91	0.50	8.17	0.00	99.61	0.26
	Hornfels	53.03	0.10	0.06	13.12	25.20	1.00	7.43	0.00	99.92	0.24
	Hornfels	53.64	0.25	-0.01	12.69	25.04	0.74	7.89	0.02	100.3	0.26
	Hornfels	53.37	0.20	-0.03	12.69	24.98	0.77	7.63	0.00	99.60	0.25
	Hornfels	53.30	0.14	0.06	11.98	25.06	0.44	9.53	-0.01	100.5	0.31
	Hornfels	53.18	0.20	0.06	12.53	25.16	0.51	8.27	0.02	99.92	0.27
	Vein	47.74	0.27	0.14	9.70	21.09	1.18	11.26	0.18	91.56	0.39
	Vein	48.97	0.81	0.15	6.27	22.66	0.19	18.58	0.02	97.65	0.61
	Vein	50.99	0.64	0.08	6.33	23.53	0.16	20.01	0.01	101.7	0.63
D10-630	100.7	46.32	0.48	0.23	8.91	22.15	0.81	11.27	-0.01	90.16	0.41
		51.42	0.62	0.12	9.32	24.11	0.51	13.95	0.00	100.0	0.45
		51.78	0.69	0.12	6.94	23.92	0.14	16.99	0.01	100.6	0.56
		51.19	0.33	0.23	9.04	23.44	1.42	14.79	0.00	100.4	0.47
		52.22	0.42	0.19	9.12	24.18	0.78	14.49	0.02	101.4	0.46
		52.06	0.57	0.33	8.22	24.06	0.83	15.76	0.01	101.8	0.51
		51.29	0.45	0.06	8.08	23.77	0.65	15.13	0.01	99.44	0.50
		50.55	0.49	0.24	7.83	23.50	1.60	14.48	-0.01	98.69	0.50
		52.07	0.51	0.14	8.64	24.36	0.41	15.09	0.01	101.2	0.49
		51.28	0.83	0.07	6.83	23.70	0.67	17.76	0.02	101.1	0.58
		52.27	0.59	0.12	8.88	24.23	0.45	14.38	0.01	100.9	0.47
		51.78	0.42	0.07	8.67	24.30	0.39	15.04	0.01	100.7	0.49
		52.06	0.51	0.22	8.84	24.11	0.74	14.46	-0.01	100.9	0.47
		51.45	0.67	0.18	8.45	24.04	0.90	16.15	0.01	101.9	0.51
		52.22	0.42	0.13	8.52	23.93	0.44	15.50	0.02	101.2	0.50
		51.69	0.11	0.13	7.41	23.69	0.36	17.92	0.01	101.3	0.57

Table A3-1 continued. Clinopyroxene compositions by microprobe analysis.

Sample ID	Depth (ft.)	SiO_2	MnO	Na_2O	MgO	CaO	Al_2O_3	FeO	K_2O	Total	%Hd
D11-785	638	46.52	0.78	0.08	6.42	26.20	0.06	15.83	0.00	95.88	0.56
		51.64	0.80	-0.02	6.67	23.75	0.05	17.06	0.02	99.98	0.57
		50.95	0.82	0.03	7.12	23.77	0.15	17.08	-0.01	99.91	0.56
		50.98	0.51	-0.04	7.31	23.71	0.13	17.04	-0.01	99.64	0.56
		51.15	0.53	0.10	7.18	23.23	0.07	17.09	-0.02	99.33	0.56
		43.78	0.51	0.07	2.97	26.41	0.19	20.42	0.01	94.35	0.78
		50.67	0.59	0.04	6.23	23.67	0.11	18.24	-0.01	99.53	0.61
D11-786	96	51.64	0.61	0.29	10.21	23.82	1.61	10.12	0.00	98.30	0.35
		51.29	0.44	0.32	9.46	24.23	3.47	10.65	0.00	99.86	0.38
		50.74	0.48	0.13	10.00	22.21	0.86	11.44	-0.02	95.83	0.38
		52.31	0.47	0.21	10.99	23.00	1.13	11.43	0.03	99.57	0.36
		50.86	0.52	0.15	9.81	23.97	0.88	12.46	0.01	98.67	0.41
		52.47	0.79	0.11	8.74	24.40	0.40	13.38	-0.01	100.3	0.45
		51.69	0.48	0.02	8.58	24.01	0.23	14.74	0.00	99.75	0.48
		53.13	0.50	0.23	10.19	22.90	1.10	11.15	0.02	99.23	0.37
		52.34	0.44	0.30	10.79	23.09	1.41	10.63	0.03	99.02	0.35
		49.29	0.45	0.20	9.82	22.21	0.51	11.17	-0.02	93.62	0.38
		49.63	0.41	0.15	9.94	22.54	0.99	10.80	-0.01	94.46	0.37
		51.88	0.84	0.06	7.61	23.56	0.30	15.39	-0.01	99.63	0.52
ERA-1B-BC-1		48.51	0.40	0.18	2.66	22.35	0.61	24.85	0.00	99.56	0.83
	UG	48.81	0.28	0.12	1.16	22.69	0.27	26.81	0.02	100.2	0.92
		48.58	0.46	0.15	2.27	22.31	0.19	25.44	-0.01	99.40	0.85
		49.29	0.49	0.16	2.02	23.00	0.30	25.35	0.00	100.6	0.86
		48.79	0.29	0.06	2.21	23.04	0.32	25.65	0.01	100.4	0.86
		48.94	0.28	0.07	1.25	22.94	0.26	28.26	-0.01	102.0	0.92
		47.76	0.21	0.19	0.85	21.80	0.28	27.48	-0.01	98.55	0.94
		49.43	0.29	0.11	2.31	23.07	0.28	26.00	-0.02	101.5	0.86
		48.69	0.40	0.06	2.29	22.98	0.16	25.69	0.03	100.3	0.85
		49.91	0.21	0.38	6.33	22.90	1.63	18.12	-0.01	99.45	0.61
		50.34	0.40	0.12	4.64	23.24	0.60	21.25	-0.01	100.6	0.71
		50.73	0.06	0.47	7.43	23.22	1.90	16.41	0.02	100.2	0.55
		50.23	0.67	-0.01	3.94	23.23	0.06	23.67	-0.01	101.8	0.75
		50.58	0.16	0.40	5.43	23.46	0.93	19.55	0.00	100.5	0.67
ERA-1B-S4	UG	49.24	0.54	0.08	3.04	23.09	0.37	24.29	0.00	100.6	0.80
		48.53	0.55	0.07	3.24	23.91	1.15	21.71	0.01	99.17	0.77
		50.08	0.50	0.05	5.38	23.41	0.10	18.96	0.01	98.49	0.65
		50.53	0.88	0.04	5.01	23.77	0.15	20.14	0.00	100.5	0.67
		50.91	0.62	0.08	5.19	23.50	0.14	20.98	0.01	101.4	0.68
		48.78	0.53	0.10	5.00	22.76	0.39	21.14	0.02	98.71	0.69
		50.83	0.42	0.10	5.24	23.33	0.55	19.36	0.00	99.83	0.66
		50.59	0.43	0.13	4.89	23.33	0.33	20.87	0.00	100.6	0.70
		43.45	0.64	0.26	5.05	19.25	0.60	17.63	0.04	86.92	0.65
		48.41	0.65	0.13	5.03	20.84	0.56	18.75	0.03	94.41	0.66

Table A3-1 continued. Clinopyroxene compositions by microprobe analysis.

Sample ID	Depth (ft.)	SiO_2	MnO	Na_2O	MgO	CaO	Al_2O_3	FeO	K_2O	Total	%Hd
ERA-1B-S4	UG	43.73	0.97	0.21	5.55	18.41	0.65	15.52	0.05	85.09	0.59
		49.70	0.58	0.33	7.74	21.53	1.17	14.21	0.04	95.31	0.50
		52.52	0.64	0.09	10.15	24.32	0.62	11.41	-0.01	99.74	0.38
		51.91	0.55	0.06	9.99	23.76	0.74	11.82	0.02	98.85	0.39
		50.34	0.62	0.09	8.78	23.44	0.33	15.53	0.02	99.15	0.49
		50.50	0.31	0.12	8.37	23.11	0.34	14.67	0.03	97.46	0.49
		50.29	0.68	0.08	5.01	23.24	0.41	21.20	0.00	100.9	0.69
		50.39	0.27	0.04	5.17	23.82	0.33	21.05	-0.02	101.0	0.69
		42.56	0.57	0.20	4.60	19.32	1.21	17.65	0.02	86.14	0.67
		49.03	0.57	0.20	4.56	22.81	1.45	20.37	0.00	98.99	0.70
		49.93	0.50	0.03	3.65	23.04	0.20	23.26	-0.02	100.6	0.77
		50.36	0.53	0.11	4.77	22.86	0.45	21.31	0.03	100.4	0.70
HEA-7-S3R	UG	50.02	0.31	0.23	3.81	23.04	0.17	23.44	-0.01	101.0	0.77
		50.21	0.43	0.13	3.43	22.57	0.23	24.45	0.03	101.5	0.79
		49.84	0.48	0.06	3.70	23.07	0.22	23.18	0.00	100.6	0.77
		48.48	0.68	0.06	3.79	21.90	0.32	23.93	0.15	99.29	0.76
		50.26	0.53	0.17	3.39	23.21	0.28	24.72	-0.01	102.5	0.79
		50.21	0.54	0.11	3.32	23.11	0.22	24.47	0.03	102.0	0.79
		49.78	0.39	0.12	3.62	23.31	0.26	23.51	0.00	101.0	0.77
		49.95	0.47	0.04	3.74	23.18	0.22	24.10	0.05	101.8	0.77
		50.14	0.42	0.01	3.50	23.32	0.22	23.97	-0.01	101.6	0.78
NBV257	UG	49.80	0.61	0.11	3.75	23.08	0.36	22.92	0.02	100.6	0.76
		50.17	0.47	0.15	3.68	23.04	0.15	22.21	0.01	99.88	0.76
		50.08	0.46	0.16	4.42	22.90	0.22	21.61	0.02	99.87	0.72
		49.54	0.43	0.07	4.15	23.14	0.19	22.48	0.03	100.0	0.74
		49.32	0.38	0.26	4.29	22.77	0.07	20.41	-0.02	97.48	0.72
		49.63	0.44	0.18	4.23	22.76	0.11	22.04	0.00	99.40	0.73
		49.93	0.39	0.18	4.19	22.49	1.02	21.32	0.01	99.52	0.73
		49.08	0.19	0.10	2.94	22.87	0.56	24.48	-0.03	100.2	0.82
		49.87	0.16	0.27	5.20	22.80	1.31	19.34	-0.02	98.95	0.67
		48.97	0.42	0.24	4.79	22.60	1.03	21.09	0.05	99.19	0.70
		48.96	0.07	0.16	5.32	22.30	1.26	20.35	0.04	98.45	0.68
		46.35	0.37	0.11	2.99	19.56	1.08	26.05	0.06	96.57	0.82
		45.42	0.55	0.12	3.96	18.07	0.49	26.82	-0.03	95.40	0.78
		48.58	0.22	0.11	3.78	22.54	0.60	21.32	0.01	97.17	0.75
		47.71	0.59	0.17	3.63	20.40	0.26	26.18	0.04	98.99	0.79
		48.66	0.45	0.20	4.31	21.65	0.19	22.69	0.05	98.20	0.74

Table A4-1. XRF analysis on pulp samples in the Gold Bowl

Drill Hole	D07-299	D07-299	D07-303	D07-305	D07-305	D07-305	D07-306	D07-306
Sample	BX 00186	BX 00200	BX 00437	BX 00531	BX 00536	BX 00549	BX 00513	BX 00521
Weight percent oxide								
F**	0.01	0.01	0.01	0.01	0.01	0.01	0.01	0.01
Na_2O	0.09	0.35	0.08	0.08	0.03	0.05	0.20	0.10
MgO	3.05	7.53	5.52	6.06	3.39	2.39	4.89	7.07
Al_2O_3	7.54	4.52	5.1	7.52	12.0	10.5	9.53	5.18
SiO_2	39.2	39.5	38.0	41.8	41.3	37.8	42.6	43.8
P_2O5	0.14	0.05	0.66	0.42	0.35	0.30	0.49	0.43
S	0.23	2.82	3.91	0.26	0.41	0.48	0.03	0.35
Cl*	0.00	0.14	0.01	0.02	0.01	0.01	0.02	0.03
K_2O	0.04	0.41	0.05	0.01	0.02	0.03	0.11	0.05
CaO	31.1	22.9	23.3	28.0	25.9	30.6	24.5	25.4
TiO_2	0.59	0.25	0.49	0.64	0.74	0.57	0.69	0.42
V*	0.02	0.00	0.00	0.03	0.03	0.03	0.02	0.02
Cr*	0.03	0.00	0.00	0.00	0.00	0.03	0.00	0.02
MnO	0.53	0.24	0.40	0.46	0.37	0.58	0.44	0.43
FeO	17.2	21.0	21.5	13.9	14.4	15.8	15.7	15.7
Co*	0.00	0.01	0.02	0.00	0.02	0.02	0.01	0.01
Rb*	0.00	0.00	0.00	0.00	0.00	0.00	0.00	0.00
Sr	0.02	0.02	0.03	0.04	0.12	0.05	0.05	0.03
Zr*	0.01	0.01	0.00	0.01	0.01	0.00	0.01	0.00
BaO*	0.02	0.02	0.00	0.00	0.00	0.00	0.02	0.02
Trace elements (parts per million)								
Cu	28	584	721	19	99	49	49	82
As	68	1104	312	208	446	300	316	272
Ag*	13	7	14	13	18	10	9	11
Te	9	19	26	45	37	46	42	90
Bi	1342	230	5607	4521	4942	4715	4170	5884
W	20	16	23	20	20	18	21	17
Mo	3	2	2	2	18	14	2	3
Pb	56	12	1	41	327	47	49	122
Zn	87	90	156	133	125	115	145	183
Sb*	8	9	7	0	30	0	1	0
Ni	20	27	29	28	114	113	32	23

Table A4-1 continued. XRF analysis on pulp samples in the Gold Bowl

Drill Hole	D07-310	D07-310	D07-316	D07-316	D07-320	D07-340	D08-430	D07-436
Sample	BX 00716	BX 00720	BX 00995	BX 00999	BX 01267	BX 01676	BX 10205	BX 10685
Weight percent oxide								
F**	0.01	0.01	0.01	0.01	0.01	0.01	0.01	0.01
Na_2O	1.44	0.13	0.08	0.55	0.05	4.83	0.10	0.09
MgO	3.41	1.67	3.48	3.93	2.98	5.66	3.23	2.53
Al_2O_3	7.76	2.59	4.72	7.36	8.42	15.2	7.95	3.10
SiO_2	31.0	12.7	38.1	41.2	37.3	52.7	34.3	26.9
P_2O5	0.30	0.13	0.25	0.33	0.13	0.34	0.25	0.06
S	6.99	16.3	6.99	3.19	0.98	0.04	0.11	12.9
Cl*	0.19	0.11	0.01	0.10	0.00	0.01	0.02	0.02
K_2O	0.64	0.27	0.07	0.43	0.04	1.04	0.05	0.13
CaO	12.1	11.7	16.9	13.7	30.6	11.6	39.8	16.0
TiO_2	0.43	0.29	0.47	0.52	0.41	1.24	0.77	0.11
V*	0.00	0.00	0.02	0.02	0.00	0.03	0.03	0.00
Cr*	0.00	0.00	0.01	0.00	0.02	0.00	0.00	0.00
MnO	0.27	0.37	0.24	0.26	0.57	0.12	0.54	0.26
FeO	34.9	53.2	27.1	25.4	17.7	6.40	12.6	37.2
Co*	0.02	0.07	0.08	0.09	0.01	0.01	0.00	0.05
Rb*	0.00	0.00	0.00	0.00	0.00	0.00	0.00	0.00
Sr	0.03	0.02	0.04	0.04	0.02	0.07	0.05	0.02
Zr*	0.01	0.01	0.00	0.03	0.01	0.01	0.01	0.01
BaO*	0.02	0.00	0.02	0.02	0.00	0.06	0.00	0.00
Trace elements (parts per million)								
Cu	921	790	1170	877	180	19	20	2033
As	106	62	300	1702	202	267	82	448
Ag*	1	3	13	21	14	12	11	4
Te	15	12	19	39	57	36	16	118
Bi	2556	1549	6737	14195	4489	4221	608	2956
W	25	25	27	146	22	15	8	45
Mo	4	2	4	19	6	14	46	205
Pb	9	13	6	9	91	173	22	18
Zn	133	118	135	232	112	111	89	102
Sb*	4	0	1	0	1	0	17	0
Ni	169	351	67	68	32	20	17	51

Table A4-1 continued. XRF Analysis of pulp samples in the Gold Bowl.

Drill Hole	D08-436	D08-436	D08-449	D08-449	D08-482	D08-482	D10-622	D10-622
Sample	BX 10686	BX 10688	BX 11351	BX 11572	BX 13871	BX 13872	BX 26054	BX 26055
Weight percent oxide								
F**	0.01	0.01	0.01	0.01	0.01	0.01	0.11	0.01
Na_2O	0.06	0.08	0.13	1.22	0.47	0.14	4.64	4.09
MgO	1.61	2.01	2.31	1.27	2.42	2.17	5.73	6.45
Al_2O_3	5.65	8.34	6.97	6.79	8.83	6.57	15.7	16.4
SiO_2	28.3	37.7	43.7	34.4	36.6	32.8	49.9	50.0
P_2O5	0.19	0.04	0.16	0.06	0.12	0.10	0.26	0.21
S	10.3	3.50	0.29	8.38	3.88	5.29	0.09	0.06
Cl*	0.02	0.03	0.02	0.00	0.01	0.00	0.13	0.08
K_2O	0.02	0.02	0.02	1.24	1.77	0.49	1.58	2.07
CaO	20.5	25.5	23.8	15.0	24.2	25.4	8.31	8.17
TiO_2	0.20	0.24	0.59	0.42	0.44	0.39	1.08	1.02
V*	0.00	0.00	0.00	0.00	0.00	0.00	0.03	0.05
Cr*	0.03	0.04	0.00	0.02	0.00	0.00	0.01	0.01
MnO	0.39	0.58	0.73	0.25	0.31	0.38	0.15	0.13
FeO	32.4	21.3	20.6	28.8	19.4	25.6	10.1	10.2
Co*	0.03	0.01	0.04	0.00	0.01	0.02	0.00	0.01
Rb*	0.00	0.00	0.00	0.00	0.01	0.00	0.01	0.01
Sr	0.04	0.03	0.04	0.02	0.05	0.05	0.04	0.04
Zr*	0.00	0.01	0.01	0.00	0.00	0.01	0.01	0.01
BaO*	0.00	0.02	0.02	0.09	0.09	0.04	0.04	0.04
Trace elements (parts per million)								
Cu	1803	675	93	1773	849	1313	42	40
As	103	113	708	757	782	237	21	24
Ag*	2	11	29	9	36	53	0	0
Te	21	70	23	38	71	36	0	1
Bi	730	2416	2446	11967	7259	2604	-2	0
W	37	23	18	44	32	26	6	3
Mo	39	6	1	87	16	15	5	4
Pb	23	334	623	42	401	490	17.5	33.8
Zn	69	119	167	3441	157	408	103	108
Sb*	17	5	5	0	0	17	11	0
Ni	42	26	38	58	35	43	20	24

Table A4-1 continued. XRF Analysis of pulp samples in the Gold Bowl.

Drill Hole	D10-622	D10-622	D10-622	D10-624	D10-624	D10-624	D10-624	D10-624
Sample	BX 26056	BX 26057	BX 26058	BX 26382	BX 26383	BX 26384	BX 26385	BX 26386
Weight percent oxide								
F**	0.10	0.01	0.01	0.01	0.01	0.01	0.01	0.01
Na_2O	4.23	4.89	0.14	2.00	0.04	0.05	0.06	0.25
MgO	5.69	4.51	4.16	3.68	2.88	2.52	2.71	3.52
Al_2O_3	16.7	15.5	8.92	12.5	10.2	9.59	10.6	8.93
$S1O_2$	49.3	50.7	40.3	44.7	37.0	36.4	38.3	46.6
P_2O5	0.19	0.23	0.26	0.29	0.26	0.22	0.18	0.21
S	0.26	0.27	0.00	0.01	0.60	0.34	0.80	1.10
Cl*	0.05	0.02	0.01	0.01	0.02	0.02	0.02	0.02
K_2O	1.55	0.84	0.03	0.02	0.02	0.03	0.04	0.15
CaO	9.28	11.9	29.0	22.8	30.9	33.2	28.8	22.8
TiO_2	0.91	0.80	0.61	1.18	0.98	1.05	0.85	0.81
V*	0.04	0.03	0.02	0.01	0.01	0.02	0.02	0.01
Cr*	0.01	0.02	0.03	0.01	0.01	0.03	0.02	0.02
MnO	0.12	0.19	0.57	0.46	0.53	0.59	0.47	0.43
FeO	9.39	9.94	15.7	12.3	16.4	15.8	16.9	15.1
Co*	0.00	0.00	0.01	0.00	0.01	0.00	0.02	0.00
Rb*	0.01	0.01	0.00	0.00	0.00	0.00	0.00	0.00
Sr	0.05	0.06	0.02	0.06	0.05	0.05	0.07	0.06
Zr*	0.00	0.01	0.00	0.01	0.01	0.00	0.01	0.01
BaO*	0.04	0.04	0.02	0.02	0.01	0.01	0.02	0.02
Trace elements (parts per million)								
Cu	171	230	19	9	38	32	97	186
As	41	46	22	21	61	81	129	49
Ag*	0	0	0	0	0	0	0	0
Te	1	0	0	0	0	0	1	0
Bi	-1	6	43	12	20	106	100	26
W	0	1	10	5	15	7	12	10
Mo	8	5	4	5	5	14	12	10
Pb	26	26	55	41	52	92	112	42
Zn	102	81	50	91	90	91	260	102
Sb*	10	8	10	17	29	30	57	21
Ni	21	27	18	16	14	16	18	21

Table A4-1 continued. XRF Analysis of pulp samples in the Gold Bowl.

Drill Hole	D10-624	D10-624	D10-624	D10-624	D10-631	D10-631	D10-631	D10-631
Sample	BX 26387	BX 26388	BX 26389	BX 26397	BX 30691	BX 30692	BX 30693	BX 30694
Weight percent oxide								
F**	0.01	0.11	0.01	0.01	0.01	0.01	0.04	0.01
Na_2O	7.28	4.43	5.93	3.51	4.23	3.85	3.27	0.79
MgO	2.74	2.97	3.03	4.70	5.36	5.65	5.90	5.22
Al_2O_3	13.8	12.2	13.7	12.8	13.9	14.1	13.3	9.21
SiO_2	55.1	45.5	52.9	48.6	49.4	48.5	48.6	39.0
P_2O5	0.25	0.27	0.28	0.47	0.21	0.20	0.20	0.21
S	0.22	2.60	0.10	0.01	0.01	0.01	0.01	0.17
Cl*	0.01	0.01	0.01	0.02	0.27	0.17	0.10	0.02
K_2O	0.70	0.05	0.06	0.11	0.59	0.89	0.69	0.12
CaO	10.8	14.9	14.4	18.0	11.8	12.8	14.5	24.1
TiO_2	1.13	1.17	1.04	1.45	1.36	1.29	1.06	1.06
V*	0.03	0.04	0.03	0.03	0.07	0.07	0.05	0.05
Cr*	0.01	0.01	0.01	0.01	0.01	0.01	0.01	0.02
MnO	0.16	0.23	0.26	0.22	0.23	0.23	0.24	0.36
FeO	5.56	13.40	8.13	9.78	12.5	12.1	11.9	13.3
Co*	0.00	0.00	0.01	0.02	0.01	0.00	0.01	0.00
Rb*	0.00	0.00	0.00	0.00	0.00	0.00	0.00	0.00
Sr	0.02	0.04	0.04	0.07	0.04	0.04	0.05	0.04
Zr*	0.01	0.01	0.01	0.01	0.01	0.00	0.00	0.01
BaO*	0.04	0.01	0.01	0.02	0.03	0.04	0.03	0.01
Trace elements (parts per million)								
Cu	41	413	27	15	10	7	13	18
As	39	50	75	36	56	26	37	64
Ag*	0	0	0	0	0	0	0	0
Te	1	1	0	0	0	1	4	39
Bi	0	4	13	73	7	59	179	1337
W	2	4	2	2	10	5	8	13
Mo	4	6	15	4	4	5	5	5
Pb	17	37	15	39	31	48	65	49
Zn	48	68	63	93	125	117	113	104
Sb*	0	5	14	25	5	11	6	12
Ni	19	29	16	15	22	21	24	17

Table A4-1 continued. XRF Analysis of pulp samples in the Gold Bowl.

Drill Hole	D10-631	D10-631	D10-631	D10-631	D10-631	D10-631	D10-631	D10-631
Sample	BX 30695	BX 30696	BX 32440	BX 32441	BX 32442	BX 32444	BX 32445	BX 32446
Weight percent oxide								
F**	0.01	0.01	0.01	0.01	0.01	0.01	0.01	0.01
Na_2O	2.91	3.28	0.28	0.09	0.77	0.61	0.06	0.05
MgO	5.64	6.51	1.36	2.13	3.08	2.30	2.54	2.65
Al_2O_3	12.7	13.8	4.18	9.05	9.13	8.27	13.5	11.3
SiO_2	46.6	48.3	44.7	40.6	53.3	41.2	40.0	37.8
P_2O5	0.21	0.20	0.18	0.19	0.23	0.24	0.19	0.19
S	0.03	0.01	0.62	0.37	0.08	0.44	0.07	0.01
Cl*	0.11	0.09	0.01	0.02	0.00	0.01	0.01	0.02
K_2O	0.38	0.84	0.09	0.04	0.80	0.14	0.01	0.01
CaO	18.0	13.4	25.1	30.2	21.3	28.2	28.5	33.4
TiO_2	1.05	1.29	0.19	0.48	0.48	0.41	0.71	0.42
V*	0.05	0.07	0.01	0.02	0.00	0.00	0.02	0.01
Cr*	0.01	0.02	0.02	0.02	0.00	0.03	0.02	0.04
MnO	0.32	0.24	0.77	0.67	0.50	0.67	0.58	0.74
FeO	11.8	11.8	20.4	14.0	9.80	17.3	13.6	13.3
Co*	0.00	0.00	0.00	0.01	0.00	0.00	0.01	0.01
Rb*	0.00	0.01	0.00	0.00	0.01	0.00	0.00	0.00
Sr	0.04	0.05	0.01	0.01	0.05	0.02	0.06	0.01
Zr*	0.01	0.01	0.00	0.00	0.01	0.00	0.01	0.01
BaO*	0.02	0.03	0.02	0.02	0.08	0.05	0.02	0.01
Trace elements (parts per million)								
Cu	13	15	36	61	8	93	9	5
As	53	22	16	11	15	29	12	9
Ag*	0	0	0	0	102	94	0	0
Te	17	0	5	1	7	2	0	0
Bi	750	8	75	1	216	5	3	0
W	7	3	18	13	9	12	12	14
Mo	4	5	50	7	5	9	15	9
Pb	230	15	64	26	3500	61	28	19
Zn	87	114	135	106	347	162	76	82
Sb*	16	7	15	7	8	11	33	0
Ni	19	20	21	22	19	22	23	20

Table A4-2. XRF Analysis of pulp samples from North of Gold Bowl.

Drill Hole	D07-379	D09-536	D07-371	D07-371	D07-371	D07-371	D07-371	D07-371
Sample	BX 09391	BX 17601	BX 09747	BX 09750	BX 09751	BX 09752	BX 09753	BX 09754
Weight percent oxide								
F**	0.01	0.01	0.01	0.01	0.01	0.01	0.01	0.01
Na_2O	0.12	0.08	0.07	0.11	0.15	1.74	5.91	3.53
MgO	1.09	1.99	3.26	1.92	1.75	2.07	2.25	2.48
Al_2O_3	4.30	5.94	6.61	8.80	8.99	11.0	15.8	13.1
SiO_2	19.2	22.8	33.6	37.8	39.1	45.0	57.0	51.8
P_2O5	0.07	0.04	0.51	0.04	0.07	0.05	0.03	0.04
S	14.8	3.43	5.37	0.06	0.04	0.09	0.07	0.82
Cl*	0.01	0.01	0.01	0.03	0.03	0.01	0.02	0.02
K_2O	0.03	0.11	0.01	0.16	0.10	0.87	1.91	2.47
CaO	16.7	35.7	24.7	35.1	33.5	26.4	9.63	16.0
TiO_2	0.07	0.06	0.44	0.53	0.47	0.59	0.81	0.67
V*	0.00	0.00	0.02	0.00	0.00	0.01	0.00	0.01
Cr*	0.00	0.02	0.03	0.03	0.03	0.03	0.01	0.02
MnO	0.27	0.45	0.47	0.57	0.55	0.45	0.17	0.29
FeO	41.5	28.7	24.7	14.8	15.2	11.5	6.27	8.60
Co*	0.05	0.02	0.01	0.01	0.01	0.00	0.00	0.00
Rb*	0.00	0.00	0.00	0.00	0.00	0.00	0.01	0.02
Sr	0.01	0.04	0.01	0.02	0.01	0.04	0.03	0.03
Zr*	0.00	0.00	0.01	0.01	0.01	0.00	0.01	0.01
BaO*	0.02	0.03	0.00	0.02	0.00	0.05	0.08	0.06
Trace elements (parts per million)								
Cu	15306	805	1503	11	13	25	5	98
As	80	105	16	5	5	3	8	162
Ag*	31	17	7	10	12	11	8	5
Te	250	52	2	2	0	1	0	0
Bi	1625	2431	9	7	18	7	4	7
W	27	23	15	8	9	8	7	12
Mo	7	2	3	5	7	4	4	3
Pb	116	121	52	30	114	39	15	27
Zn	132	124	108	102	99	90	70	114
Sb*	0	0	6	5	10	13	4	6
Ni	705	32	29	21	24	23	20	13

Table A4-2 continued. XRF Analysis of pulp samples from North of Gold Bowl.

Drill Hole	D07-371	D07-371	D07-371	D07-371	D07-371	D07-371	D07-371	D07-371
Sample	BX 09756	BX 09758	BX 09760	BX 09762	BX 09766	BX 09767	BX 09768	BX 09769
Weight percent oxide								
F**	0.01	0.01	0.01	0.01	0.01	0.01	0.01	0.01
Na_2O	0.01	0.52	0.08	0.07	2.89	0.11	0.06	5.09
MgO	1.97	1.22	0.69	0.62	4.29	1.73	2.16	3.33
Al_2O_3	8.97	6.16	3.16	3.14	13.2	6.07	7.38	15.9
SiO_2	36.5	29.0	18.6	16.2	54.4	30.2	33.4	56.8
P_2O5	0.05	0.04	0.04	0.05	0.42	0.24	0.32	0.46
S	0.63	8.89	0.02	0.14	0.23	0.20	0.19	0.31
Cl*	0.03	0.00	0.01	0.02	0.01	0.03	0.02	0.02
K_2O	0.02	1.00	0.19	0.14	2.30	0.15	0.23	2.82
CaO	32.9	23.2	72.7	74.8	12.8	47.2	42.5	7.18
TiO_2	0.52	0.37	0.38	0.40	1.01	0.49	0.57	1.02
V*	0.02	0.00	0.00	0.01	0.00	0.00	0.00	0.00
Cr*	0.03	0.03	0.02	0.02	0.02	0.03	0.02	0.02
MnO	0.64	0.28	0.38	0.32	0.20	0.55	0.58	0.09
FeO	14.4	28.9	3.60	3.88	7.90	12.8	12.5	6.57
Co*	0.01	0.01	0.00	0.00	0.00	0.01	0.00	0.01
Rb*	0.00	0.00	0.00	0.00	0.01	0.00	0.00	0.01
Sr	0.02	0.02	0.04	0.04	0.04	0.03	0.04	0.03
Zr*	0.01	0.00	0.01	0.01	0.01	0.01	0.01	0.02
BaO*	0.02	0.07	0.04	0.00	0.14	0.02	0.03	0.18
Trace elements (parts per million)								
Cu	416	1940	2	7	94	66	65	79
As	5	107	8	4	1	3	3	5
Ag*	18	13	21	22	4	14	15	4
Te	1	3	2	0	2	1	1	1
Bi	19	141	4	7	5	5	5	6
W	17	91	6	9	6	10	10	6
Mo	5	3	2	2	7	3	2	2
Pb	272	366	7	15	11	12	15	10
Zn	1540	192	64	182	107	155	91	69
Sb*	12	9	5	12	2	9	13	10
Ni	23	44	13	13	21	18	16	17

Table A4-2 continued. XRF Analysis of pulp samples from North of Gold Bowl.

Drill Hole	D07-371	D07-371	D07-371	D07-371	D07-371	D07-371	D07-371	D07-376
Sample	BX 09770	BX 09771	BX 09772	BX 09774	BX 09775	BX 09776	BX 09780	BX 08731
Weight percent oxide								
F**	0.01	0.01	0.01	0.01	0.01	0.01	0.01	0.01
Na_2O	0.14	0.15	0.20	0.07	0.04	0.10	0.14	0.05
MgO	1.52	0.75	0.73	0.69	0.39	1.41	1.27	2.64
Al_2O_3	3.72	2.84	2.00	2.53	2.25	3.90	4.41	6.82
SiO_2	39.4	46.1	44.4	34.3	36.2	36.7	28.0	34.8
P_2O5	0.12	0.07	0.07	0.08	0.06	0.10	0.13	0.46
S	4.15	0.91	0.54	1.41	0.36	0.91	0.20	3.69
Cl*	0.02	0.02	0.03	0.01	0.02	0.02	0.02	0.00
K_2O	0.15	0.04	0.04	0.04	0.02	0.06	0.28	0.01
CaO	26.2	23.8	24.9	33.6	36.4	33.8	59.0	27.1
TiO_2	0.24	0.16	0.10	0.06	0.03	0.23	0.29	0.35
V*	0.00	0.00	0.00	0.00	0.00	0.00	0.00	0.01
Cr*	0.02	0.02	0.01	0.03	0.03	0.02	0.02	0.02
MnO	0.88	1.01	1.01	0.39	0.38	0.47	0.41	0.49
FeO	23.3	24.1	25.9	26.6	23.8	22.2	5.65	23.3
Co*	0.02	0.00	0.00	0.02	0.00	0.01	0.00	0.00
Rb*	0.00	0.00	0.00	0.00	0.00	0.00	0.00	0.00
Sr	0.01	0.01	0.01	0.00	0.00	0.01	0.04	0.01
Zr*	0.00	0.00	0.00	0.00	0.00	0.00	0.01	0.01
BaO*	0.03	0.00	0.00	0.00	0.00	0.00	0.05	0.00
Trace elements (parts per million)								
Cu	846	231	63	993	165	411	34	2146
As	95	13	13	153	130	105	3	10
Ag*	6	6	6	16	13	13	16	10
Te	1	2	3	1	3	1	2	0
Bi	13	12	9	53	57	8	7	8
W	25	15	7	273	305	66	8	23
Mo	3	3	5	11	13	12	3	4
Pb	73	23	13	145	63	36	28	12
Zn	208	102	96	117	65	120	128	180
Sb*	3	7	7	12	1	8	13	11
Ni	37	25	22	22	22	29	15	35

Table A4-2 continued. XRF Analysis of pulp samples from North of Gold Bowl.

Drill Hole	D07-376	D07-376	D07-376	D07-376	D07-376	D07-376	D07-376	D07-376
Sample	BX 08732	BX 08733	BX 08735	BX 08736	BX 08737	BX 08738	BX 08739	BX 08742
Weight percent oxide								
F**	0.01	0.01	0.01	0.01	0.01	0.01	0.01	0.01
Na_2O	0.04	0.10	0.06	0.09	0.07	0.12	0.04	0.06
MgO	1.73	2.10	2.55	1.54	3.49	5.24	2.46	2.87
Al_2O_3	6.50	7.18	9.44	6.57	7.71	9.75	9.67	6.15
SIO_2	28.3	36.2	38.9	36.9	37.6	43.2	37.5	31.2
P_2O5	0.45	0.30	0.37	0.26	0.46	0.53	0.46	0.51
S	6.94	2.43	0.31	4.14	1.26	0.06	0.38	4.38
Cl*	0.01	0.00	0.01	0.00	0.01	0.00	0.01	0.00
K_2O	0.00	0.03	0.02	0.09	0.01	0.02	0.02	0.02
CaO	25.2	28.1	30.6	27.5	29.5	24.7	31.0	21.6
TiO_2	0.73	0.40	0.50	0.40	0.47	0.64	0.72	0.37
V*	0.02	0.00	0.00	0.00	0.02	0.00	0.02	0.02
Cr*	0.02	0.02	0.02	0.04	0.03	0.02	0.02	0.04
MnO	0.41	0.55	0.61	0.41	0.49	0.44	0.56	0.34
FeO	29.4	21.9	16.6	20.5	18.6	15.2	17.1	32.3
Co*	0.00	0.01	0.00	0.00	0.00	0.00	0.01	0.01
Rb*	0.00	0.00	0.00	0.00	0.00	0.00	0.00	0.00
Sr	0.01	0.01	0.01	0.02	0.01	0.05	0.01	0.01
Zr*	0.01	0.01	0.01	0.01	0.01	0.02	0.01	0.00
BaO*	0.00	0.00	0.00	0.00	0.00	0.00	0.00	0.02
Trace elements (parts per million)								
Cu	1837	5126	74	9744	2354	29	218	700
As	17	37	9	23	10	9	13	21
Ag*	7	19	10	27	13	5	10	0
Te	2	2	2	2	2	1	2	2
Bi	12	11	6	6	8	9	7	10
W	18	10	12	7	11	11	13	16
Mo	4	4	6	6	1	4	6	3
Pb	14	15	10	38	15	12	80	45
Zn	119	410	69	770	168	120	138	74
Sb*	7	15	13	16	4	22	15	12
Ni	42	29	13	35	22	18	23	34

Table A4-2 continued. XRF Analysis of pulp samples from North of Gold Bowl.

Drill Hole	D07-376	D07-376	D07-376	D07-376	D07-376	D07-376	D07-376	D07-376
Sample	BX 08743	BX 08744	BX 08745	BX 08746	BX 08748	BX 08749	BX 08750	BX 08751
Weight percent oxide								
F**	0.01	0.01	0.01	0.01	0.01	0.01	0.01	0.01
Na_2O	0.04	0.09	0.06	0.10	0.07	0.04	0.06	0.06
MgO	3.28	3.33	3.29	2.82	3.78	1.37	2.27	2.40
Al_2O_3	7.31	12.3	4.82	7.44	6.92	9.56	6.77	6.00
SiO_2	34.7	41.2	29.5	39.6	39.9	35.3	29.3	29.0
P_2O5	0.45	0.49	0.47	0.36	0.40	0.30	0.30	0.32
S	3.78	0.21	9.60	1.29	1.93	1.92	5.09	4.64
Cl*	0.00	0.01	0.01	0.00	0.00	0.01	0.01	0.01
K_2O	0.01	0.02	0.00	0.06	0.02	0.01	0.02	0.02
CaO	25.2	25.0	21.2	26.6	26.5	30.2	21.0	20.5
TiO_2	0.37	0.65	0.34	0.45	0.54	0.51	0.41	0.34
V*	0.01	0.01	0.00	0.00	0.01	0.02	0.00	0.02
Cr*	0.04	0.01	0.04	0.02	0.01	0.05	0.04	0.03
MnO	0.41	0.36	0.34	0.60	0.49	0.54	0.35	0.35
FeO	24.1	16.3	30.1	20.3	19.2	20.0	34.4	36.1
Co*	0.00	0.00	0.00	0.01	0.00	0.00	0.00	0.00
Rb*	0.00	0.00	0.00	0.00	0.00	0.00	0.00	0.00
Sr	0.01	0.06	0.01	0.03	0.02	0.01	0.01	0.01
Zr*	0.01	0.01	0.00	0.01	0.01	0.01	0.00	0.01
BaO*	0.00	0.00	0.00	0.00	0.00	0.02	0.00	0.00
Trace elements (parts per million)								
Cu	2696	46	2012	1787	1072	609	853	2042
As	13	10	15	101	18	13	27	34
Ag*	11	6	2	13	7	12	-1	6
Te	0	2	4	2	2	2	2	2
Bi	9	7	13	26	5	5	8	7
W	16	13	19	16	15	12	18	26
Mo	4	10	5	8	4	11	7	9
Pb	49	13	24	122	30	183	141	56
Zn	179	80	114	324	136	51	77	139
Sb*	18	16	2	10	11	11	6	12
Ni	32	14	44	44	23	31	42	43

Table A4-2 continued. XRF Analysis of pulp samples from North of Gold Bowl.

Drill Hole	D07-376	D07-376	D07-376	D07-376
Sample	BX 08755	BX 08756	BX 08757	BX 08757
Weight percent oxide				
F**	0.01	0.01	0.01	0.01
Na_2O	0.05	0.06	0.13	0.09
MgO	1.33	1.56	3.55	3.24
Al_2O_3	10.2	6.89	5.72	8.56
SiO_2	36.4	26.7	36.2	38.7
P_2O5	0.35	0.26	0.39	0.24
S	0.28	0.95	2.96	1.04
Cl*	0.01	0.01	0.01	0.01
K_2O	0.01	0.16	0.02	0.02
CaO	33.7	45.1	28.9	29.2
TiO_2	0.51	0.59	0.25	0.46
V*	0.02	0.01	0.00	0.02
Cr*	0.04	0.02	0.02	0.03
MnO	0.67	0.72	0.63	0.55
FeO	16.4	16.8	20.8	17.7
Co*	0.00	0.00	0.00	0.00
Rb*	0.00	0.00	0.00	0.00
Sr	0.00	0.03	0.02	0.01
Zr*	0.01	0.01	0.01	0.01
BaO*	0.00	0.02	0.00	0.02
Trace elements (parts per million)				
Cu	96	316	806	1800
As	5	7	8	17
Ag*	9	22	9	40
Te	2	3	0	6
Bi	5	30	5	76
W	12	27	15	28
Mo	7	5	7	6
Pb	97	450	38	1244
Zn	59	292	156	822
Sb*	10	7	5	12
Ni	18	18	38	31

Table A4-3. XRF Analysis of pulp samples from the Southwest Zone.

Drill Hole	D07-366	D07-366	D07-366	D07-385	D07-385	D07-385	D07-390	D07-390
Sample	BX 02459	BX 02460	BX 02463	BX 03128	BX 03130	BX 03132	BX 02677	BX 02679
Weight percent oxide								
F**	0.01	0.01	0.01	0.01	0.01	0.01	0.01	0.01
Na_2O	0.04	0.06	0.04	0.11	1.25	0.92	0.07	0.08
MgO	2.26	5.24	6.46	2.32	1.96	2.21	1.77	2.42
Al_2O_3	0.60	4.12	0.57	1.83	10.3	6.34	4.54	1.23
SiO_2	28.8	30.8	40.2	17.2	41.0	33.4	35.7	30.7
P_2O5	0.04	0.12	0.02	0.04	0.16	0.13	0.15	0.10
S	6.48	0.56	0.03	1.26	1.38	1.43	1.13	1.35
Cl*	0.00	0.03	0.01	0.07	0.08	0.11	0.01	0.01
K_2O	0.05	0.14	0.07	0.63	2.96	2.39	0.07	0.03
CaO	16.1	31.7	22.4	59.8	24.3	32.3	34.5	39.8
TiO_2	0.02	0.26	0.02	0.13	0.72	0.52	0.17	0.11
V*	0.00	0.00	0.00	0.00	0.02	0.01	0.00	0.00
Cr*	0.02	0.02	0.00	0.02	0.03	0.00	0.05	0.03
MnO	0.12	0.26	0.24	0.26	0.20	0.32	0.44	0.37
FeO	44.4	24.2	29.5	16.0	15.3	19.6	20.9	23.0
Co*	0.02	0.01	0.00	0.00	0.00	0.01	0.01	0.00
Rb*	0.00	0.00	0.00	0.01	0.02	0.02	0.00	0.00
Sr	0.01	0.05	0.01	0.05	0.04	0.06	0.01	0.01
Zr*	0.00	0.00	0.00	0.00	0.01	0.01	0.00	0.00
BaO*	0.02	0.00	0.02	0.04	0.08	0.05	0.03	0.00
Trace elements (parts per million)								
Cu	710	298	178	918	443	353	2143	3946
As	339	691	182	181	294	72	27	48
Ag*	10	24	9	19	11	13	22	21
Te	37	63	15	10	24	38	23	12
Bi	8157	11909	2278	95	405	462	610	887
W	35	31	25	7	15	14	12	74
Mo	2	3	1	8	161	25	39	1
Pb	44	179	28	22	17	13	211	74
Zn	133	165	98	40	35	39	176	178
Sb*	0	0	1	5	5	0	9	15
Ni	69	28	28	22	38	32	25	19

Table A4-3 continued. XRF Analysis of pulp samples from the Southwest Zone.

Drill Hole	D07-390	D08-414	D08-414	D08-414	D08-476	D08-476	D08-476	D08-477
Sample	BX 02698	BX 04693	BX 04695	BX 04697	BX 12949	BX 12961	BX 13340	BX 13422
Weight percent oxide								
F**	0.01	0.01	0.01	0.01	0.01	0.01	0.01	0.01
Na_2O	0.08	0.09	0.10	0.09	1.26	0.31	0.65	0.46
MgO	2.64	1.79	2.34	2.34	3.18	5.68	3.19	4.34
Al_2O_3	6.21	0.67	0.73	1.70	9.85	6.65	9.00	6.93
SiO_2	38.0	15.5	19.5	22.1	40.3	43.1	38.8	40.4
P_2O5	0.07	0.05	0.05	0.05	0.29	0.32	0.22	0.23
S	0.24	1.20	0.86	1.86	1.41	3.41	1.60	3.26
Cl*	0.02	0.02	0.03	0.02	0.01	0.08	0.14	0.27
K_2O	0.07	0.04	0.04	0.07	1.37	1.42	3.80	1.22
CaO	31.6	11.1	14.9	23.4	19.3	17.5	19.9	14.3
TiO_2	0.38	0.07	0.05	0.07	0.40	0.49	0.79	0.33
V*	0.00	0.00	0.00	0.00	0.02	0.03	0.02	0.02
Cr*	0.03	0.03	0.03	0.04	0.01	0.00	0.00	0.02
MnO	0.30	0.10	0.15	0.22	0.48	0.27	0.24	0.26
FeO	19.9	69.2	61.1	47.9	21.5	20.3	21.2	27.6
Co*	0.04	0.01	0.01	0.01	0.07	0.01	0.00	0.02
Rb*	0.00	0.00	0.00	0.00	0.01	0.00	0.02	0.00
Sr	0.04	0.00	0.00	0.01	0.04	0.02	0.02	0.02
Zr*	0.01	0.00	0.00	0.00	0.01	0.00	0.01	0.00
BaO*	0.03	0.00	0.01	0.02	0.09	0.09	0.11	0.04
Trace elements (parts per million)								
Cu	296	568	1010	1164	1585	1149	386	1209
As	418	95	51	95	648	27	639	38
Ag*	34	2	5	8	10	32	6	8
Te	6	99	96	37	21	35	65	51
Bi	1065	289	289	258	825	537	782	852
W	15	49	33	25	15	33	18	25
Mo	10	2	5	2	365	33	66	163
Pb	537	11	8	11	32	719	14	24
Zn	176	93	89	75	202	294	77	144
Sb*	12	0	0	0	11	4	4	0
Ni	25	67	47	55	222	82	39	104

Table A4-3 continued. XRF Analysis of pulp samples from the Southwest Zone.

Drill Hole	D08-479	D08-479	D08-479	D08-481	D08-481	D08-481	D09-491	D09-491
Sample	BX 13335	BX 13339	BX 13342	BX 15173	BX 15253	BX 15254	BX 15664	BX 15665
Weight percent oxide								
F**	0.01	0.01	0.01	0.01	0.01	0.01	0.01	0.01
Na_2O	0.25	0.26	1.40	0.17	0.06	0.07	0.14	0.13
MgO	1.33	2.67	1.99	2.63	1.53	1.86	2.73	3.38
Al_2O_3	7.12	8.15	7.01	8.90	1.03	1.49	3.78	2.52
SiO_2	39.2	36.4	29.2	41.4	21.6	25.6	37.9	34.5
P_2O5	0.17	0.16	0.14	0.17	0.04	0.08	0.08	0.04
S	6.24	5.21	1.07	1.72	2.50	5.33	3.32	4.49
Cl*	0.02	0.13	0.05	0.05	0.01	0.02	0.09	0.03
K_2O	0.52	3.04	1.84	0.72	0.04	0.05	0.34	0.50
CaO	17.9	15.5	40.4	21.2	44.5	33.1	24.4	25.9
TiO_2	0.52	0.56	0.62	0.58	0.05	0.04	0.22	0.11
V*	0.01	0.02	0.00	0.00	0.00	0.00	0.00	0.00
Cr*	0.02	0.00	0.00	0.00	0.02	0.00	0.02	0.02
MnO	0.24	0.20	0.25	0.34	0.35	0.30	0.32	0.30
FeO	26.0	27.2	15.3	21.6	27.7	31.7	26.4	27.8
Co*	0.02	0.01	0.02	0.00	0.01	0.01	0.00	0.02
Rb*	0.00	0.01	0.01	0.22	0.00	0.00	0.00	0.01
Sr	0.03	0.02	0.04	0.05	0.02	0.01	0.02	0.02
Zr*	0.01	0.01	0.01	0.01	0.00	0.00	0.01	0.00
BaO*	0.02	0.09	0.09	0.07	0.00	0.00	0.02	0.02
Trace elements (parts per million)								
Cu	997	1072	367	273	474	976	685	1007
As	63	346	346	50	161	113	7	17
Ag*	5	5	16	17	16	11	7	16
Te	52	148	59	46	68	47	32	49
Bi	1086	1030	1887	1134	2758	1403	200	537
W	15	16	16	27	27	31	14	15
Mo	66	185	29	66	1	3	16	12
Pb	11	11	13	282	68	39	13	71
Zn	68	82	48	124	70	61	64	85
Sb*	6	0	11	5	0	0	1	6
Ni	109	55	30	20	22	41	22	24

Table A4-3 continued. XRF Analysis of pulp samples from the Southwest Zone.

Drill Hole	D09-492	D09-492	D09-492	D09-493	D09-493	D09-524	D09-528	D09-528
Sample	BX 15738	BX 15740	BX 15747	BX 18232	BX 18233	BX 19197	BX 19372	BX 19373
Weight percent oxide								
F**	0.01	0.01	0.01	0.01	0.01	0.01	0.01	0.01
Na_2O	0.11	0.11	0.08	0.24	0.10	0.10	0.11	0.13
MgO	5.81	6.22	4.66	4.92	4.85	1.73	2.36	1.93
Al_2O_3	0.59	0.68	0.81	2.57	1.43	1.75	1.43	4.57
SiO_2	40.9	42.3	38.1	36.1	36.3	33.4	35.8	34.7
P_2O5	0.02	0.02	0.03	0.03	0.02	0.12	0.14	0.05
S	2.32	3.03	3.95	1.83	2.49	2.52	3.16	0.25
Cl*	0.03	0.03	0.03	0.05	0.03	0.00	0.01	0.01
K_2O	0.02	0.03	0.04	0.44	0.27	0.35	0.10	1.08
CaO	27.7	22.4	24.5	32.4	33.7	34.7	27.8	36.3
TiO_2	0.02	0.00	0.00	0.07	0.04	0.27	0.08	0.11
V*	0.00	0.00	0.00	0.00	0.00	0.00	0.00	0.00
Cr*	0.02	0.02	0.00	0.02	0.02	0.02	0.02	0.02
MnO	0.33	0.35	0.33	0.35	0.33	0.19	0.34	0.46
FeO	22.0	24.6	27.4	20.8	20.3	24.3	28.0	19.8
Co*	0.00	0.01	0.01	0.00	0.01	0.01	0.01	0.00
Rb*	0.00	0.00	0.00	0.01	0.00	0.00	0.00	0.01
Sr	0.01	0.00	0.00	0.04	0.03	0.02	0.00	0.01
Zr*	0.00	0.00	0.00	0.00	0.00	0.00	0.00	0.00
BaO*								
Trace elements (parts per million)								
Cu	339	514	642	365	356	1691	2350	410
As	11	28	20	4	51	62	54	90
Ag*	12	9	8	13	10	17	15	14
Te	39	81	42	16	8	22	20	18
Bi	87	416	261	43	36	1569	1325	2320
W	12	15	15	15	14	20	20	18
Mo	2	1	1	5	4	171	281	51
Pb	17	19	19	60	14	32	77	26
Zn	56	67	57	98	72	164	265	170
Sb*	3	0	0	7	8	16	6	0
Ni	19	17	17	14	16	40	44	17

Table A4-3 continued. XRF Analysis of pulp samples from the Southwest Zone.

Drill Hole	D09-538	D09-538	D09-538	D10-568	D10-568	D10-596	D10-596	D10-713
Sample	BX 17446	BX 17447	BX 17448	BX 29533	BX 29547	BX 29314	BX 29317	BX 46104
Weight percent oxide								
F**	0.01	0.01	0.01	0.01	0.01	0.01	0.01	0.01
Na_2O	0.10	0.06	0.23	0.28	0.09	0.39	0.13	0.06
MgO	2.27	4.36	2.46	1.94	1.69	2.56	3.33	1.89
Al_2O_3	2.85	8.15	2.44	4.82	0.64	4.71	6.99	4.19
SiO_2	39.9	35.4	28.1	33.3	17.6	30.3	36.8	28.6
P_2O5	0.11	0.35	0.04	0.13	0.02	0.08	0.19	0.23
S	2.31	4.28	4.71	3.76	1.25	1.59	3.53	9.18
Cl*	0.02	0.01	0.02	0.03	0.02	0.29	0.01	0.00
K_2O	0.04	0.01	0.10	1.02	0.10	0.59	0.04	0.14
CaO	25.0	24.9	16.7	24.5	18.7	33.9	25.5	19.4
TiO_2	0.07	0.56	0.02	0.27	0.02	0.26	0.40	0.26
V*	0.00	0.00	0.00	0.00	0.00	0.00	0.00	0.00
Cr*	0.02	0.02	0.00	0.01	0.02	0.02	0.02	0.03
MnO	0.52	0.29	0.22	0.34	0.14	0.36	0.47	0.34
FeO	26.7	21.1	44.5	29.3	58.9	24.9	22.0	35.1
Co*	0.01	0.01	0.01	0.01	0.07	0.00	0.02	0.01
Rb*	0.00	0.00	0.00	0.01	0.00	0.00	0.00	0.00
Sr	0.00	0.05	0.01	0.02	0.01	0.01	0.03	0.02
Zr*	0.00	0.01	0.00	0.00	0.00	0.00	0.01	0.01
BaO*	0.00	0.00	0.02	0.06	0.00	0.03	0.01	0.02
Trace elements (parts per million)								
Cu	538	1399	630	1796	1500	363	1002	3715
As	29	58	154	8	1511	71	138	48
Ag*	7	28	5	7	7	6	10	10
Te	29	178	41	20	19	15	15	49
Bi	581	776	3573	39	4656	166	2975	270
W	20	19	33	19	43	16	26	24
Mo	3	18	1	81	1	2	5	3
Pb	9	542	66	10	0	8	9	154
Zn	86	123	124	64	115	72	161	262
Sb*	8	0	0	0	14	5	10	3
Ni	24	191	56	31	68	22	57	178

Table A4-3 continued. XRF Analysis of pulp samples from the Southwest Zone.

Drill Hole	D06-255	D06-255	D06-261	D06-261	D06-261	D06-261	D06-261	D06-261
Sample	11136	11137	11227	11228	11239	11241	11242	11243
Weight percent oxide								
F**	0.01	0.01	0.01	0.01	0.01	0.01	0.01	0.01
Na_2O	0.10	0.09	0.73	0.41	0.10	0.12	0.09	0.07
MgO	1.67	1.57	1.48	1.54	3.62	3.97	4.17	2.64
Al_2O_3	1.54	2.91	7.06	6.87	0.55	0.57	0.47	0.41
SiO_2	26.8	28.5	34.1	26.5	18.9	22.4	24.5	21.0
P_2O5	0.07	0.07	0.15	0.09	0.01	0.02	0.01	0.04
S	3.02	2.24	0.72	0.62	0.64	0.65	0.32	2.78
Cl*	0.00	0.01	0.01	0.04	0.02	0.02	0.02	0.01
K_2O	0.03	0.05	2.52	3.01	0.03	0.03	0.03	0.01
CaO	16.4	21.7	34.9	43.2	14.2	27.1	45.0	31.4
TiO_2	0.04	0.07	0.46	0.56	0.04	0.06	0.03	0.03
V*	0.01	0.01	0.02	0.01	0.00	0.00	0.00	0.00
Cr*	0.05	0.02	0.02	0.02	0.03	0.03	0.00	0.05
MnO	0.17	0.23	0.29	0.41	0.10	0.19	0.31	0.22
FeO	45.5	25.2	17.2	16.4	61.7	44.8	24.9	41.1
Co*	0.00	0.01	0.00	0.01	0.00	0.00	0.01	0.01
Rb*	0.00	0.00	0.01	0.02	0.00	0.00	0.00	0.00
Sr	0.00	0.01	0.03	0.04	0.00	0.00	0.02	0.01
Zr*	0.00	0.00	0.00	0.01	0.00	0.00	0.00	0.00
BaO*	0.01	0.02	0.14	0.16	0.02	0.00	0.02	0.02
Trace elements (parts per million)								
Cu	105	210	1148	245	133	234	81	656
As	315	87	5	5	39	67	32	22
Ag*	65	40	13	14	0	6	15	3
Te	10	5	0	0	1	31	39	4
Bi	7009	1570	4	5	10	176	172	60
W	42	50	7	13	35	26	8	17
Mo	2	2	17	17	2	2	2	1
Pb			15	5	7	8	6	6
Zn	44	44	85	47	80	65	49	57
Sb*	0	0	13	10	15	6	5	11
Ni	1	1	36	19	49	34	14	32

Table A4-3 continued. XRF Analysis of pulp samples from the Southwest Zone.

Drill Hole	D06-261	D06-261	D06-261	D06-261	D06-261	D06-261	D06-261	D06-261
Sample	11244	11245	11246	11247	11248	11249	11251	11252
Weight percent oxide								
F**	0.01	0.13	0.01	0.07	0.14	0.01	0.01	0.01
Na_2O	0.09	0.13	0.04	0.13	0.13	0.24	0.23	0.04
MgO	3.61	6.21	14.0	7.84	7.09	5.47	4.77	8.25
Al_2O_3	0.69	0.82	0.79	1.27	2.36	2.90	2.28	3.90
SiO_2	28.5	32.7	8.78	29.4	28.2	25.1	22.5	9.33
P_2O5	0.05	0.04	0.02	0.05	0.02	0.09	0.08	0.04
S	1.37	0.46	0.03	0.33	0.74	1.13	0.90	0.02
Cl*	0.01	0.02	0.00	0.04	0.03	0.06	0.07	0.00
K_2O	0.03	0.03	0.01	0.17	0.62	0.70	0.27	0.50
CaO	40.0	38.7	73.1	43.7	43.1	43.4	49.3	74.5
TiO_2	0.03	0.04	0.05	0.09	0.17	0.19	0.19	0.25
V*	0.00	0.00	0.00	0.00	0.01	0.00	0.01	0.01
Cr*	0.00	0.01	0.00	0.00	0.01	0.01	0.01	0.00
MnO	0.01	0.36	0.16	0.27	0.30	0.24	0.22	0.10
FeO	25.6	20.3	2.87	16.6	16.9	20.2	19.0	2.87
Co*	0.01	0.00	0.00	0.00	0.01	0.00	0.00	0.00
Rb*	0.00	0.00	0.00	0.00	0.01	0.01	0.00	0.01
Sr	0.02	0.02	0.08	0.03	0.03	0.04	0.06	0.10
Zr*	0.00	0.00	0.00	0.00	0.01	0.01	0.01	0.00
BaO*	0.02	0.03	0.02	0.00	0.03	0.02	0.01	0.02
Trace elements (parts per million)								
Cu	224	69	0	60	520	700	464	31
As	19	9	3	7	9	13	11	5
Ag*	9	13	23	13	13	15	15	25
Te	6	4	1	2	4	12	6	1
Bi	67	30	6	21	62	146	61	8
W	14	6	0	7	3	6	2	3
Mo	2	2	2	2	3	3	2	2
Pb	8	4	3	5	7	7	6	3
Zn	51	49	7	43	47	48	44	17
Sb*	11	7	8	0	6	1	14	9
Ni	14	8	2	10	10	15	14	6

Table A4-3 continued. XRF Analysis of pulp samples from the Southwest Zone.

Drill Hole	D06-261	D06-261	D06-261	D06-261	D06-261	D06-261	D06-261	D06-270
Sample	11253	11254	11255	11256	11257	11258	11259	BX 11342
Weight percent oxide								
F**	0.01	0.22	0.01	0.15	0.01	0.01	0.01	0.17
Na_2O	0.24	0.17	0.06	0.10	0.12	0.03	0.01	0.07
MgO	7.54	11.4	1.69	3.16	4.50	7.59	11.7	2.61
Al_2O_3	3.43	5.67	1.15	1.17	1.22	2.21	4.00	8.08
SiO_2	32.5	32.0	22.0	28.8	35.2	7.60	12.9	39.5
P_2O5	0.06	0.05	0.09	0.01	0.02	0.01	0.03	0.27
S	0.59	0.69	4.62	0.54	1.39	0.08	0.07	0.03
Cl*	0.08	0.03	0.02	0.03	0.04	0.00	0.00	0.03
K_2O	0.89	2.62	0.08	0.20	0.15	0.09	0.06	0.02
CaO	34.1	31.4	32.1	45.3	33.0	80.6	68.9	31.9
TiO_2	0.23	0.35	0.03	0.00	0.03	0.08	0.19	0.65
V*	0.00	0.01	0.00	0.00	0.00	0.00	0.00	0.02
Cr*	0.02	0.01	0.05	0.01	0.01	0.01	0.00	0.03
MnO	0.26	0.22	0.20	0.37	0.35	0.10	0.08	0.62
FeO	19.9	15.0	37.4	20.0	23.7	1.42	1.73	15.9
Co*	0.01	0.01	0.01	0.01	0.01	0.00	0.00	0.01
Rb*	0.01	0.03	0.00	0.00	0.00	0.00	0.00	0.00
Sr	0.02	0.01	0.01	0.02	0.01	0.12	0.19	0.00
Zr*	0.01	0.01	0.00	0.00	0.00	0.00	0.00	0.01
BaO*	0.03	0.05	0.02	0.03	0.02	0.02	0.02	0.02
Trace elements (parts per million)								
Cu	463	410	1754	224	881	9	4	13
As	16	15	164	74	115	4	14	133
Ag*	13	11	0	14	10	26	23	0
Te	6	2	4	1	3	0	0	5
Bi	63	38	340	118	261	7	5	318
W	8	34	1653	14	23	2	4	12
Mo	1	2	5	3	3	6	5	3
Pb	6	7	7	6	7	4	3	27.2
Zn	65	58	41	54	70	9	14	71
Sb*	8	7	9	4	12	3	6	3
Ni	17	14	34	10	17	4	9	14

Table A4-3 continued. XRF Analysis of pulp samples from the Southwest Zone.

Drill Hole	D06-270	D06-270	D06-270	D06-270	D06-270	D06-270	D06-270	D06-270
Sample	BX 11343	BX 11344	BX 11347	BX 11348	BX 11349	BX 11351	BX 11353	BX 11354
Weight percent oxide								
F**	0.16	0.01	0.01	0.01	0.01	0.01	0.01	0.01
Na_2O	0.03	0.06	0.04	0.06	0.10	0.14	0.06	0.07
MgO	2.43	2.28	0.67	2.40	2.33	2.39	1.61	2.16
Al_2O_3	7.25	6.55	8.70	4.33	6.65	6.98	5.51	4.64
SiO_2	39.7	38.6	37.2	41.7	44.6	44.4	39.0	41.5
P_2O5	0.26	0.20	0.08	0.09	0.13	0.16	0.13	0.14
S	0.02	0.16	0.32	0.16	0.26	0.22	0.05	0.34
Cl*	0.01	0.02	0.01	0.01	0.01	0.01	0.01	0.01
K_2O	0.02	0.02	0.05	0.05	0.03	0.02	0.03	0.02
CaO	31.8	30.4	31.8	26.5	22.7	23.6	29.7	26.8
TiO_2	0.57	0.35	0.28	0.14	0.38	0.59	0.17	0.10
V*	0.01	0.01	0.01	0.01	0.02	0.02	0.01	0.00
Cr*	0.03	0.03	0.04	0.02	0.01	0.00	0.03	0.03
MnO	0.59	0.57	0.56	0.63	0.72	0.65	0.55	0.53
FeO	16.9	18.2	17.8	20.8	19.9	20.2	19.5	20.1
Co*	0.02	0.11	0.11	0.02	0.01	0.06	0.15	0.09
Rb*	0.00	0.00	0.00	0.00	0.00	0.00	0.00	0.00
Sr	0.00	0.00	0.00	0.00	0.04	0.05	0.00	0.00
Zr*	0.01	0.00	0.00	0.00	0.01	0.01	0.01	0.00
BaO*	0.01	0.01	0.01	0.02	0.01	0.00	0.02	0.01
Trace elements (parts per million)								
Cu	17	24	861	41	33	74	17	283
As	176	1276	1204	126	47	677	1228	1251
Ag*	102	0	0	0	0	0	0	0
Te	2	23	6	1	0	28	23	16
Bi	86	1940	346	144	25	2652	1387	1683
W	13	24	15	10	9	12	17	9
Mo	3	8	8	4	6	4	3	8
Pb	21	58	369	74	162	821	1690	589
Zn	103	91	475	130	156	140	106	115
Sb*	6	0	1	0	11	14	2	1
Ni	19	42	40	14	24	37	77	83

Table A4-3 continued. XRF Analysis of pulp samples from the Southwest Zone.

Drill Hole	D06-270	D06-270	D06-272	D06-272	D06-272	D06-272	D06-272	D06-272
Sample	BX 11357	BX 11358	11365	11366	11367	11368	11369	11370
Weight percent oxide								
F**	0.11	0.09	0.01	0.01	0.01	0.01	0.01	0.01
Na_2O	1.70	1.58	0.25	0.33	0.31	0.29	0.31	0.24
MgO	2.07	2.25	3.92	2.15	1.96	1.84	1.91	1.75
Al_2O_3	11.9	9.43	8.65	5.06	5.37	5.82	4.72	2.83
SiO_2	59.7	60.1	40.3	34.9	37.4	37.4	34.2	31.4
P_2O5	0.16	0.25	0.27	0.13	0.15	0.14	0.01	0.10
S	0.01	0.00	2.25	6.36	3.85	3.41	3.39	5.80
Cl*	0.01	0.01	0.02	0.24	0.22	0.19	0.15	0.06
K_2O	2.29	1.72	0.22	0.57	0.51	0.49	0.47	0.31
CaO	12.3	15.4	22.3	15.0	18.2	19.7	22.6	26.3
TiO_2	0.48	0.56	0.56	0.29	0.35	0.37	0.35	0.17
V*	0.01	0.01	0.01	0.01	0.00	0.00	0.02	0.00
Cr*	0.02	0.02	0.02	0.02	0.02	0.02	0.02	0.03
MnO	0.27	0.38	0.44	0.26	0.31	0.38	0.36	0.30
FeO	7.71	6.97	20.7	34.5	31.3	29.8	31.1	30.4
Co*	0.00	0.00	0.00	0.01	0.01	0.00	0.00	0.00
Rb*	0.01	0.00	0.00	0.00	0.00	0.00	0.00	0.00
Sr	0.04	0.02	0.04	0.01	0.01	0.01	0.01	0.01
Zr*	0.02	0.00	0.00	0.00	0.00	0.00	0.00	0.00
BaO*	0.17	0.10	0.02	0.02	0.00	0.03	0.04	0.04
Trace elements (parts per million)								
Cu	12	8	599	1402	984	1181	1200	1832
As	48	22	16	11	14	4	13	33
Ag*	0	0	7	0	3	5	4	5
Te	0	0	1	6	9	4	13	31
Bi	7	7	6	14	17	9	39	67
W	5	4	19	22	29	20	18	12
Mo	3	3	26	217	3	1	2	48
Pb	34	34	9	11	9	8	11	11
Zn	96	101	68	91	90	83	89	63
Sb*	11	10	7	13	14	7	4	0
Ni	19	27	34	42	27	25	29	29

Table A4-3 continued. XRF Analysis of pulp samples from the Southwest Zone.

Drill Hole	D06-272	D06-272	D06-272	D06-272	D06-272	D06-272	D06-272	D06-272
Sample	11371	11372	11373	11374	11375	11377	11378	11379
Weight percent oxide								
F**	0.01	0.01	0.01	0.01	0.01	0.01	0.01	0.01
Na_2O	0.22	0.12	0.12	0.13	0.24	0.15	0.13	0.09
MgO	2.99	2.52	2.25	2.86	2.16	3.29	1.99	1.55
Al_2O_3	2.14	2.12	3.16	3.48	3.94	2.32	1.53	0.67
SiO_2	40.7	38.9	37.1	38.0	35.3	32.6	18.7	14.0
P_2O5	0.10	0.13	0.11	0.15	0.12	0.05	0.07	0.04
S	2.89	3.97	3.42	2.13	0.63	3.19	1.21	0.33
Cl*	0.04	0.02	0.01	0.02	0.03	0.03	0.03	0.03
K_2O	0.25	0.03	0.05	0.14	0.74	0.17	0.27	0.08
CaO	21.3	21.3	25.3	27.1	33.9	30.5	22.1	21.1
TiO_2	0.13	0.16	0.14	0.11	0.15	0.11	0.11	0.03
V*	0.00	0.00	0.00	0.00	0.00	0.00	0.00	0.00
Cr*	0.01	0.00	0.00	0.02	0.00	0.02	0.03	0.02
MnO	0.40	0.40	0.39	0.40	0.47	0.44	0.17	0.13
FeO	28.5	29.7	27.6	25.1	22.1	26.7	52.9	61.8
Co*	0.00	0.00	0.02	0.00	0.00	0.02	0.16	0.02
Rb*	0.00	0.00	0.00	0.00	0.00	0.00	0.00	0.00
Sr	0.01	0.01	0.01	0.01	0.03	0.01	0.01	0.01
Zr*	0.00	0.01	0.00	0.00	0.01	0.00	0.00	0.00
BaO*	0.02	0.00	0.00	0.00	0.06	0.03	0.03	0.00
Trace elements (parts per million)								
Cu	2463	2232	1875	2543	979	1579	464	114
As	6	105	15	4	9	377	2960	142
Ag*	5	9	7	9	11	13	8	9
Te	29	14	2	1	9	4	6	2
Bi	50	2541	314	11	80	352	2778	94
W	10	15	18	213	13	123	40	32
Mo	4	2	2	3	0	2	3	1
Pb	8	61	14	8	8	21	23	10
Zn	99	97	65	77	76	73	94	70
Sb*	0	0	7	6	11	13	17	18
Ni	22	38	32	22	14	26	71	45

Table A4-3 continued. XRF Analysis of pulp samples from the Southwest Zone.

Drill Hole	D06-272	D06-272	D06-272	D06-272	D06-273	D06-273	D06-273	D06-273
Sample	11380	11381	11382	11383	11387	11388	11389	11390
Weight percent oxide								
F**	0.01	0.01	0.01	0.01	0.01	0.01	0.01	0.01
Na_2O	0.10	0.10	0.08	0.05	0.17	0.20	0.20	0.12
MgO	2.18	3.60	2.05	0.96	2.29	2.65	2.49	2.24
Al_2O_3	0.50	0.78	0.78	0.25	2.14	3.07	3.21	1.44
SiO_2	19.4	33.3	14.6	1.03	37.7	39.5	39.6	29.1
P_2O5	0.02	0.03	0.02	0.01	0.14	0.14	0.10	0.05
S	0.28	0.14	0.64	0.02	4.49	3.83	1.77	0.75
Cl*	0.02	0.03	0.02	0.00	0.07	0.11	0.08	0.03
K_2O	0.06	0.14	0.11	0.02	0.13	0.21	0.15	0.06
CaO	21.9	31.8	75.0	96.7	20.9	18.1	25.6	43.3
TiO_2	0.02	0.04	0.08	0.00	0.14	0.26	0.13	0.07
V*	0.00	0.00	0.00	0.00	0.01	0.01	0.01	0.00
Cr*	0.01	0.02	0.01	0.00	0.03	0.03	0.01	0.02
MnO	0.16	0.37	0.19	0.06	0.42	0.37	0.41	0.51
FeO	54.8	29.5	6.21	0.75	31.3	31.4	26.1	22.1
Co*	0.00	0.00	0.00	0.00	0.01	0.02	0.01	0.01
Rb*	0.00	0.00	0.00	0.00	0.00	0.00	0.00	0.00
Sr	0.00	0.02	0.08	0.12	0.01	0.01	0.02	0.03
Zr*	0.00	0.00	0.01	0.00	0.00	0.00	0.00	0.00
BaO*	0.00	0.00	0.04	0.00	0.02	0.03	0.02	0.02
Trace elements (parts per million)								
Cu	104	28	139		972	835	283	113
As	342	59	138	25	72	41	59	15
Ag*	11	10	25	29	3	2	11	10
Te	22	9	0	1	2	2	3	13
Bi	4716	224	29	4	15	21	12	139
W	33	14	2	1	18	13	10	4
Mo	2	2	4	2	19	188	2	1
Pb	6	11	7	7	9	12	9	10
Zn	110	77	15	6	89	111	96	86
Sb*	19	9	12	8	13	7	17	0
Ni	53	15	7	5	25	28	18	12

Table A4-3 continued. XRF Analysis of pulp samples from the Southwest Zone.

Drill Hole	D06-273	D06-273	D06-273	D06-273	D06-273	D06-273	D06-273	D06-273
Sample	11391	11392	11393	11394	11396	11397	11398	1399
Weight percent oxide								
F**	0.15	0.01	0.01	0.01	0.01	0.21	0.01	0.32
Na_2O	0.10	0.02	0.12	0.11	0.10	0.12	0.17	0.12
MgO	3.51	2.10	3.38	4.04	2.83	4.58	3.94	2.83
Al_2O_3	1.31	3.07	1.77	0.67	0.64	0.75	1.04	1.02
SiO_2	25.6	18.9	39.8	23.2	19.3	30.4	31.5	29.2
P_2O5	0.01	0.01	0.10	0.02	0.03	0.04	0.05	0.04
S	4.01	2.08	1.40	0.20	0.79	0.36	2.96	2.29
Cl*	0.00	0.00	0.01	0.01	0.01	0.01	0.01	0.01
K_2O	0.07	0.04	0.06	0.03	0.03	0.04	0.04	0.04
CaO	19.7	46.7	23.1	13.2	14.9	16.3	13.6	12.0
TiO_2	0.01	0.03	0.06	0.01	0.00	0.01	0.02	0.02
V*	0.00	0.00	0.00	0.00	0.00	0.00	0.00	0.00
Cr*	0.04	0.02	0.01	0.00	0.03	0.00	0.00	0.00
MnO	0.19	0.37	0.48	0.14	0.12	0.20	0.22	0.19
FeO	44.7	26.2	29.6	57.7	59.2	45.7	43.9	50.9
Co*	0.01	0.01	0.01	0.00	0.01	0.01	0.00	0.00
Rb*	0.00	0.00	0.00	0.00	0.00	0.00	0.00	0.00
Sr	0.01	0.07	0.01	0.00	0.01	0.01	0.00	0.00
Zr*	0.00	0.00	0.00	0.00	0.00	0.00	0.00	0.00
BaO*	0.02	0.03	0.02	0.01	0.00	0.02	0.02	0.01
Trace elements (parts per million)								
Cu	789	252	286	35	131	65	231	237
As	226	55	23	280	865	461	1019	409
Ag*	6	18	4	2	28	10	16	6
Te	19	12	21	9	18	10	21	24
Bi	3465	1167	227	6377	18966	10598	20309	9551
W	29	10	8	34	59	32	45	46
Mo	5	7	1	1	2	2	5	5
Pb	38	22	9	21	47	53	285	86
Zn	125	59	117	162	251	193	264	186
Sb*	3	17	0	0	0	0	0	0
Ni	36	15	20	36	55	48	61	60

Table A4-3 continued. XRF Analysis of pulp samples from the Southwest Zone.

Drill Hole	D06-273	D06-273	D06-273	D06-273	D06-276	D06-276	D06-276	D06-276
Sample	11400	11401	11402	11403	11430	11431	11432	11433
Weight percent oxide								
F**	0.01	0.01	0.01	0.01	0.01	0.01	0.01	0.01
Na_2O	6.21	1.74	3.07	0.06	1.39	0.19	0.12	0.14
MgO	2.70	3.70	2.84	1.58	8.18	5.81	2.94	2.88
Al_2O_3	15.9	11.3	13.7	0.82	17.2	17.3	6.98	4.26
SiO_2	55.0	43.7	51.6	8.22	46.9	36.9	30.9	29.4
P_2O5	0.29	0.24	0.27	0.02	0.22	0.33	0.11	0.11
S	0.03	0.26	0.04	0.04	0.01	0.47	2.92	4.19
Cl*	0.01	0.02	0.01	0.00	0.04	0.02	0.03	0.05
K_2O	2.00	0.87	2.79	0.08	1.54	1.91	0.92	1.35
CaO	8.38	18.3	17.5	83.7	11.8	15.9	29.2	30.3
TiO_2	0.48	0.45	0.55	0.03	0.74	0.84	0.42	0.36
V*	0.01	0.01	0.00	0.00	0.03	0.03	0.02	0.02
Cr*	0.01	0.01	0.01	0.01	0.02	0.06	0.02	0.02
MnO	0.11	0.24	0.13	0.13	0.16	0.24	0.34	0.32
FeO	8.57	19.00	7.00	5.17	11.6	19.8	24.8	26.3
Co*	0.01	0.00	0.00	0.00	0.01	0.01	0.01	0.01
Rb*	0.01	0.01	0.01	0.00	0.01	0.01	0.01	0.01
Sr	0.04	0.04	0.06	0.06	0.04	0.03	0.05	0.05
Zr*	0.01	0.01	0.01	0.00	0.01	0.01	0.01	0.00
BaO*	0.17	0.09	0.28	0.04	0.07	0.12	0.03	0.05
Trace elements (parts per million)								
Cu	0	43	3	12	119	211	715	1146
As	14	40	7	40	34	20	3	7
Ag*	4	5	8	29	6	8	11	9
Te	1	3	1	2	2	0	2	10
Bi	90	522	156	212	5	6	8	25
W	4	10	4	1	7	11	3	11
Mo	4	11	5	3	4	220	343	103
Pb	7	6	7	11	6	7	8	9
Zn	53	92	50	16	84	139	97	81
Sb*	12	21	1	11	1	5	0	6
Ni	9	13	5	2	29	28	24	26

Table A4- 3 continued. XRF Analysis of pulp samples from the Southwest Zone.

Drill Hole	D06-276	D06-276	D06-276	D06-276	D06-276	D06-276	D06-276	D06-276
Sample	11434	11435	11436	11437	11438	11439	11441	11442
Weight percent oxide								
F**	0.19	0.01	0.01	0.01	0.05	0.01	0.01	0.01
Na_2O	0.15	0.19	0.22	0.18	0.09	0.19	0.16	0.13
MgO	3.32	3.51	3.43	4.01	4.28	3.53	3.12	3.55
Al_2O_3	4.38	3.32	4.57	3.99	3.46	9.68	9.32	8.91
SiO_2	28.7	31.3	34.8	36.3	27.0	34.9	35.9	34.2
P_2O5	0.14	0.16	0.08	0.05	0.13	0.14	0.15	0.16
S	4.07	2.94	1.17	2.16	2.51	1.17	1.70	2.69
Cl*	0.03	0.04	0.03	0.03	0.02	0.05	0.13	0.06
K_2O	1.19	0.48	0.48	0.66	0.66	2.37	3.38	3.58
CaO	32.7	34.9	36.9	31.9	41.7	23.7	19.3	20.5
TiO_2	0.28	0.24	0.21	0.15	0.52	0.63	0.57	0.43
V*	0.01	0.01	0.02	0.01	0.02	0.01	0.02	0.02
Cr*	0.01	0.01	0.00	0.02	0.00	0.01	0.01	0.02
MnO	0.21	0.26	0.35	0.31	0.34	0.30	0.29	0.30
FeO	24.3	22.4	17.5	19.9	18.9	23.0	25.8	25.2
Co*	0.00	0.01	0.00	0.01	0.01	0.01	0.01	0.01
Rb*	0.01	0.00	0.00	0.01	0.01	0.02	0.02	0.03
Sr	0.03	0.03	0.04	0.03	0.03	0.03	0.03	0.02
Zr*	0.00	0.00	0.00	0.00	0.01	0.01	0.01	0.00
BaO*	0.06	0.00	0.03	0.02	0.03	0.11	0.09	0.09
Trace elements (parts per million)								
Cu	1551	1138	589	1565	659	410	819	799
As	12	13	15	14	10	9	7	10
Ag*	11	10	13	10	10	7	9	7
Te	13	3	26	18	19	5	2	3
Bi	46	26	69	50	61	15	5	9
W	22	10	7	8	9	9	8	16
Mo	183	278	49	182	326	50	1	5
Pb	16	18	14	11	10	7	8	11
Zn	67	74	69	84	56	103	112	104
Sb*	15	11	4	12	4	9	3	8
Ni	23	18	17	17	22	11	21	30

Table A4-3 continued. XRF Analysis of pulp samples from the Southwest Zone.

Drill Hole	D06-276	D06-276	D06-276	D06-276	D06-276	D06-276	D06-289	D06-289
Sample	11443	11444	11445	11446	11447	11448	11617	11618
Weight percent oxide								
F**	0.01	0.01	0.01	0.01	0.01	0.01	0.01	0.01
Na_2O	0.10	0.21	0.11	0.06	0.16	0.05	0.84	0.04
MgO	1.71	2.79	2.86	2.23	2.53	0.83	7.14	3.69
Al_2O_3	11.1	6.18	9.26	9.45	6.23	2.12	16.7	6.07
SiO_2	37.8	34.9	33.1	33.3	37.5	8.04	48.0	37.2
P_2O5	0.36	0.20	0.15	0.16	0.18	0.03	0.30	0.16
S	2.16	3.09	2.59	1.74	3.41	0.08	0.11	2.81
Cl*	0.05	0.12	0.04	0.03	0.05	0.02	0.01	0.02
K_2O	1.17	1.18	2.01	1.13	1.20	0.41	2.75	0.06
CaO	24.6	23.6	18.8	20.9	16.2	85.8	11.1	23.5
TiO_2	0.84	0.52	0.61	0.72	0.54	0.18	0.73	0.30
V*	0.03	0.02	0.01	0.01	0.02	0.01	0.04	0.00
Cr*	0.03	0.02	0.01	0.01	0.01	0.01	0.02	0.02
MnO	0.34	0.38	0.28	0.30	0.30	0.12	0.15	0.30
FeO	19.3	26.6	30.0	29.8	31.5	2.17	11.8	25.6
Co*	0.01	0.01	0.01	0.01	0.00	0.00	0.00	0.00
Rb*	0.01	0.01	0.02	0.01	0.01	0.00	0.01	0.00
Sr	0.08	0.02	0.02	0.01	0.01	0.08	0.03	0.04
Zr*	0.02	0.01	0.01	0.01	0.01	0.00	0.01	0.01
BaO*	0.04	0.03	0.05	0.05	0.04	0.05	0.17	0.02
Trace elements (parts per million)								
Cu	2234	1071	590	392	791	12	285	399
As	13	10	7	8	15	31	97	7
Ag*	13	7	3	8	4	33	7	12
Te	2	6	9	33	17	1	3	3
Bi	8	22	28	46	33	5	21	8
W	11	9	7	67	12	1	10	8
Mo	5	2	2	3	1	2	7	140
Pb	19	11	8	9	16	8	13	8
Zn	72	82	117	118	125	13	65	71
Sb*	39	0	2	8	16	7	12	14
Ni	30	34	22	19	27	5	33	14

Table A4-3 continued. XRF Analysis of pulp samples from the Southwest Zone.

Drill Hole	D06-289	D06-289	D06-289	D06-289	D06-289	D06-289	D06-292	D06-292
Sample	11619	11620	11622	11623	11624	11625	11650	11651
Weight percent oxide								
F**	0.01	0.01	0.01	0.01	0.01	0.01	0.01	0.01
Na_2O	0.13	0.13	0.14	1.14	0.09	0.08	0.24	0.10
MgO	3.50	3.04	2.75	3.16	1.31	1.11	4.44	4.38
Al_2O_3	16.7	0.99	1.02	4.62	1.24	1.08	3.64	1.96
SiO_2	40.5	29.0	25.9	27.6	17.8	27.4	40.4	29.9
P_2O5	0.06	0.02	0.01	0.11	0.04	0.03	0.10	0.04
S	1.81	0.59	0.40	2.78	0.55	0.53	2.52	2.57
Cl*	0.03	0.04	0.02	0.02	0.03	0.02	0.00	0.00
K_2O	0.11	0.08	0.09	0.49	0.12	0.06	0.29	0.21
CaO	23.6	25.4	21.8	22.4	66.5	50.9	22.8	35.8
TiO_2	0.05	0.02	0.02	0.15	0.12	0.11	0.13	0.04
V*	0.00	0.00	0.00	0.00	0.00	0.00	0.01	0.01
Cr*	0.01	0.00	0.02	0.03	0.02	0.02	0.01	0.02
MnO	0.33	0.29	0.21	0.19	0.24	0.31	0.40	0.31
FeO	28.3	40.1	47.1	36.6	11.8	18.3	24.8	24.2
Co*	0.00	0.00	0.00	0.01	0.00	0.00	0.01	0.00
Rb*	0.00	0.00	0.00	0.00	0.00	0.00	0.00	0.00
Sr	0.01	0.01	0.01	0.02	0.04	0.03	0.02	0.04
Zr*	0.00	0.00	0.00	0.00	0.00	0.00	0.00	0.00
BaO*	0.03	0.03	0.03	0.04	0.02	0.00	0.05	0.04
Trace elements (parts per million)								
Cu	372	127	120	605	102	86	1372	2155
As	37	292	183	251	46	118	7	9
Ag*	7	6	9	10	22	15	7	11
Te	36	38	59	70	1	2	2	2
Bi	428	1148	4130	5042	17	12	6	6
W	19	19	34	35	7	10	13	10
Mo	25	2	2	3	4	6	100	21
Pb	18	31	42	68	5	7	14	7
Zn	82	95	118	112	26	36	241	185
Sb*	5	15	32	74	2	11	10	9
Ni	20	26	32	47	9	15	36	26

Table A4-3 continued. XRF Analysis of pulp samples from the Southwest Zone.

Drill Hole	D06-292	D06-292	D06-292	D06-292	D06-292	D06-292	D06-29	D06-292
Sample	11652	11653	11654	11656	11657	11659	11660	11661
Weight percent oxide								
F**	0.08	0.01	0.01	0.01	0.01	0.01	0.01	0.01
Na_2O	0.16	0.24	0.03	0.08	0.10	0.04	0.17	0.30
MgO	6.99	5.38	0.25	3.31	4.18	0.95	1.35	0.81
Al_2O_3	1.97	2.40	0.13	0.63	0.48	0.98	2.62	1.80
SiO_2	32.8	34.9	93.9	33.8	41.1	11.6	6.88	4.75
P_2O5	0.02	0.04	0.01	0.02	0.02	0.07	0.03	0.02
S	2.17	2.44	0.26	3.39	2.59	0.56	0.06	0.15
Cl*	0.01	0.03	0.02	0.01	0.02	0.02	0.00	0.00
K_2O	0.35	0.71	0.01	0.09	0.06	0.04	0.45	0.27
CaO	36.2	33.0	4.19	38.4	28.0	72.2	85.5	89.5
TiO_2	0.03	0.10	0.00	0.00	0.00	0.09	0.24	0.12
V*	0.00	0.01	0.00	0.00	0.00	0.00	0.00	0.01
Cr*	0.02	0.01	0.02	0.02	0.01	0.02	0.02	0.01
MnO	0.32	0.25	0.02	0.34	0.38	0.35	0.12	0.08
FeO	18.8	20.2	1.13	19.8	22.9	13.0	2.35	1.94
Co*	0.02	0.01	0.00	0.00	0.01	0.01	0.00	0.00
Rb*	0.01	0.01	0.00	0.00	0.00	0.00	0.01	0.00
Sr	0.00	0.05	0.00	0.04	0.02	0.05	0.10	0.10
Zr*	0.00	0.01	0.00	0.00	0.00	0.00	0.00	0.00
BaO*	0.00	0.06	0.00	0.02	0.00	0.00	0.08	0.05
Trace elements (parts per million)								
Cu	337	512	28	743	608	120	5	19
As	9	4	1	7	8	12	27	8
Ag*	12	12	1	12	6	21	24	25
Te	0	1	0	2	2	2	1	0
Bi	7	6	5	11	13	4	4	4
W	5	7	0	6	9	3	2	2
Mo	12	3	8	2	2	3	4	5
Pb	8	7	7	6	5	5	6	6
Zn	52	61	1	47	89	27	15	25
Sb*	5	8	0	5	10	8	6	1
Ni	10	16	0	17	19	11	4	5

Table A4-3 continued. XRF Analysis of pulp samples from the Southwest Zone.

Drill Hole	D06-292	D06-292	D06-292	D07-322	D07-322	D07-322	D07-322	D07-322
Sample	11662	11663	11664	BX 01401	BX 01403	BX 01404	BX 01405	BX 01406
Weight percent oxide								
F**	0.01	0.01	0.01	0.01	0.01	0.21	0.01	0.01
Na_2O	0.06	0.04	0.06	1.65	0.18	0.16	0.11	0.10
MgO	0.84	0.64	1.08	4.89	7.23	2.82	3.13	4.70
Al_2O_3	0.80	0.61	0.34	11.2	1.53	2.52	2.01	0.80
SiO_2	5.30	5.16	5.83	36.9	43.0	39.2	39.2	35.1
P_2O5	0.04	0.02	0.01	0.24	0.07	0.15	0.14	0.08
S	0.19	0.65	0.82	4.40	0.57	3.17	3.22	2.11
Cl*	0.02	0.02	0.00	0.02	0.01	0.01	0.01	0.00
K_2O	0.10	0.02	0.01	1.45	0.13	0.04	0.03	0.02
CaO	85.9	82.9	81.9	16.0	26.1	23.1	23.7	23.9
TiO_2	0.12	0.09	0.05	0.53	0.08	0.15	0.11	0.05
V*	0.01	0.00	0.00	0.01	0.00	0.01	0.00	0.00
Cr*	0.02	0.02	0.02	0.01	0.01	0.03	0.02	0.00
MnO	0.21	0.19	0.19	0.34	0.38	0.38	0.40	0.31
FeO	6.25	9.52	9.47	22.0	20.6	27.8	27.6	32.7
Co*	0.00	0.00	0.01	0.01	0.01	0.01	0.00	0.00
Rb*	0.00	0.00	0.00	0.01	0.00	0.00	0.00	0.00
Sr	0.07	0.06	0.08	0.03	0.01	0.01	0.00	0.01
Zr*	0.00	0.00	0.00	0.01	0.00	0.00	0.00	0.00
BaO*	0.03	0.03	0.00	0.08	0.03	0.00	0.02	0.02
Trace elements (parts per million)								
Cu	35	206	172	1667	519	2056	1817	843
As	5	8	8	20	15	12	9	28
Ag*	26	25	24	5	7	2	5	0
Te	0	1	0	3	4	3	2	7
Bi	5	4	4	18	123	20	27	218
W	5	4	7	13	11	13	11	12
Mo	4	6	14	123	3	6	2	3
Pb	4	6	5	12	6	9	7	12
Zn	17	18	20	82	99	106	88	93
Sb*	12	8	14	7	0	15	6	0
Ni	9	7	19	277	20	43	38	27

Table A4-3 continued. XRF Analysis of pulp samples from the Southwest Zone.

Drill Hole	D06-292	D06-292	D06-292	D06-292	D06-292	D06-292	D06-29	D06-292
Sample	11652	11653	11654	11656	11657	11659	11660	11661
Weight percent oxide								
F**	0.08	0.01	0.01	0.01	0.01	0.01	0.01	0.01
Na_2O	0.17	0.24	0.03	0.08	0.10	0.04	0.17	0.30
MgO	6.99	5.38	0.25	3.31	4.18	0.95	1.35	0.81
Al_2O_3	1.97	2.40	0.13	0.63	0.48	0.98	2.62	1.80
SiO_2	32.8	34.9	93.9	33.8	41.1	11.6	6.88	4.75
P_2O5	0.02	0.04	0.00	0.02	0.02	0.07	0.03	0.02
S	2.17	2.44	0.26	3.39	2.59	0.56	0.06	0.15
Cl*	0.01	0.03	0.02	0.01	0.02	0.02	0.00	0.00
K_2O	0.36	0.71	0.01	0.09	0.06	0.04	0.45	0.27
CaO	36.2	33.0	4.19	38.4	28.0	72.2	85.5	89.5
TiO_2	0.03	0.10	0.00	0.00	0.00	0.09	0.24	0.12
V*	0.00	0.01	0.00	0.00	0.00	0.00	0.00	0.01
Cr*	0.02	0.01	0.03	0.02	0.01	0.02	0.02	0.01
MnO	0.32	0.25	0.02	0.34	0.38	0.35	0.12	0.08
FeO	18.8	20.2	1.13	19.8	22.9	13.0	2.35	1.94
Co*	0.01	0.01	0.00	0.00	0.01	0.01	0.00	0.00
Rb*	0.00	0.01	0.00	0.00	0.00	0.00	0.01	0.00
Sr	0.00	0.05	0.00	0.04	0.02	0.05	0.10	0.11
Zr*	0.00	0.01	0.00	0.00	0.00	0.00	0.00	0.00
BaO*	0.00	0.06	0.00	0.02	0.00	0.00	0.08	0.05
Trace elements (parts per million)								
Cu	337	512	28	743	608	120	5	19
As	9	4	1	7	8	12	27	8
Ag*	12	12	1	12	6	21	24	25
Te	0	1	0	2	2	2	1	0
Bi	7	6	5	11	13	4	4	4
W	5	7	0	6	9	3	2	2
Mo	12	3	8	2	2	3	4	5
Pb	8	7	7	6	5	5	6	6
Zn	52	61	1	47	89	27	15	25
Sb*	5	8	0	5	10	8	6	1
Ni	10	16	0	17	19	11	4	5

Table A4-3 continued. XRF Analysis of pulp samples from the Southwest Zone.

Drill Hole	D07-322	D07-322	D07-322	D07-322	D07-322	D07-323	D07-323	D07-323
Sample	BX 01407	BX 01408	BX 01409	BX 01410	BX 01412	BX 01436	BX 01437	BX 01438
Weight percent oxide								
F**	0.01	0.01	0.21	0.01	0.01	0.01	0.01	0.08
Na_2O	0.16	0.13	0.11	0.09	0.19	0.12	0.22	0.10
MgO	3.51	2.55	2.56	2.01	4.20	1.76	2.36	1.80
Al_2O_3	0.51	0.57	0.56	0.58	1.24	10.70	3.72	4.29
SiO_2	30.3	14.8	18.5	21.7	40.4	38.9	38.5	38.9
P_2O5	0.03	0.02	0.03	0.03	0.03	0.16	0.11	0.08
S	0.48	1.18	1.51	1.71	1.11	1.73	1.76	0.92
Cl*	0.01	0.02	0.02	0.02	0.06	0.04	0.08	0.01
K_2O	0.02	0.06	0.07	0.07	0.18	0.87	0.24	0.04
CaO	19.1	13.5	9.73	14.0	27.8	22.0	25.9	30.4
TiO_2	0.03	0.02	0.00	0.01	0.04	0.41	0.27	0.22
V*	0.00	0.00	0.00	0.00	0.00	0.01	0.01	0.01
Cr*	0.03	0.03	0.00	0.00	0.01	0.02	0.02	0.01
MnO	0.18	0.14	0.10	0.09	0.40	0.01	0.38	0.48
FeO	45.5	65.4	65.4	58.8	24.2	22.9	26.2	22.5
Co*	0.01	0.20	0.09	0.06	0.00	0.01	0.00	0.01
Rb*	0.00	0.00	0.00	0.00	0.00	0.00	0.00	0.00
Sr	0.01	0.01	0.00	0.01	0.01	0.05	0.01	0.00
Zr*	0.00	0.00	0.00	0.00	0.00	0.01	0.00	0.00
BaO*	0.03	0.01	0.00	0.02	0.03	0.07	0.02	0.02
Trace elements (parts per million)								
Cu	343	345	516	500	229	1024	1553	757
As	205	5312	3050	1261	27	16	17	11
Ag*	0	2	0	5	11	7	11	11
Te	8	27	38	29	5	2	3	4
Bi	432	9464	8381	6632	288	10	11	13
W	25	46	37	37	16	13	14	14
Mo	3	2	2	3	1	12	7	3
Pb	8	0	0	0	11	42	18	11
Zn	80	159	158	129	71	135	181	108
Sb*	8	0	0	13	19	17	12	1
Ni	20	85	77	72	16	29	28	18

Table A4-3 continued. XRF Analysis of pulp samples from the Southwest Zone.

Drill Hole	D07-323	D07-323	D07-323	D07-323	D07-323	D07-323	D07-323	D07-323
Sample	BX 01439	BX 01440	BX 01443	BX 01445	BX 01446	BX 01448	BX 01449	BX 01450
Weight percent oxide								
F**	0.12	0.01	0.01	0.01	0.01	0.01	0.01	0.01
Na_2O	0.19	0.13	0.12	0.07	0.14	0.11	0.13	0.12
MgO	2.56	3.11	2.31	1.35	2.92	4.83	4.66	2.88
Al_2O_3	3.78	1.57	3.11	5.95	1.37	0.31	0.39	0.62
SiO_2	41.8	41.4	40.0	32.9	32.6	36.1	32.2	22.7
P_2O5	0.12	0.09	0.13	0.04	0.09	0.03	0.02	0.02
S	1.29	0.97	2.93	0.65	3.65	1.10	0.80	1.21
Cl*	0.05	0.02	0.01	0.01	0.01	0.01	0.01	0.01
K_2O	0.17	0.06	0.03	0.04	0.02	0.00	0.02	0.05
CaO	23.3	26.8	23.4	36.9	25.3	21.7	18.5	16.6
TiO_2	0.22	0.15	0.14	0.12	0.12	0.00	0.03	0.02
V*	0.01	0.00	0.00	0.02	0.01	0.00	0.00	0.00
Cr*	0.01	0.00	0.00	0.02	0.02	0.01	0.01	0.02
MnO	0.35	0.38	0.39	0.51	0.32	0.26	0.21	0.15
FeO	25.9	25.0	27.1	21.3	32.8	35.4	42.9	54.9
Co*	0.01	0.01	0.00	0.01	0.00	0.00	0.01	0.15
Rb*	0.00	0.00	0.00	0.00	0.00	0.00	0.00	0.00
Sr	0.01	0.01	0.00	0.01	0.01	0.01	0.01	0.00
Zr*	0.00	0.00	0.00	0.00	0.01	0.00	0.00	0.00
BaO*	0.02	0.02	0.02	0.02	0.01	0.02	0.02	0.02
Trace elements (parts per million)								
Cu	744	1268	2329	479	1076	1066	739	358
As	17	8	16	8	177	56	400	3051
Ag*	5	10	6	9	15	8	0	0
Te	25	15	9	0	8	2	2	5
Bi	110	47	110	83	4028	280	368	2550
W	13	6	11	7	25	11	17	37
Mo	6	4	6	3	5	4	2	2
Pb	12	15	7	5	107	9	6	2
Zn	149	173	156	65	123	88	84	101
Sb*	0	3	9	7	5	7	4	0
Ni	29	24	35	21	39	34	31	56

Table A4-3 continued. XRF Analysis of pulp samples from the Southwest Zone.

Drill Hole	D07-323	D07-323	D07-323	D07-323	D07-323	D07-323	D07-325	D07-325
Sample	BX 01451	BX 01452	BX 01454	BX 01456	BX 01459	BX 10455	BX 01484	BX 01489
Weight percent oxide								
F**	0.01	0.01	0.01	0.01	0.01	0.01	0.01	0.01
Na_2O	0.09	0.13	0.13	0.18	0.04	0.18	0.07	1.36
MgO	1.55	2.37	1.50	3.48	10.7	4.10	14.7	4.71
Al_2O_3	0.47	0.49	0.73	0.92	1.46	1.08	5.89	16.3
SiO_2	14.9	18.3	13.8	31.2	7.11	39.2	24.6	47.3
P_2O5	0.05	0.06	0.03	0.02	0.02	0.01	0.03	0.41
S	1.20	1.05	1.72	0.59	0.13	0.50	0.08	0.45
Cl*	0.01	0.02	0.04	0.04	0.02	0.06	0.00	0.00
K_2O	0.04	0.05	0.08	0.16	0.12	0.16	0.03	2.08
CaO	11.6	12.3	14.1	25.8	76.4	21.6	50.0	15.9
TiO_2	0.03	0.03	0.02	0.02	0.08	0.00	0.27	0.69
V*	0.00	0.00	0.00	0.00	0.00	0.00	0.00	0.03
Cr*	0.00	0.02	0.00	0.02	0.02	0.02	0.02	0.02
MnO	0.08	0.10	0.10	0.22	0.12	0.26	0.12	0.23
FeO	68.5	64.3	66.9	36.9	3.63	32.4	4.09	10.2
Co*	0.26	0.06	0.01	0.01	0.00	0.04	0.00	0.00
Rb*	0.00	0.00	0.00	0.00	0.00	0.00	0.00	0.01
Sr	0.00	0.00	0.01	0.01	0.07	0.00	0.04	0.03
Zr*	0.00	0.00	0.00	0.00	0.01	0.00	0.01	0.01
BaO*	0.02	0.01	0.01	0.02	0.04	0.03	0.00	0.16
Trace elements (parts per million)								
Cu	438	410	822	234	1	161	0	464
As	4459	1849	1071	163	4	344	20	13
Ag*	0	0	1	9	25	8	20	7
Te	22	19	28	22	0	12	1	0
Bi	6561	5534	8140	3345	19	2670	16	4
W	39	39	33	23	1	22	2	11
Mo	4	4	3	2	3	5	3	3
Pb	0	0	0	30	4	5	5	15
Zn	131	125	140	98	13	95	33	100
Sb*	0	1	26	15	7	19	8	11
Ni	94	76	51	25	6	26	12	38

Table A4-3 continued. XRF Analysis of pulp samples from the Southwest Zone.

Drill Hole	D07-325	D07-325	D07-325	D07-325	D07-325	D07-325	D07-325	D07-325
Sample	BX 01491	BX 01492	BX 01493	BX 01494	BX 01495	BX 01496	BX 01498	BX 01500
Weight percent oxide								
F**	0.01	0.01	0.01	0.01	0.01	0.01	0.01	0.01
Na_2O	0.18	0.10	0.06	0.07	0.14	0.12	0.06	0.09
MgO	3.29	4.55	10.6	13.7	10.0	6.80	5.98	3.87
Al_2O_3	4.26	1.21	0.55	0.55	0.84	0.77	0.36	0.59
SiO_2	35.5	38.6	62.4	58.5	46.8	42.8	35.8	28.5
P_2O5	0.14	0.08	0.01	0.01	0.03	0.03	0.03	0.04
S	1.85	3.31	0.06	0.02	0.15	1.58	1.98	0.99
Cl*	0.02	0.01	0.01	0.01	0.01	0.01	0.02	0.02
K_2O	0.87	0.04	0.08	0.02	0.05	0.04	0.02	0.07
CaO	30.7	23.0	11.9	16.4	25.5	24.6	27.1	24.3
TiO_2	0.21	0.06	0.02	0.02	0.12	0.14	0.03	0.02
V*	0.00	0.00	0.00	0.00	0.00	0.00	0.00	0.00
Cr*	0.03	0.02	0.01	0.01	0.02	0.02	0.00	0.02
MnO	0.29	0.31	0.24	0.22	0.28	0.29	0.30	0.22
FeO	22.1	28.6	14.1	10.4	16.0	22.7	28.1	41.1
Co*	0.02	0.01	0.00	0.00	0.01	0.01	0.01	0.00
Rb*	0.00	0.00	0.00	0.00	0.00	0.00	0.00	0.00
Sr	0.02	0.00	0.00	0.00	0.00	0.00	0.01	0.01
Zr*	0.01	0.00	0.00	0.00	0.00	0.00	0.00	0.00
BaO*	0.09	0.00	0.00	0.00	0.00	0.00	0.00	0.00
Trace elements (parts per million)								
Cu	3449	1197	25	3	35	524	1319	259
As	43	11	0	7	8	15	15	91
Ag*	18	4	4	5	5	6	7	7
Te	31	16	0	2	2	2	1	12
Bi	95	128	16	19	14	120	209	640
W	6	16	5	4	11	12	83	16
Mo	32	11	2	2	1	2	1	3
Pb	20	11	4	5	4	10	8	19
Zn	109	90	70	64	61	79	68	110
Sb*	12	11	8	12	13	18	13	13
Ni	27	33	7	7	13	20	22	36

Table A4-3 continued. XRF Analysis of pulp samples from the Southwest Zone.

Drill Hole	D07-325	D07-325	D07-326	D07-326	D07-326	D07-326	D07-326	D07-326
Sample	BX 01502	BX 01504	BX 01521	BX 01522	BX 01523	BX 01524	BX 01525	BX 01526
Weight percent oxide								
F**	0.01	0.01	0.01	0.01	0.01	0.01	0.01	0.01
Na_2O	0.04	0.05	0.06	0.06	0.12	1.40	0.17	0.39
MgO	5.83	1.13	0.64	1.50	1.34	1.51	2.13	2.40
Al_2O_3	0.57	0.25	2.59	8.42	7.56	9.87	6.03	5.71
SiO_2	6.71	1.12	8.67	39.1	36.5	36.1	36.5	31.8
P_2O5	0.02	0.01	0.02	0.15	0.15	0.16	0.15	0.10
S	0.49	0.01	14.00	1.40	1.00	1.63	3.26	2.15
Cl*	0.02	0.04	0.02	0.01	0.04	0.02	0.02	0.09
K_2O	0.10	0.04	0.48	0.17	0.49	2.17	0.74	0.83
CaO	78.9	96.2	27.4	30.1	31.3	26.7	24.4	31.0
TiO_2	0.04	0.02	0.08	0.51	0.60	0.67	0.36	0.14
V*	0.00	0.00	0.00	0.00	0.02	0.00	0.02	0.00
Cr*	0.02	0.04	0.05	0.03	0.02	0.00	0.02	0.02
MnO	0.22	0.08	0.23	0.35	0.33	0.26	0.33	0.44
FeO	6.70	0.90	44.8	17.9	20.4	19.3	25.4	24.5
Co*	0.00	0.00	0.05	0.00	0.00	0.00	0.00	0.01
Rb*	0.00	0.00	0.00	0.00	0.00	0.01	0.00	0.01
Sr	0.09	0.15	0.04	0.07	0.04	0.03	0.03	0.02
Zr*	0.00	0.00	0.00	0.01	0.01	0.00	0.01	0.00
BaO*	0.00	0.00	0.03	0.03	0.05	0.13	0.06	0.07
Trace elements (parts per million)								
Cu	147	0	2850	800	692	595	2779	2090
As	71	0	5975	46	10	9	8	14
Ag*	31	30	0	9	9	11	10	8
Te	3	0	2	0	1	0	21	10
Bi	520	4	34	7	7	5	44	33
W	4	2	45	15	10	12	13	147
Mo	2	1	4	4	3	30	150	4
Pb	9	6	21	13	22	17	14	11
Zn	18	5	25	61	75	72	127	62
Sb*	15	12	0	14	8	5	0	0
Ni	8	7	1729	130	47	30	28	24

Table A4-3 continued. XRF Analysis of pulp samples from the Southwest Zone.

Drill Hole	D07-326	D07-326	D07-356	D07-356	D07-356	D07-356	D07-356	D07-356
Sample	BX 01527	BX 01528	BX 02429	BX 02430	BX 02431	BX 02432	BX 02433	BX 02434
Weight percent oxide								
F**	0.01	0.01	0.01	0.01	0.01	0.01	0.01	0.13
Na_2O	0.11	0.07	5.25	2.84	0.62	0.26	0.34	0.26
MgO	4.10	3.75	5.85	6.16	5.18	4.08	5.33	2.43
Al_2O_3	1.00	0.78	16.6	16.8	11.8	8.02	13.2	9.37
SiO_2	23.7	3.73	53.9	50.7	44.1	23.1	36.5	27.0
P_2O5	0.03	0.01	0.42	0.42	0.24	0.10	0.14	0.16
S	2.84	0.08	0.02	0.12	1.12	1.03	0.30	1.56
Cl*	0.02	0.02	0.01	0.02	0.01	0.01	0.01	0.04
K_2O	0.10	0.09	1.19	1.94	1.25	0.69	2.04	1.96
CaO	22.4	89.8	8.73	11.1	18.1	41.5	27.5	40.6
TiO_2	0.05	0.05	0.65	0.68	0.64	0.51	0.74	0.74
V*	0.00	0.00	0.03	0.03	0.02	0.02	0.02	0.03
Cr*	0.04	0.01	0.04	0.03	0.02	0.02	0.01	0.03
MnO	0.19	0.07	0.09	0.16	0.41	0.58	0.41	0.54
FeO	44.3	1.36	7.11	8.77	16.2	19.8	13.0	14.7
Co*	0.26	0.00	0.00	0.00	0.01	0.01	0.01	0.01
Rb*	0.00	0.00	0.01	0.01	0.00	0.00	0.01	0.01
Sr	0.02	0.12	0.06	0.04	0.04	0.06	0.04	0.05
Zr*	0.00	0.00	0.01	0.01	0.01	0.01	0.01	0.01
BaO*	0.03	0.03	0.04	0.09	0.11	0.07	0.26	0.16
Trace elements (parts per million)								
Cu	1280	15	89	300	466	462	281	371
As	4259	10	6	14	26	178	62	1380
Ag*	3	28	3	5	6	10	10	10
Te	8	2	1	1	1	1	0	1
Bi	1523	7	5	5	7	10	7	6
W	26	0	6	6	13	9	7	8
Mo	2	2	1	2	5	1	1	5
Pb	13	6	9	14	17	8	14	12
Zn	92	13	58	60	92	54	43	30
Sb*	11	9	5	5	8	0	11	8
Ni	70	5	58	47	155	97	63	96

Table A4-3 continued. XRF Analysis of pulp samples from the Southwest Zone.

Drill Hole	D07-357	D07-357	D07-357	D07-357	D07-357	D07-357	D07-357	D07-357
Sample	BX 02546	BX 02557	BX 02582	BX 02539	BX 02540	BX 02541	BX 02543	BX 02544
Weight percent oxide								
F**	0.01	0.01	0.01	0.01	0.01	0.01	0.01	0.01
Na_2O	0.10	0.13	0.05	2.13	2.45	1.84	0.15	0.21
MgO	2.18	4.72	8.45	6.52	6.79	4.89	2.67	2.41
Al_2O_3	4.91	0.64	2.74	16.4	14.5	14.2	5.31	5.82
SiO_2	26.2	25.4	13.2	49.4	49.8	42.3	38.2	37.3
P_2O5	0.10	0.02	0.02	0.39	0.57	0.32	0.13	0.13
S	2.78	0.16	0.02	0.14	0.48	0.76	2.22	1.15
Cl*	0.05	0.01	0.00	0.01	0.00	0.01	0.04	0.06
K_2O	1.30	0.03	0.14	1.63	1.05	1.85	1.29	2.02
CaO	40.0	17.2	73.4	16.5	15.5	22.5	25.0	29.0
TiO_2	0.31	0.02	0.13	0.68	0.71	0.68	0.25	0.36
V*	0.00	0.00	0.01	0.03	0.03	0.00	0.00	0.01
Cr*	0.03	0.02	0.02	0.03	0.02	0.02	0.02	0.01
MnO	0.38	0.16	0.10	0.18	0.16	0.27	0.30	0.35
FeO	21.2	51.4	1.62	5.86	7.69	10.2	24.1	20.9
Co*	0.01	0.00	0.00	0.00	0.00	0.00	0.00	0.00
Rb*	0.00	0.00	0.00	0.01	0.00	0.01	0.00	0.01
Sr	0.03	0.01	0.07	0.06	0.06	0.05	0.02	0.01
Zr*	0.00	0.00	0.01	0.01	0.01	0.01	0.00	0.01
BaO*	0.10	0.00	0.02	0.08	0.05	0.11	0.08	0.13
Trace elements (parts per million)								
Cu	2012	64	0	110	331	174	1448	762
As	13	37	2	19	12	41	24	6
Ag*	14	6	26	5	5	6	12	6
Te	10	2	0	1	0	1	12	8
Bi	33	20	4	3	5	4	27	21
W	8	21	0	3	4	8	11	10
Mo	55	2	2	5	6	2	9	88
Pb	13	5	4	19	14	10	94	13
Zn	77	80	14	73	85	63	67	49
Sb*	9	7	6	9	4	6	3	3
Ni	27	33	6	25	49	56	28	20

Table A4-3 continued. XRF Analysis of pulp samples from the Southwest Zone.

Drill Hole	D07-357	D07-357	D07-357	D07-357	D07-357	D07-357	D07-357	D07-357
Sample	BX 02545	BX 02548	BX 02551	BX 02552	BX 02553	BX 02554	BX 02555	BX 02556
Weight percent oxide								
F**	0.01	0.01	0.01	0.01	0.01	0.01	0.01	0.01
Na_2O	0.15	0.16	0.09	0.08	0.08	0.09	0.10	0.11
MgO	3.91	2.94	2.84	4.41	3.33	3.71	5.28	4.33
Al_2O_3	6.20	5.24	4.93	2.63	0.79	0.47	0.75	0.80
SiO_2	36.4	36.2	32.7	37.5	25.2	29.2	28.0	21.8
P_2O5	0.12	0.12	0.11	0.12	0.04	0.02	0.01	0.02
S	1.15	1.27	1.05	1.23	1.22	2.27	0.42	0.70
Cl*	0.07	0.05	0.03	0.00	0.00	0.00	0.02	0.01
K_2O	1.82	1.46	0.59	0.07	0.03	0.01	0.03	0.06
CaO	27.8	29.4	34.9	28.2	42.1	24.8	16.5	31.1
TiO_2	0.41	0.37	0.29	0.16	0.07	0.03	0.03	0.04
V*	0.00	0.01	0.00	0.00	0.00	0.00	0.00	0.00
Cr*	0.02	0.02	0.02	0.01	0.00	0.02	0.02	0.02
MnO	0.33	0.36	0.40	0.37	0.35	0.27	0.16	0.22
FeO	21.3	22.0	21.7	24.9	26.6	38.4	48.6	40.8
Co*	0.00	0.01	0.00	0.01	0.00	0.06	0.03	0.00
Rb*	0.01	0.01	0.00	0.00	0.00	0.00	0.00	0.00
Sr	0.02	0.01	0.02	0.02	0.02	0.00	0.01	0.14
Zr*	0.01	0.01	0.01	0.00	0.00	0.00	0.00	0.00
BaO*	0.11	0.09	0.05	0.03	0.03	0.00	0.00	0.02
Trace elements (parts per million)								
Cu	1077	1404	1803	1951	225	218	88	252
As	5	9	12	18	13	712	575	67
Ag*	10	8	13	10	14	9	2	8
Te	6	17	14	8	3	14	9	3
Bi	33	76	33	26	80	4561	159	23
W	10	9	15	12	15	27	27	21
Mo	22	36	6	2	1	2	2	3
Pb	11	24	37	60	22	16	16	13
Zn	58	68	69	98	52	100	77	51
Sb*	7	0	13	14	8	0	5	5
Ni	19	22	16	21	18	51	45	34

Table A4-3 continued. XRF Analysis of pulp samples from the Southwest Zone.

Drill Hole	D07-357	D07-357	D07-357	D07-357	D07-357	D07-357	D07-357	D07-357
Sample	BX 02558	BX 02562	BX 02563	BX 02564	BX 02565	BX 02566	BX 02567	BX 02568
Weight percent oxide								
F**	0.01	0.01	0.01	0.12	0.54	0.01	0.01	0.01
Na_2O	0.07	0.13	0.11	0.10	0.07	0.01	0.08	0.01
MgO	3.65	8.36	9.93	10.60	12.80	7.02	5.74	5.95
Al_2O_3	0.63	5.21	5.66	6.66	7.55	3.59	2.14	3.67
SiO_2	32.0	14.9	17.8	35.7	27.6	11.4	34.0	8.97
P_2O5	0.05	0.03	0.08	0.04	0.07	0.04	0.05	0.01
S	2.14	0.21	0.45	0.46	0.46	0.14	2.06	0.21
Cl*	0.00	0.01	0.00	0.05	0.03	0.02	0.02	0.00
K_2O	0.02	0.24	0.47	2.79	2.16	0.37	0.06	0.55
CaO	23.7	64.5	58.8	27.2	35.9	69.5	30.9	75.3
TiO_2	0.03	0.26	0.24	0.34	0.34	0.22	0.06	0.20
V*	0.00	0.00	0.00	0.00	0.00	0.00	0.00	0.01
Cr*	0.02	0.00	0.00	0.00	0.00	0.00	0.02	0.01
MnO	0.26	0.19	0.14	0.16	0.15	0.23	0.34	0.15
FeO	37.4	5.75	6.09	15.6	12.1	7.34	24.3	4.81
Co*	0.00	0.00	0.00	0.00	0.00	0.00	0.01	0.00
Rb*	0.00	0.00	0.01	0.03	0.02	0.01	0.00	0.01
Sr	0.01	0.10	0.11	0.03	0.04	0.08	0.02	0.10
Zr*	0.00	0.02	0.01	0.01	0.01	0.01	0.00	0.00
BaO*	0.00	0.03	0.07	0.05	0.05	0.00	0.00	0.04
Trace elements (parts per million)								
Cu	352	43	54	164	204	151	824	65
As	24	5	6	7	4	8	29	12
Ag*	5	25	19	10	20	22	11	25
Te	13	1	1	5	1	0	8	0
Bi	138	9	10	43	14	12	255	35
W	18	6	5	3	6	6	25	4
Mo	2	2	6	5	3	2	1	2
Pb	12	6	4	7	9	3	7	5
Zn	64	21	22	59	45	22	67	18
Sb*	1	5	3	0	12	8	8	10
Ni	33	11	9	9	13	8	26	13

Table A4-3 continued. XRF Analysis of pulp samples from the Southwest Zone.

Drill Hole	D07-357	D07-357	D07-357	D07-357	D07-357	D07-357	D07-357	D07-357
Sample	BX 02571	BX 02572	BX 02573	BX 02575	BX 02576	BX 02580	BX 02581	BX 02583
Weight percent oxide								
F**	0.01	0.06	0.01	0.01	0.01	0.01	0.01	0.01
Na_2O	0.03	0.11	0.06	2.01	1.01	0.36	0.06	0.05
MgO	7.42	10.10	2.93	7.64	8.84	11.60	2.40	1.53
Al_2O_3	3.13	4.87	1.22	6.79	4.45	6.74	0.52	0.79
SiO_2	9.18	15.70	8.94	37.6	36.4	38.8	6.62	9.62
P_2O5	0.03	0.04	0.02	0.14	0.11	0.16	0.01	0.01
S	0.11	0.05	0.31	0.97	1.07	1.68	0.07	0.03
Cl*	0.00	0.02	0.00	0.04	0.03	0.02	0.01	0.02
K_2O	0.31	0.43	0.17	0.88	0.37	0.44	0.01	0.03
CaO	75.8	62.4	81.2	30.5	31.9	25.1	87.4	79.1
TiO_2	0.17	0.21	0.09	0.66	0.60	0.83	0.04	0.00
V*	0.00	0.00	0.00	0.01	0.02	0.00	0.00	0.00
Cr*	0.00	0.00	0.01	0.00	0.01	0.02	0.02	0.00
MnO	0.15	0.11	0.11	0.14	0.17	0.10	0.14	0.21
FeO	3.45	5.79	4.80	12.5	14.7	13.9	2.60	8.50
Co*	0.00	0.00	0.00	0.00	0.03	0.01	0.00	0.00
Rb*	0.01	0.01	0.00	0.01	0.00	0.00	0.00	0.00
Sr	0.15	0.12	0.10	0.04	0.04	0.06	0.13	0.07
Zr*	0.00	0.02	0.00	0.00	0.00	0.01	0.00	0.00
BaO*	0.03	0.00	0.03	0.03	0.02	0.02	0.00	0.00
Trace elements (parts per million)								
Cu	30	30	69	173	215	437	10	0
As	4	9	5	23	310	29	3	37
Ag*	28	23	26	10	9	9	29	26
Te	1	0	0	7	4	1	0	0
Bi	59	34	4	229	230	9	14	18
W	3	2	3	2	6	7	3	1
Mo	3	2	1	28	47	3	2	2
Pb	4	5	5	11	10	8	5	8
Zn	14	19	14	50	56	60	12	23
Sb*	2	5	12	10	16	19	15	5
Ni	6	6	10	11	14	14	5	5

Table A4-3 continued. XRF Analysis of pulp samples from the Southwest Zone.

Drill Hole	D07-367	D07-367	D07-367	D07-367	D07-392	D07-392	D07-392	D07-392
Sample	BX 02489	BX 02490	BX 02491	BX 02492	BX 03219	BX 03220	BX 03221	BX 03222
Weight percent oxide								
F**	0.01	0.01	0.01	0.01	0.01	0.01	0.01	0.01
Na_2O	0.06	0.03	0.03	0.07	0.13	0.11	6.99	0.20
MgO	3.94	1.22	1.31	3.40	2.44	2.40	2.24	4.24
Al_2O_3	1.07	0.21	0.24	0.96	7.02	8.10	16.3	9.31
SiO_2	31.1	7.59	3.81	26.7	41.2	41.4	55.0	43.9
P_2O5	0.04	0.02	0.02	0.04	0.21	0.21	0.29	0.27
S	1.93	0.81	0.73	0.07	0.02	0.03	0.08	0.03
Cl*	0.01	0.01	0.00	0.02	0.01	0.01	0.02	0.00
K_2O	0.02	0.01	0.00	0.02	0.29	0.05	1.15	0.08
CaO	26.8	78.2	87.7	49.8	29.2	27.6	8.88	21.7
TiO_2	0.02	0.00	0.00	0.04	0.58	0.62	0.71	1.06
V*	0.00	0.00	0.00	0.00	0.00	0.02	0.00	0.02
Cr*	0.02	0.03	0.01	0.02	0.02	0.01	0.02	0.02
MnO	0.30	0.19	0.12	0.36	0.69	0.57	0.19	0.45
FeO	34.6	11.6	5.91	18.4	18.0	18.8	7.96	18.4
Co*	0.00	0.00	0.00	0.00	0.00	0.00	0.01	0.00
Rb*	0.00	0.00	0.00	0.00	0.00	0.00	0.00	0.00
Sr	0.01	0.04	0.06	0.02	0.01	0.03	0.02	0.04
Zr*	0.00	0.00	0.00	0.00	0.01	0.01	0.01	0.01
BaO*	0.00	0.04	0.00	0.00	0.04	0.02	0.08	0.03
Trace elements (parts per million)								
Cu	334	168	78	186	4	23	63	662
As	76	10	14	12	16	20	11	16
Ag*	6	24	29	16	10	8	3	27
Te	14	1	3	1	1	0	0	9
Bi	746	27	85	8	7	7	17	145
W	26	8	2	11	16	16	6	10
Mo	1	1	1	2	5	7	8	6
Pb	15	4	6	7	7	12	69	97
Zn	75	18	10	50	98	134	102	298
Sb*	9	3	10	4	10	10	2	18
Ni	32	12	9	12	21	22	10	17

Table A4-3 continued. XRF Analysis of pulp samples from the Southwest Zone.

Drill Hole	D07-392	D07-392	D07-392	D07-392	D07-392	D07-392	D07-392	D07-392
Sample	BX 03225	BX 03226	BX 03227	BX 03228	BX 03231	BX 03232	BX 03236	BX 03237
Weight percent oxide								
F**	0.01	0.01	0.01	0.01	0.01	0.01	0.01	0.01
Na_2O	0.13	0.18	0.10	0.08	0.09	0.09	0.07	0.10
MgO	2.50	2.06	2.68	2.43	3.07	1.16	1.76	2.44
Al_2O_3	8.22	4.35	3.62	3.69	4.67	7.06	5.91	5.09
SiO_2	43.4	37.4	42.4	41.2	41.6	38.3	40.4	41.6
P_2O5	0.19	0.12	0.18	0.17	0.33	0.14	0.17	0.20
S	0.13	2.83	1.09	1.35	1.21	0.21	0.15	0.50
Cl*	0.01	0.01	0.00	0.00	0.01	0.01	0.00	0.00
K_2O	0.06	0.16	0.09	0.06	0.27	0.07	0.05	0.10
CaO	25.7	26.3	26.3	26.5	26.0	31.8	30.1	27.1
TiO_2	0.66	0.25	0.27	0.30	0.87	0.38	0.35	0.43
V*	0.02	0.00	0.00	0.00	0.02	0.01	0.00	0.00
Cr*	0.02	0.00	0.02	0.02	0.02	0.02	0.02	0.02
MnO	0.44	0.56	0.49	0.51	0.36	0.55	0.52	0.39
FeO	18.5	25.1	22.6	23.5	21.3	20.1	20.3	21.6
Co*	0.00	0.01	0.00	0.00	0.00	0.01	0.01	0.01
Rb*	0.00	0.00	0.00	0.00	0.00	0.00	0.00	0.00
Sr	0.05	0.01	0.00	0.00	0.05	0.00	0.00	0.02
Zr*	0.01	0.00	0.00	0.00	0.00	0.00	0.00	0.00
BaO*	0.00	0.00	0.03	0.00	0.03	0.00	0.02	0.03
Trace elements (parts per million)								
Cu	2	3577	715	1863	1178	326	118	568
As	8	50	19	27	36	27	26	87
Ag*	5	22	10	22	10	9	10	11
Te	2	33	8	6	6	5	3	29
Bi	15	521	131	131	136	189	102	1571
W	12	23	11	12	17	23	13	18
Mo	2	257	12	4	26	6	3	5
Pb	12	297	75	105	18	9	5	4
Zn	125	406	197	266	226	124	83	163
Sb*	12	8	6	7	12	9	5	0
Ni	24	38	28	27	25	21	22	27

Table A4-3 continued. XRF Analysis of pulp samples from the Southwest Zone.

Drill Hole	D07-392	D07-392	D07-392	D07-392	D07-392	D07-392	D07-392	D07-392
Sample	BX 03238	BX 03239	BX 03240	BX 03241	BX 03242	BX 03243	BX 03244	BX 03245
Weight percent oxide								
F**	0.01	0.01	0.01	0.01	0.01	0.01	0.01	0.01
Na_2O	0.45	2.29	5.11	2.76	2.89	4.45	3.40	3.19
MgO	2.52	2.16	2.53	2.23	2.34	1.84	1.79	2.44
Al_2O_3	11.5	13.6	13.1	13.5	13.3	12.4	12.7	13.6
SiO_2	48.8	55.5	56.4	62.1	61.8	66.7	62.4	56.2
P_2O5	0.18	0.20	0.18	0.21	0.21	0.18	0.17	0.21
S	0.04	0.17	0.01	0.35	0.72	0.58	0.19	0.13
Cl*	0.01	0.00	0.00	0.02	0.01	0.01	0.02	0.02
K_2O	2.79	5.49	2.50	3.92	3.48	2.13	1.99	1.86
CaO	18.7	10.8	10.4	7.56	7.10	5.36	9.61	12.1
TiO_2	0.83	0.80	0.73	0.78	0.73	0.62	0.64	0.69
V*	0.03	0.02	0.03	0.02	0.02	0.00	0.02	0.02
Cr*	0.03	0.02	0.01	0.03	0.02	0.02	0.02	0.02
MnO	0.28	0.17	0.15	0.10	0.10	0.08	0.14	0.20
FeO	13.6	8.67	8.55	6.23	7.01	5.49	6.74	9.20
Co*	0.00	0.00	0.00	0.00	0.00	0.00	0.00	0.00
Rb*	0.00	0.01	0.01	0.01	0.01	0.01	0.01	0.01
Sr	0.04	0.02	0.02	0.03	0.02	0.02	0.03	0.03
Zr*	0.01	0.01	0.01	0.01	0.01	0.01	0.01	0.01
BaO*	0.23	0.00	0.13	0.20	0.15	0.08	0.13	0.11
Trace elements (parts per million)								
Cu	64	157	59	203	315	254	129	203
As	11	9	22	11	46	27	32	58
Ag*	8	6	5	4	4	3	6	5
Te	1	0	0	2	0	1	1	3
Bi	53	15	10	6	5	6	8	90
W	6	8	5	7	11	10	7	10
Mo	2	2	2	3	4	5	10	36
Pb	9	10	12	13	13	11	11	20
Zn	106	86	81	50	52	42	51	77
Sb*	9	7	3	7	4	4	3	3
Ni	30	31	27	23	23	22	18	20

Table A4-3 continued. XRF Analysis of pulp samples from the Southwest Zone.

Drill Hole	D07-392	D07-392	D07-392	D07-392	D07-392	D07-392	D07-392	D07-392
Sample	BX 03246	BX 03246	BX 03247	BX 03248	BX 03249	BX 03250	BX 03251	BX 03256
Weight percent oxide								
F**	0.01	0.01	0.01	0.01	0.01	0.01	0.01	0.01
Na_2O	2.70	2.69	0.81	1.22	0.81	2.47	1.20	0.26
MgO	2.31	2.34	2.33	2.34	2.48	2.35	1.88	1.93
Al_2O_3	13.2	13.4	11.5	14.4	9.72	12.0	7.34	9.20
SiO_2	55.0	55.0	43.7	50.3	45.7	48.8	39.9	40.6
P_2O5	0.19	0.18	0.18	0.23	0.19	0.16	0.11	0.26
S	0.29	0.30	0.59	0.11	0.09	0.30	2.73	0.32
Cl*	0.03	0.03	0.02	0.01	0.01	0.01	0.00	0.00
K_2O	1.61	1.59	2.14	3.81	1.25	2.20	0.89	0.27
CaO	12.6	12.4	24.9	14.8	20.9	15.9	20.7	26.2
TiO_2	0.72	0.70	0.69	0.83	0.67	0.66	0.40	0.75
V*	0.00	0.00	0.02	0.01	0.02	0.02	0.02	0.02
Cr*	0.02	0.00	0.02	0.02	0.02	0.02	0.02	0.02
MnO	0.19	0.18	0.28	0.29	0.37	0.25	0.39	0.58
FeO	11.0	10.9	12.5	11.2	17.5	14.7	23.3	19.2
Co*	0.00	0.00	0.00	0.00	0.01	0.01	0.04	0.01
Rb*	0.00	0.00	0.01	0.01	0.00	0.01	0.00	0.00
Sr	0.03	0.03	0.04	0.03	0.04	0.03	0.02	0.09
Zr*	0.01	0.01	0.01	0.01	0.01	0.00	0.01	0.01
BaO*	0.09	0.09	0.17	0.27	0.07	0.09	0.03	0.05
Trace elements (parts per million)								
Cu	175	167	354	153	124	166	3899	118
As	73	67	41	41	136	232	659	1097
Ag*	7	5	8	3	6	7	18	21
Te	3	3	4	1	3	1	13	3
Bi	84	82	190	161	458	97	3850	63
W	12	13	21	13	13	11	11	11
Mo	13	12	8	10	39	36	31	7
Pb	17	19	14	12	10	10	3	511
Zn	80	81	98	121	142	119	372	201
Sb*	9	5	6	5	0	4	0	13
Ni	27	27	18	21	21	24	50	20

Table A4-3 continued. XRF Analysis of pulp samples from the Southwest Zone.

Drill Hole	D07-392	D07-392	D08-413	D08-413	D08-413	D08-413	D08-413	D08-413
Sample	BX 03257	BX 03258	BX 04641	BX 04646	BX 04647	BX 04649	BX 04650	BX 04651
Weight percent oxide								
F**	0.01	0.01	0.01	0.01	0.01	0.01	0.01	0.01
Na_2O	0.06	0.11	0.15	0.17	0.14	0.07	0.16	0.10
MgO	1.87	2.37	2.15	2.78	3.12	3.51	2.38	6.32
Al_2O_3	7.22	6.44	5.52	2.70	1.18	0.38	0.98	0.76
SiO_2	41.8	39.9	38.0	41.2	41.1	29.9	17.0	35.8
P_2O5	0.20	0.25	0.14	0.13	0.12	0.04	0.05	0.03
S	0.07	0.03	2.52	3.15	3.65	2.12	2.82	0.15
Cl*	0.01	0.02	0.07	0.07	0.03	0.01	0.03	0.02
K_2O	0.03	0.03	0.14	0.12	0.04	0.01	0.05	0.04
CaO	27.4	30.3	24.5	22.1	23.1	15.0	13.1	31.5
TiO_2	0.53	0.59	0.38	0.16	0.09	0.00	0.03	0.03
V*	0.02	0.00	0.02	0.00	0.00	0.00	0.00	0.00
Cr*	0.01	0.02	0.03	0.03	0.03	0.05	0.07	0.02
MnO	0.60	0.71	0.50	0.36	0.40	0.15	0.10	0.33
FeO	20.0	19.2	25.7	26.8	26.7	47.7	62.6	24.9
Co*	0.00	0.02	0.00	0.02	0.01	0.08	0.12	0.00
Rb*	0.00	0.00	0.00	0.00	0.00	0.00	0.00	0.00
Sr	0.05	0.00	0.02	0.01	0.00	0.00	0.01	0.02
Zr*	0.01	0.01	0.00	0.00	0.00	0.00	0.00	0.00
BaO*	0.02	0.00	0.02	0.02	0.01	0.01	0.00	0.02
Trace elements (parts per million)								
Cu	18	2	548	608	1097	506	482	28
As	128	129	10	20	36	1422	2182	43
Ag*	9	10	6	7	10	2	0	14
Te	3	2	2	13	39	7	8	3
Bi	9	10	9	244	896	8626	2665	500
W	11	13	27	11	12	48	37	9
Mo	9	5	186	1	0	4	3	1
Pb	47	7	7	10	20	76	10	11
Zn	140	90	70	76	72	144	98	65
Sb*	11	6	13	19	0	0	8	2
Ni	28	27	26	28	27	54	67	16

Table A4-3 continued. XRF Analysis of pulp samples from the Southwest Zone.

Drill Hole	D09-489	D09-489	D09-489	D09-492	D09-492	D09-492	D09-492	D09-492
Sample	BX 15667	BX 15668	BX 15669	BX 15737	BX 15738	BX 15739	BX 15740	BX 15741
Weight percent oxide								
F**	0.01	0.01	0.01	0.01	0.01	0.01	0.01	0.01
Na_2O	0.34	0.14	0.12	0.05	0.12	0.08	0.11	0.13
MgO	2.60	2.39	3.15	5.03	5.64	5.17	6.12	6.50
Al_2O_3	6.65	4.08	3.14	0.93	0.63	0.72	0.66	0.71
SiO_2	29.1	33.5	29.5	30.1	38.5	38.8	41.1	42.8
P_2O5	0.07	0.07	0.06	0.01	0.01	0.02	0.02	0.01
S	1.47	2.64	2.53	2.25	2.15	2.14	2.92	2.27
Cl*	0.02	0.09	0.03	0.01	0.02	0.02	0.02	0.02
K_2O	1.01	0.42	0.50	0.02	0.02	0.03	0.03	0.02
CaO	20.6	19.5	21.3	22.1	25.3	22.7	20.9	21.0
TiO_2	0.38	0.22	0.09	0.02	0.02	0.01	0.01	0.01
V*	0.01	0.00	0.01	0.00	0.00	0.00	0.00	0.00
Cr*	0.01	0.01	0.01	0.01	0.02	0.02	0.02	0.02
MnO	0.34	0.37	0.24	0.20	0.33	0.34	0.33	0.31
FeO	16.1	20.1	20.4	18.9	20.2	21.8	22.6	21.1
Co*	0.01	0.00	0.00	0.01	0.00	0.00	0.01	0.00
Rb*	0.01	0.00	0.01	0.00	0.00	0.00	0.00	0.00
Sr	0.03	0.02	0.02	0.02	0.01	0.01	0.00	0.00
Zr*	0.00	0.00	0.00	0.00	0.00	0.00	0.00	0.00
BaO*	0.04	0.02	0.03	0.01	0.00	0.01	0.01	0.01
Trace elements (parts per million)								
Cu	319	712	610	698	340	376	489	354
As	9	16	16	21	21	20	35	23
Ag*	18	24	27	23	29	20	32	30
Te	1	16	32	31	43	19	95	58
Bi	6	180	217	59	99	38	455	154
W	8	13	16	10	11	9	10	18
Mo	2	5	3	5	0	1	2	1
Pb	19	15	25	30	24	16	1	16
Zn	80	53	79	69	74	53	56	72
Sb*	0	0	0	0	0	0	0	0
Ni	108	103	1	107	1	1	111	1

Table A4-3 continued. XRF Analysis of pulp samples from the Southwest Zone.

Drill Hole	D09-492	D09-492	D09-492	D09-492	D09-492	D09-492	D09-492	D09-492
Sample	BX 15742	BX 15743	BX 15744	BX 15745	BX 15746	BX 15747	BX 15748	BX 15738
Weight percent oxide								
F**	0.01	0.01	0.01	0.01	0.01	0.01	0.01	0.01
Na_2O	0.14	0.14	0.12	0.09	0.11	0.10	0.07	0.11
MgO	3.74	4.87	4.37	4.05	4.91	4.60	3.86	5.98
Al_2O_3	2.12	1.21	1.69	0.80	0.70	0.71	0.99	0.64
SiO_2	36.9	39.4	37.0	30.5	36.4	35.7	31.8	42.1
P_2O5	0.04	0.02	0.03	0.04	0.03	0.02	0.03	0.02
S	4.95	2.45	2.59	0.75	2.21	3.70	4.87	2.34
Cl*	0.04	0.05	0.05	0.02	0.03	0.03	0.01	0.02
K_2O	0.14	0.10	0.16	0.04	0.04	0.04	0.03	0.03
CaO	20.7	23.4	24.4	24.5	26.0	22.6	24.3	26.9
TiO_2	0.03	0.04	0.08	0.01	0.01	0.01	0.01	0.02
V*	0.01	0.00	0.00	0.00	0.00	0.00	0.00	0.00
Cr*	0.02	0.02	0.02	0.01	0.02	0.01	0.01	0.02
MnO	0.31	0.31	0.31	0.24	0.30	0.34	0.29	0.31
FeO	26.7	21.9	23.1	14.8	23.1	25.0	25.5	21.4
Co*	0.01	0.00	0.01	0.01	0.01	0.01	0.01	0.01
Rb*	0.00	0.00	0.00	0.00	0.00	0.00	0.00	0.00
Sr	0.01	0.01	0.01	0.01	0.01	0.01	0.02	0.01
Zr*	0.00	0.00	0.00	0.00	0.00	0.00	0.00	0.00
BaO*	0.02	0.02	0.03	0.01	0.02	0.02	0.01	0.00
Trace elements (parts per million)								
Cu	969	386	357	136	282	598	778	341
As	59	34	21	17	21	29	45	16
Ag*	26	23	22	22	21	30	27	10
Te	43	29	20	21	18	46	52	37
Bi	344	270	53	55	51	281	558	90
W	15	13	11	11	11	16	13	14
Mo	0	8	2	2	3	2	0	1
Pb	1	3	23	16	18	13	1	17
Zn	61	63	53	41	57	88	46	56
Sb*	0	0	0	0	0	0	0	0
Ni	1	1	1	1	4	1	1	17

Table A4-3 continued. XRF Analysis of pulp samples from the Southwest Zone.

Drill Hole	D09-492	D09-492	D09-492	D09-492	D09-492	D09-526	D09-526	D09-526
Sample	BX 15740	BX 15741	BX 15742	BX 15747	BX 15748	BX 19285	BX 19286	BX 19287
Weight percent oxide								
F**	0.01	0.01	0.01	0.01	0.01	0.01	0.01	0.01
Na_2O	0.11	0.14	0.13	0.09	0.07	0.10	0.12	0.10
MgO	6.41	6.69	3.93	4.91	4.23	1.50	2.67	2.81
Al_2O_3	0.69	0.69	2.11	0.73	1.08	2.96	2.08	1.93
SiO_2	43.4	45.7	38.6	38.9	34.8	25.3	34.2	34.2
P_2O5	0.02	0.02	0.04	0.04	0.03	0.09	0.09	0.09
S	3.13	2.44	5.24	4.04	5.37	2.04	1.15	0.87
Cl*	0.03	0.03	0.05	0.03	0.02	0.01	0.01	0.00
K_2O	0.02	0.03	0.14	0.03	0.03	0.04	0.04	0.04
CaO	21.8	22.0	21.4	24.0	26.0	27.1	22.1	22.9
TiO_2	0.00	0.00	0.04	0.00	0.00	0.11	0.10	0.18
V*	0.00	0.00	0.00	0.00	0.00	0.01	0.01	0.01
Cr*	0.02	0.02	0.02	0.02	0.00	0.02	0.02	0.01
MnO	0.36	0.33	0.33	0.35	0.33	0.27	0.32	0.32
FeO	23.9	21.9	27.7	26.7	27.8	18.6	19.2	18.1
Co*	0.00	0.00	0.01	0.01	0.01	0.01	0.01	0.01
Rb*	0.00	0.00	0.00	0.00	0.00	0.00	0.00	0.00
Sr	0.00	0.00	0.01	0.01	0.02	0.01	0.01	0.01
Zr*	0.00	0.00	0.00	0.00	0.00	0.00	0.00	0.00
BaO*	0.00	0.00	0.02	0.00	0.00	0.01	0.02	0.02
Trace elements (parts per million)								
Cu	494	360	998	621	817	3664	2157	1199
As	31	17	55	22	42	61	112	173
Ag*	10	8	5	10	13	45	39	37
Te	79	48	37	41	44	25	31	41
Bi	408	139	317	255	523	1406	2617	2780
W	8	9	13	9	13	13	12	14
Mo	1	1	2	1	1	3	2	4
Pb	17	10	19	21	24	0.5	0.5	0.5
Zn	66	66	64	58	59	353	294	233
Sb*	0	8	0	9	0	0	0	0
Ni	21	19	23	20	23	104	104	1

Table A4-3 continued. XRF Analysis of pulp samples from the Southwest Zone.

Drill Hole	D09-526	D09-534	D09-534	D09-534	D09-534	D09-534	D09-545	D09-545
Sample	BX 19288	BX 17126	BX 17127	BX 17128	BX 17129	BX 17130	BX 21346	BX 21347
Weight percent oxide								
F**	0.01	0.01	0.01	0.01	0.01	0.01	0.01	0.01
Na_2O	0.09	0.15	0.08	0.09	0.09	0.12	0.78	1.39
MgO	2.67	4.04	2.29	1.66	3.28	4.80	1.96	1.34
Al_2O_3	0.60	2.30	0.35	1.81	1.01	1.22	4.80	7.00
SiO_2	29.4	27.9	16.9	17.0	22.3	26.7	20.3	38.7
P_2O5	0.05	0.06	0.04	0.02	0.01	0.02	0.15	0.16
S	1.85	0.91	0.21	0.32	0.45	0.30	1.41	0.39
Cl*	0.00	0.02	0.01	0.01	0.01	0.02	0.01	0.04
K_2O	0.03	1.01	0.05	0.67	0.32	0.15	1.15	1.44
CaO	24.9	27.1	35.7	37.9	31.8	28.6	30.7	19.3
TiO_2	0.07	0.11	0.05	0.03	0.03	0.13	0.23	0.44
V*	0.00	0.01	0.00	0.00	0.00	0.01	0.01	0.02
Cr*	0.02	0.01	0.01	0.01	0.01	0.01	0.01	0.01
MnO	0.28	0.19	0.19	0.20	0.21	0.22	0.61	0.43
FeO	19.9	11.7	15.7	10.2	15.3	15.1	9.75	10.8
Co*	0.00	0.01	0.01	0.00	0.02	0.00	0.11	0.01
Rb*	0.00	0.00	0.00	0.00	0.00	0.00	0.00	0.01
Sr	0.00	0.01	0.01	0.02	0.01	0.02	0.02	0.02
Zr*	0.00	0.01	0.00	0.00	0.00	0.00	0.00	0.00
BaO*	0.02	0.06	0.01	0.05	0.02	0.02	0.04	0.06
Trace elements (parts per million)								
Cu	2615	1738	108	124	121	95	233	95
As	70	205	104	167	368	106	1687	2088
Ag*	33	19	27	21	25	21	299	18
Te	28	8	112	28	5	8	29	1
Bi	1216	92	2024	266	54	85	1546	3
W	13	37	15	9	20	16	15	5
Mo	1	5	1	2	6	2	271	4
Pb	1	1	1	1	1	1	920	1
Zn	229	62	49	49	70	68	656	92
Sb*	0	0	0	0	0	0	296	32
Ni	1	9	104	1	104	1	7	1

Table A4-3 continued. XRF Analysis of pulp samples from the Southwest Zone.

Drill Hole	D09-545	D09-545	D09-545	D09-545	D09-545	D09-545	D07-321	D07-321
Sample	BX 21348	BX 21349	BX 21350	BX 21346	BX 21347	BX 21349	BX 01291	BX 01292
Weight percent oxide								
F**	0.01	0.01	0.01	0.01	0.01	0.01	0.01	0.01
Na_2O	0.10	2.16	2.91	0.94	1.56	2.16	0.47	0.11
MgO	0.78	1.48	3.07	2.37	1.51	1.48	4.00	4.07
Al_2O_3	2.83	8.16	11.6	5.88	7.97	8.17	9.76	10.4
SiO_2	40.1	46.5	57.0	25.3	44.7	46.6	34.0	35.0
P_2O5	0.13	0.10	0.26	0.19	0.19	0.10	0.17	0.15
S	0.30	1.54	0.28	1.82	0.47	1.54	2.91	3.70
Cl*	0.01	0.01	0.02	0.02	0.05	0.01	0.01	0.01
K_2O	0.06	2.62	2.39	1.52	1.73	2.62	0.30	0.85
CaO	22.2	18.9	12.3	42.0	23.5	18.9	23.1	21.4
TiO_2	0.19	0.43	0.62	0.34	0.55	0.43	0.65	0.52
V*	0.01	0.01	0.02	0.01	0.02	0.01	0.02	0.02
Cr*	0.02	0.02	0.01	0.02	0.01	0.02	0.02	0.02
MnO	0.71	0.35	0.27	0.89	0.54	0.35	0.24	0.20
FeO	12.0	7.87	7.10	14.3	13.8	7.86	24.2	23.3
Co*	0.01	0.00	0.00	0.16	0.01	0.00	0.01	0.01
Rb*	0.00	0.01	0.01	0.01	0.01	0.01	0.00	0.00
Sr	0.02	0.02	0.03	0.03	0.03	0.02	0.05	0.03
Zr*	0.00	0.01	0.01	0.01	0.01	0.01	0.01	0.01
BaO*	0.01	0.12	0.11	0.06	0.08	0.12	0.03	0.08
Trace elements (parts per million)								
Cu	82	97	22	217	101	105	760	906
As	33	5163	348	1698	2145	5445	6	4
Ag*	20	11	2	255	9	8	12	7
Te	0	3	0	23	1	2	2	2
Bi	4		0	1437	22	12	14	11
W	13	9	5	15	5	6	7	11
Mo	2	4	2	275	4	4	1	2
Pb	11	1	1	1632	24	30	9	11
Zn	68	514	100	689	96	415	134	113
Sb*	0	0	0	271	23	15	3	0
Ni	1	45	70	23	16	22	30	27

Table A4-4. XRF Analysis of pulp samples from the W Southwest Zone.

Drill Hole	D07-321	D07-333	D07-333	D07-333	D07-333	D07-333	D07-333	D07-333
Sample	BX 01294	BX 02181	BX 02182	BX 02183	BX 02184	BX 02184	BX 02185	BX 02187
Weight percent oxide								
F**	0.11	0.01	0.01	0.01	0.01	0.01	0.01	0.01
Na_2O	0.17	5.77	1.30	0.23	0.19	0.13	0.12	0.14
MgO	3.17	2.73	4.53	5.01	5.86	5.14	4.44	4.62
Al_2O_3	14.5	17.9	8.54	4.61	2.61	2.72	6.31	4.68
SiO_2	37.3	50.7	35.3	35.2	41.7	38.2	42.0	39.0
P_2O5	0.22	0.41	0.18	0.14	0.22	0.12	0.11	0.13
S	0.89	0.75	3.24	4.06	1.37	4.60	1.87	1.63
Cl*	0.01	0.00	0.03	0.04	0.01	0.01	0.00	0.02
K_2O	3.03	2.14	1.19	1.84	0.16	0.17	0.07	0.15
CaO	27.6	10.6	20.5	21.7	25.9	21.2	22.9	26.3
TiO_2	0.59	0.84	0.55	0.37	0.09	0.12	0.15	0.07
V*	0.03	0.03	0.02	0.01	0.00	0.00	0.00	0.00
Cr*	0.03	0.03	0.02	0.02	0.02	0.00	0.02	0.04
MnO	0.20	0.07	0.20	0.19	0.26	0.24	0.25	0.32
FeO	11.8	7.72	24.1	26.3	21.4	27.1	21.5	22.7
Co*	0.00	0.00	0.06	0.00	0.01	0.01	0.01	0.00
Rb*	0.02	0.01	0.01	0.02	0.00	0.00	0.00	0.00
Sr	0.05	0.04	0.04	0.04	0.03	0.02	0.04	0.03
Zr*	0.02	0.01	0.01	0.01	0.01	0.00	0.01	0.01
BaO*	0.20	0.13	0.03	0.05	0.04	0.00	0.00	0.03
Trace elements (parts per million)								
Cu	279	1763	866	1221	913	1384	1221	1053
As	4	2	691	14	7	8	10	11
Ag*	13	7	13	9	10	1	10	9
Te	12	2	7	15	11	30	20	29
Bi	30	7	22	63	39	159	89	128
W	9	6	7	13	10	16	7	16
Mo	1	3	54	15	9	138	37	33
Pb	10	7	20	15	13	11	23	19
Zn	61	61	87	80	97	95	134	139
Sb*	6	2	4	3	11	0	4	6
Ni	11	23	38	42	29	31	38	30

Table A4-4 continued. XRF Analysis of pulp samples from the W Southwest Zone.

Drill Hole	D07-333	D07-333	D07-333	D07-333	D07-333	D07-333	D07-334	D07-334
Sample	BX 02188	BX 02190	BX 02192	BX 02193	BX 02194	BX 02195	BX 02197	BX 02199
Weight percent oxide								
F**	0.01	0.01	0.01	0.01	0.01	0.01	0.01	0.01
Na_2O	0.20	0.12	0.19	0.04	0.06	0.05	1.71	2.09
MgO	5.28	4.39	4.19	2.24	1.35	1.14	10.3	5.93
Al_2O_3	6.64	2.37	5.36	2.50	1.35	1.47	17.5	11.0
SiO_2	39.9	31.9	28.4	48.0	56.4	37.7	46.7	58.3
P_2O5	0.22	0.10	0.09	0.04	0.02	0.02	0.45	0.33
S	4.07	5.54	6.61	5.39	0.48	0.13	1.10	1.82
Cl*	0.03	0.01	0.02	0.03	0.04	0.02	0.02	0.03
K_2O	0.89	0.27	0.44	0.07	0.13	0.23	2.25	1.31
CaO	16.3	25.6	23.6	23.3	35.4	55.8	7.03	9.85
TiO_2	0.16	0.10	0.16	0.09	0.04	0.04	0.87	0.52
V*	0.00	0.00	0.00	0.00	0.00	0.00	0.01	0.02
Cr*	0.02	0.04	0.02	0.02	0.03	0.03	0.01	0.02
MnO	0.23	0.28	0.20	0.12	0.10	0.12	0.12	0.10
FeO	25.9	28.9	30.3	17.9	4.48	3.11	11.7	8.53
Co*	0.00	0.00	0.01	0.00	0.00	0.00	0.00	0.00
Rb*	0.01	0.00	0.00	0.00	0.00	0.00	0.01	0.01
Sr	0.03	0.02	0.04	0.04	0.05	0.07	0.02	0.02
Zr*	0.00	0.00	0.01	0.00	0.01	0.00	0.01	0.01
BaO*	0.04	0.03	0.03	0.00	0.00	0.03	0.07	0.05
Trace elements (parts per million)								
Cu	921	1497	1297	1302	82	9	192	429
As	11	11	6	8	2	10	3	10
Ag*	5	12	11	14	11	18	7	8
Te	12	72	44	9	0	0	2	1
Bi	60	331	208	166	6	5	6	9
W	11	18	19	8	0	0	11	8
Mo	45	312	251	17	11	6	2	5
Pb	14	11	29	78	10	6	29	44
Zn	128	101	136	60	31	27	117	49
Sb*	8	6	9	13	7	6	8	7
Ni	32	47	41	29	12	8	19	19

Table A4-4 continued. XRF Analysis of pulp samples from the W Southwest Zone.

Drill Hole	D07-334	D07-334	D07-334	D07-334	D07-338	D07-338	D07-338	D07-338
Sample	BX 02201	BX 02203	BX 02204	BX 02205	BX 02236	BX 02238	BX 02239	BX 02240
Weight percent oxide								
F**	0.01	0.01	0.01	0.01	0.01	0.01	0.01	0.01
Na_2O	0.07	1.53	0.15	0.14	0.14	0.27	0.07	0.08
MgO	6.19	5.23	1.58	1.85	5.07	4.59	4.38	4.38
Al_2O_3	3.92	9.66	5.35	7.34	4.65	9.22	6.42	5.34
SiO_2	41.8	32.8	23.9	21.9	41.1	38.8	29.9	33.4
P_2O5	0.15	0.19	0.11	0.11	0.16	0.11	0.17	0.14
S	1.47	4.23	0.63	0.55	2.84	2.18	7.63	3.41
Cl*	0.03	0.03	0.02	0.01	0.03	0.05	0.03	0.04
K_2O	0.98	0.73	1.17	1.75	0.13	3.03	1.70	1.64
CaO	27.6	22.3	61.5	60.6	20.1	14.7	15.5	24.2
TiO_2	0.31	0.58	0.44	0.07	0.13	0.74	0.16	0.18
V*	0.01	0.00	0.00	0.02	0.00	0.01	0.00	0.00
Cr*	0.03	0.02	0.01	0.02	0.02	0.01	0.04	0.03
MnO	0.53	0.20	0.13	0.10	0.23	0.21	0.15	0.25
FeO	12.0	22.3	4.91	4.71	25.2	25.9	33.5	26.7
Co*	0.01	0.00	0.00	0.00	0.01	0.01	0.01	0.00
Rb*	0.01	0.00	0.01	0.01	0.00	0.02	0.01	0.02
Sr	0.06	0.05	0.07	0.06	0.03	0.02	0.02	0.04
Zr*	0.01	0.01	0.01	0.01	0.00	0.01	0.00	0.01
BaO*	0.05	0.04	0.06	0.06	0.00	0.07	0.03	0.04
Trace elements (parts per million)								
Cu	306	1020	114	5	1342	715	2306	752
As	3647	86	33	80	6	0	4	0
Ag*	20	7	19	23	8	6	0	9
Te	102	1	2	1	1	4	3	2
Bi	664	13	5	6	12	14	17	8
W	13	11	8	6	18	14	14	9
Mo	488	2	4	3	182	22	69	13
Pb	67	32	67	96	16	23	21	30
Zn	35	116	20	30	108	146	115	95
Sb*	6	3	1	10	3	6	6	1
Ni	16	26	8	9	63	35	78	32

Table A4-4 continued. XRF Analysis of pulp samples from the W Southwest Zone.

Drill Hole	D07-338	D07-338	D07-338	D07-338	D07-338	D07-338	D07-338	D07-338
Sample	BX 02242	BX 02243	BX 02244	BX 02245	BX 02246	BX 02247	BX 02248	BX 02249
Weight percent oxide								
F**	0.00	0.00	0.00	0.00	0.00	0.00	0.00	0.00
Na_2O	0.00	0.00	0.10	0.00	1.80	1.10	1.90	2.00
MgO	3.90	4.30	4.80	4.70	3.00	5.00	6.00	5.60
Al_2O_3	4.90	4.60	6.20	8.40	11.9	13.8	15.2	16.0
SiO_2	33.7	35.4	35.1	33.4	35.1	33.4	39.5	40.6
P_2O5	0.10	0.10	0.10	0.10	0.30	0.20	0.30	0.30
S	2.00	1.20	1.20	1.90	2.20	0.90	2.30	2.90
Cl*	0.00	0.00	0.10	0.00	0.10	0.00	0.00	0.00
K_2O	1.30	1.60	1.90	1.80	2.40	1.10	1.60	1.90
CaO	30.4	32.3	29.7	22.9	15.7	23.4	15.1	12.5
TiO_2	0.20	0.20	0.30	0.30	0.80	0.60	0.70	0.70
V*	0.00	0.00	0.00	0.00	0.00	0.00	0.00	0.00
Cr*	0.00	0.00	0.00	0.00	0.00	0.00	0.00	0.00
MnO	0.30	0.30	0.20	0.20	0.20	0.30	0.20	0.10
FeO	22.8	19.7	19.9	26.1	26.2	19.8	16.9	17.2
Co*	0.00	0.00	0.00	0.00	0.00	0.00	0.00	0.00
Rb*	0.00	0.00	0.00	0.00	0.00	0.00	0.00	0.00
Sr	0.00	0.10	0.10	0.00	0.00	0.00	0.00	0.00
Zr*	0.00	0.00	0.00	0.00	0.00	0.00	0.00	0.00
BaO*	0.00	0.10	0.1	0.00	0.10	0.10	0.10	0.10
Trace elements (parts per million)								
Cu	323	218	248	385	657	656	680	719
As	3	5	1	3	0	5	6	5
Ag*	15	14	12	9	5	12	8	6
Te	9	22	3	5	1	6	1	1
Bi	23	87	9	17	8	9	8	7
W	6	6	137	12	14	9	7	12
Mo	17	16	18	32	21	4	2	3
Pb	31	36	42	39	16	11	29	13
Zn	77	65	71	102	120	113	112	116
Sb*	7	5	7	14	5	0	0	0
Ni	16	15	14	25	29	21	29	35

Table A4-4 continued. XRF Analysis of pulp samples from the W Southwest Zone.

Drill Hole	D07-338	D07-338	D07-338	D07-338
Sample	BX 02250	BX 02251	BX 02252	BX 02253
Weight percent oxide				
F**	0.01	0.01	0.01	0.01
Na_2O	0.53	1.37	0.09	0.20
MgO	2.52	3.82	1.36	1.54
Al_2O_3	15.5	11.5	2.79	3.54
SiO_2	34.4	29.8	7.65	11.4
P_2O5	0.26	0.22	0.05	0.06
S	2.43	4.15	0.15	0.16
Cl*	0.02	0.02	0.02	0.00
K_2O	3.76	1.42	0.51	0.70
CaO	25.6	25.3	83.1	79.4
TiO_2	0.74	0.63	0.23	0.35
V*	0.01	0.04	0.00	0.00
Cr*	0.02	0.02	0.02	0.02
MnO	0.24	0.19	0.22	0.09
FeO	13.7	21.2	3.62	2.39
Co*	0.01	0.00	0.00	0.00
Rb*	0.02	0.01	0.00	0.01
Sr	0.04	0.04	0.09	0.06
Zr*	0.01	0.01	0.01	0.00
BaO*	0.19	0.09	0.05	0.04
Trace elements (parts per million)				
Cu	437	934	26	9
As	56	10	20	27
Ag*	12	8	28	27
Te	2	7	0	2
Bi	8	28	5	3
W	36	14	6	6
Mo	3	9	11	22
Pb	27	19	10	16
Zn	63	104	39	96
Sb*	18	8	8	10
Ni	24	38	17	35

Table A4-5. Gold compositions by microprobe analysis.

Sample ID	Depth	%Ag	%Au	%Hg	Totals	Fineness
BH-UG-11	UG	19.01	82.88	0.21	102.09	813
		18.97	83.36	0.09	102.42	815
		19.01	82.00	0.05	101.06	812
		18.68	83.24	0.04	101.96	817
		18.63	83.72	0.02	102.38	818
		18.89	83.51	0.07	102.47	816
		26.92	75.52	-0.04	102.41	737
		26.87	74.90	0.03	101.79	736
		24.43	77.29	-0.02	101.70	760
		23.18	78.31	0.03	101.52	772
		22.39	77.90	0.00	100.29	777
		23.12	77.69	0.02	100.84	771
		23.71	77.72	-0.01	101.42	766
		23.65	76.75	0.03	100.43	764
		23.32	76.75	0.05	100.12	767
		23.78	77.83	-0.16	101.45	766
		24.99	77.54	0.07	102.59	756
BH-UG-16	UG	7.62	93.28	0.07	100.96	924
		7.73	93.54	0.07	101.33	924
		7.78	94.37	0.14	102.29	924
		7.60	92.25	0.01	99.86	924
		7.60	92.62	0.11	100.32	924
		7.66	92.55	0.12	100.33	924
		7.62	93.92	0.02	101.56	925
		7.60	92.95	0.07	100.62	924
BH-UG-2	UG	8.98	87.16	0.01	96.16	907
		9.29	87.87	0.02	97.19	904
		10.10	89.00	0.06	99.16	898
		11.77	90.21	0.17	102.15	885
		10.46	90.39	0.04	100.89	896
		9.76	91.08	-0.06	100.78	903

Table A4-5 continued. Gold compositions by microprobe analysis.

Sample ID	Depth	%Ag	%Au	%Hg	Totals	Fineness
BH-UG-8	UG	6.96	91.08	0.06	98.09	929
		7.21	91.68	0.02	98.91	927
		7.63	92.99	0.01	100.62	924
		7.69	91.58	0.00	99.27	923
		7.92	91.72	0.02	99.66	921
		7.47	89.38	0.04	96.89	923
		9.54	90.49	0.05	100.08	905
C-5	60.5	19.11	82.42	0.08	101.62	812
		19.01	82.20	0.01	101.22	812
		20.01	80.53	0.15	100.69	801
		20.05	80.33	0.10	100.49	800
		18.46	83.04	0.06	101.57	818
C-5	73	21.18	77.94	-0.03	99.08	786
		20.94	77.80	0.10	98.84	788
		20.59	79.01	-0.11	99.49	793
		21.72	77.02	0.05	98.80	780
		18.43	81.88	0.00	100.31	816
		20.07	81.83	0.01	101.91	803
		19.36	81.70	0.05	101.11	808
		20.79	77.25	-0.06	97.99	788
		22.29	78.33	0.05	100.67	778
		22.06	78.47	0.04	100.58	781
		20.27	80.11	0.04	100.42	798
		19.61	80.73	0.03	100.37	805
D02-198	213.5	9.66	91.20	-0.02	100.84	904
		9.65	92.03	0.15	101.83	905
		8.38	90.79	0.06	99.24	916
		8.32	91.17	0.14	99.64	916
		10.45	90.45	-0.03	100.87	896
		0.20	99.31	0.09	99.59	998
		0.23	99.51	0.01	99.75	998
D02-199	430	12.78	84.28	0.02	97.08	868
		13.36	82.95	0.16	96.47	861
		11.52	87.39	0.17	99.09	884
		11.44	84.50	0.04	95.98	881
D02-208	75	9.37	91.66	0.01	101.04	907
		9.28	91.88	0.11	101.27	908
		9.28	91.18	0.03	100.49	908
		9.26	86.70	0.11	96.08	903

Table A4-5 continued. Gold compositions by microprobe analysis.

Sample ID	Depth	%Ag	%Au	%Hg	Totals	Fineness
D07-404	12.5	8.15	89.73	0.13	98.01	917
		9.46	91.79	0.03	101.29	907
		9.18	92.98	0.02	102.18	910
		9.31	93.54	0.09	102.95	909
		8.84	90.75	0.01	99.60	911
		8.82	91.88	0.08	100.78	912
		8.11	89.28	0.09	97.48	917
		8.31	90.65	0.00	98.96	916
		8.60	92.64	-0.03	101.22	915
		8.79	92.12	0.06	100.97	913
		8.69	91.87	0.12	100.68	914
		8.47	90.33	0.18	98.98	914
D09-545	692.5	39.02	61.06	0.10	100.18	610
		38.60	61.71	0.22	100.53	615
D10-622	159	26.55	73.75	-0.02	100.28	735
		26.66	72.99	-0.12	99.53	732
		26.05	74.23	-0.03	100.26	740
		25.88	74.74	0.05	100.67	743
		26.23	75.59	0.02	101.85	742
		26.13	74.00	0.08	100.22	739
		38.03	63.55	0.10	101.68	626
		37.42	64.84	-0.01	102.25	634
D10-630	100.7	17.54	84.20	0.02	101.76	828
		17.81	82.29	0.01	100.12	822
		17.66	83.30	0.06	101.03	825
		18.12	83.41	0.02	101.55	822
		17.89	79.59	0.12	97.60	816